EXAMINATION OF A SEMI-ANALYTIC FINITE ELEMENT METHOD FOR PLATE BENDING PROBLEMS

by

K. M. HUSSAIN M.Sc.

A thesis submitted for the degree of

Doctor of Philosophy

The University of Aston in Birmingham

August 1975

Faculty of Engineering

Department of Mechanical Engineering

Head of Department,
Professor A. J. Ede.

Supervisor,
Mr. T. H. Richards.

SUMMARY

In this thesis the Semi-Analytic Finite Element Method of analysis of laterally loaded rectangular plates is examined. A computer program is described in which the eigenfunctions of free vibration of uniform beams are used as the analytic functions. Rectangular plates with any combination of simply supported, clamped or free edges and with any variation of loading or flexural rigidity, including plates with holes or rigid inclusions, may be solved.

In developing the computer program, various schemes were implemented to reduce the influence of errors inherent in the beam eigenfunctions and for the reduction of computer storage requirement so that it may be possible to process the program on a relatively small digital computer. A description of these schemes is given in this thesis.

Using the computer program, the behaviour of the analytic functions in respect of numerical stability and convergence is examined on a comparative basis and the effects of load and rigidity variation on these characteristics are established.

Extensive tests are carried out to check the accuracy of the method under various conditions of loading and rigidity variations. Also, the rate of convergence of the semi-analytic method is compared with other finite element formulations.

Finally, the results from the semi-analytic method, for three plate problems, are compared with those from an experimental technique, namely the Moire method.

NOTATION

a	Length of the strip element.
b	Width of the strip element.
D	Flexural rigidity.
E	Young's Modulus.
h	Plate thickness.
M	Number of harmonics.
M_x, M_y	Bending moments.
M_{xy}	Twisting moment.
M_x^*, M_y^*, Q^*	Applied line loads.
p_0, q	Applied pressure
Q_x, Q_y	Shearing forces
u, v	Displacements.
V_x, V_y	Effective shearing forces.
w	Deflection.
x, y, z	Cartesian co-ordinates.
Y	Beam eigenfunction.
Y_m	m^{th} mode of the beam eigenfunction.
w_{im}	Harmonic deflection parameter on nodal line i.
δ^{*m}	Harmonic prescribed displacement.
χ_x, χ_y	Curvatures.
χ_{xy}	Twist
$\varepsilon_x, \varepsilon_y$	Direct strains.
γ_{xy}	Shearing strain.
$\sigma_x, \sigma_y, \sigma_z$	Direct stresses.
$\tau_{xy}, \tau_{yz}, \tau_{zx}$	Shearing stresses.
μ	Parameter related to the natural frequencies of free vibration of uniform beams.

ν	Poisson's Ratio.
θ_x, θ_y	Rotations.
θ_{im},	Harmonic rotation parameter on nodal line i.
Φ_r^{mn}	Products of eigenfunctions and their derivatives.
$[B]$, $[\bar{B}]$, $[\bar{\bar{B}}]$ $[N]$	Matrices containing functions of position in the displacement model.
$[D]$	Elasticity matrix.
$[D^*]$	Defined by $D = D\ D^*$.
$\{f\}_e$	Element load vector.
$\{f^m\}_e$	Harmonic element load vector.
$\{F\}$	Overall load vector.
$\{F^m\}$	Harmonic overall load vector.
$[J]_r$	Matrices involved in element stiffness matrix.
$[k]_e$	Element stiffness matrix.
$[k^m]$	Harmonic element stiffness matrix.
$[K]$	Overall stiffness matrix
$[K^m]$	Harmonic overall stiffness matrix.
$\{M\}$	Moments vector.
$\{\alpha\}$	Generalised co-ordinates.
$\{\delta\}_e$	Element displacement vector.
$\{\delta^m\}_e$	Harmonic element displacement vector.
$\{\delta\}$	Overall displacement vector.
$\{\varepsilon\}$	Strain vector.
$\{\sigma\}$	Stress vector.
$\{\chi\}$	Curvatures vector.

CONTENTS

CHAPTER 1

CHAPTER ONE

INTRODUCTION.

1.1 The Plate Bending Problem.

A plate is a flat structural element whose thickness is small when compared to its in-plane dimensions. Plates are used frequently in the engineering fields. Ships, air-planes, containers, bridges, architectural structures and instruments are but a few types of structures in which plates, invariably, constitute a major part.

The load carrying nature of the plate is categorized by four types of plates:

1. Thin Plates with Small Deflections. This type of plate carries the load by internal bending and twisting moments and transverse shears in a manner similar to beams.
2. Membranes. These are thin plates which possess no flexural rigidity. They carry the load by axial forces and central shears (i.e. shears in the plane of the plate). They compare to the plates in type 1 as do strings to beams.
3. Thin Plates with Large Deflections. The load carrying nature of this type of plate combines those in 1 and 2.
4. Thick Plates. The internal forces in a thick plate are those relating to a three dimensional body.

The subject matter which covers each of these types of plates is extremely large. It is the first type of plates which concerns the study carried out for this thesis.

The analytic solutions of problems of plates of this type, and indeed all other types, is restricted to simple cases of geometry, loading and boundary conditions. For complex problems, various approximate and numerical methods are employed. In the event that a digital computer is available, the finite element method is, probably, the most widely used method for the analysis of plate bending problems, because of its versatility and high level of accuracy when a sufficient number of finite elements is considered. However, this method is hampered by the large volume of input data which is not only tedious and time consuming, but also prone to human errors.

The finite strip method was suggested by Cheung [1] as a semi-analytic finite element method for the analysis of laterally loaded rectangular plates, in which computer storage requirement, solution time and input data are reduced.

The project described in this thesis was concerned with the extension of the finite strip method to deal with more boundary conditions than was originally attempted and to examine the applicability of the method to plate problems with severe loading and rigidity variations. A more detailed description of the scope of this investigation will be given at the end of the introduction. First, a brief historical account of the development of plate theory which leads up to the finite element method and the semi-analytic technique, will be given here.

1.2 Historical Development.

An account of the history of the development of the mathematical theory of plates is given in ref. [2]. A brief summary from this and other references, [3] and [4], are given here.

The earliest investigations of plates were concerned with vibration. Euler, Bernoulli and Germain attempted to obtain the differential equation of the vibrating plate and although Germain succeeded, with the help of Lagrange, in deriving the correct differential equation of the vibrating plate, the fundamentals, upon which the derivation of the equation is based, were not justified.

The first satisfactory theory of plate bending was developed by Navier. In a paper which he presented to the Academy of Sciences, in 1820, Navier arrived at the well-known governing differential equation of a laterally loaded plate, viz.

$$D\left(\frac{\partial^4 w}{\partial x^4} + 2\,\frac{\partial^4 w}{\partial x^2\,\partial y^2} + \frac{\partial^4 w}{\partial y^4}\right) = p.$$

where p is the applied pressure and D is the flexural rigidity of the plate.

Navier also stated the correct boundary conditions for simply supported edges and solved this problem in the form of a double sine series. This "exact" solution represented the first satisfactory solution to a problem in plate bending.

Poisson also obtained the differential equation of the plate and discussed the boundary conditions, but required three conditions to be satisfied for a free edge, viz. the normal bending moment, the twisting moment and the shear force.

The assumptions upon which the theory of plates is based were laid down by Kirchhoff in 1850. His hypotheses were (1) that lines normal to the middle plane before bending remain so after bending, and (2) that the middle plane does not suffer deformation during small deflections. Establishing a correct expression for the potential energy of the bent plate and using the principle of virtual work he arrived at the differential equation governing the bending of a plate. Further, Kirchhoff showed that there must only be two boundary conditions at the edge and not three as Poisson supposed.

In 1867, Thomson and Tait explained in their "Treatise on Natural Philosophy" the significance of the reduction in the boundary conditions thus providing the first formal demonstration of St. Venant's principle which replaces one system of forces by another one statically equivalent. Thomson also explained why Kirchhoff's theory is accurate enough only if the deflections are small when compared to the thickness of the plate.

Around the turn of the century structural steel replaced wood in the construction of ships and the use of thin plates gained impetus bringing about advances in plate theories and the methods of solution of the problem.

In 1899, M. Levy developed a method of solution for rectangular plates with two opposite edges simply supported and arbitrary boundary conditions on the other two edges. The study of various geometric forms and loading conditions followed. However, rigorous solutions to the plate bending problem remained limited. Consequently, engineers resorted to approximate methods of solutions. Noteable amongst these are the methods by Ritz, Galerkin, Vlasov and Kantorovich where the solution of the problem is reduced to the evaluation of simple integrals and the solutions of simultaneous algebraic equations.

The approximation in these methods is due to the replacement of the unknown function which represents the true deflection anywhere on the plate by an assumed one that approximates to it. Other methods of approximation are numerical ones. They involve mathematical and geometric idealisation. One such method is the finite difference method where the partial differential equation of the plate is replaced by the equivalent difference equation. The latter is applied to a discrete number of points on the plate located at the joints of the network called the finite difference mesh, and the resulting set of equations together with the difference equations representing the boundary conditions are solved yielding the deflection of the plate at the mesh points. As the number of mesh points increases, the resulting number of equations becomes too large to solve by hand, even with the aid of such techniques as the Relaxation method [5]. Thus, when extreme accuracy is required, the finite difference mesh must be fine and the consequent increase in the number of equations necessitates the use of either a pure resistance electrical analogue computer [6] or a digital computer. In a problem where the use of a digital computer is proposed another method of analysis may become more attractive for its versatility and higher convergence rate [4]. It is the finite element method.

1.3 The Finite Element Method.

Hrenikoff [7] is considered to have made the earliest attempt at using a discrete element system to represent a continuum. In 1941 he introduced the Framework Method for the solution of problems in elasticity. In this method the elastic continuum is replaced by a definite pattern of beams and bars that possess such elastic properties as to make the deformations of the framework at the intersection of the members equivalent to those of the original continuum at the same points. The lack of high-speed digital computers at that time and some inherent difficulties in the representation of arbitrary geometries prevented the wide use of this method.

In 1956, soon after the invention of high-speed digital computers, Turner, Clough, Martin and Topp [8] introduced the Finite Element Method which later proved to be one of the most powerful tools in engineering analysis.

The notion upon which the finite element method was based is that no matter what the state of strain in an elastic body is, the complexity of the function which describes it can be reduced, with good accuracy, by considering small regions of the elastic body, and assuming that simple functions represent the strains within each region. This concept is similar in principle to that in which any function can be represented by segments of low order polynomials and if the segments are small enough, straight lines can give a good representation of what may have been a high degree polynomial.

On the above basis the finite element analysis involves dividing the continuum into a number of finite elements interconnected at discrete nodes. A function is assumed to represent the state of displacement within each element, in terms of the nodal displacements (the shape function). A stiffness matrix is then obtained for each element either by a direct stiffness method which uses the notion of stiffness influence coefficients [9], or by using the principle of minimum potential energy [10] whereby the assumed displacements and the consequent strains and stresses are substituted into the expression for the potential energy which is then minimized with respect to the nodal displacements yielding an equilibrium equation with a stiffness matrix and a force vector.

The equations governing the behaviour of the overall structure are obtained by assembling the element stiffness matrices and element force vectors into an overall stiffness matrix and an overall force vector. For this purpose either the equilibrium and compatibility conditions are used directly, or the principle of minimum potential energy is applied to the overall structure.

The statements of the boundary conditions are then incorporated into the overall equations and the solution of the equations follows.

Although the final sets of equations resulting from the two methods of formulation of the problem are identical, the interpretation of the finite element method differs in the variational formulation from that in the direct stiffness method. In the latter, the continuum is assumed to be made up of small structural elements "welded" together at certain points and the procedure follows similar lines to those in the analysis of framed structures. In the variational formulation no physical division of the continuum is assumed. Instead, the continuum is partitioned, by imaginary lines, into sub-regions and a solution or a displacement model is assumed to apply to each sub-region. Thus a pattern of solutions is assumed to apply to the overall structure with the proviso that the solutions match at certain points on the boundaries of the sub-regions. In the variational formulation, the zones are also referred to as elements and the term "division into elements" is, generally, used regardless of formulation.

Applying the variational principle to the assumed displacement models is similar to the Rayleigh-Ritz method of solution of boundary-value problems [11]. The difference being that in the Rayleigh-Ritz method, a smooth continuous function is assumed to apply to the problem as a whole rather than to sub-regions within the continuum. The variational formulation of the finite element method is, therefore, a piece-wise application of the Rayleigh-Ritz method.

The variational formulation allowed a more rigorous, mathematical study of the method to be carried out. In particular a theoretical account of the conditions necessary for convergence of the solution was possible [12]. With a more mathematical approach to the finite element method, the scope of application of the method became wider.

The finite element method was, initially, developed to yield structural data of sufficient accuracy to be adequate for subsequent dynamic and aeroelastic analyses [8]. However, engineers from various fields, including structural mechanics, soon realised the tremendous potential that the method has and set out to develop it. In structural analysis, a great deal of work has been carried out on improving the accuracy of the method and its rate of convergence by studying various formulations, types of elements and functions, [13] and [14].

The finite element problem may now be formulated with displacements as basic unknowns (the displacement approach) together with an application of the principle of minimum potential energy, or it may be formulated with stresses as basic unknowns (the equilibrium approach) in which case the principle of minimum complementary energy may be used. Alternatively, a mixed formulation is also possible, whereby both stresses and displacements are basic unknowns. The Hellinger-Reissner principle may be applied to the mixed formulation. Each formulation may be more suitable for one problem than another. Ref. [10] gives a detailed description of these approaches and their suitability to various problems.

Attempts at improving the accuracy of the results with a reduction in the number of elements have been concentrated on testing various types of elements and displacement (or stress) models. Amongst the most outstanding contributors in this field are Zienkiewicz [15], Irons [16] and Argyris [17].

Accuracy of the results from a finite element method of analysis may be improved by dividing the continuum into a larger number of elements. Alternatively, a higher degree polynomial may be used for the shape function. Since the shape function is a function of the nodal displacements, this can be achieved either by increasing the number of nodes on each element or by increasing the number of degrees of freedom per node. However, the number of elements is sometimes governed by the need for a reasonable representation of the boundary. In this case, elements with straight edges are inefficient.

Considerable improvement to the formulation of the finite element method was achieved by the introduction of the "Isoparametric Element" concept [15]. In this type of element, curved-boundary elements are allowed in conjunction with a curvilinear co-ordinate system [18]. The geometry of the element and the shape function are described in terms of the same parameters and are of the same order, hence the term "isoparametric element".

In fields of engineering other than structural mechanics, the finite element method has, successfully, been applied to a variety of problems including soil and rock mechanics, heat conduction, seepage, fluid mechanics and hydraulics [10].

There are two serious disadvantages of the finite element method. The first is the need for a relatively large, high-speed computer to perform the calculations, because even the most efficient finite element computer program requires a large amount of computer storage and time. The second and, perhaps, the most serious disadvantage is the large amount of data necessary to produce reasonably accurate results. The disadvantage here is twofold. Firstly, the process of data preparation is tedious and time consuming. Secondly, with a large amount of data there is a relatively greater risk of making a human error. The erroneous results may be of such a nature as to appear acceptable and, therefore, go undetected.

Attempts have been made to automate the process of discretization to some degree [19] but this has not been completely accomplished because some engineering judgement is often necessary when generating the finite element mesh.

In any problem where a great deal of effort, time and cost are necessary for the solution and when all known possibilities for the reduction of these factors, whilst maintaining the generality of the solution method, have been exploited, a further reduction is sought through special techniques. Such a reduction is, invariably, achieved at the expense of a loss in the generality of the solution method. The Semi-Analytic approach, which is applicable to the finite element method, represents one of these special methods.

1.4 The Semi-Analytic Finite Element Method.

In many rpoblems it is possible to reduce a three dimensional problem into a two dimensional one by assuming that stresses or strains in one direction are negligible, as in the cases of plane stress or plane strain, provided that there are acceptable grounds for making such assumptions.

In the finite element method of analysis, another, entirely different, method of reducing the dimensions is called "The Semi-Analytic Technique". In this method, the displacements, strains and stresses in one direction are assumed to vary according to some known function which satisfies the boundary conditions at the extreme points of this direction. Consequently, the continuum need not be divided into elements in the direction along which the state of displacements is specified by the analytic function.

This technique was applied to axisymmetric solids with axisymmetric or non-axisymmetric loads [20] and to axisymmetric solids with asymmetric properties [21]. Application of the technique to rectangular plate bending problems was suggested by Cheung [1] who called it the finite strip method. The plate is assumed to be divided in one direction into strips across whose width the deflection is assumed to be in the form of a third order polynomial. In the longitudinal direction, a set of functions is chosen to represent the variation of the deflection. The eigenfunctions of free vibration of uniform beams were employed. The boundary conditions at the edges of the strips being satisfied by the appropriate eigenfunctions.

The method of solution follows a similar procedure to that employed for the finite element method.

In the previous section it was stated that a reduction in solution time is usually achieved at the expense of a loss in generality. The semi-analytic method is, generally, restricted to rectangular plate problems, although under certain circumstances non-rectangular edges may be treated. However, the extensive use of rectangular plates in industry allows the method to be a great deal more useful than it would, otherwise, be.

1.5 Scope of Investigation.

Any method which reduces the amount of work, time and cost necessary for the solution of a particular problem deserves close attention. The finite strip method has been presented as such [1]. This project, therefore, aimed at developing the method and examining, more closely, its various aspects and exploring its potential.

Cheung applied the method to rectangular plates with two opposite edges simply supported or clamped or simply supported-clamped [22] but, although he pointed out that appropriately selected eigenfunctions may be used to solve bending problems of plates with other boundary conditions, no formal investigation had been, as far as is known, carried out to study the numerical stability, convergence or accuracy of the method when applied to boundary conditions other than those mentioned above. The applicability of the semi-analytic method to problems of plates with severe variation in rigidity, such as plates with holes, had not been explored.

A major part of this project was to develop a computer program based on the semi-analytic method. The computer program is to be able to solve problems of rectangular plates with any combination of simply supported, clamped and free boundary conditions. Also any variation in the applied load or flexural rigidity is to be accomodated.

In developing the computer program, various ideas have been implemented for the reduction of the errors inherent in computer-evaluation of some of the eigenfunctions and their integrals, and for reducing the computer storage requirement.

The computer program has been used to examine the numerical stability and the rates of convergence of the various eigenfunctions for a specific number of strips and the effect of load and rigidity variation on these quantities has been studied.

The program was also used to appraise the accuracy of the method and to test its capability to represent severe variations in the flexural rigidity. In particular, the effect of the singularity of the bending moments, at the corners of a rectangular hole, on the solution and the extent of error propagation has been examined.

The convergence rate of the method, as a function of solution time, was compared with other formulations of the finite element method.

The Moire method was used for an experimental analysis of some plates, including those with rigidity variations, and the results were compared with computer predicitions based on the finite strip method.

The aims of this project were achieved. However, it was not possible, in the time given for the project, to test the suitability of a number of schemes, which were envisaged during the work carried out here. for the analysis of rectangular plates with mixed boundary conditions and for the solution of certain types of non-rectangular plates. Consequently, a number of suggestions, for further work, were made.

CHAPTER 2

CHAPTER TWO

SMALL DEFLECTIONS OF THIN PLATES

2.1. Classical Theory.

The so-called classical theory of plates is based on the theory of elasticity. A mathematical model which describes the physical behaviour of the plate is established after making certain assumptions regarding this behaviour and the material properties of the plate. Compatibility conditions provide the means for a displacement-strain relationship. Hook's Law, then, relates the stresses to the strains. Finally, the equations of equilibrium are employed to obtain the governing differential equation of the plate.

2.1.1. Assumptions.

A plate is, like all other structural elements, strictly, a three dimensional continuum, the exact analysis of which requires the application of three dimensional theory of elasticity. The analysis can, however, be reduced to a two dimensional one and the development of an approximate theory of plate bending facilitated by making certain assumptions.

A distinguishing feature of a plate type member is that one of its characteristic dimensions -the thickness- is small compared with the other two. Because of this, plausible assumptions about its behaviour are:

1. The middle surface of the plate is not strained. This implies that the middle surface during bending is a neutral surface.

2. The stresses normal and tangential to the middle plane are small when compared with the other stresses.
3. Lines normal to the middle surface before bending remain normal after bending. They merely rotate through the same angle as the middle surface. The implication of this assumption is that the effect of shear forces on the deflection of the plate is negligible.

The first assumption can be shown to be acceptable to a good degree of accuracy if the deflection is small compared to the plate thickness [23]. The validity of the second and the third assumptions depends to a large extent on the ratio of plate thickness to the lateral dimensions of the plate [24]. The degree of load concentration plays an important part in neglecting the effect of shear on deformation.

The classical theory of plates also assumes that the material of the plate is elastic, homogeneous and isotropic.

2.1.2 Derivation of the Governing Differential Equation.

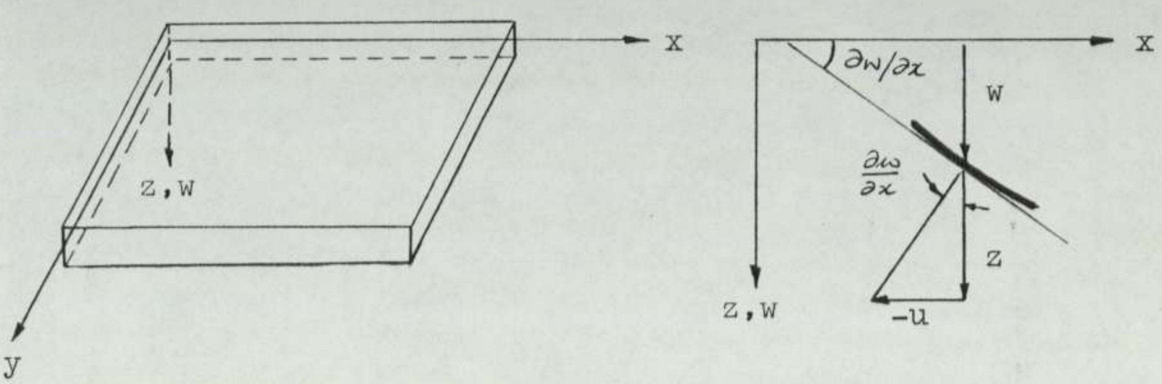

Fig.(2.1).

If the displacement, in the x direction, of a point on a normal to the neutral surface at distance z is u(x,y,z) then,

$$u = -z \frac{\partial w}{\partial x} \qquad \text{from fig.(2.1.) and assumption 3,}$$

similarly, for the displacement in the y direction v(x,y,z):

$$v = -z \frac{\partial w}{\partial y}$$

From theory of elasticity, the conditions for compatibility will be given by:

$$\begin{aligned} \varepsilon_x &= \frac{\partial u}{\partial x} = -z \frac{\partial^2 w}{\partial x^2} \;, \\ \varepsilon_y &= \frac{\partial v}{\partial y} = -z \frac{\partial^2 w}{\partial y^2} \;, \\ \gamma_{xy} &= \frac{\partial u}{\partial y} + \frac{\partial v}{\partial x} = -2z \frac{\partial^2 w}{\partial x \, \partial y} \end{aligned} \qquad (2.1.)$$

In the light of the assumptions made, an element is very nearly in a state of plane stress, then Hook's Law takes the form:

$$\begin{Bmatrix} \sigma_x \\ \sigma_y \\ \tau_{xy} \end{Bmatrix} = \frac{E}{1-\nu^2} \begin{bmatrix} 1 & \nu & 0 \\ \nu & 1 & 0 \\ 0 & 0 & \frac{1-\nu}{2} \end{bmatrix} \begin{Bmatrix} \varepsilon_x \\ \varepsilon_y \\ \gamma_{xy} \end{Bmatrix}$$

and substituting for the strains from equations (2.1.), the stress vector becomes:

$$\begin{Bmatrix} \sigma_x \\ \sigma_y \\ \tau_{xy} \end{Bmatrix} = -\frac{Ez}{1-\nu^2} \begin{bmatrix} 1 & \nu & 0 \\ \nu & 1 & 0 \\ 0 & 0 & \frac{1-\nu}{2} \end{bmatrix} \begin{Bmatrix} \frac{\partial^2 w}{\partial x^2} \\ \frac{\partial^2 w}{\partial y^2} \\ 2\frac{\partial^2 w}{\partial x \, \partial y} \end{Bmatrix} \qquad (2.2.)$$

For equilibrium, these stresses have to satisfy the equations:

$$\frac{\partial \sigma_x}{\partial x} + \frac{\partial \tau_{xy}}{\partial y} + \frac{\partial \tau_{xz}}{\partial z} = 0$$

$$\frac{\partial \tau_{yx}}{\partial x} + \frac{\partial \sigma_y}{\partial y} + \frac{\partial \tau_{yz}}{\partial z} = 0 \qquad (2.3.)$$

$$\frac{\partial \tau_{zx}}{\partial x} + \frac{\partial \tau_{zy}}{\partial y} + \frac{\partial \sigma_z}{\partial z} = 0$$

Although plane stress is assumed in the analysis, the loads which have to be in equilibrium are three directional, viz., σ_x, σ_y, τ_{xy} in the plane of the plate and p, the applied pressure, normal to the plane of the plate. To equilibrate p, the shearing stresses τ_{zx} and τ_{zy} need to be considered. The three dimensional nature of the equations of equilibrium must, therefore, be maintained.

To establish the equilibrium equations for the plate, the stresses across the thickness of the plate are examined:

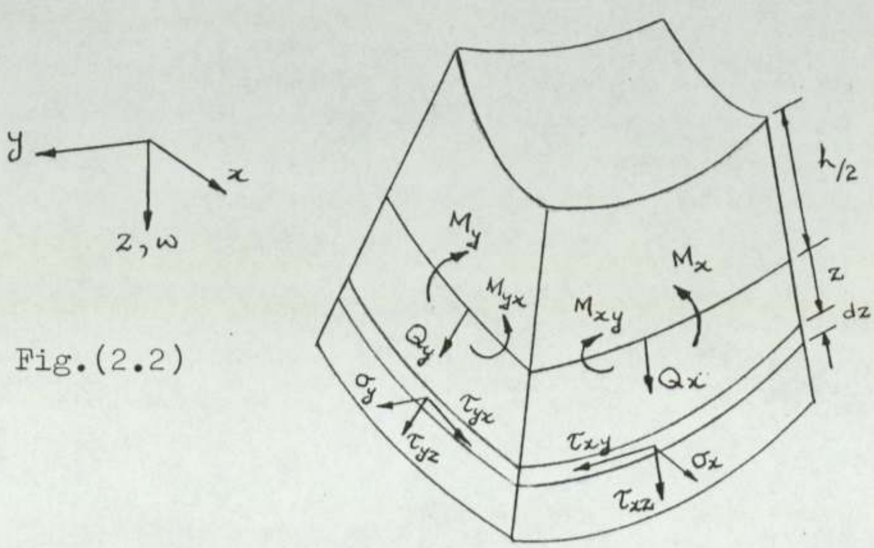

Fig.(2.2)

From Fig.(2.2.) the bending moments and shear forces per unit length are given by:

$$\left.\begin{aligned}
M_x &= \int_{-h/2}^{h/2} \sigma_x \cdot z\,dz && \text{(a)}\\
M_y &= \int_{-h/2}^{h/2} \sigma_y \cdot z\,dz && \text{(b)}\\
M_{xy} &= \int_{-h/2}^{h/2} \tau_{xy} \cdot z\,dz = M_{yx} && \text{(c)}\\
Q_x &= \int_{-h/2}^{h/2} \tau_{xz}\,dz && \text{(d)}\\
Q_y &= \int_{-h/2}^{h/2} \tau_{yz}\,dz && \text{(e)}
\end{aligned}\right\} \qquad (2.4.)$$

Multiplying the first and second equations (2.3.) by z and integrating all three equations w.r.t z from -h/2 to h/2 gives

$$\left.\begin{aligned}
&\frac{\partial}{\partial x}\int_{-h/2}^{h/2} \sigma_x\, z\,dz + \frac{\partial}{\partial y}\int_{-h/2}^{h/2} \tau_{xy}\, z\,dz + \int_{-h/2}^{h/2} \frac{\partial \tau_{xz}}{\partial z}\, z\,dz = 0 && \text{(a)}\\
&\frac{\partial}{\partial x}\int_{-h/2}^{h/2} \tau_{yx}\, z\,dz + \frac{\partial}{\partial y}\int_{-h/2}^{h/2} \sigma_y\, z\,dz + \int_{-h/2}^{h/2} \frac{\partial \tau_{yz}}{\partial z}\, z\,dz = 0 && \text{(b)}\\
&\frac{\partial}{\partial x}\int_{-h/2}^{h/2} \tau_{zx}\,dz + \frac{\partial}{\partial y}\int_{-h/2}^{h/2} \tau_{zy}\,dz + \int_{-h/2}^{h/2} \frac{\partial \sigma_z}{\partial z}\,dz = 0 && \text{(c)}
\end{aligned}\right\} (2.5.)$$

Substituting equations (2.4.) into equations (2.5.) yields the equilibrium equation for the plate

$$\frac{\partial M_x}{\partial x} + \frac{\partial M_{xy}}{\partial y} - Q_x = 0 \qquad \text{(a)}$$

$$\frac{\partial M_{yx}}{\partial x} + \frac{\partial M_y}{\partial y} - Q_y = 0 \qquad \text{(b)} \qquad (2.6.)$$

$$\frac{\partial Q_x}{\partial x} + \frac{\partial Q_y}{\partial y} + p = 0 \qquad \text{(c)}$$

The third term in each of equations (2.5a) and (2.5b) was integrated by parts subject to the conditions $\tau_{xz} = \tau_{yz} = 0$ at $z = \pm h/2$. The third term of equation (2.5c) was subject to the condition $\sigma_z = 0$ at $z = h/2$, $\sigma_z = -p$ at $z = -h/2$.

Substituting equations (2.2.) into the first and second equations (2.3.) then integrating across the thickness yields the expressions for τ_{xz} and τ_{yz}:

$$\tau_{xz} = \frac{E(4z^2 - h^2)}{8(1 - \nu^2)} \cdot \frac{\partial}{\partial x} \left(\frac{\partial^2 w}{\partial x^2} + \frac{\partial^2 w}{\partial y^2} \right)$$

$$\tau_{yz} = \frac{E(4z^2 - h^2)}{8(1 - \nu^2)} \cdot \frac{\partial}{\partial y} \left(\frac{\partial^2 w}{\partial x^2} + \frac{\partial^2 w}{\partial y^2} \right) \qquad (2.7.)$$

Substituting into equations (2.4d) and (2.4e) then into (2.6c) gives the differential equation of the deflection surface for the plate

$$\frac{\partial^4 w}{\partial x^4} + 2\frac{\partial^4 w}{\partial x^2 \partial y^2} + \frac{\partial^4 w}{\partial y^4} = \frac{p}{D} \qquad (2.8.)$$

or more compactly:

$$\nabla^4 w = p/D$$

where
$$D = \frac{Eh^3}{12(1 - \nu^2)}$$

Substituting equations (2.2.) and equations (2.7.) into equation (2.4.) gives the expressions for the bending moments and shear forces:

$$M_x = - D \left(\frac{\partial^2 w}{\partial x^2} + \nu \frac{\partial^2 w}{\partial y^2} \right)$$

$$M_y = - D \left(\frac{\partial^2 w}{\partial y^2} + \nu \frac{\partial^2 w}{\partial x^2} \right)$$

$$M_{xy} = - D (1 - \nu) \frac{\partial^2 w}{\partial x \partial y} \qquad (2.9.)$$

$$Q_x = - D \frac{\partial}{\partial x} \left(\frac{\partial^2 w}{\partial x^2} + \frac{\partial^2 w}{\partial y^2} \right)$$

$$Q_y = - D \frac{\partial}{\partial y} \left(\frac{\partial^2 w}{\partial x^2} + \frac{\partial^2 w}{\partial y^2} \right)$$

From equations (2.2.), (2.7.) and (2.9.) the stresses are obtained in terms of the bending moments and shear forces

$$\sigma_x = \frac{12z}{h^3} M_x \ , \ \sigma_y = \frac{12z}{h^3} M_y \ , \ \tau_{xy} = \frac{12z}{h^3} M_{xy}$$

$$\tau_{xz} = \frac{3Q_x}{2h} \left(1 - \frac{4z^2}{h^2} \right) , \ \tau_{yz} = \frac{3Q_y}{2h} \left(1 - \frac{4z^2}{h^2} \right) \qquad (2.10)$$

The maximum values of the stresses σ_x, σ_y and τ_{xy} occur at $z = \pm h/2$ and the maximum values of τ_{xz} and τ_{yz} occur at $z = 0$. Thus:

$$\begin{Bmatrix} \sigma_x \\ \sigma_y \\ \tau_{xy} \end{Bmatrix}_{max.} = \pm \frac{6}{h^2} \begin{Bmatrix} M_x \\ M_y \\ M_{xy} \end{Bmatrix} \qquad (2.11)$$

and

$$\begin{Bmatrix} \tau_{xz} \\ \\ \tau_{yz} \end{Bmatrix}_{max} = \frac{3}{2h} \begin{Bmatrix} Q_x \\ \\ Q_y \end{Bmatrix} \qquad (2.12.)$$

For a more detailed and general study of the classical theory of plates, reference may be made to the well-known classic "Theory of Plates and Shells" [23].

2.2. Variational Approach.

Variational Calculus is the mathematical process of establishing the conditions required for determining a functional such that another functional is stationary. A functional is a function which depends on the whole path of one or more functions rather than a number of independent variables.

Most problems which employ the Finite Element Method for their solution are based on a variational principle in their formulation. However, it is possible to formulate the finite element problem on a non-variational basis

2.2.1. Principle of Minimum Potential Energy.

This is one of the principles employed in formulating a finite element problem. It states: Of all possible displacement patterns a body can assume which satisfy compatibility and geometric boundary conditions, the one which satisfies the equilibrium requirement makes the potentail energy a minimum.

Minimizing a functional, F, implies the vanishing of its first variation δF. The variation notation δ is similar to the total differential in calculus, i.e. if $F=F(x,w',w'')$, then $\delta F = \frac{\partial F}{\partial w}\delta w + \frac{\partial F}{\partial w'}\delta w' + \frac{\partial F}{\partial w''}\delta w''$. It also exhibits the commutative property with differentiation and integration, i.e.

$$\delta\left(\frac{dw}{dx}\right) = \frac{d}{dx}(\delta w) \text{ and } \delta\int F\,dx = \int \delta F\,dx.$$

The variational formulation will now be developed for the plate problem.

It can be shown [23] that the potential energy of a rectangular plate with flexural rigidity D and in plane dimensions a × b, under an applied pressure p(x,y), is given by:

$$V = \int_0^a\int_0^b \left\{ \frac{D}{2}\left[\left(\frac{\partial^2 w}{\partial x^2}\right)^2 + \left(\frac{\partial^2 w}{\partial y^2}\right)^2 + 2\nu\frac{\partial^2 w}{\partial x^2}\cdot\frac{\partial^2 w}{\partial y^2} + 2(1-\nu)\left(\frac{\partial^2 w}{\partial x\,\partial y}\right)^2\right] - pw\right\} dxdy \qquad (2.13.)$$

The first variation of V is

$$\delta V = \int_0^a\int_0^b\left\{\frac{D}{2}\left[2\left(\frac{\partial^2 w}{\partial x^2}\right)\delta\left(\frac{\partial^2 w}{\partial x^2}\right) + 2\left(\frac{\partial^2 w}{\partial y^2}\right)\delta\left(\frac{\partial^2 w}{\partial y^2}\right) + 2\nu\left(\frac{\partial^2 w}{\partial x^2}\,\delta\left(\frac{\partial^2 w}{\partial y^2}\right) + \frac{\partial^2 w}{\partial y^2}\,\delta\left(\frac{\partial^2 w}{\partial x^2}\right)\right) + 2(1-\nu)\cdot 2\frac{\partial^2 w}{\partial x\,\partial y}\,\delta\left(\frac{\partial^2 w}{\partial x\,\partial y}\right)\right] - p\,\delta w\right\} dxdy \quad (2.14.)$$

This can be regarded as a "virtual" change in V consequent on letting the plate execute a virtual displacement δw. Integrating the terms in the square brackets, successively, by parts aiming at reducing the variation of second order derivitives such as $\delta\left(\frac{\partial^2 w}{\partial x^2}\right)$ to first order derivitives, $\delta\left(\frac{\partial w}{\partial x}\right)$, and zero order δw, and tidying up gives for the first variation of the potential energy:

$$\delta V = \int_o^a\int_o^b \left\{ D \left[\frac{\partial^4 w}{\partial x^4} + 2\frac{\partial^4 w}{\partial x^2 \partial y^2} + \frac{\partial^4 w}{\partial y^4}\right] - p\right\} \delta w \, dxdy$$

$$+ \int_o^a D\left\{\left[\frac{\partial^2 w}{\partial x^2} + \nu \frac{\partial^2 w}{\partial y^2}\right] \delta\left(\frac{\partial w}{\partial x}\right)\right\}_{x=o}^{x=b} dy$$

$$+ \int_o^b D\left\{\left[\frac{\partial^2 w}{\partial y^2} + \nu \frac{\partial^2 w}{\partial x^2}\right] \delta\left(\frac{\partial w}{\partial y}\right)\right\}_{y=o}^{y=a} dx$$

$$- \int_o^a D\left\{\left[\frac{\partial^3 w}{\partial x^3} + (2-\nu) \frac{\partial^3 w}{\partial x \partial y^2}\right] \delta w\right\}_{x=o}^{x=b} dy$$

$$- \int_o^b D\left\{\left[\frac{\partial^3 w}{\partial y^3} + (2-\nu) \frac{\partial^3 w}{\partial y \partial x^2}\right] \delta w\right\}_{y=o}^{y=a} dx$$

$$+ 2(1-\nu) D \left\{\left[\frac{\partial^2 w}{\partial x \partial y} \delta w\right]_{x=o}^{x=b}\right\}_{y=o}^{y=a}$$

$$= 0 \quad \text{for minimum potential energy} \qquad (2.15)$$

Details of the integration are given in appendix (1).

Since the variations δw, $\delta(\frac{\partial w}{\partial x})$ and $\delta(\frac{\partial w}{\partial y})$ are arbitrary in the region of the plate and are zero on the boundary only if w, $\frac{\partial w}{\partial x}$ and $\frac{\partial w}{\partial y}$, respectively, are prescribed, then each term in equation (2.15) must vanish independently.

A fundamental lemma of variational calculus [11] states that for any function $\varphi(x)$ continuous in the interval $[x_1, x_2]$, if $\int_{x_1}^{x_2} \varphi(x)\eta(x)\,dx=0$, where $\eta(x)$ is any continuous differentiable function satisfying $\eta(x_1) = \eta(x_2) = 0$, then $\varphi \equiv 0$ for $x_1 \leqslant x \leqslant x_2$.

It follows from the above lemma and from equation (2.15) that:

$$D\left[\frac{\partial^4 w}{\partial x^4} + 2\frac{\partial^4 w}{\partial x^2 \partial y^2} + \frac{\partial^4 w}{\partial y^4}\right] - p = 0 \qquad \text{(a)}$$

$$\left\{D\left[\frac{\partial^2 w}{\partial x^2} + \nu \frac{\partial^2 w}{\partial y^2}\right] \delta\left(\frac{\partial w}{\partial x}\right)\right\}_{x=o}^{x=b} = 0 \qquad \text{(b)}$$

$$\left\{D\left[\frac{\partial^2 w}{\partial y^2} + \nu \frac{\partial^2 w}{\partial x^2}\right] \delta\left(\frac{\partial w}{\partial y}\right)\right\}_{y=o}^{y=a} = 0 \qquad \text{(c)}$$

$$\left\{D\left[\frac{\partial^3 w}{\partial x^3} + (2-\nu)\frac{\partial^3 w}{\partial x\, \partial y^2}\right] \delta w\right\}_{x=o}^{x=b} = 0 \qquad \text{(d)} \qquad (2.16)$$

$$\left\{D\left[\frac{\partial^3 w}{\partial y^3} + (2-\nu)\frac{\partial^3 w}{\partial y\, \partial x^2}\right] \delta w\right\}_{y=o}^{y=a} = 0 \qquad \text{(e)}$$

$$2(1-\nu)\, D \left\{\left[\frac{\partial^2 w}{\partial x\, \partial y}\ \delta w\right]_{x=o}^{x=b}\right\}_{y=o}^{y=a} = 0 \qquad \text{(f)}$$

Expression (a) is the familiar differential equation of the plate problem. Written more compactly it is

$$\nabla^4 w = \frac{p}{D}\ .$$

Expressions (b) through (f) give the natural and geometric boundary conditions which must be satisfied. Thus on the edges x=o and x=b it is required that

either $\frac{\partial w}{\partial x}$ is prescribed, hence $\delta\left(\frac{\partial w}{\partial x}\right) = 0$

or $M_x = D\left[\frac{\partial^2 w}{\partial x^2} + \nu \frac{\partial^2 w}{\partial y^2}\right] = 0$, also

either w is prescribed, hence $\delta w = 0$

or $V_x = D\left[\frac{\partial^3 w}{\partial x^3} + (2-\nu)\frac{\partial^3 w}{\partial x\, \partial y^2}\right] = 0.$

where V_x is the effective shear force.

Similarly, on the edges y=o and y=a it is required that

either $\frac{\partial w}{\partial y}$ is prescribed or $M_y=0$, and

either w is prescribed or $V_y=0$.

From expression (f) the corner conditions must be satisfied: either w is prescribed or $R=2(1-\nu)D\frac{\partial^2 w}{\partial x\,\partial y}=0$ on each corner where R is a concentrated reaction at each corner.

2.2.2. Effective Shear Force and Corner Reactions.

The natural boundary conditions pertaining to the normal moments are readily visualized from physical considerations. The effective shear force and concentrated corner reactions, on the other hand, need some clarification. Along the edge of a rectangular plate , three quantities that are relevant to the natural boundary conditions prevail. These are the moment normal to the edge, the twisting moment and the shearing force. However, only two natural boundary conditions result from the variational formulation. They are the normal bending moment and the "effective" shear force. Obviously, the two conditions relating to the twisting moment and shear force have been reduced to one. Thomson and Tait in their treatise "Natural Philosophy" pointed out the significance of this reduction in the number of natural boundary conditions.

Because the governing differential equation is of the 4th order, no more than two boundary conditions may be imposed on each edge. The twisting moment is the result of shear forces above and below the neutral axis and parallel to it, Fig(2.2.). By Saint Venant's Principle, these forces may be replaced by forces normal to the neutral axis producing the same twisting moment with only a local change to the stress distribution field around the upper and lower edges.

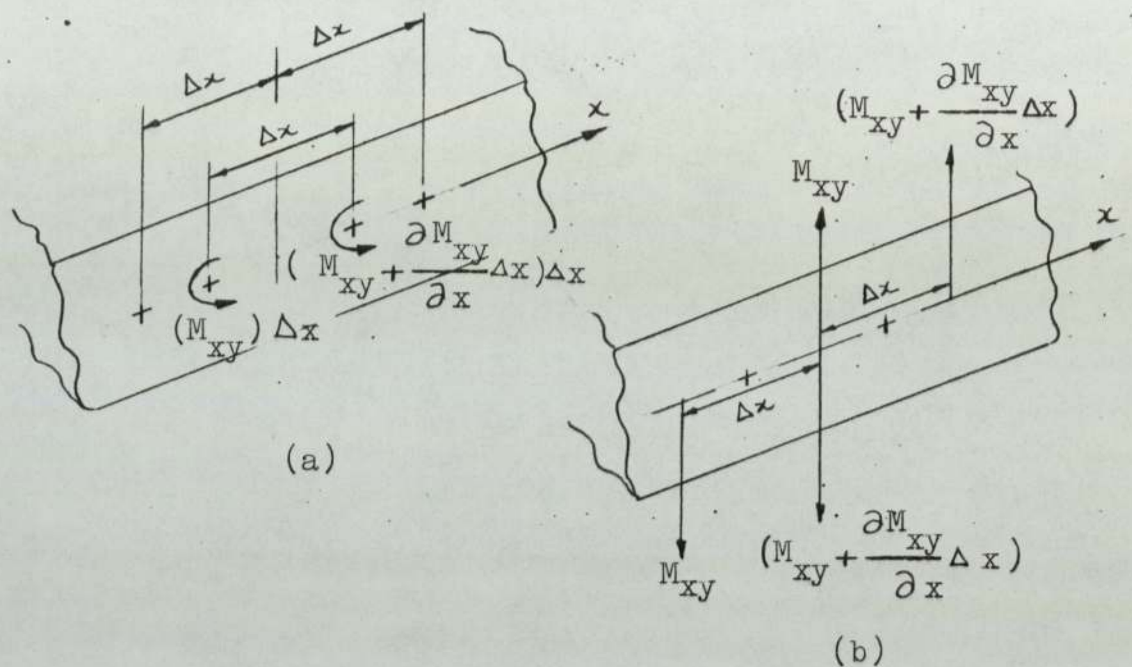

Fig.(2.3)

Considering a small length $2\Delta x$ of an edge parallel to the x-axis, and representing the variation in the twisting moment as a one term Taylor series, the value of the twisting moment at two points Δx apart will be as shown in Fig.(2.3a), where M_{xy} is the twisting moment per unit length (i.e. M_{xy} has the units of force). These moments are now replaced by forces, normal to the neutral axis, whose magnitudes and separation are as shown in Fig.(2.3b). It can be seen that the nett force acting along the edge due to the twisting moment will be $+\dfrac{\partial M_{xy}}{\partial x}$ per unit length. Adding this to the shear force distribution on the edge, the effective shear force will be:

$$V_y = (Q_y + \frac{\partial M_{xy}}{\partial x})$$

Similarly,

$$V_x = (Q_x + \frac{\partial M_{xy}}{\partial y}) \qquad (2.17)$$

Using the expressions for Q_x, Q_y and M_{xy} from (2.9.) the effective shear forces will be:

$$V_y = -D\left[\frac{\partial^3 w}{\partial y^3} + (2-\nu)\frac{\partial^3 w}{\partial y\,\partial x^2}\right]$$

and

$$V_x = -D\left[\frac{\partial^3 w}{\partial x^3} + (2-\nu)\frac{\partial^3 w}{\partial x\,\partial y^2}\right] \qquad (2.18)$$

which are identical to the expressions obtained from the variational formulation (2.15).

If there is a discontinuity in the rate of turn of the tangent to the edge, as is the case for plates with straight edges, then from the preceeding argument regarding the representation of the twisting moment by a shear force, there will remain a concentrated force at the discontinuity (i.e. the corner of the straight edges). The value of this force will be $2M_{xy}$. Fig.(2.3c) clarifies this point further.

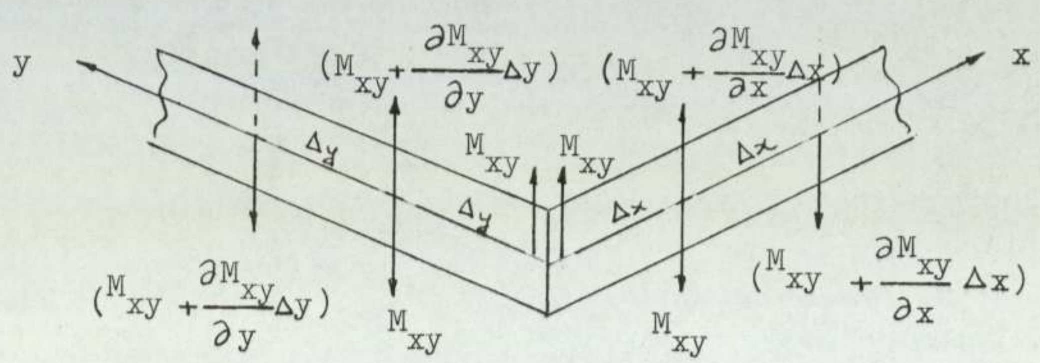

Fig.(2.3c).

Once again if the expression for M_{xy} is used, the corner forces will be given by

$$R = 2D(1-\nu)\frac{\partial^2 w}{\partial x\,\partial y} \quad \text{as in expression (f).}$$

Thus a plate with straight edges supported in some way along one or more of these edges will have, not only a distributed shearing force at the edge, but also a concentrated force at the corner.

Two adjacent, free edges will not have such a force because in this case w is arbitrary and condition (f) will only be satisfied if R=0.

In the case of clamped, adjacent edges, R will also be zero because the normal slope ($\frac{\partial w}{\partial n}$) along the whole of the edges is constant (=0) and therefore the rate of change with respect to the tangential direction (i.e. $\frac{\partial}{\partial t}\left(\frac{\partial w}{\partial n}\right)$) is zero, thus $\frac{\partial^2 w}{\partial x\,\partial y} = 0$, hence R=0.

The variational formulation yielded the differential equation governing the flexure of thin plates with small deflections. It also yielded the natural and geometric boundary conditions to be satisfied for the solution of the problem.

A very important point was also apparent from this formulation. If the problem is formulated by using variational methods, then either the geometric or the natural boundary conditions need to be satisfied. For example, if the plate was simply supported along the edge x=b and the geometric boundary conditions were to be satisfied, then, referring back to expression (b), by allowing $\left[\delta\left(\frac{\partial w}{\partial x}\right)\right]_{x=b}$ to remain arbitrary implies $[M_x]_{x=b}=0$ which is the appropriate natural boundary condition.

2.3. Solution of the Governing Differential Equation.

The so-called classical theory of plates is based on the theory of elasticity. The mathematical model which describes the physical behaviour of the plate was established after making certain assumptions regarding this behaviour and the material properties of the plate. Compatibility conditions provided the means for a displacement-strain relationship, then Hook's Law related the stresses to the strains. The equations of equilibrium provided the final means for establishing the governing differential equation of the plate.

Rigorous solution of the plate bending problem requires the solution of the governing differential equation

$$\nabla^4 w = p/D \qquad (2.19)$$

subject to satisfying the boundary conditions of the particular plate problem. Such solutions are only available for a limited number of cases of plate geometry, loading and boundary conditions. In the majority of cases rigorous solutions are either unavailable or extremely cumbersome. A brief survey of some of the available "exact", approximate and numerical methods will be given here.

2.3.1. Exact Solutions.

a. The Circular Plate.

The circular clamped plate under uniform pressure is one of the problems for which a rigorous solution is easily obtained [4]. The availability of a simple function, namely $w = C(x^2+y^2-r_0^2)^2$ where r_0 is the radius of the plate and C is a constant, which satisfies the differential equation (2.19) and the boundary conditions, is the reason for the ease with which the solution to this particular problem is obtained. The constant C is evaluated by substituting the function into the differential equation.

Although somewhat more elaborate, rigorous solutions for problems of circular plates with boudary conditions other than clamped, and loading other than uniform pressure, may be obtained [25]. In these cases, the governing differential equation is, usually, stated in polar coordinates (r, θ), viz.,

$$\nabla_p^4 w = \frac{p(r,\theta)}{D} \tag{2.20}$$

where

$$\nabla_p^4 = \left(\frac{\partial^2}{\partial r^2} + \frac{1}{r^2}\frac{\partial^2}{\partial \theta^2} + \frac{1}{r}\frac{\partial}{\partial r}\right)\left(\frac{\partial^2}{\partial r^2} + \frac{1}{r^2}\frac{\partial^2}{\partial \theta^2} + \frac{1}{r}\frac{\partial}{\partial r}\right)$$

The solution of equation (2.20) may be taken in the form:

$$w = w_H + w_P \tag{2.21}$$

where w_H is the solution of the homogeneous differential equation

$$\nabla_p^4 w = 0 \tag{2.22}$$

and w_P is the particular solution of equation (2.20).

The solution as given by equation (2.21) may be interpreted as the superposition of the solution, w_H, due to edge forces only and the solution, w_P, due to the applied load.

A general solution to equation (2.22) was obtained by Clebsch [23] in the form:

$$w(r,\theta) = R_0(r) + \sum_{m=1}^{\infty} R_m(r)\cos m\theta + \sum_{m=1}^{\infty} R'_m(r)\sin m\theta \tag{2.23}$$

where R_0, R_1, R_2, ..., R'_1, R'_2, ... are functions of r only.

Substitution of equation (2.23) into equation (2.22) results in a set of ordinary differential equations whose solutions give expressions for R_0, R_m and R'_m ($m=1,2,\ldots$). These expressions contain constants which are determined from implementation of the boundary conditions.

The special case of circular plate problems possessing rotational symmetry is simplified by the fact that in this case the governing differential equation is reduced to an ordinary differential equation, in r only, which can be integrated directly if the load is represented as a continuous function of r. The constants of integration are evaluated from the boundary conditions. The case of rotationally symmetric circular plates with variable rigidity is one of the rare cases that can be solved analytically with relative ease [23]. The variation in the rigidity (as a function of r) has to be considered when the governing differential equation is derived. The resulting ordinary differential equation will have variable coefficients.

b. Simply Supported Rectangular Plates - Navier's Method.

Mathematically exact solutions of special cases of rectangular plates are also available. The simply supported rectangular plate, for example, was solved in 1820 by Navier using double sine series [23]. The deflection within the plate was expressed as the sum:

$$w(x,y) = \sum_{m=1}^{\infty} \sum_{n=1}^{\infty} W_{mn} \sin \frac{m\pi x}{a} \sin \frac{n\pi y}{b} \qquad (2.24)$$

where W_{mn} are unknown constants.

The series in (2.24) satisfies the boundary conditions of simply supported edges (at $x=o,a$ and $y=o,b$).

The applied load was also expressed as a double sine series by use of the usual Fourier methods. Thus:

$$p(x,y) = \sum_{m=1}^{\infty} \sum_{n=1}^{\infty} P_{mn} \sin \frac{m\pi x}{a} \sin \frac{n\pi y}{b} \qquad (2.25)$$

where P_{mn} are the Fourier coefficients.

Substitution of equations (2.24) and (2.25) into equation (2.19) yields an algebraic equation which can be solved to give the unknown constants W_{mn}. The bending and twisting moments, shear forces and stresses can be obtained from expressions (2.9) through (2.12).

The Navier solution is mathematically exact, though not in practice because the series is always truncated to a finite number of terms. The deflection series, however, converges quite rapidly in the case of distributed loads. For discontinuous or concentrated loads the rate of convergence is slower. This is reflected by the relative weakness of the Fourier method in representing discontinuous functions. The rate of convergence of the series for the moments and shear forces is also slow because these quantities involve derivatives of expression (2.24) and the truncation error is magnified when the function is differentiated.

c. Levy's Method.

A more general, though more cumbersome, method for the solution of rectangular plates was introduced by Levy [23]. For this method to be suitable the plate has to be simply supported on two opposite edges (x=o,a say). The deflection of the plate is expressed as a single sine series

$$w(x,y) = \sum_{m=1}^{\infty} Y_m \sin \frac{m\pi x}{a} \qquad (2.26)$$

where Y_m is an unknown function of y only. The series satisfies the boundary conditions at the simply supported edges. The unknown function Y_m is determined subject to satisfying the governing differential equation and the boundary conditions at the other two edges. If the solution is taken in the form

$$w = w_H + w_P$$

where w_H is the solution to the homogeneous differential equation $\nabla^4 w = o$ and w_p is the particular solution of equation (2.19), the series (2.26) can be taken to represent w_H. Substitution into $\nabla^4 w = o$ gives a 4th. order ordinary differential equation, in Y_m, whose general solution is easily obtained by standard methods [26]. The boundary conditions provide the means of determining the constants in the general solution. The particular solution can be determined easily only if the applied load is the same on all sections perpendicular to the simply supported edges (i.e. $p=p(x)$). The assumption is then made that the component w_p of the deflection is independent of y. This assumption reduces the governing differential equation for the plate, (2.13), to that of a strip, i.e.

$$\frac{d^4 w_P}{dx^4} = \frac{p(x)}{D}. \qquad (2.27)$$

This equation can be integrated directly and the constants of integration can be evaluated using the boundary conditions at x=o,a. Alternatively, since w_H is in the form of a series, the solution to equation (2.27) can be obtained by representing w_P and $p(x)$ as a single sine series and proceeding as in the Navier method.

Mansfield [27] suggests the form of the particular integral for a number of loading cases that are functions of y as well as x.

The Navier and the Levy methods are in effect applications in the separation of variables technique for the solution of partial differential equations. In the first, both functions of the variables are of a known form, and in the second only one function is known and the other is established by solution of the resulting ordinary differential equation.

d. Rectangular Plates with One or More Edges Clamped.

Timoshenko [23] introduced a method to deal with rectangular plates with one or more clamped edges. The method involves solving the problem of a plate under lateral load but with all edges simply supported, then superposing the solution for a plate bent by a bending moment applied normal to the edge which is clamped in the original problem. The magnitude of the moment is such that it renders the normal slope produced at the relevant edge by the lateral load, equal to zero.

2.3.2. Approximate Methods.

Rigorous methods for solution of plate problems have been shown to deal only with a limited number of relatively simple cases of plate geometry, loading and boundary conditions. As these variables become more complex, the exact analysis becomes sometimes difficult and mostly impossible. The numerical and approximate methods, then, become the only means for plate stressing.

Variational principles form the basis to a number of methods for the approximate solution of plate problems. The Ritz, Galerkin, Vlasov and Kantorovich methods are some of the more widely known and used variational methods.

a. The Ritz Method.

The Ritz method [4], [26], [27], [24] involves replacing the required deflection function by a set of linearly independent functions - assuming that the required function can be represented by such functions - so that the assumption is made that

$$w(x,y) = \sum_{m=1}^{M} \sum_{n=1}^{M} W_{mn} \varphi_{mn}(x,y) \qquad (2.28)$$

where W_{mn} are unknown constants.

The functions $\varphi_{mn}(x,y)$, which are called co-ordinate functions, must satisfy, at least, the geometric boundary conditions. These functions are generally taken as the product of two functions, i.e.

$$\varphi_{mn}(x,y) = X_m(x) . Y_n(y). \qquad (2.29)$$

Various functions for a number of boundary conditions are suggested by E.H.Mansfield [27] and R.Szilard [4].

If the function (2.28) is substituted into the expression for the potential energy (2.13) the latter will be a function of the unknown constants W_{mn} and the variables x and y. Thus:

$$V = \iint \sum_{m=1}^{M} \sum_{n=1}^{M} F(W_{mn}, x, y)\, dx\, dy \qquad (2.30)$$

Applying the principle of minimum potential energy (section 2.2.1.) implies:

$$\frac{\partial V}{\partial W_{mn}} = \iint \sum_{m=1}^{M} \sum_{n=1}^{M} \frac{\partial}{\partial W_{mn}} \left[F(W_{mn}, x, y) \right] dx\, dy = 0 \quad (2.31)$$

$$m, n = 1, 2, \ldots, M$$

Equation (2.31) yields M^2 simultaneous algebraic equations from which the unknown constants W_{mn} are determined.

It can be shown [24] that for the Ritz method, as $M \to \infty$, V approaches the exact value of the potential energy provided that the set of co-ordinate functions is complete in the energy space [28].

In effect the Ritz method is one whereby successive approximations to the true solution are obtained. Generally, the number of approximations, M, is predetermined because, unless the functions X_m and Y_n (equation 2.29) are orthogonal (Appendix A2.2), the value of the constants W_{mn} depends on M.

Application of the Ritz method is not restricted to plate problems. It can be applied to any boundary value problem for which a functional, such as V, is available.

The accuracy of the Ritz solution for a specific value of M depends on how closely the true function is approximated by the assumed function.

b. The Galerkin Method.

In the Galerkin method [24], once again a set of functions is assumed to represent the deflection of the plate (equation 2.28). However, now φ_{mn} have to satisfy both geometric and natural boundary conditions. The constants W_{mn}

are determined in a different way from that employed in the Ritz method. The plate is assumed to execute a virtual deflection δw. The consequent virtual work done by the applied load will be $\iint p \, \delta w \, dx \, dy$. Now using the differential equation (2.19) this virtual work can also be written as $\iint D\nabla^4 w \, \delta w \, dx \, dy$. Therefore:

$$\iint p \;\delta w \, dx \, dy = \iint D\nabla^4 w \;\delta w \, dx \, dy$$

$$\text{or} \qquad (D\nabla^4 w - p) \;\delta w \, dx \, dy = 0 \qquad (2.32)$$

Equation (2.32) was, in fact, an intermediate result when the variational formulation of the plate problem was carried out (equation 2.15).

Strictly speaking equation (2.32) is only valid if w is the exact solution to the differential equation. For approximate solutions the validity of the equation is maintained if a term by term variation of deflection is considered [4].

Using the assumed functions, the virtual deflection will be

$$\delta w = \sum \sum \delta w_{mn} \;\varphi_{mn}\,(x,y) \qquad (2.33)$$

Substituting equation (2.33) into (2.32) and remembering that the virtual deflection is arbitrary, the following system of equations is obtained:

$$(\nabla^4 w - p/D)\;\varphi_{mn} \, dx \, dy = 0 \quad (m,n = 1,2,\ldots M) \qquad (2.34)$$

where the operator ∇^4 acts on the deflection functions as a whole and the functions φ_{mn} are considered for each value of m and n individually.

Substitution of the assumed deflection functions (2.28) into equation (2.34) yields a set of simultaneous algebraic equations which, when solved, would yield the required constants W_{mn} $(m,n = 1,2,...M)$. In effect, the equality in equation (2.32) is forced by adjusting the arbitrary constants W_{mn}.

The reason for the requirement that the assumed deflection pattern must satisfy both the geometric and natural boundary conditions in the Galerkin method, whereas satisfaction of the geometric boundary conditions is sufficient for the Ritz method, is apparent from equation (2.15). In the Ritz method the assumed deflection is substituted into the potential energy which is then minimized. Consequently the boundary conditions, as given by expressions (b) through (f) equation (2.16), are satisfied implicitly if only the geometric boundary conditions are satisfied. In the Galerkin method, on the other hand, only the first term of equation (2.15) is employed. The remaining terms of the equation, i.e. those relating to the boundary conditions, are satisfied only if both the geometric and natural boundary conditions are satisfied.

As a general method for the solution of boundary value problems, Galerkin's method has the advantage over that of Ritz in that it does not require the availability of a functional such as V (equation 2.30). However, for problems in the theory of elasticity it can be shown that the coefficients obtained from a Galerkin solution are identical to those obtained from the Ritz method for the same set of co-ordinate functions [24]. Nevertheless, the set of algebraic simultaneous equations in W_{mn} are obtained more quickly from Galerkin's method [24].

c. Kantorovich Method.

A major drawback in the Ritz and Galerkin methods is their dependence, for accuracy, on the choice of co-ordinate functions. An alternative process which offers a method less dependant on the choice of functions was developed by Kantorovich [24]. The partial generalisation is, however, achieved at the expense of labour.

Although the derivation of the Kantorovich method is based on the functional (such as V) rather than on virtual displacement, from the resulting equations the method may be considered as a generalisation of Galerkin's method in, basically, the same way that Levy generalises Navier's method. The deflection is assumed to be in the form of equations (2.28) and (2.29). However, now only one of the functions, say Y_n, is chosen such that it satisfies the boundary conditions at two opposing edges. The other function is obtained by solving the ordinary differential equation which arises from an analysis similar to that in the Galerkin method. The constants that arise from the solution are evaluated by inserting the geometric and natural boundary conditions.

The approximate methods summarised above are based on choosing a set of functions which approximates part or the whole of the solution. They reduce the solution of the problem to the solution of simultaneous algebraic equations. Although these methods can be cumbersome and laborious they do, nevertheless, provide a useful tool for the solution of some plate problems when computers are not available.

2.3.3. Numerical Methods.

These are particular approaches to the approximate methods. They differ from those mentioned in the preceeding section in that the problem is examined for a discrete number of points on the plate rather than for the continuum.

a. The Finite Differences Method.

The approximation in this method [4] pertains to replacing the derivatives in the governing differential equation of the problem and its boundary conditions by their difference equivalent for a number of chosen points, called nodes, located at the joints of the finite difference mesh.

The central difference equivalent of a derivative of a function f(x) at a point is given by

$$f_i' \approx \triangle f_i = \frac{f_{i+1} - f_{i-1}}{2h}$$

where $\triangle$ is the difference operator corresponding to D in differentiation. f_{i+1} and f_{i-1} are the values of the function at points $i+1$ and $i-1$, a small distance, h, to the right and left of point i (Fig.2.4).

Fig.(2.4).

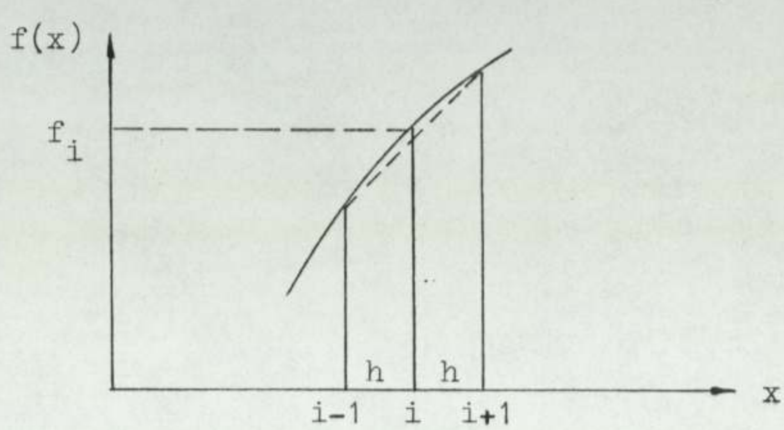

Replacing derivatives by differences in this way means replacing the slope of the tangent at point i by the slope of the chord joining points i+1 and i-1.

Higher differences are used to replace higher derivatives. Partial difference operators are obtained on the same basis as partial derivatives, i.e. by operating on each variable in turn keeping the others constant each time.

The difference equation equivalent to the partial differential equation of the plate problem is given by:

$$\nabla^4 w \approx \frac{1}{h^4}\Big\{20w_{i,j} - 8(w_{i+1,j} + w_{i-1,j} + w_{i,j+1} + w_{i,j-1}) + 2(w_{i+1,j+1} + w_{i+1,j-1} + w_{i-1,j+1} + w_{i-1,j-1}) + w_{i,j+2} + w_{i,j-2} + w_{i+2,j} + w_{i-2,j}\Big\} = p_{i,j}/D \qquad (2.35)$$

Equation (2.35) assumes that the distance between the nodes is the same, h, in both directions. $p_{i,j}$ is the applied pressure at node i,j.

To facilitate the finite difference analysis, a pattern is usually drawn showing the factor by which the value of the independent variable, which is unknown, is multiplied at each relevant node of the dependent variables' mesh. The finite difference pattern for the plate problem would be as shown in fig.(2.5).

The finite difference analysis starts with the division of the plate into a mesh. Generally, a square mesh is used but in some cases other types, such as tringular, hexagonal or quadrilateral mesh, may be preferable. The finite difference equation for these types of mesh [5] will, however, be different from equation (2.35).

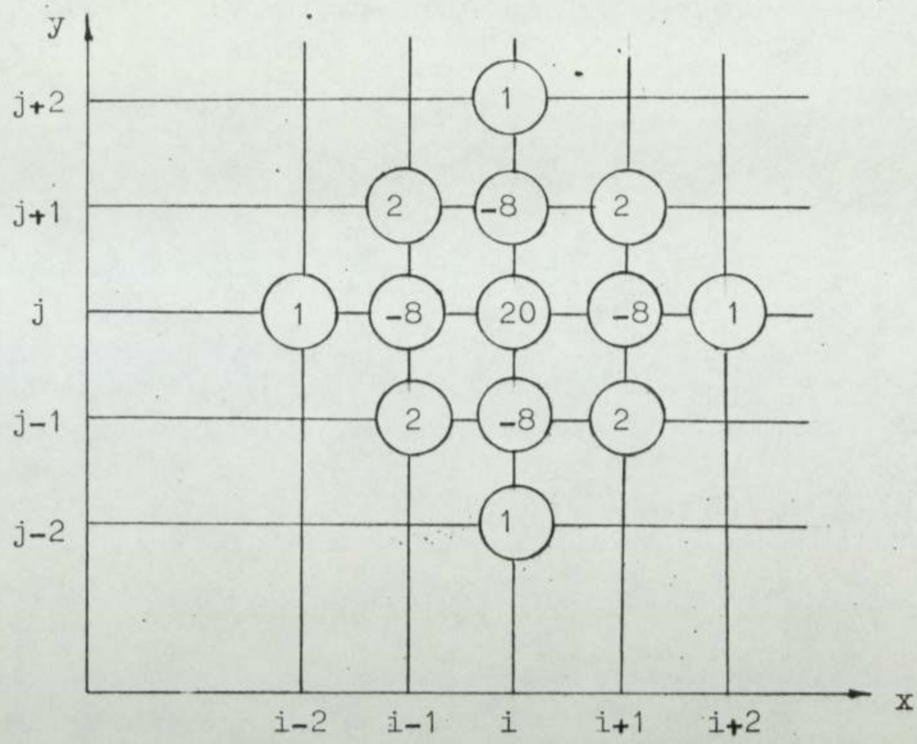

Fig.(2.5).

The appropriate finite difference equation is applied to each node in turn. Fictitious nodes may have to be introduced outside the boundary of the plate, but the deflection at these nodes is expressed in terms of the deflection of the interior nodes via the boundary conditions. The partial differential equations representing the boundary conditions are also written in finite difference form. The system of similtaneous algebraic equations can, then, be solved to give the unknown nodal displacements.

The finite difference method is computer-programmable, but in the absence of a computer, relatively simple cases can be solved by hand. The most laborious part of the analysis is the solution of the equation. For this purpose the Relaxation Method [5] for the solution of linear equations is particularly useful. The relaxation method is one whereby an initial guess $\{x^0\}$ is made at the solution vector of the system of equations

$$[A]\{x\} - \{B\} = 0 \qquad (2.36)$$

If $\{x^0\} \neq \{x\}$ then there will be a residual when $\{x^0\}$ is substituted into (2.36). This residual will be given by:

$$\{R\} = [A]\{x^0\} - \{B\}$$

Increments are added to the initial guess and to subsequent approximations until the residuals become negligible.

The relaxation method, when applied to a finite difference analysis, is simplified by the fact that the changes in the values of the approximation at each node, due to an incremental increase (or decrease) in one of the nodal values, are known because these changes follow a pattern identical to the finite difference pattern. Detailed description of the application of the relaxation method to finite difference analysis is given by Salvadori and Baron [5].

Another method for the solution of the finite difference equations is an experimental one. It is the electrical resistance network method which was developed by S.C. Redshaw [6], [29]. By using the expressions for the bending moments, the governing differential equation of the plate may be reduced to two second order partial differential equations, viz.

$$\frac{\partial^2 M}{\partial x^2} + \frac{\partial^2 M}{\partial y^2} = -\,{}^{p}/_{D}$$

$$\text{and} \quad \frac{\partial^2 w}{\partial x^2} + \frac{\partial^2 w}{\partial y^2} = -M \qquad (2.37)$$

where M is defined as $\dfrac{(M_x + M_y)}{D(1+\nu)}$

The finite difference form of equations (2.37) is analogous to the equations relating the electrical potentials to the resistances in an electrical network of a specific nature. Details of the network, the derivation of the equations and the analogy are given in reference [29].

C.T. Harnden and K.R. Rushton [30] applied the electrical resistance method to the analysis of plates with variable thickness. The governing differential equation of such a plate is given by:

$$\nabla^2(D\nabla^2 w) - \left\{(1-\nu)\left[\frac{\partial^2 D}{\partial x^2}\frac{\partial^2 w}{\partial y^2} - 2\frac{\partial^2 D}{\partial x\partial y}\frac{\partial^2 w}{\partial x\partial y} + \frac{\partial^2 D}{\partial y^2}\frac{\partial^2 w}{\partial x^2}\right]\right\} = p$$

Taking the term in the brackets $\{\ \}$ to the right-hand side, this term together with the applied load are assumed to make up a new "external" load which, in the first instance, is unknown. Employing the form (2.37) of the equation and using the electrical network method, the problem can be solved by an iterative process in which the term $\{\ \}$ is, initially, assumed to be zero, then using the solution, the term $\{\ \}$ is evaluated and the applied load is modified to include this term. The problem is, then, re-solved and the process repeated until the difference between two successive solutions is acceptably small.

The method of electrical resistance network has been applied, successfully, to other problems such as that of thermal stresses in thick-walled tubes by T.H. Richards [31].

(b) Hrenikoff's Method.

In 1940, Hrenikoff [7] developed a method for the structural analysis of elastic continuua, which approximates the continuum by a definite, though not unique, pattern of beams and bars assembled in a framework. The elastic properties of the members in the framework are obtained by consideration of the deformations in the framework which are equivalent to those in the original continuum. In a modified form of the method [32], the properties of the members for the plate bending problem are obtained by considering a rectangular cell with diagonal members and equating the rotations at the nodes of the cell with those of a plate element of the same dimensions when both are subjected to statically equivalent moments and torques. Once these properties are obtained the analysis then follows the standard matrix-displacement method for the solution of the equivalent framework.

Without the aid of a computer this method can be quite laborious, particularly in the case of complex problems. If a computer is available then the finite element method will prove to be more powerful and versatile.

(c) The Finite Element Method.

This method is probably the most significant development in structural analysis in recent years. With electronic computers continually becoming more powerful the finite element method rapidly gains more popularity amongst engineers and already it is being used for the analysis of problems other than those relating to structural mechanics [10].

The method, which will be described in more detail in the next chapter, basically involves replacing the actual continuum by a structure which consists of a discrete number of elements connected at their nodal points. A function is then chosen to represent the state of displacements and/or stresses within the element. The procedure which then follows resembles that of the Ritz method. The difference being that the Ritz process is applied to the structure as a whole, whereas in the finite element method the analysis is carried out on each finite element in turn, then the overall problem is examined from the point of view of a structure comprising the assemblage of these elements.

An important feature of the finite element method is its ability to deal with arbitrary shape regions and arbitrary loading and boundary conditions. However, the number of elements into which the overall structure must be divided, for a given accuracy, depends to a large extent on the complexity of the geometry, boundary and loading conditions and as the problem becomes more complex so the number of required elements must grow. The storage requirement demanded of the computer, the amount of work necessary for the preparation of the data and the computer time required for processing the programme, are linked to the size and complexity of the problem. Even with today's high-speed computers the cost of processing computer programmes can be considerable. It is for this reason that modifications to the finite element method are sought in order to deal with particular types of problems that possess certain geometric conditions which, when taken into account, can reduce the amount of work and cost necessary to analyse the problem. One such modification is the semi-analytic method of analysis.

(d) The Finite Strip Method.

In the semi-analytic method of analysis the variation of displacements along one direction of the continuum is described by a set of continuous functions that satisfy the boundary conditions at the extreme points of the body in that direction, whilst along the remaining directions the continuum is divided into elements and a displacement function is employed to describe the displacements within the elements in these directions.

This method of analysis was applied to axi-symmetric solids [20], [21], [33]. In this case the displacements are assumed to vary in the circumferential direction according to the form of a Fourier series. There are no boundary conditions to be satisfied at the extreme points, save for the compatibility of the functions at $\theta = 0$ and $\theta = 2\pi$ which is satisfied by the trigonometric functions of the Fourier series.

Y.K. Cheung applied the semi-analytic approach to the problems of plates with two opposite edges simply supported [1], and to the problems of elastic slabs [22] and to the problems of folded plate structures [34]. He named the method "The Finite Strip Method".

2.3.4 Concluding Remarks

In this section various methods for the solution of plate bending problems were discussed. It was found that analytical solution of the plate problem is very difficult and laborious except for cases of relatively simple geometry, boundary and loading conditions. For more complex problems, approximate methods are necessary. Under this category, the methods of Ritz, Galerkin and Kantorovich were outlined. All these methods depend, for accuracy of solution, on how closely the assumed deflection function approximates the actual deflection surface.

Finally, numerical methods were discussed as the means for solving bending problems of plates of arbitrary geometry, boundary and loading conditions. A very important feature that these methods possess is that they are computer programmable.

The most powerful and most versatile of these methods is the finite element method. The use of this method requires the availability of a computer. Once a computer programme is available the critical factors in the efficiency of the analysis, for a given degree of accuracy, are the amount of data required for input into the computer and the cost of processing the programme. The importance of the first factor is twofold. First there is the amount of time spent by the programme user to prepare the data, and secondly the vulnerability to human errors increases with an increase in the size of the data to be prepared.

Finally a method for the analysis of rectangular plates was mentioned, in which the deflection in one direction is expressed as an analytic function satisfying the boundary conditions at the extreme points in this direction. This results in a reduction in the required amount of data and the computer time necessary for processing the programme. The method, as applied to rectangular plates, was introduced by Y.K. Cheung who called it "The Finite Strip Method", and applied it to a limited number of cases of boundary conditions and thickness variation. It was the aim of the project described in this thesis to extend the application of the method to a much wider range of boundary and loading conditions and rigidity variation and to make a study of its numerical stability, convergence and accuracy.

CHAPTER 3

CHAPTER THREE

THE FINITE ELEMENT METHOD.

3.1. Introduction to the Displacement Approach.

The use of the Finite Element Method for the solution of problems in elastic continuua consists of the following steps:

1. The continuum is divided by imaginary lines and thus replaced by a structure composed of an assemblage of a discrete number of elements called "finite elements". The mesh of lines intersect at discrete points called "nodes". The finite elements may, in general, be of triangular, rectangular or quadrilateral shape in the case of two dimensional problems. For three dimensional problems, tetrahedra, hexahedra or rectangular prisms are used. In some cases, to improve accuracy and to reduce the required number of elements, curved boundary elements have been used
2. A suitable function is chosen to describe the state of displacement within each element in terms of generalized co-ordinates. The basis for choosing a displacement function will be given later.
3. By substituting the co-ordinates of the nodes into the displacement function and solving for the generalized co-ordinates in terms of nodal displacements then substituting back into the displacement function, this function will be in terms of the nodal displacements and will then be called the "shape function". It will

be noted here that in order to be able to obtain the shape function in this way, the number of generalized co-ordinates must be equal to the number of nodes per element, multiplied by the number of displacement components per node. It is possible to formulate the shape function directly by using interpolation functions

4. Using well-known relationships in solid mechanics, the strains and stresses, (curvatures and moments in the case of plate flexure), and hence, the total potential energy of the element may be obtained in terms of the nodal displacements.
5. Minimizing the total potential energy of the element with respect to the nodal displacements, an equilibrium equation for the element arises, from which an element stiffness matrix and an element force vector are recognised.
6. The equilibrium equations for the overall structure are, then, stated by adding contributions of element stiffnesses and loads to the appropriate locations in the overall stiffness matrix and overall load vector.
7. The geometric boundary conditions are imposed.
8. The equations are solved yielding the unknown nodal displacements.

Stated mathematically, the above procedure can be summarized as follows:

Let the displacements within the element be given by:

$$\{u\} = [s]\{\alpha\} \qquad (3.1.)$$

where $\{u\}$ is a vector which contains all possible displacements, within the element, in the direction of the co-ordinate axes. $\{s\}$ are functions of position and $\{\alpha\}$ are the generalised co-ordinates.

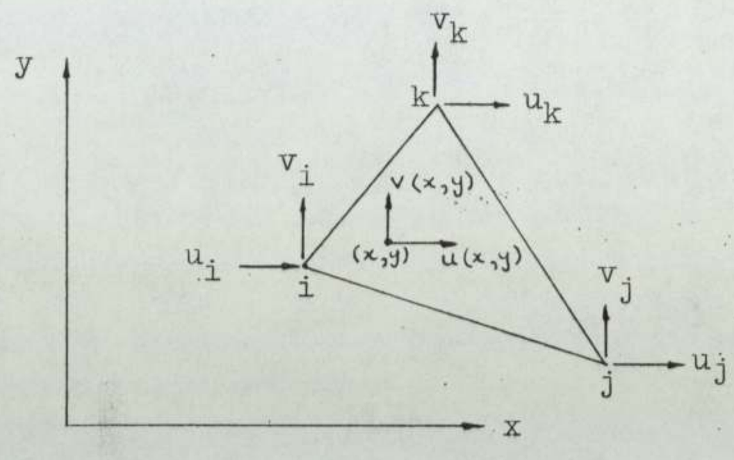

Fig.(3.1) A triangular element in a plane stress or plane strain region.

Substituting the values of x and y, at each node, into equation (3.1), the nodal displacements will be:

$$\{\delta\}_e = [A]\{\alpha\} \tag{3.2}$$

In the case of the element in fig.(3.1), the nodal displacements are:

$$\{\delta\}_e = \left[u_i \quad v_i \quad u_j \quad v_j \quad u_k \quad v_k\right]^T$$

From equations (3.1) and (3.2), the element displacements will be:

$$\{u\} = [s]\,[A]^{-1}\{\delta\}_e$$

$$= [N]\{\delta\}_e \tag{3.3}$$

where $[N] = [s][A]^{-1}$

Since the matrix $[A]$ has to be square so that it may be inverted, it follows from equation (3.2) that $\{\alpha\}$ must be of the same order as $\{\delta\}_e$ as stated in section (3.1), item (3).

By appropriate differentiation of the displacements, the strains (curvatures, for plate bending) can be determined anywhere within the element. Thus:

$$\{\varepsilon\} = [B]\{\delta\}_e \qquad (3.4)$$

where $\{\varepsilon\}$ is the strains vector and $[B]$ contains appropriate derivatives of $[N]$.

Using the stress-strain relationship, the stresses (moments) are obtained from equation (3.4). If no initial stresses or strains are assumed then,

$$\{\sigma\} = [D]\{\varepsilon\} \qquad (3.5)$$

where $\{\sigma\}$ is the stress vector and $[D]$ is the elasticity matrix. Substituting for $\{\varepsilon\}$ from (3.4) into (3.5), the stress vector becomes:

$$\{\sigma\} = [D]\,[B]\{\delta\}_e \qquad (3.6)$$

The strain energy density for a linear elastic system is given by:

$$dU = \tfrac{1}{2}\{\varepsilon\}^T\{\sigma\}\,dv \qquad (3.7)$$

where v is the volume of the elastic body.

The total potential energy for the element will, therefore, be given by:

$$V_e = \tfrac{1}{2}\iiint_{vol.}\{\varepsilon\}^T\{\sigma\}\,dvol - \iiint_{vol.}\{u\}^T\{\overline{X}\}\,dvol$$

$$- \iint_{S_T}\{u\}^T\{\overline{T}\}\,dS_T \qquad (3.8)$$

where dvol is the volume of the element and s_T is the part of the surface over which tractions are specified. The second integral represents the work done by the body forces and the third integral represents the work done by surface tractions.

Now, substituting for $\{\varepsilon\}$ from equation (3.4), for $\{\sigma\}$ from equation (3.6) and for $\{u\}$ from equation (3.3), the potential energy of the element will be

$$V_e = \tfrac{1}{2} \iiint_{vol.} \{\delta\}_e^T [B]^T [D][B]\{\delta\}_e \, dvol$$

$$- \iiint_{vol.} \{\delta\}_e^T [N]^T \{\bar{X}\} \, dvol$$

$$- \iint_{s_T} \{\delta\}_e^T [N]^T \{\bar{T}\} \, ds_T \qquad (3.9)$$

Applying the principle of minimum potential energy to the element implies $\delta V_e = 0$.

Therefore,

$$\delta V_e = \delta \{\delta\}_e^T \Big(\iiint_{vol.} [B]^T [D][B] dvol \, \{\delta\}_e - \iiint_{vol.} [N]^T \{\bar{X}\} dvol$$

$$- \iint_{s_T} [N]^T \{\bar{T}\} \, ds_T \Big) = 0 \qquad (3.10)$$

Since $\delta\{\delta\}_e^T$ is arbitrary, then:

$$\iiint_{vol.} [B]^T [D][B] dvol \, \{\delta\}_e - \iiint_{vol.} [N]^T \{\bar{X}\} dvol$$

$$- \iint_{s_T} [N]^T \{\bar{T}\} ds_T = 0 \qquad (3.11)$$

Comparing equation (3.11) with the characteristic relationship of elastic bodies, i.e. $k\delta = f$, where k, δ and f are the stiffness, displacement and force parameters for the elastic body, the element stiffness matrix will be given by

$$[k]_e = \iiint_{vol} [B]^T [D][B] \, dvol \qquad (3.12)$$

and the load vector by

$$\{f\}_e = \iiint_{vol} [N]^T \{\overline{X}\} \, dvol + \iint_{s_T} [N]^T \{\overline{T}\} \, ds_T \qquad (3.13)$$

Substitution of equations (3.12) and (3.13) into equation (3.9) gives an expression for the potential energy of the element in terms of the element stiffness matrix and element load vector, i.e.

$$V_e = \tfrac{1}{2} \{\delta\}_e^T [k]_e \{\delta\}_e - \{\delta\}_e^T \{f\}_e \qquad (3.14)$$

Equation (3.14) is the typical form of the potential energy of a finite degree of freedom (discrete) system.

When the stiffness matrix and force vector for the overall structure are assembled according to the rules of assembly that will be given later, an equilibrium equation for the overall problem will be obtained. This will be of the form

$$[K]\{\delta\} = \{F\} \qquad (3.15)$$

After inserting the boundary conditions into equation (3.15), they can be solved to yield the unknown nodal displacements $\{\delta\}$. The solution to the problem then follows from equations (3.3) and (3.6).

3.2. Convergence Requirements - Bases for Choosing a Displacement Function.

Dividing a continuum into a discrete number of elements implies the reduction of the infinite number of degrees of freedom to a finite number. As the subdivisions are made smaller with a consequent increase in the number of degrees of freedom, the discretized structure approaches the original continuum. It does not, however, follow that the solution approaches the exact solution to the problem unless the function chosen to represent the displacements within the elements satisfies certain convergence requirements. Some of these requirements are essential, whilst others only accelerate convergence. These requirements are:

1. The displacement function should represent the actual displacement pattern as closely as possible.
2. The number of generalised co-ordinates in the displacement function must be equal to the total number of degrees of freedom of the element. This is necessary for the eventual solution of the equations.
3. The function must be continuous within the element. Also, if the highest derivative in the energy functional is the n^{th}, then the displacements and, preferably, their derivatives to an order $\geqslant(n-1)$ must be compatible along common boundaries of the elements.

The necessity for the first part of this requirement is obvious. For the second part, a mathematical justification can be presented thus: If a small transition zone is assumed at the inter-element boundary and if the $(n-1)$ derivative is continuous whilst the n^{th} derivative has a finite discontinuity at this zone, then, on evaluating the potential energy of the structure as the sum of the potential energy of all the elements plus the potential energy at the transition zones, the contribution of the latter will be zero because the actual volume of the transition zone is zero. If, on the other hand, the (n-1) derivative has a finite discontinuity then the n^{th} derivative will tend to infinity at the discontinuity. Consequently, the contribution of potential energy of the transition zone will be unknown (an infinite potential energy density multiplied by zero volume).

4. The displacement function and some of its derivatives must include constant terms. The necessity for this requirement becomes clear if the element size is imagined to be getting smaller and smaller. As the size becomes infinitesimal, so the displacements and strains (curvatures, in the case of plate bending) approach constant values.

   The constant terms in the displacement function and its derivatives are, in fact, the rigid body modes. Hence, this requirement states, implicitly, that the displacement function must include the rigid body modes.

Finite Element formulations which satisfy the third requirement above are called "conforming" and those which satisfy the fourth requirement are called "complete".

In some cases, such as plate bending problems, it is difficult to establish displacement functions that satisfy full compatibility of slopes along common boundaries of elements. However, functions violating this requirement, i.e. non-conforming functions, whilst maintaining continuity of deflection, and satisfying the completeness requirement, have been used with satisfactorily converging results [35]. It is not possible in these cases to prove convergence.

3.3. The Semi-Analytical Approach.

In the most general cases of finite element method analysis, the continuum has to be divided into elements in three directions (or four, if the time dimension is included). In these cases, where the total number of degrees of freedom (hence unknowns) is large, the major drawback in the finite element method is highlighted. The cost of solution and the need for larger, more capable, computers increases disproportionately with an increased number of degrees of freedom. As in analytical methods of analysis, it is often possible to reduce a three dimensional problem into a two dimensional one simply by assuming that the stress or strain in one direction is negligible as in the plane stress or plane strain cases.

Another , entirely different, method of reducing the number of dimensions is called the semi-analytical method. In this method, the displacements, strains and stresses in one direction are assumed to vary according to a known analytical function which satisfies the boundary conditions at the extreme points of this direction. It follows, then, that the continuum need not be divided into elements in the direction along which the state of displacement is described by the analytical function.

In the finite element method, displacement approach, the displacements within the elements are given by an equation in the form

$$\{u\} = [N]\{\delta\}_e$$

where $[N] = [N(x,y,z)]$

If a function, f(z), is chosen to represent the displacement along the whole of the length in the z direction and if this function satisfies the boundary conditions at the extreme points, then the element may be chosen to cover the whole of the length in the z direction (Fig.3.2). The displacement function would then be of the form

$$\{u\} = [N(x,y)f(z)]\{\delta\}_e.$$

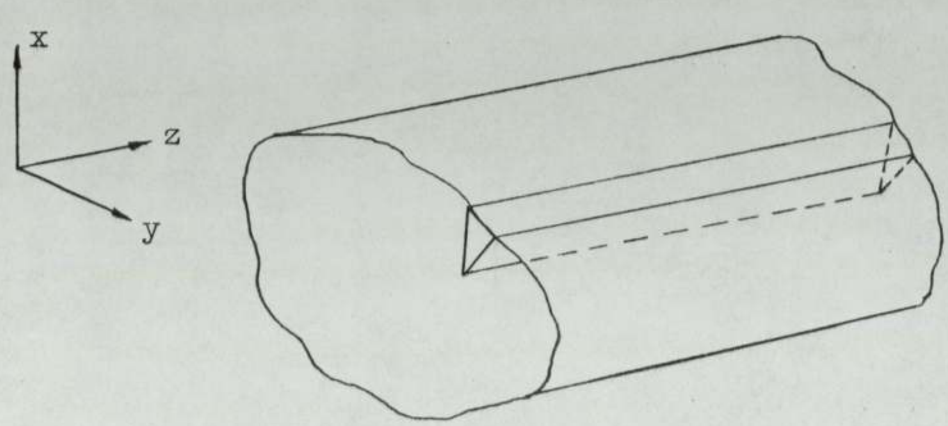

Fig.(3.2)

$\{\delta\}_e$ are, now, nodal displacement parameters rather then nodal displacements, because the "nodes" in this case are lines and not points.

elements of cross sections similar to those used in plane stress or plane strain problems. The elements are interconnected at nodal circles (fig.3.3). The displacements in all three directions are assumed to vary with θ according to the form of a Fourier series. In the r and z directions the variation is often assumed to be linear.

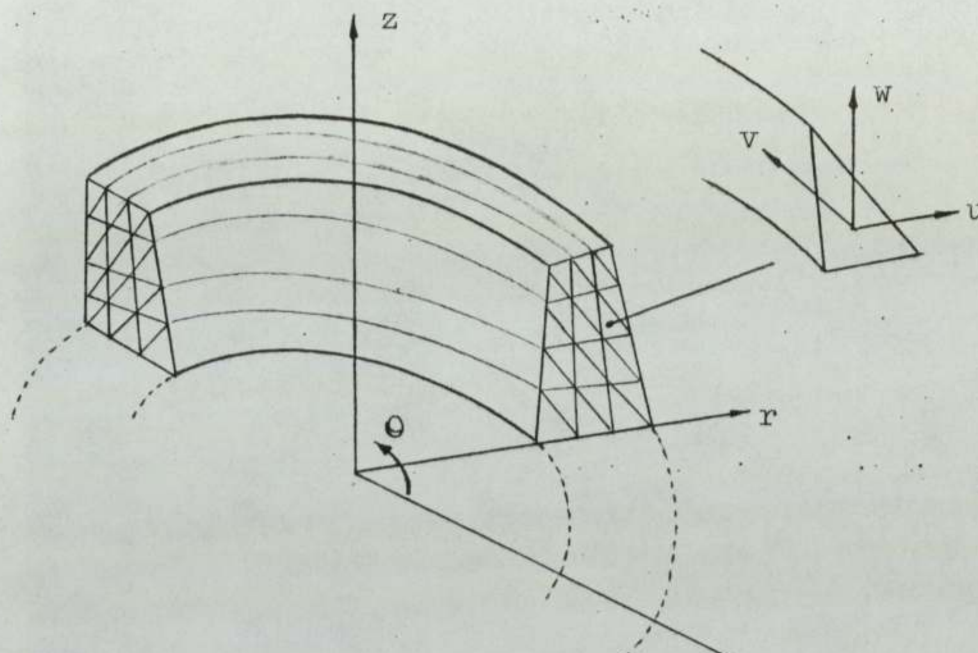

Fig.(3.3).

The displacements will, then, be of the form:

$$u = \sum_m (b_{1m} + b_{2m}\, r + b_{3m}\, z)\cos m\theta + \sum_m (b_{4m} + b_{5m}\, r + b_{6m}\, z)\sin m\theta$$

If the problem is symmetric about a plane containing the r and z axes, then if θ is measured from this plane, use may be made of the symmetry by neglecting the sin $m\theta$ terms for u and v and the cos $m\theta$ terms for w.

Generally, no one function is sufficient to describe the displacement in the z direction. Instead, a system of linearly independent functions is chosen so that a closer approximation to the true displacement is obtained as more functions are taken. This notion is identical to the Ritz method for the solution of boundary value problems (section 2.3.2a).

The number of functions taken to represent the displacements in the z direction may be thought of as a number of "analytic divisions" of the element in this direction. Thus the continuum is divided into a number of "analytical elements" in one direction and finite elements in the other directions.

The displacement functions may now be written as

$$\{u\} = \sum_{m=1}^{M} [N(x,y)\, \varphi_m(z)]\, \{\delta\}_e$$

where M represents the number of analytic functions $\varphi_m(z)$. Both $N(x,y)$ and $\varphi_m(z)$ have to satisfy the requirements laid down in section (3.2). In addition, φ_m has to satisfy the boundary conditions at the ends. Consequently, for φ_m the requirement that the function should include rigid body modes will be irrelevant except in the cases of free - free and simply supported - free end conditions when rigid body deflection and rigid body rotation must be present in the first case, and rigid body rotation in the second.

The semi-analytic approach to the finite element method can be applied in axisymmetric solids with non-symmetric loading [20]. The solid is divided into axisymmetric

In the case of axisymmetric material properties, the orthogonality property (appendix A2.2) can be employed to uncouple the modes. On the other hand, if the material properties vary in the circumferential direction, then the Fourier expansion can be employed to represent this variation [21]. However, it will not be possible to apply the orthogonality property in this case.

The semi-analytic treatment of the plate bending problem is given in detail in the next chapter.

CHAPTER 4

CHAPTER FOUR

THE SEMI-ANALYTIC TREATMENT OF THE PLATE BENDING PROBLEM.

4.1 Introduction.

For the solution of plate bending problems by the finite element method, the plate has to be divided into elements in both of the in-plane directions. At least three nodal parameters per node must prevail in the displacement function (one deflection and two rotations). Using a semi-analytical technique the plate need only be divided into strips, interconnected at nodal lines (Fig.4.1a).

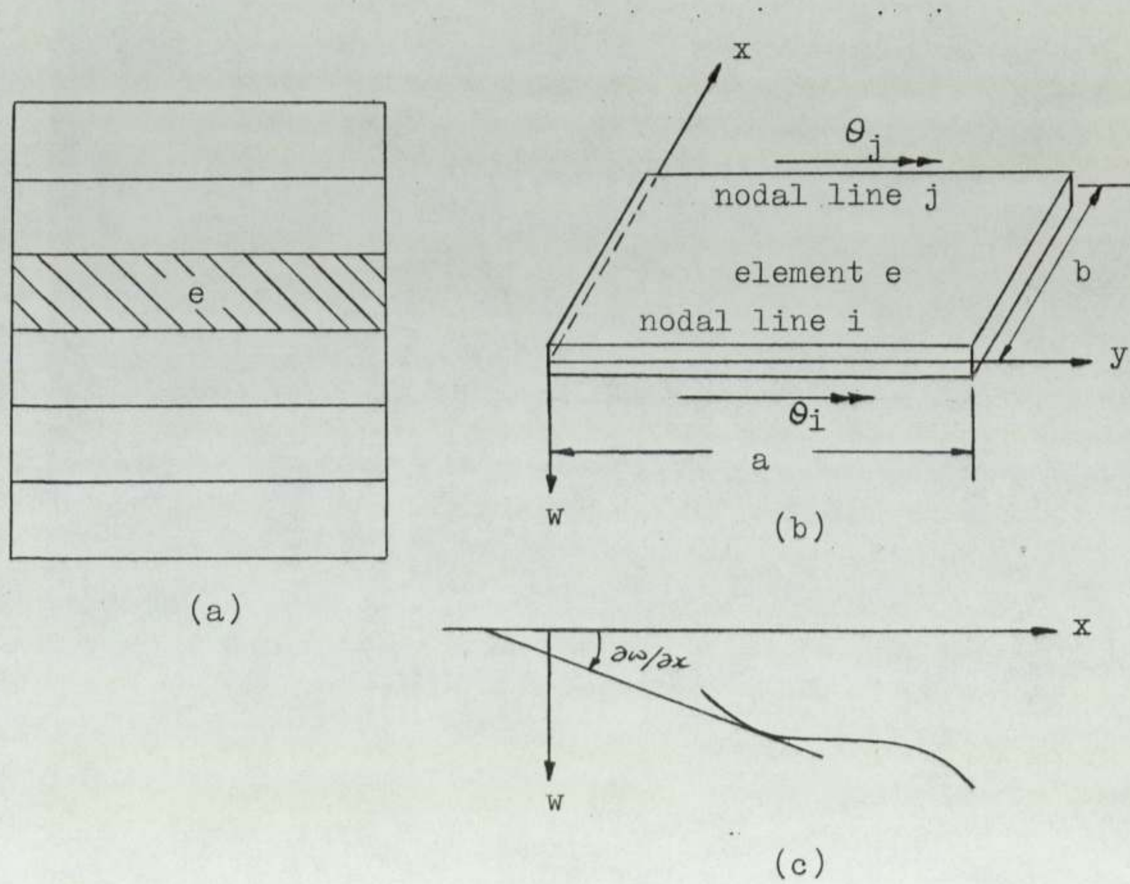

Fig.(4.1)

An analytic function must be chosen to represent the deflection in the "long" direction (y-direction). This function must satisfy pre-chosen boundary conditions at the ends ($y=o$ and $y=a$).

In the x-direction, a polynomial may be used to represent the deflection within the strip. The degree of the polynomial is established from the number of nodes per element (two nodal lines in this case) and the number of displacement parameters per node required to describe the problem fully and to ensure inter-element continuity of deflection and slopes (section 3.1 item 3 and section 3.2, item 3).

Although the deflection of the middle surface completely defines a plate bending problem, the need for the slope normal to the edge of the strip to be uniquely defined in order to ensure inter-element compatibility of slopes, necessitates the specification of a normal slope parameter in the function. Using a cartesian co-ordinate system, this normal slope will be given by:

$$\theta_x = -\frac{\partial w}{\partial x} \qquad \text{Fig. 4.1b and c.}$$

In the y-direction, if a set of continuous functions is employed, then the slope $\theta_y = \frac{\partial w}{\partial y}$ will automatically be continuous anywhere within the strip, including the edges of the strip. Also, if the same number of functions (harmonics or modes) are used for each strip then compatibility of the slope θ_y at common boundaries is assured.

Thus, the nodal parameters which must be specified in the displacement function, to ensure continuity of deflection and slopes across common boundaries, are the deflection amplitude and the normal rotation amplitude.

It will be seen, in section (4.4), that the use of a continuous function in the y-direction also ensures the continuity of the twist term $\frac{\partial^2 w}{\partial x \, \partial y}$ along a nodal line.

4.2 The Displacement Function in the x-Direction.

Since the number of parameters required to describe the problem is four for each strip, one deflection and one rotation per nodal line, then the polynomial representing the variation of w in the x-direction will be cubic. Thus:

$$f(x) = A_1 + A_2 x + A_3 x^2 + A_4 x^3 \tag{4.1}$$

Following the procedure outlined in section (3.1) this function can be written in terms of the nodal parameters. Then:

$$f(x) = \left[\left(1 - \frac{3x^2}{b^2} + \frac{2x^3}{b^3}\right) \quad \left(-x + \frac{2x^2}{b} - \frac{x^3}{b^2}\right) \quad \left(\frac{3x^2}{b^2} - \frac{2x^3}{b^3}\right) \quad \left(\frac{x^2}{b} - \frac{x^3}{b^2}\right) \right] \begin{Bmatrix} w_i \\ \theta_i \\ w_j \\ \theta_j \end{Bmatrix} \tag{4.2}$$

where w_i, θ_i, w_j and θ_j are the deflection and rotation amplitudes on nodal lines i and j. b is the width of the strip.

In a more compact form, the function can be written as:

$$f(x) = [N]\{\delta\}_e \tag{4.3}$$

4.3 The Analytic Function.

In principle, any function, or set of functions, that satisfies the boundary conditions at the ends of the strip, may be employed to represent the variation of w in the y-direction. However, since numerical stability plays an important part in the eventual solution of the equations the right choice of analytic functions is important. Orthogonal functions have been shown to yield a system of equations that is very stable [28]. Such functions are the eigenfunctions of the free vibration of a uniform beam [36]. These functions are known to satisfy the differential equation

$$\frac{d^4Y}{dy^4} = \frac{\mu^4}{a^4} Y \tag{4.4}$$

where μ is a parameter related to the natural frequencies of free vibration, a is the length of the beam.

The solution to equation (4.4) has the form:

$$Y = A \sin\frac{\mu y}{a} + B \cos\frac{\mu y}{a} + C \text{ sh } \frac{\mu y}{a} + D \text{ ch } \frac{\mu y}{a} \tag{4.5}$$

Substitution of the boundary conditions into equation (4.5) gives four equations from which a transcendental equation in μ is obtained. Three of the constants A, B, C and D, are obtained in terms of the fourth. Using the arbitrary nature of these constants, one of them is assigned the value 1 and the rest are evaluated accordingly. Evaluation of these constants and the roots of the transcendental equation for the clamped-clamped case is given in Appendix (2) . The transcendental equation pertinent to a particular set of boundary conditions is called "The Characteristic Equation".

The solution of the characteristic equation gives an infinite set of roots μ_m (m=1,2,...∞). Therefore, the general solution of equation (4.4) will be in the form:

$$Y = \sum_{m=1}^{\infty} (A_m \sin \frac{\mu_m y}{a} + B_m \cos \frac{\mu_m y}{a} + C_m \,\mathrm{sh} \frac{\mu_m y}{a} + D_m \,\mathrm{ch} \frac{\mu_m y}{a}) \qquad (4.6)$$

The constants A_m, B_m, C_m and D_m, the characteristic equations and a number of their roots, for six sets of boundary conditions, are given in table (4.1). Fig.(4.2) shows the shape of the deflection curve along the y-axis for the first three modes of the six sets of boundary conditions.

The deflection anywhere within the strip will now be given by:

$$w = \sum_{m=1}^{M} f_m(x).Y_m(y) \qquad (4.7)$$

where $f_m(x)$ is given by equation (4.2), with the nodal displacement amplitudes $[\, w_i \quad \theta_i \quad w_j \quad \theta_j \,]^T$ replaced by $[\, w_{im} \quad \theta_{im} \quad w_{jm} \quad \theta_{jm} \,]^T$. $Y_m(y)$ is the m^{th} mode of equation (4.6).

An interesting feature of the beam eigenfunctions is that in the cases where the boundary conditions are the same at both ends of the beam, the odd modes are symmetric and the even modes are skew symmetric. This fact is demonstrated in Fig.(4.2). It follows from this , that when the geometry, loading and boundary conditions are symmetric about y=a/2, then the even terms of the deflection function are zero.

$$Y_r = A_r \sin\frac{\mu_r y}{a} + B_r \cos\frac{\mu_r y}{a} + C_r \,\mathrm{sh}\frac{\mu_r y}{a} + D_r \,\mathrm{ch}\frac{\mu_r y}{a}$$

case No.	end conditions	constants				α_r	characteristic equation	first 4 roots of charac. eqn.	general formula $r>4$
		A_r	B_r	C_r	D_r				
1	SS - SS	1	0	0	0	——	$\sin\mu_r = 0$	$\pi, 2\pi, 3\pi, 4\pi$	$r\pi$
2	C - C	1	$-\alpha_r$	-1	α_r	$\dfrac{\sin\mu_r - \mathrm{sh}\,\mu_r}{\cos\mu_r - \mathrm{ch}\,\mu_r}$	$\cos\mu_r \,\mathrm{ch}\,\mu_r = 1$	4.7300, 7.8532, 10.9956, 14.1372	$\dfrac{2r+1}{2}\pi$
3	F - F	1	$-\alpha_r$	1	$-\alpha_r$	$\dfrac{\sin\mu_r - \mathrm{sh}\,\mu_r}{\cos\mu_r - \mathrm{ch}\,\mu_r}$	$\cos\mu_r \,\mathrm{ch}\,\mu_r = 1$	4.7300, 7.8532, 10.9956, 14.1372	$\dfrac{2r+1}{2}\pi$
4	C - F	1	$-\alpha_r$	-1	α_r	$\dfrac{\sin\mu_r + \mathrm{sh}\,\mu_r}{\cos\mu_r + \mathrm{ch}\,\mu_r}$	$\cos\mu_r \,\mathrm{ch}\,\mu_r = -1$	1.8751, 4.6941, 7.8548, 10.9955	$\dfrac{2r-1}{2}\pi$
5	SS - C	1	0	$-\alpha_r$	0	$\dfrac{\sin\mu_r}{\mathrm{sh}\,\mu_r}$	$\tan\mu_r = \tanh\mu_r$	3.9266, 7.0685, 10.2102, 13.3520	$\dfrac{4r+1}{4}\pi$
6	SS - F	1	0	α_r	0	$\dfrac{\sin\mu_r}{\mathrm{sh}\,\mu_r}$	$\tan\mu_r = \tanh\mu_r$	3.9266, 7.0685, 10.2102, 13.3520	$\dfrac{4r+1}{4}\pi$

code for end conditions: SS simply-supported, C clamped, F free

Table (4.1)

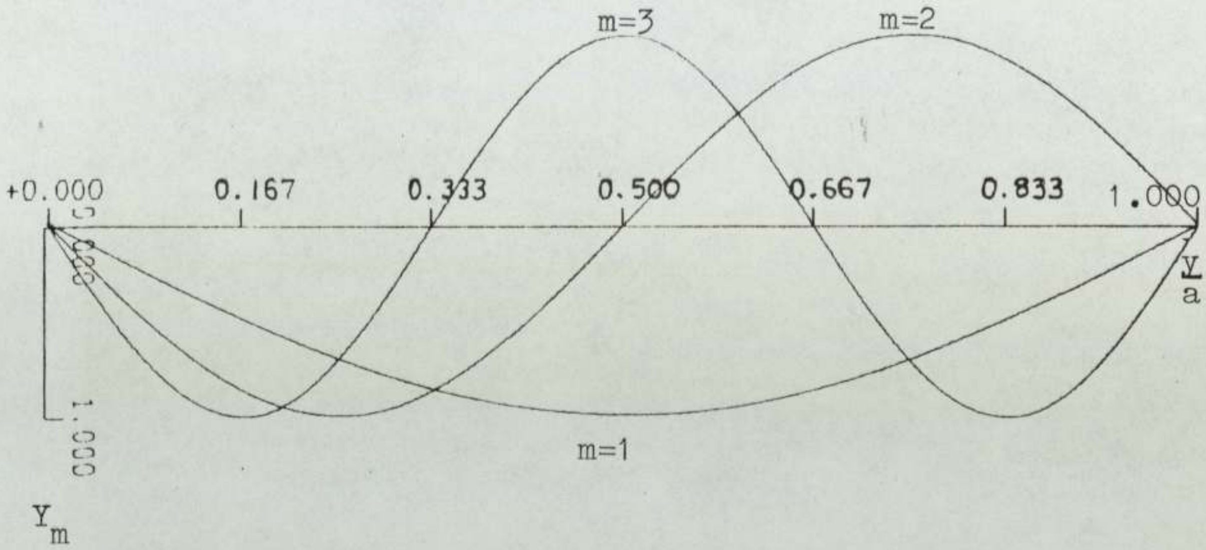

(a) Simply Supported-Simply Supported

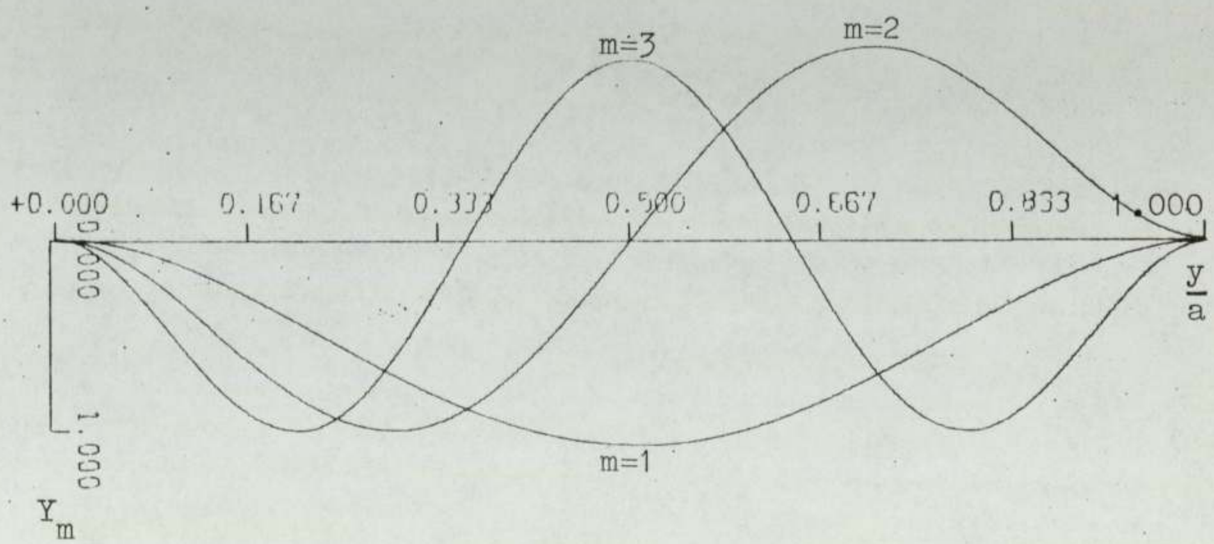

(b) Clamped-Clamped

Fig.(4.2) Shapes of the beam eigenfunctions.

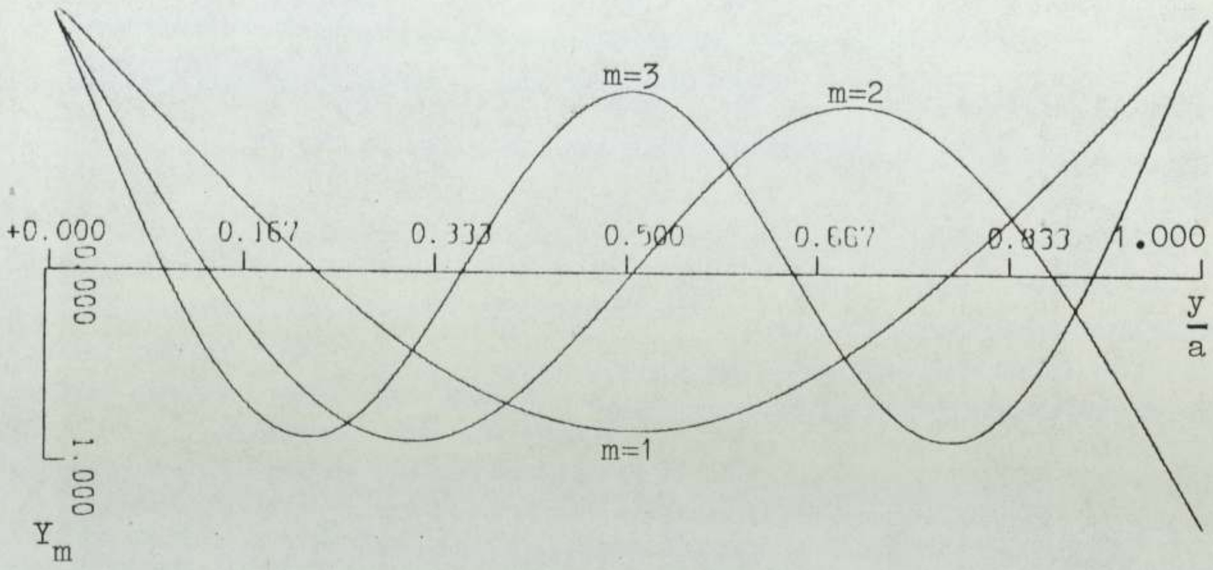

(c) Free-Free

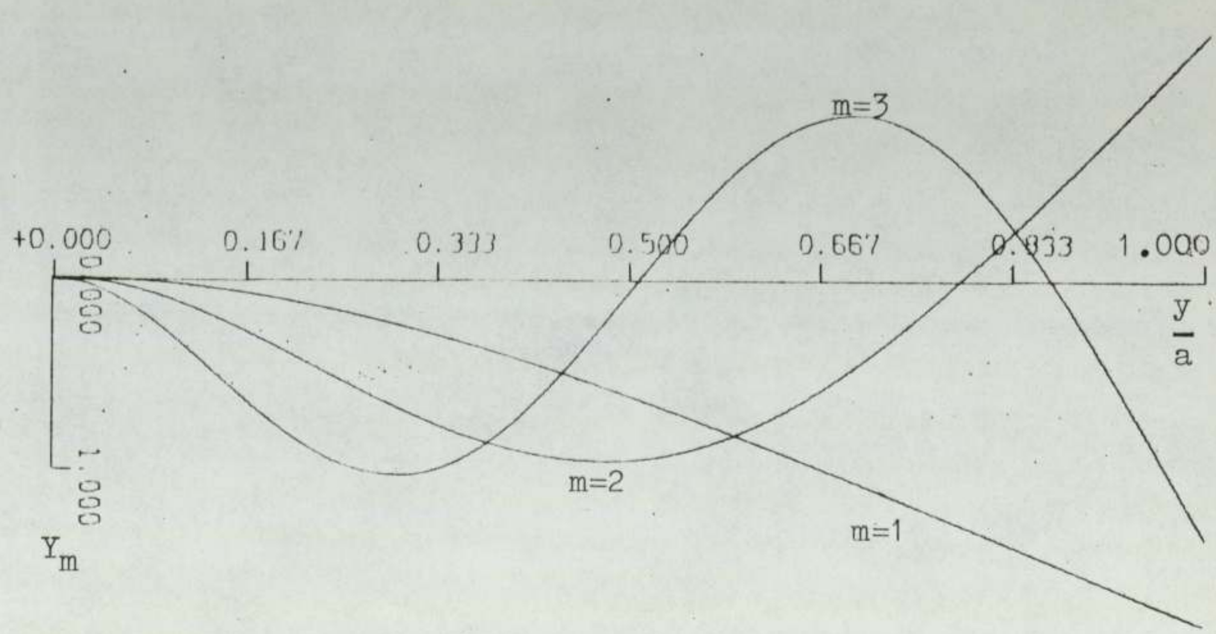

(d) Clamped-Free

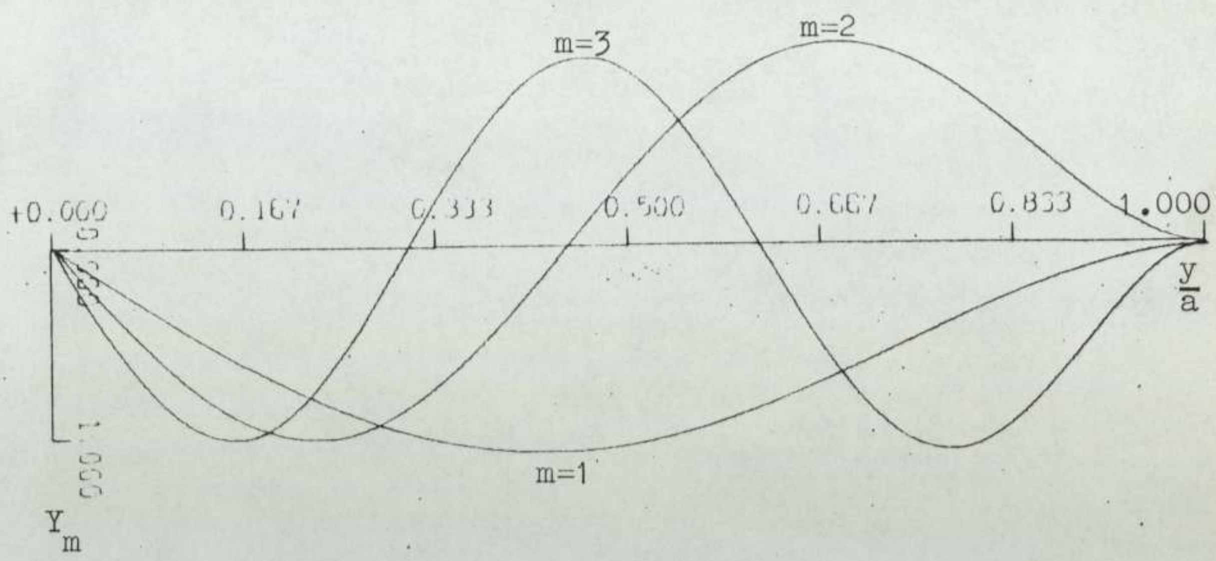

(e) Simply Supported-Clamped

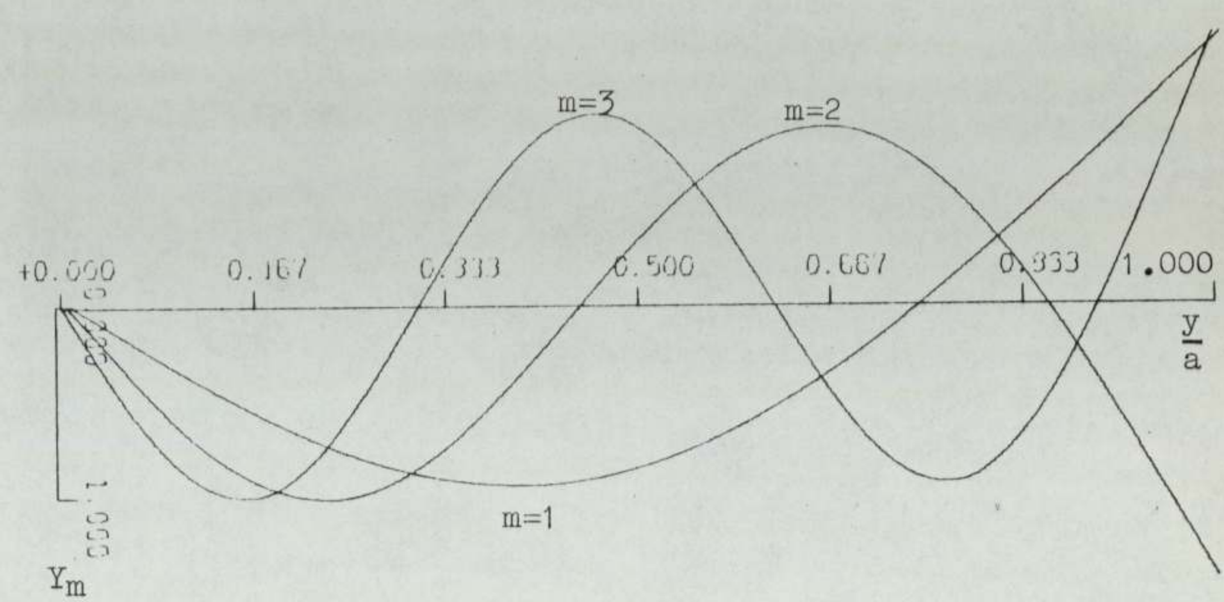

(f) Simply Supported-Free

4.4 Continuity of Deflection, Slopes, Curvatures and Twist.

In a classical finite element investigation of a plate bending problem where four-node rectangular elements are used with three parameters specified per node, one deflection and two rotations, the deflection is uniquely defined at the boundary of the element and continuity of deflection across element boundaries is ensured. The normal slopes, on the other hand, are continuous at the nodes only. Elsewhere at common boundaries, the normal slopes are discontinuous [35]. The curvatures and twist are discontinuous at common nodes as well as common boundaries.

In the semi-analytic approach, the continuity of a function at a "node" implies continuity at the whole length of the common boundary since the node in this case represents the whole of the edge of the strip. A formal investigation of the continuity of deflection, slopes, curvatures and twist for the semi-analytic approach will be given here.

A common boundary for two strips is given by x=b for element (e) and x=0 for element (e+1) as shown in Fig.(4.3).

Fig.(4.3)

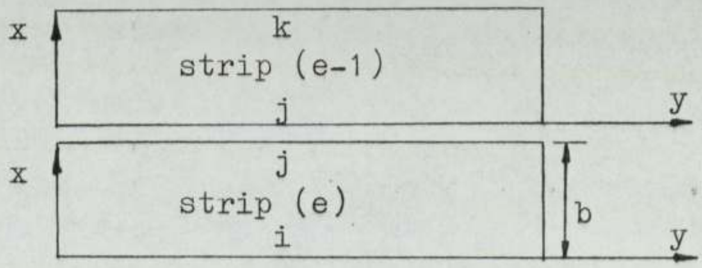

Using equations (4.7) and (4.2), with the appropriate alterations to the subscripts of the nodal parameters, to evaluate the deflection, slopes, curvatures and twist from the point of view of both elements, these quantities will be as given in the table below:

Function	value at x = 0 element (e+1)	value at x = b element (e)
w	$w_{jm}\ Y_m$	$w_{jm}\ Y_m$
$\theta_x = -\dfrac{\partial w}{\partial x}$	$\theta_{jm}\ Y_m$	$\theta_{jm}\ Y_m$
$\theta_y = \dfrac{\partial w}{\partial y}$	$w_{jm}\ Y'_m$	$w_{jm}\ Y'_m$
$\chi_x = -\dfrac{\partial^2 w}{\partial x^2}$	$\left[\dfrac{6}{b^2}(w_{jm} - w_{km}) - \dfrac{2}{b}(\theta_{km} + 2\,\theta_{jm})\right] Y_m$	$\left[\dfrac{6}{b^2}(w_{jm} - w_{im}) + \dfrac{2}{b}(\theta_{im} + 2\,\theta_{jm})\right] Y_m$
$\chi_y = -\dfrac{\partial^2 w}{\partial y^2}$	$-\,w_{jm}\ Y''_m$	$-\,w_{jm}\ Y''_m$
$\chi_{xy} = -2\dfrac{\partial^2 w}{\partial x\,\partial y}$	$2\,\theta_{jm}\ Y'_m$	$2\,\theta_{jm}\ Y'_m$

where the summation sign has been dropped for convenience, $Y'_m = dY_m/dy$ and $Y''_m = d^2Y_m/dy^2$.

Now, bearing in mind that Y_m is a continuous differentiable function with continuous derivatives, then it is obvious that apart from the curvature χ_x all the functions above are continuous across common element boundaries for all values of y, i.e. for the whole length of the element boundary. The curvature χ_x at x = 0 of element (e+1) is a function of the displacement parameters of the nodal lines j and k, whilst at x = b of element (e) (i.e. along the same line) this quantity is a function of the displacement parameters of the nodal lines i and j. Therefore, in general, the curvature χ_x is discontinuous across the transition zone from one strip to the neighbouring one. However, since the potential energy functional does not contain any derivatives higher than that in the curvature term χ_x, the discontinuity of this term at the transition zone will not, in itself, cause any errors to occur in the value of the potential energy of the overall structure (section 3.2).

It may be observed that the key to the continuity of a function, at the common boundary of two elements, lies with the parameters which specify the value of the function at the common boundary. If these parameters are pertinent to no other nodal line but the one in question then continuity is inevitable. If, on the other hand, parameters of other nodal lines are involved then discontinuity occurs.

Although, as stated, this discontinuity at the common boundary does not in itself affect the potential energy of the system, its consequences may appear at a nodal line on the boundary of the plate when the function must take a specific value, because of boundary conditions. For example, at a simply supported edge the curvature χ_x should be zero. However, the parameters which specify this function at the simply supported edge also specify the function at other points on the element where it is non-zero. It is, then, unlikely that the condition $\chi_x=0$ is satisfied because these parameters will be chosen, through minimization of potential energy, as to give the least error in the potential energy of the whole plate. However, if the size of the edge element is small, then the error in the value of the function at the edge would be small.

The bending moment is a function of the curvatures χ_x

and χ_y. Now, at a simply supported edge, both of these functions should vanish. χ_y will, in fact, be zero at the edge, whilst χ_x will have a non-zero value as has already been stated. The residual moment at the simply supported edge due to the non-vanishing of χ_x will be very small as will be confirmed in some of the test cases in section(7.8).

4.5 Rigid Body Modes.

One of the requirements discussed in section (3.2) that the assumed displacement function must satisfy is that it should be able to represent the rigid body modes, i.e. the elements must be able to deflect and rotate without being strained. In the semi-analytic approach to the plate bending problem the function satisfies this requirement, in the x-direction, due to the presence of the constants A_1 and A_2 (equation 4.1). In the y-directions the analytic function satisfies specific boundary conditions and thus, the question of rigid body modes arises only in the cases of free-free edges where rigid body deflection and rigid body rotation should be represented, and simply supported-free edges where the rigid body rotation must be present.

The functions given in table (4.1), cases 3 and 6, do not include these modes. The terms $1, (\frac{1}{2} - \frac{y}{a})$ and $\frac{y}{a}$ need to be added to the relevant cases to represent rigid body deflection and rotation. Hence the deflection functions for the free-free and the simply supported-free cases will be respectively:

$$w = \sum_{m=1}^{M-2} f_m(x)\, Y_m(y) + f_{M-1}(x)\,.\,1 + f_M(x).(\tfrac{1}{2} - \tfrac{y}{a}) \quad (4.8)$$

and

$$w = \sum_{m=1}^{M-1} f_m(x)\, Y_m(y) + f_M(x) \cdot \frac{y}{a} \qquad (4.9)$$

where $Y_m(y)$ is as given in table (4.1) for the respective cases. This choice of function for the rigid body modes maintains the orthogonality property of the analytic functions (Appendix A2.3).

4.6 Boundary Conditions - The Beam and the Plate.

On two opposing edges of the plate the boundary conditions must be satisfied by the analytic functions. Now, the functions employed are beam functions and the boundary conditions they satisfy are those rotating to a beam. The validity of application of these functions to a plate need to be examined.

The boundary condition of zero deflection is straightforward, for if the beam function satisfies this condition then, referring back to the expression for the assumed deflection shape (equation 4.7), the condition is satisfied for the whole edge of the plate. The zero normal slope condition is similarly satisfied along the whole edge if the beam eigenfunction satisfies this condition.

The condition of zero normal bending moment for the beam implies $\frac{\partial^2 w}{\partial y^2} = 0$ and that for the plate implies $(\frac{\partial^2 w}{\partial y^2} + \nu \frac{\partial^2 w}{\partial x^2}) = 0$. However, since the supported edge is a rectilinear one then $\frac{\partial^2 w}{\partial x^2} = 0$. Thus, for the plate, the condition to be satisfied is $\frac{\partial^2 w}{\partial y^2} = 0$ as in the beam and the argument follows similar lines to those of the deflection. The problem of a free edge condition is a different matter. Here, the effective shear force, as well as the normal bending moment, must be zero for the plate. Neither of these conditions is completely satisfied by the beam function as the expressions below will show:

For the beam:

$$\frac{\partial^2 w}{\partial y^2} = 0 \quad \text{and} \quad \frac{\partial^3 w}{\partial y^3} = 0$$

For the plate:

$$\frac{\partial^2 w}{\partial y^2} + \nu \frac{\partial^2 w}{\partial x^2} = 0 \text{ and } \quad \frac{\partial^3 w}{\partial y^3} + (2-\nu)\frac{\partial^3 w}{\partial y\, \partial x^2} = 0$$

The natural boundary conditions for a free edge are, therefore, only approximately satisfied by the beam eigenfunction. Although the energy formulation allows the satisfaction of geometric boundary conditions to be sufficient for convergence in the energy space whilst the natural boundary conditions are satisfied implicitly (section 2.2.2), this will not occur in the case of the free edge beam function. This statement is verified by considering the expressions for the normal and tangential bending moments.

In effect, the deflection is assumed to be in the form

$$w = X(x).Y(y)$$

The tangential bending moment will be given by:

$$M_x = - D\,(X''\,Y + \nu\,Y''\,X)$$

Now, if the function Y(y) is the beam eigenfunction, then $Y''(y{=}a) = Y'''(y{=}a) = 0$ and $Y(y{=}a) \neq 0$, where y=a is the free edge.

Therefore, the tangential bending moment at the free edge will be

$$(M_x)_{y=a} = - D(X'' \, Y)_{y=a} \neq 0$$

The normal bending moment M_y is given by:

$$M_y = - D(Y'' \, X + \nu \, X'' \, Y)$$

The value of this moment at the free edge will be

$$(M_y)_{y=a} = - D(\nu \, X'' \, Y)_{y=a} \neq 0$$

Similar argument applies to the effective shear force.

Therefore, the normal bending moment and the effective shear force are not zero at the free edge. The reason for the paradox lies in the fact that in the energy formulation no assumptions are made about the form of the deflection function, whereas in the semi-analytic method described here, the deflection is assumed to be of a specific form satisfying certain conditions, viz. $w = X(x).Y(y)$, $Y''(a) = Y'''(a) = 0$.

It is interesting to consider that if, for a free edge, the method of Kantorovich (section 2.3.2 c) were used to establish the analytic function subject to the satisfaction of the boundary conditions, then this function would not be the beam eigenfunction employed here. The Kantorovich function would, in fact, be of such a form that neither of the two terms constituting the normal bending moment, i.e. $Y'' \, X$ and $\nu X'' \, Y$, is zero at the edge individually, but their sum is. It follows, then, that for the Kantorovich function $Y_K''(a) \neq 0$. The argument regarding the effective shear force is similar

The implication of the non-satisfaction of the natural boundary conditions for a free edge is that there will be a residual normal bending moment and a residual shear force at the free edge, which may cause the solution to converge to one differing slightly from the true solution. The errors in the solution would be more pronounced when the bending moments and shear forces are evaluated near the free edge.

Two methods are suggested here to reduce this error. The first involves solving the problem, evaluating the residual moment and residual shear force, then re-solving the problem with these residuals as applied loads in the opposite direction, together with the original load.

The second method is the one whereby the free edge is simulated by imagining the plate to be longer in the y-direction than it actually is, and assigning a zero value to the flexural rigidity of the additional length (Fig.4.4).

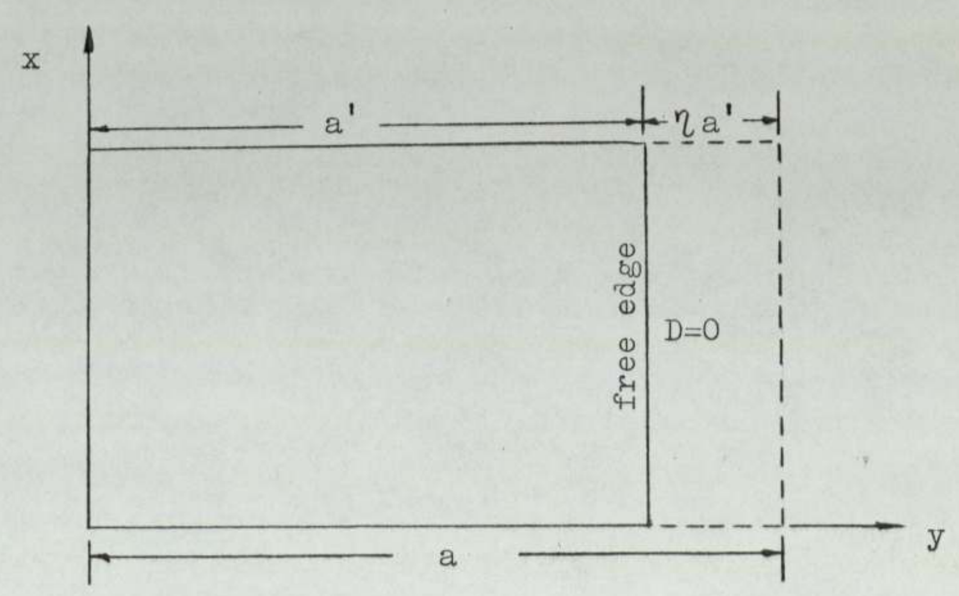

Fig.(4.4)

The original length of the plate in the y-direction is a' and that of the substitute plate is $a=a'(1+\eta)$ where η is a quantity small enough to maintain the general shape of the deflection curve of the beam (Fig.4.2) and large enough to keep the free edge away from the restrictions imposed by the beam function on its second and third derivatives. Various values of η were tested after the development of the computer program. It was found that $\eta=0.2$ gives the best results from the points of view of convergence rate as well as reduction in the value of the residual normal bending moment.

Effectively, this method replaces the beam function by one which, up to a point, has the same shape as the beam function, but without the free edge boundary conditions of the beam.

4.7 The Element Stiffness Matrix.

From equations (4.3) and (4.7), the deflection within each element of the plate will be given by

$$w = \sum_{m=1}^{m=M} [N]\{\delta^m\}_e \; Y_m \tag{4.10}$$

where

$$N = \left[\left(1 - \frac{3x^2}{b^2} + \frac{2x^3}{b^3}\right) \; \left(-x + \frac{2x^2}{b} - \frac{x^3}{b^2}\right) \; \left(\frac{3x^2}{b^2} - \frac{2x^3}{b^3}\right) \; \left(\frac{x^2}{b} - \frac{x^3}{b^2}\right)\right]$$

and

$$\{\delta^m\}_e = \left[w_{im} \;\; \theta_{im} \;\; w_{jm} \;\; \theta_{jm}\right]_e^T$$

The curvatures and twist of the element are then given by

$$\{\chi\}_e = \begin{Bmatrix} -\dfrac{\partial^2 w}{\partial x^2} \\ -\dfrac{\partial^2 w}{\partial y^2} \\ -2\dfrac{\partial^2 w}{\partial x\,\partial y} \end{Bmatrix} = \sum_{m=1}^{m=M} \begin{bmatrix} -[N'']\,Y_m \\ -[N]\,Y''_m \\ -2[N']\,Y'_m \end{bmatrix} \{\delta^m\}_e \tag{4.11}$$

where

$$[N'] = \frac{d}{dx}[N], \quad [N''] = \frac{d^2}{dx^2}[N], \quad Y'_m = \frac{dY_m}{dy}, \quad Y''_m = \frac{d^2Y_m}{dy^2}.$$

or

$$\{\chi\}_e = \sum_{m=1}^{m=M} \left([B]Y_m + [\bar{B}]Y'_m + [\bar{\bar{B}}]Y''_m\right)\{\delta^m\}_e \tag{4.12}$$

$$= \sum_{m=1}^{m=M} [C^m]\,\{\delta^m\}_e \tag{4.13}$$

where

$$[B] = \begin{bmatrix} -[N''] \\ \\ [0] \\ \\ [0] \end{bmatrix} , \quad [\bar{B}] = \begin{bmatrix} [0] \\ \\ [0] \\ \\ -2[N'] \end{bmatrix} \qquad (4.14)$$

$$[\bar{\bar{B}}] = \begin{bmatrix} [0] \\ -[N] \\ [0] \end{bmatrix} , \quad [C^m] = [B]Y_m + [\bar{B}]Y'_m + [\bar{\bar{B}}]Y''_m$$

The element moments are

$$\{M\}_e = \begin{Bmatrix} M_x \\ \\ M_y \\ \\ M_{xy} \end{Bmatrix} = D[D^*]\{\chi\}_e \qquad (4.15)$$

where

$$D = \frac{Eh^3}{12(1-\nu^2)} , \quad [D^*] = \begin{bmatrix} 1 & \nu & 0 \\ \nu & 1 & 0 \\ 0 & 0 & \frac{1-\nu}{2} \end{bmatrix}$$

h = thickness of element.

An expression for the potential energy of a plate under a distributed load, alternative to that given in chapter (2) can be shown to be

$$V = \tfrac{1}{2} \iint_{\text{area}} \{M\}^T\{\chi\} \, dxdy - \iint_{\text{area}} q \; w \; dxdy \qquad (4.16)$$

Substituting for $\{M\}$, $\{\chi\}$ and w from (4.15), (4.13) and (4.10) the potential energy for the element will be:

$$V_e = \tfrac{1}{2}\int_0^a\int_0^b \sum_m\sum_n D\,\{\delta^m\}_e^T [C^m]^T [D^*][C^n]\{\delta^n\}_e \, dx\, dy$$

$$-\int_0^a\int_0^b q\sum_m [N]\{\delta^m\}_e \, Y_m \, dx\, dy \qquad (4.17)$$

Minimizing the potential energy of the element implies

$$\frac{\partial V_e}{\partial\{\delta^j\}_e} = 0.$$

Therefore,

$$\frac{\partial V_e}{\partial\{\delta^j\}_e} = \tfrac{1}{2}\int_0^a\int_0^b D\Big(\sum_m\sum_n \{\delta^m\}_e^T[C^m]^T[D^*][C^n]\,\frac{\partial\{\delta^n\}_e}{\partial\{\delta^j\}_e}$$

$$+\sum_m\sum_n \frac{\partial\{\delta^m\}_e}{\partial\{\delta^j\}_e}\,[C^m]^T[D^*][C^n]\{\delta^n\}_e\Big)\, dx\, dy$$

$$-\int_0^a\int_0^b q\sum_m [N]\,\frac{\partial\{\delta^m\}_e}{\partial\{\delta^j\}_e}\; Y_m \; dx\, dy = 0$$

$$j = 1,2,\ldots,M$$

Simplifying:

$$0 = \tfrac{1}{2}\int_0^a\int_0^b D\Big(\sum_m\Big[\{\delta^m\}_e^T[C^m]^T[D^*][C^j]\Big]^T$$

$$+\sum_n [C^j]^T[D^*][C^n]\{\delta^n\}_e\Big)\, dx\, dy - \int_0^a\int_0^b q\,[N]^T\, Y_j\, dx\, dy$$

$$j = 1,2,\ldots,M$$

Transposing the first term, changing the summation subscript m to n and the subscript j to m and interchanging the summation and integration operations gives:

$$\sum_{n=1}^{M} \int_0^a \int_0^b D[C^m]^T [D^*][C^n] \{\delta^n\}_e \; dx\, dy$$

$$= \int_0^a \int_0^b q \; [N]^T \; Y_m \;\; dx\, dy \qquad (4.18)$$

$$m = 1,2,\ldots,M$$

Equations (4.18) are the equilibrium equations for the element. These equations can be stated in the following form

$$\sum_{n=1}^{M} [k^{mn}]_e \{\delta^n\}_e = \{f^m\}_e \qquad m = 1,2,\ldots,M \qquad (4.19)$$

where

$$\underset{4x4}{[k^{mn}]_e} = \int_0^a \int_0^b D \, [C^m]^T [D^*][C^n] \, dx\, dy$$

$$\underset{4x1}{\{f^m\}_e} = \int_0^a \int_0^b q \, [N]^T \; Y_m \;\; dx\, dy \qquad (4.20)$$

$[k^{mn}]_e$, $\{\delta^n\}_e$ and $\{f^n\}_e$ will be referred to as the harmonic element stiffness matrix, harmonic element nodal displacements vector and harmonic load vector respectively.

Substituting equation (4.20) into equation (4.17), the potential energy of the element will be obtained in terms of the harmonic element stiffness matrix and harmonic load vector:

$$V_e = \tfrac{1}{2}\sum_m \sum_n \{\delta^m\}_e^T [K^{mn}]_e \{\delta^n\}_e - \sum_m \{\delta^m\}_e^T \{f^m\}_e \qquad (4.21)$$

Substituting for $[C]$ from (4.14) into (4.20), and neglecting the null matrices that arise on multiplying out the matrices $[\bar{B}]^T[D^*][B]$, $[B]^T[D^*][\bar{B}]$, $[\bar{\bar{B}}]^T[D^*][\bar{B}]$ and $[\bar{B}]^T[D^*][\bar{\bar{B}}]$, the harmonic element stiffness matrix will be given by:

$$\begin{aligned}
[k^{mn}]_e = & \int_0^b\int_0^a D\, Y_m\, Y_n\, [B]^T[D^*][B]\; dx\, dy \\
& + \int_0^b\int_0^a D\, Y''_m\, Y_n [\bar{\bar{B}}]^T[D^*][B]\; dx\, dy \\
& + \int_0^b\int_0^a D\, Y_m\, Y''_n [B]^T[D^*][\bar{\bar{B}}]\; dx\, dy \\
& + \int_0^b\int_0^a D\, Y'_m\, Y'_n [\bar{B}]^T[D^*][\bar{B}]\; dx\, dy \\
& + \int_0^b\int_0^a D\, Y''_m\, Y''_n [\bar{\bar{B}}]^T[D^*][\bar{\bar{B}}]\; dx\, dy \qquad (4.22)
\end{aligned}$$

or

$$[k^{mn}]_e = \sum_{r=1}^{5} \int_0^b\int_0^a D\; \Phi_r^{mn}[J]_r\; dx\, dy \qquad (4.23)$$

where

$$\Phi_1^{mn} = Y_m\, Y_n \;,\quad \Phi_2^{mn} = Y''_m\, Y_n \;,\quad \Phi_3^{mn} = Y_m\, Y''_n \;,$$

$$\Phi_4^{mn} = Y'_m\, Y'_n \;,\quad \Phi_5^{mn} = Y''_m\, Y''_n \;,$$

$$[J]_1 = [B]^T[D^*][B],\; [J]_2 = [\bar{\bar{B}}]^T[D^*][B],\; [J]_3 = [B]^T[D^*][\bar{\bar{B}}]$$

$$[J]_4 = [\bar{B}]^T[D^*][\bar{B}],\; [J]_5 = [\bar{\bar{B}}]^T[D^*][\bar{\bar{B}}]$$

4.7.1 Symmetry of the Element Stiffness Matrix.

Expanding equation (4.19), the element equilibrium equations can be written as:

$$\begin{bmatrix} [k^{11}]_e & [k^{12}]_e \cdots & [k^{1n}]_e \cdots & [k^{1M}]_e \\ [k^{21}]_e & [k^{22}]_e \cdots & [k^{2n}]_e \cdots & [k^{2M}]_e \\ \vdots & \vdots & \vdots & \vdots \\ [k^{m1}]_e & [k^{m2}]_e \cdots & [k^{mn}]_e \cdots & [k^{mM}]_e \\ \vdots & \vdots & \vdots & \vdots \\ [k^{M1}]_e & [k^{M2}]_e \cdots & [k^{Mn}]_e \cdots & [k^{MM}]_e \end{bmatrix} \begin{Bmatrix} \{\delta^1\}_e \\ \{\delta^2\}_e \\ \vdots \\ \{\delta^m\}_e \\ \vdots \\ \{\delta^M\}_e \end{Bmatrix} = \begin{Bmatrix} \{f^1\}_e \\ \{f^2\}_e \\ \vdots \\ \{f^n\}_e \\ \vdots \\ \{f^M\}_e \end{Bmatrix} \qquad (4.24)$$

or

$$[k]_e \{\delta\}_e = \{f\}_e \qquad (4.25)$$

where $[k]_e$, $\{\delta\}_e$ and $\{f\}_e$ are the element stiffness matrix, element nodal displacement vector and element load vector respectively and are distinct from the harmonic element stiffness matrix and harmonic element nodal displacements and load vectors.

Now, if the harmonic element stiffness matrix (equation 4.22) is transposed and the modes m and n interchanged, it will be found that:

$$[k^{mn}]_e = [k^{nm}]_e^T$$

It becomes apparent, therefore, that the element stiffness matrix (equation 4.24) is symmetric.

4.7.2 Representation of the Flexural Rigidity.

In general, the flexural rigidity, D, may vary with x and y, due to a variation in the thickness or the properties of the plate, or both, and since the harmonic element stiffness matrix (equation 4.22) involves the evaluation of integrals of functions of D, the variation of D with x and y has to be taken into account when the integrals are evaluated.

Although it is possible to represent D(x,y) as a Fourier series to generalise an arbitrary function D(x,y), the error incurred in the inevitable truncation of the Fourier series, particularly in the case of step variation, makes an alternative method of representation of D more attractive. This method involves carrying out the integration process in the y direction in a discrete, pre-chosen number of steps and assuming the variation of D to be linear in both directions over each step. Thus, if the number of steps is NS and the end limits for each step are $y \in [a_{s-1}, a_s]$ (s=1,2,...NS, $a_0 = 0$, $a_{NS} = a$) and $x \in [o, b]$, then the flexural rigidity for each step will be

$$D_s = D_{1s}\, x + D_{2s}\, y + D_{3s} \qquad (s=1,2,\dots,NS) \quad (4.26)$$

and the harmonic element stiffness matrix will be given by:

$$\begin{aligned}
[k^{mn}]_e &= \sum_{r=1}^{5} \sum_{s=1}^{NS} \int_{a_{s-1}}^{a_s} \int_{o}^{b} (D_{1s}\, x + D_{2s}\, y + D_{3s})\, \Phi_r^{mn} [J]_r \, dxdy \\
&= \sum_{r=1}^{5} \left\{ \int_{o}^{b} x[J]_r \, dx \sum_{s=1}^{NS} D_{1s} \int_{a_{s-1}}^{a_s} \Phi_r^{mn} \, dy \right. \\
&\quad + \int_{o}^{b} [J]_r \, dx \, \Big(\sum_{s=1}^{NS} D_{2s} \int_{a_{s-1}}^{a_s} y \, \Phi_r^{mn} \, dy \\
&\quad \left. + \sum_{s=1}^{NS} D_{3s} \int_{a_{s-1}}^{a_s} \Phi_r^{mn} \, dy \Big) \right\} \qquad (4.27)
\end{aligned}$$

The matrices $\int_0^b [J]_r \, dx$ and $\int_0^b x[J]_r \, dx$ and the integrals of the function which constitute $\int_0^a \Phi_r^{mn} \, dy$ are given in Appendix (3).

If the flexural rigidity of the element is uniform then the required number of steps is one, and the values of D_{15} and D_{25} in equation (4.26) are zero. This reduces the expression for the harmonic element stiffness matrix to:

$$[k^{mn}]_e = D_3 \sum_{r=1}^{5} \int_0^a \Phi_r^{mn} \, dy \int_0^b [J]_r \, dy \qquad (4.28)$$

Now, because of the orthogonality property, appendix (A2.2), the integrals $\int_0^a \Phi_1^{mn} \, dy$ and $\int_0^a \Phi_5^{mn} \, dy$ are zero for $m \neq n$, for any combination of simply supported, clamped or free boundary conditions.

To establish the order of magnitude, O, of the matrices $[k^{mn}]_e$ in comparison to that of the matrices $[k^{mm}]_e$, the five terms in the harmonic stiffnes matrix $[k^{mm}]_e$, equation (4.23), are examined:

It can be seen from appendix (A2.2), that the order of magnitude of integrals $\int_0^a \Phi_r^{mm} \, dy$ (r=1,2,3,4,5) is given by:

$$O\left(\int_0^a \Phi_1^{mm} \, dy\right) = a \, ,$$

$$O\left(\int_0^a \Phi_2^{mm} \, dy\right) = O\left(\int_0^a \Phi_3^{mm} \, dy\right) = O\left(\int_0^a \Phi_4^{mm} \, dy\right) = \left(\frac{\mu_m}{a}\right)^2 . a$$

$$O\left(\int_0^a \Phi_5^{mm} \, dy\right) = \left(\frac{\mu_m}{a}\right)^4 . \, a$$

Values of μ_m, for various boundary conditions, are given in appendix (A4.3).

From appendix (A3.1), the order of magnitude of elements in equivalent locations in the matrices $\int_0^b [J]_r \, dx$ are:

$$O\left(\int_0^b [J]_1 \, dx\right) = \frac{1}{b^3}$$

$$O\left(\int_0^b [J]_2 \, dx\right) = O\left(\int_0^b [J]_3 \, dx\right) = O\left(\int_0^b [J]_4 \, dx\right) = \frac{1}{b}$$

$$O\left(\int_0^b [J]_5 \, dx\right) = b.$$

Therefore, the order of magnitude of the five terms contributing to the harmonic element stiffness matrix will be:

$$O\,(T_1) = \eta \cdot \frac{1}{b^2}$$

$$O\,(T_2) = O(T_3) = O(T_4) = \frac{\mu_m^2}{\eta} \cdot \frac{1}{b^2}$$

$$O\,(T_5) = \frac{\mu_m^4}{\eta^3} \cdot \frac{1}{b^2}$$

where

$$T_1 = \int_0^a \Phi_1^{mm} \, dy \cdot \int_0^b [J]_1 \, dx \,.$$

etc.

and

$$\eta = \frac{a}{b} \,.$$

Hence

$$O\,(T_2) = O(T_3) = O(T_4) = \left(\frac{\eta}{\mu_m}\right)^2 O(T_5)$$

Also,

$$O(T_2) = O(T_3) = O(T_4) = (\frac{\mu_m}{\eta})^2 \, O(T_1).$$

Therefore, in general, either T_1 or T_5 makes the largest contribution to the stiffness matrix depending on whether $(\frac{\eta}{\mu_m})$ is greater than or less than 1.0. The case where this ratio is equal to 1.0 would, for any particular problem, occur for one value of μ_m only.

A procedure IFIFI, which was developed for the computer program, was used to evaluate the integrals $\int_0^a \Phi_r^{mn}\, dy$ (r=1,2,..5) for the various boundary conditions and for a number of values of m and n. It was observed, for all boundary conditions that:

$$\int_0^a \Phi_r^{mn}\, dy \;(m > n) < \int_0^a \Phi_r^{nn}\, dy < \int_0^a \Phi_r^{mm}\, dy \quad r=2,3,4.$$

The ratio $\int_0^a \Phi_r^{mn}\, dy \;(m \neq n) \,/ \int_0^a \Phi_r^{mm}\, dy$ was, in many cases as low as 0.01.

Thus, the matrix $[k^{mn}]_e$ for $m \neq n$ is small when compared with $[k^{mm}]_e$ for two reasons. Firstly, by virtue of the fact that the two terms which make the greater contribution to $[k^{mm}]_e$ are missing from $[k^{mn}]_e$ and secondly, because the values of the integrals $\int_0^a \Phi_r^{mn}\, dy$ are smaller than those of $\int_0^a \Phi_r^{mm}\, dy$ (r=2,3,4)

It can be concluded from the above that equation(4.24), though still coupled (i.e. the modes are interdependent), will have a coefficient matrix $[k]_e$ that contains predominant submatrices $[k^{mm}]_e$ on the leading diagonal. The numerical stability of the equations will, then, be reinforced.

The particular case of simply supported-simply supported plate is simplified further due to the fact that the orthogonality property reduces all the integrals $\int_0^a \Phi_r^{mn}\,dy$ (r=1,...5) to zero for $m \neq n$. This is because the function for this case of boundary conditions is $\sin \frac{m\pi y}{a}$ which is orthogonal, as are its derivatives. This reduces the harmonic element stiffness matrix $[k^{mn}]_e$ to zero when $m \neq n$, which results in the uncoupling of equations (4.24), i.e.

$$[k^{mm}]_e \{\delta^m\}_e = \{f^m\}_e \quad m=1,2,\ldots,M \qquad (4.29)$$

It follows from equation (4.29) that the equilibrium equations for the whole plate are uncoupled. Thus the complete analysis can be carried out for each mode separately resulting in a much-reduced solution time.

In the case where the flexural rigidity of the plate varies with x only, one of two methods may be employed. In the first, D is assumed to be piece-wise constant, i.e. D does not vary within each element though its value is different from one element to the next. The expression for the harmonic element stiffness matrix will then be as in equation (4.28). In the second method the variation within the element is approximated by a linear function. In this case, referring to equation (4.26), $D=D_1 x + D_3$ and the harmonic element stiffness matrix will be given by

$$[k^{mn}]_e = \sum_{r=1}^{5} \left\{ \int_0^b x\,[J]_r\,dx \,.\, D_1 \int_0^a \Phi_r^{mn}\,dy + \int_0^b [J]_r\,dx \,.\, D_3 \int_0^a \Phi_r^{mn}\,dy \right\}$$

In both of these methods the preceeding argument regarding the orthogonality property holds.

If the plate rigidity varies in the y-direction only then once again either of two methods may be applied to represent this variation. In both methods the integration has to be carried out over a discrete number of steps as described earlier in this section. The rigidity for each step may be assumed either constant or linear. In these cases the harmonic element element stiffness matrix will respectively be:

$$\left[k^{mn}\right]_e = \sum_{r=1}^{5} \sum_{s=1}^{NS} D_{3s} \int_{a_{s-1}}^{a_s} \Phi_r^{mn}\, dy \cdot \int_0^b [J]_r\, dx$$

and

$$\left[k^{mn}\right]_e = \sum_{r=1}^{5} \left\{ \int_0^b [J]_r\, dx \left(\sum_{s=1}^{NS} D_{1s} \int_{a_{s-1}}^{a_s} y\, \Phi_r^{mn}\, dy + \sum_{s=1}^{NS} D_{3s} \int_{a_{s-1}}^{a_s} \Phi_r^{mn}\, dy \right) \right\}$$

In both cases the orthogonality property is disturbed because the eigenfunctions are orthogonal with respect to a weighting function of unity. For varying sections, D is under the integral sign and the weighting function is, thus, not unity. If the integral is broken up into steps each with a constant value for D, then the interval of integration is not the correct one for the orthogonality property to apply.

The orthogonality (or quasi-orthogonality) property is very important from the point of view of numerical stability. The orientation of the plate problem should be chosen so as to allow this property to be applied whenever possible. Thus, for a plate whose flexural rigidity varies in one direction only this direction should be made to coincide with the x-axis, i.e. the plate should be divided in such a way as to allow the strips to have constant rigidities along their y-axis.

For plates whose rigidities vary in both directions, any combination of the previous methods of representation may be used. In the computer program which was developed on the basis of the theory presented here, the user may choose the method of representation of the flexural rigidity by means of a code which will be described later. The choice of a linearly varying flexural rigidity involves very little additional computational time on the part of the computer. This choice should therefore, be made whenever it involves a reduction in the number of strips (in the x-direction) or a reduction in the number of steps (in the y-direction) and little additional manual effort.

Plates with step-variation in their flexural rigidity arise frequently in practice. Typically, plate thickness is increased over part of the plate area as a means of reinforcement. For such plates, the methods discussed earlier give an exact representation of the flexural rigidity. Fig.(4.5) shows a strip with step variation in its rigidity. The harmonic element stiffness matrix for this strip would be:

$$[k^{mn}]_e = \sum_{r=1}^{5} \left\{ \left(D_1 \int_0^{a_1} \Phi_r^{mn} \, dy + D_2 \int_{a_1}^{a_2} \Phi_r^{mn} \, dy + D_3 \int_{a_2}^{a} \Phi_r^{mn} \, dy \right) \int_0^b [J]_r \, dx \right\}$$

Fourier series representation of this type of variation in the flexural rigidity can only be an approximation which may be crude unless a large number of terms in the series is taken.

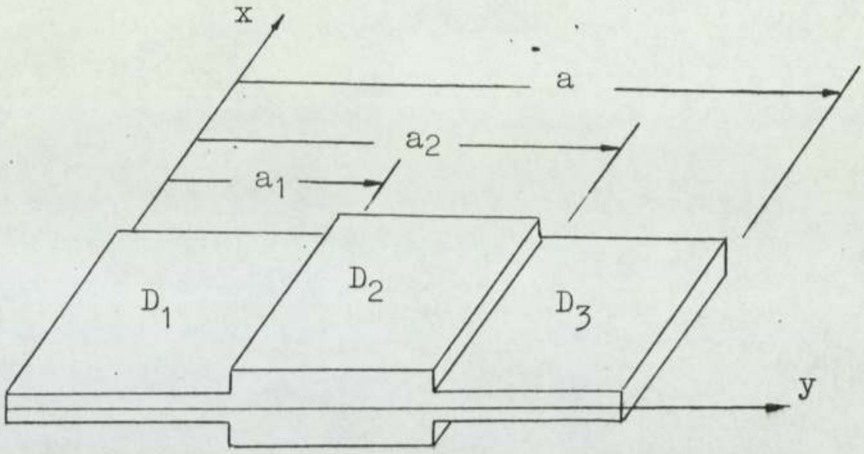

Fig.(4.5)

For piece-wise linear representation of D_s (equation 4.26) the coefficients D_{1s}, D_{2s} and D_{3s} are required. These may be at hand in simple cases. However, if the flexural rigidity varies with x and y according to some known function, these constants need to be evaluated. A method is employed whereby the number of steps and their end limits are decided, then the flexural rigidity is evaluated at the four corners of each step using the known function, then a plane is chosen to represent the variation of D_s. Now, since only three values are required to define a plane uniquely, it is necessary to obtain the optimum plane from the four values of rigidity at the corners of each step. For this purpose the method of least squares is employed (appendix 5).

In implementing these ideas in a computer program, a code is used to differentiate between the various cases.

4.8 The Element Force Vector

In equation (4.20), the harmonic element force vector was found to be

$$\left\{f^m\right\}_e = \int_0^a \int_0^b q\,[N]^T\,Y_m\,dx\,dy \tag{4.30}$$

This expression for the harmonic element force vector was obtained, in effect, by differentiating the work done by the applied load with respect to the harmonic nodal displacement vector. Although expression (4.30) was obtained for a distributed load over the area of the strip, no assumptions were made regarding the nature of the distribution. The harmonic element force vector can be obtained for any type of load simply by considering the work done by the applied load. Contrary to many statements on the subject [20], [33], [1], [35] etc., the applied load need not be expanded into the same series as the analytic function which describes the deflection. An expression for the work done can be obtained directly from the applied load and the assumed deflection function. Differentiation with respect to the nodal displacements, then, yields the force vector. Because of the othogonality property, the resulting force vector is the same in both cases as will be shown for the case of a distributed load.

4.8.1 Distributed Load Over Part of the Element

The pressure q(x,y) is applied over the shaded area of the element (fig. 4.6). The conventional method of obtaining the force vector is by expressing the applied load as a series of the same form as the assumed deflection, i.e.

$$q(x,y) = \sum_{m=1}^{M} q_m\,Y_m(y) \tag{4.31}$$

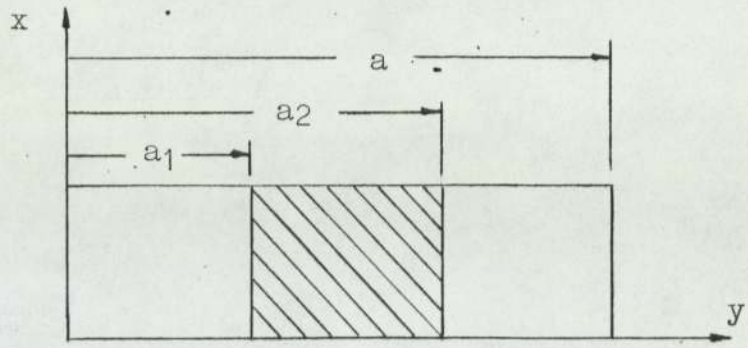

Fig.(4.6)

Multiplying both sides of equation (4.31) by Y_n and integrating over the length of the strip, the following will be obtained:

$$\int_0^a q(x,y)\, Y_n\, dy = \sum_{m=1}^{M} \int_0^a q_m\, Y_m\, Y_n\, dy$$

Applying the orthogonality property of the beam eigenfunctions and neglecting the zero value of the left hand side outside the limits $y \in [a_1 , a_2]$, the expression for q_m will be obtained. Thus,

$$q_m = \frac{\int_{a_1}^{a_2} q(x,y)\, Y_m\, dy}{\int_0^a Y_m^2\, dy} \tag{4.32}$$

The harmonic element force vector is obtained by considering the work done (W.D.) by the applied load and differentiating with respect to the harmonic element displacement parameters. Thus,

$$\text{W.D.} = \int_0^a \int_0^b q(x,y)\, w(x,y)\, dx\, dy$$

On substituting for q from (4.31) and for w from (4.10), the work done will be

$$\text{W.D.} = \sum_{n=1} \sum_{m=1} \int_0^a \int_0^b q_m\, Y_m\, [N]\, \{\delta^n\}_e\, Y_n\, dx\, dy$$

On using the orthogonality property, the work done will be:

$$W.D. = \sum_m \int_0^a \int_0^b q_m [N] \{\delta^m\}_e Y_m^2 \, dx \, dy$$

Substituting for q_m from equation (4.32), the work done becomes:

$$W.D. = \sum_m \int_{a_1}^{a_2} \int_0^b q(x,y) \, Y_m [N]\{\delta^m\}_e \, dx \, dy \qquad (4.33)$$

The harmonic element force vector will, then, be given by:

$$\{f^j\}_e = \frac{\partial W.D.}{\partial\{\delta^j\}_e} = \int_{a_1}^{a_2} \int_0^b q(x,y) \, [N]^T \, Y_j \, dx \, dy \qquad (4.34)$$

$$j=1,2,\ldots,M$$

It is obvious that expression (4.33) for the work done may be obtained directly by considering the work done per unit area, i.e. $q(x,y)\,w$, and integrating over the area of the strip to which the pressure is applied, i.e. $x \in [o,b]$, $y \in [a_1, a_2]$. The harmonic element force vector is then obtained as before. This direct method is used to obtain the various load vectors for all loading conditions that are treated here.

4.8.2 Representation of an Applied Pressure.

Similar ideas are implemented, in representing an applied pressure which may vary in both the x and y directions, to those employed in the representation of the flexural rigidity. The integration with respect to y (equation 4.30) is carried out in a discrete number of steps, NS, over each of which the applied pressure is assumed to vary linearly in both directions. Thus:

$$q_s = q_{1s} \, x + q_{2s} \, y + q_{3s} \qquad (s=1,2,\ldots,NS)$$

The harmonic element force vector will then be given by:

$$\{f^m\}_e = \int_0^b x\ [N]^T\ dx \ . \sum_{s=1}^{NS} q_{1s} \int_{a_{s-1}}^{a_s} Y_m\ dy$$
$$+ \int_0^b [N]^T\ dx \left\{ \sum_{s=1}^{NS} q_{2s} \int_{a_{s-1}}^{a_s} y\ Y_m\ dy + \sum_{s=1}^{NS} q_{3s} \int_{a_{s-1}}^{a_s} Y_m\ dy \right\} \qquad (4.35)$$

The vectors $\int_0^b [N]^T$ and $\int_0^b x\ [N]^T$ are given in Appendix (A3.3).

Evaluation of the coefficients q_{1s} , q_{2s} and q_{3s} is achieved in a manner identical to that used for the flexural rigidity.

4.8.3 Implication of the Element Force Vector.

Recalling equations (4.19), the equilibrium equations for the element were

$$\sum_{n=1}^{M} [k^{mn}]_e\ \{\delta^n\}_e = \{f^m\}_e \qquad m=1,2,\ldots,M$$

or,

$$\sum_{n=1}^{M} \begin{bmatrix} k_{11} & k_{12} & k_{13} & k_{14} \\ k_{21} & k_{22} & k_{23} & k_{24} \\ k_{31} & k_{32} & k_{33} & k_{34} \\ k_{41} & k_{42} & k_{43} & k_{44} \end{bmatrix}_e^{mn} \begin{Bmatrix} w_1 \\ \theta_1 \\ w_2 \\ \theta_2 \end{Bmatrix}_e^{n} = \begin{Bmatrix} f_1 \\ f_2 \\ f_3 \\ f_4 \end{Bmatrix}_e^{m} \qquad (4.36)$$

If, in equations (4.36), θ_1, w_2 and θ_2 were made zero then the remaining load-displacement relationship would be

$$\sum_{n=1}^{M} k_{11}^{mn}\ w_1^n = f_1^m$$

Comparison of this relationship with that for a basic spring system would indicate that f_1 corresponds to an external force applied to nodal line 1. Similarly f_3 corresponds to an external force applied to nodal line 2 and f_2 and f_4 correspond to external moments applied to nodal lines 1 and 2 respectively, i.e.

$$\{f^m\}_e = \begin{bmatrix} F_1^m & M_1^m & F_2^m & M_2^m \end{bmatrix}^T$$

In effect , the distributed load is replaced by an equivalent system of forces and moments applied to the nodal lines of the element.

4.8.4 <u>Other Types of Loading.</u>

The harmonic element force vector will now be obtained for line loads and concentrated loads applied to a nodal line of an element.

When the equilibrium equations of the elements are assembled to yield the equilibrium equations of the whole plate, the nodal forces and the unknown nodal displacement parameters are those relating to the nodal lines of the overall structure, i.e. the global nodal lines. For this reason it is more convenient to treat loads applied to the nodal lines from the point of view of the overall structure rather than the element.

<u>a. Line Force.</u>

A uniform line force Q* is applied to nodal line k from y=c to y=d (Fig.4.7)

b. Line Moments M_x^* and M_y^*

Uniform line moments M_x^* and M_y^* applied to nodal line k from y=c to y=d (Figs.4.8)

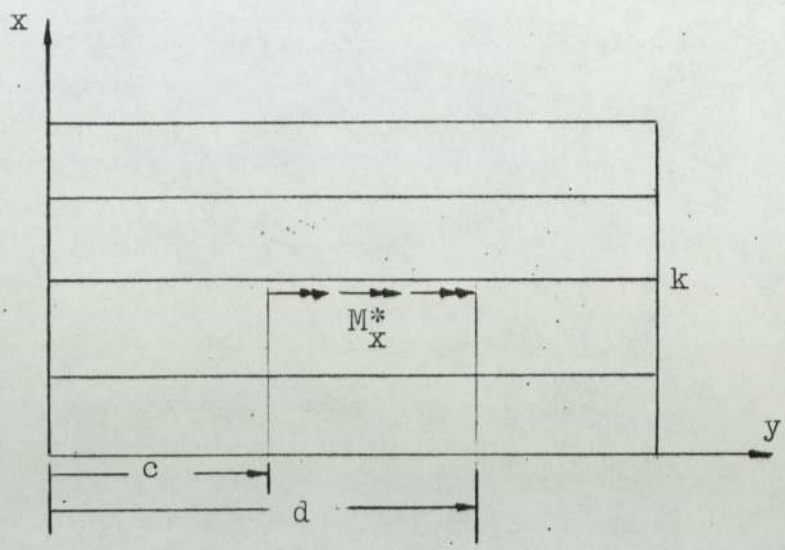

Figs.(4.8)

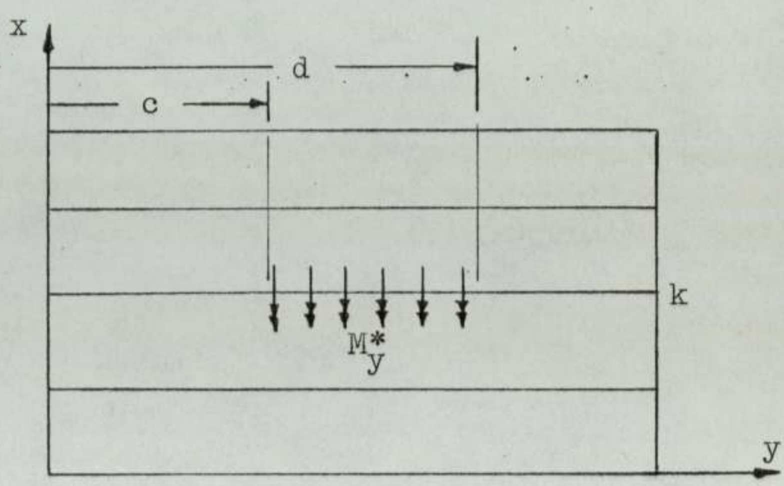

The work done in these cases is in rotating through θ_x and θ_y respectively.

$$(\theta_x)_k = -\left(\frac{\partial w}{\partial x}\right)_k = -\sum_{m=1}^{M} f'(x)_k \, Y_m = \sum_{m=1}^{M} \theta_{km} \, Y_m$$

where θ_{km} is the rotation parameter at nodal line k.

$$(\theta_y)_k = \left(\frac{\partial w}{\partial y}\right)_k = \sum_{m=1}^{M} f(x)_k \, Y'_m = \sum_{m=1}^{M} w_{km} \, Y'_m$$

The work done by the line moment M^*_x is

$$W.D. = \int_c^d M^*_x \sum_{m=1}^{M} \theta_{km} \, Y_m \, dy$$

$$= M^*_x \sum_{m=1}^{M} \theta_{km} \int_c^d Y_m \, dy$$

The non-zero value in the harmonic force vector is in the location of the bending moment on node k. Therefore,

$$M_k^j = \frac{\partial W.D.}{\partial \theta_{kj}} = M^*_x \int_c^d Y_j \, dy \qquad j=1,2,\ldots,M$$

The work done by the line moment M^*_y is

$$W.D. = M^*_y \sum_{m=1}^{M} w_{km} \int_c^d Y'_m \, dy$$

The non-zero value in this case is in the location of the force on node k.

$$F_k^j = \frac{\partial W.D.}{\partial w_{kj}} = M^*_y \int_c^d Y'_j \, dy \qquad j=1,2,\ldots,M$$

The treatment of line loads in the y-direction has been based on uniform distribution. Variable loads, therefore, have to be considered by superposing a discrete number of piecewise constant line loads (Fig.4.9)

Fig.(4.9)

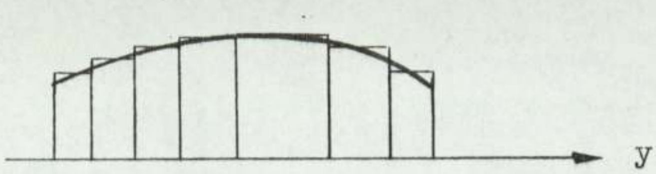

Line loads in the x-direction must be replaced by concentrated loads applied at the nodal lines. Sufficient accuracy is achieved, particularly if the width of the element is small, by simply lumping the line load into two concentrated loads applied at the nodal lines. Representation of the line forces may be improved by applying concentrated moments as well as concentrated forces at the nodal lines in such a magnitude as to make the work done by the representative system of loads equivalent to that of the actual load.

c. Concentrated Loads.

If a concentrated force P* is applied to node k at y=c, then the work done by this force will be

$$\begin{aligned} W.D. &= P^* (w)_{k,y=c} \\ &= P^* \sum_{m=1}^{M} f(x)_k \; Y_m \; (y=c) \\ &= P^* \sum_{m=1}^{M} w_{km} \; Y_m \; (y=c) \end{aligned}$$

$$F_k^j = \frac{\partial W.D.}{\partial w_{kj}} = P^* \; Y_j \; (y=c) \qquad j=1,2,\ldots,M$$

Similarly, for a concentrated moment M^*_{cx} and a concentrated moment M^*_{cy}, the harmonic load vector will contain non-zero values at the following respective locations:

$$M_k^j = M^*_{cx} \; Y_j(y=c) \text{ , and} \qquad j=1,2,\ldots,M.$$

$$F_k^j = M^*_{cy} \; Y_j'(y=c)$$

Having described the behaviour of a single element, the behaviour of the overall structure must be investigated in relation to the assemblage of stiffnesses and forces of all the elements. This will be the subject of the next chapter.

CHAPTER 5

CHAPTER FIVE.

THE OVERALL STRUCTURE.

The behaviour of the overall problem may be investigated either by considering the compatibility of the displacements and the equilibrium of the overall structure in a direct way or by applying the principle of minimum potential energy to the overall structure. Since the later method has been applied to the element, it will be used to establish the behaviour of the assemblage of elements.

5.1 Assembly of the Overall Stiffness Matrix and Overall Load Vector.

5.1.1 General Procedure.

The potential energy of an element was obtained in terms of the element stiffness matrix and load vector (equation 3.14). This was found to be:

$$V_e = \tfrac{1}{2} \{\delta\}_e^T [k]_e \{\delta\}_e - \{\delta\}_e^T \{f\}_e \tag{5.1}$$

Therefore, if the number of elements in the overall structure is NE then the potential energy of the overall structure will be:

$$V = \tfrac{1}{2} \sum_{e=1}^{NE} \{\delta\}_e^T [k]_e \{\delta\}_e - \sum_{e=1}^{NE} \{\delta\}_e^T \{f\}_e \tag{5.2}$$

The vector $\{\delta\}_e$ represents the nodal displacements for the element e. Thus, for an element with two nodes and one degree of freedom per node, the nodal displacement and load vectors will be

$$\{\delta\}_e = \begin{Bmatrix} \delta_1 \\ \delta_2 \end{Bmatrix} \quad \text{and} \quad \{f\}_e = \begin{Bmatrix} f_1 \\ f_1 \end{Bmatrix}$$

Now, if these vectors are transformed to ones with global numbering containing the total number of degrees of freedom, then the element nodal displacements and element nodal forces vectors become

$$\{\delta_e\} = \begin{Bmatrix} 0 \\ 0 \\ \vdots \\ \delta_{e_1} \\ \delta_{e_2} \\ \vdots \\ 0 \\ 0 \end{Bmatrix} \begin{array}{c} \cdots\cdots \text{ row } 1 \cdots\cdots \\ \cdots\cdots \text{ row } 2 \cdots\cdots \\ \\ \cdots\cdots \text{ row } e_1 \cdots\cdots \\ \cdots\cdots \text{ row } e_2 \cdots\cdots \\ \\ \\ \\ \end{array} \begin{Bmatrix} 0 \\ 0 \\ \vdots \\ f_{e_1} \\ f_{e_2} \\ \vdots \\ 0 \\ 0 \end{Bmatrix} = \{f_e\}$$

where e_1 and e_2 are the global node numbers which correspond to the first and second degrees of freedom of element e.

The vectors $\{\delta_e\}$ and $\{f_e\}$ are distinguished from $\{\delta\}_e$ and $\{f\}_e$ by taking the suffix e inside the brackets to indicate that the only non-zero locations in the first pair of vectors are those attributed to element e. The same convention will be applied to the element stiffness matrix.

If the general nature of the equilibrium equations $[k]_e \{\delta\}_e = \{f\}_e$ is to be maintained, then the element stiffness matrix has to take the form:

$$[k_e] = \begin{array}{cc} \left[\begin{array}{cc} \begin{bmatrix} k_{e_1 e_1} & k_{e_1 e_2} \\ k_{e_2 e_1} & k_{e_2 e_2} \end{bmatrix} & \\ \begin{array}{cc} \vdots & \vdots \end{array} & \end{array}\right] & \begin{array}{l} \cdots\cdots \text{ row } e_1 \\ \cdots\cdots \text{ row } e_2 \\ \\ \\ \end{array} \\ \begin{array}{cc} \text{col } e_1 & \text{col } e_2 \end{array} & \end{array}$$

where
$$\begin{bmatrix} k_{e_1 e_2} & k_{e_1 e_2} \\ k_{e_2 e_1} & k_{e_2 e_2} \end{bmatrix} = \begin{bmatrix} k_{11} & k_{12} \\ k_{21} & k_{22} \end{bmatrix}_e$$

All other locations in the matrix $[k_e]$ are zero.

If the equation $[k_e]\{\delta_e\} = \{f_e\}$ is expanded it would yield the same result as the equation $[k]_e\{\delta\}_e = \{f\}_e$.

Therefore, equation (5.2) can be re-written as:

$$V = \tfrac{1}{2}\sum_{e=1}^{NE}\{\delta_e\}^T[k_e]\{\delta_e\} - \sum_{e=1}^{NE}\{\delta_e\}^T\{f_e\}$$

Expanding the summation, the total potential energy becomes:

$$\begin{aligned} V = \tfrac{1}{2}(& \{\delta_1\}^T[k_1]\{\delta_1\} + \{\delta_2\}^T[k_2]\{\delta_2\} + \cdots \\ & + \{\delta_e\}^T[k_e]\{\delta_e\} + \cdots + \{\delta_{NE}\}^T[k_{NE}]\{\delta_{NE}\}) \\ & - (\{\delta_1\}^T\{f_1\} + \{\delta_2\}^T\{f_2\} + \cdots + \{\delta_e\}^T\{f_e\} + \cdots \\ & + \{\delta_{NE}\}^T\{f_{NE}\}) \end{aligned} \tag{5.3}$$

Now, if, in equation (5.3), the extended element displacement vectors $\{\delta_e\}$ are replaced by the overall nodal displacement vector $\{\delta\}$ which contains all the nodal displacements of the structure, the equation will not be affected because the zero locations in the stiffness matrices and force vectors will nullify the effect of the displacements added to each of the vectors $\{\delta_e\}$.

Hence,

$$V = \frac{1}{2}\Big(\{\delta\}^T[k_1]\{\delta\} + \{\delta\}^T[k_2]\{\delta\} + \dots + \{\delta\}^T[k_e]\{\delta\} + \dots + \{\delta\}^T[k_{NE}]\{\delta\}\Big) - \Big(\{\delta\}^T\{f_1\} + \{\delta\}^T\{f_2\} + \dots + \{\delta\}^T\{f_e\} + \dots + \{\delta\}^T\{f_{NE}\}\Big) \tag{5.4}$$

Using the distributive law $[A]([B] + [C])[D] = [A][B][D] + [A][C][D]$, equation (5.4) becomes:

$$V = \frac{1}{2}\Big(\{\delta\}^T([k_1] + [k_2] + \dots + [k_e] + \dots + [k_{NE}])\{\delta\}\Big) - \Big(\{\delta\}^T(\{f_1\} + \{f_2\} + \dots + \{f_e\} + \dots + \{f_{NE}\})\Big)$$

or,

$$V = \frac{1}{2}\{\delta\}^T[K]\{\delta\} - \{\delta\}^T\{F\} \tag{5.5}$$

where

$$[K] = \sum_{e=1}^{e=NE}[k_e] \qquad \text{and} \qquad \{F\} = \sum_{e=1}^{e=NE}\{f_e\}$$

Minimization of the total potential energy gives:

$$\frac{\partial V}{\partial \{\delta\}} = [K]\{\delta\} - \{F\} = 0$$

or

$$[K]\{\delta\} = \{F\}$$

Thus, $[K]$ and $\{F\}$ are the overall stiffness matrix and overall force vector.

From the preceeding discussion, it is easily recognised that knowing the global numbers of the nodes of each element, the locations, into which the element stiffnesses and loads must be inserted in the overall stiffness matrix and load vector, are immediately established.

As some elements will have common global node numbers, some locations will contain the sum of the appropriate stiffnesses and loads of these elements.

If the number of degrees of freedom per node was N, then δ_{e_1} and δ_{e_2} would be replaced by vectors of order N. e_1 and e_2 would represent N values, the first of which is N $\times$(the global node number -1)$+1$. For subsequent values, 1 is added. This is made clear by the following displacement vector:

$$\begin{array}{l} \text{global} \\ \text{node 1} \cdots\cdots \\ \\ \text{node 2} \cdots\cdots \\ \\ \\ \text{node e} \cdots\cdots \\ \\ \end{array} \left\{ \begin{array}{c} \\ \{\delta_1\} \;\; N \times 1 \\ \\ \{\delta_2\} \;\; N \times 1 \\ \vdots \\ \\ \{\delta_e\} \;\; N \times 1 \\ \vdots \end{array} \right\} \begin{array}{l} \cdots\cdots \text{row } 1 \\ \cdots\cdots \text{row } N \\ \cdots\cdots \text{row } N+1 \\ \cdots\cdots \text{row } 2N \\ \\ \cdots\cdots \text{row } N(e-1)+1 \\ \cdots\cdots \text{row } Ne \\ \\ \end{array}$$

5.1.2 Assembly of the Harmonic Stiffness Matrices and Load Vectors.

Following a procedure similar to that given in the previous section, the overall stiffness matrix can be obtained.

From equation (4.21), the potential energy of the element was given by:

$$V = \frac{1}{2}\sum_{m}\sum_{n}\{\delta^m\}_e^T[k^{mn}]_e\{\delta^n\}_e - \sum_{m}\{\delta^m\}_e^T\{f^m\}_e$$

Therefore, for the whole structure, the total potential energy is given by:

$$V = \frac{1}{2}\sum_{m}\sum_{n}\{\delta^m\}^T[K^{mn}]\{\delta^n\} - \sum_{m}\{\delta^m\}^T\{F^m\} \qquad (5.6)$$

where

$$[K^{mn}] = \sum_{e=1}^{e=NE}[k_e^{mn}] \quad \text{and} \quad \{F^m\} = \sum_{e=1}^{e=NE}\{f_e^m\} \qquad (5.7)$$

Now,

$$\frac{\partial V}{\partial\{\delta^j\}} = \sum_{m=1}^{m=M}[K^{jm}]\{\delta^m\} - \{F^j\} = 0 \qquad j=1,2,\ldots M \qquad (5.8)$$

Replacing m by n and j by m, equation (5.8) becomes

$$\sum_{n=1}^{n=M}[K^{mn}]\{\delta^n\} = \{F^m\} \qquad m=1,2,\ldots M \qquad (5.9)$$

$[K^{mn}]$, $\{\delta^n\}$ and $\{F^m\}$ are the harmonic overall stiffness matrix, harmonic overall nodal displacement parameters and harmonic overall load vector.

Written out in extended form, equation (5.9) becomes:

$$\begin{bmatrix} [K^{11}] & [K^{12}] & \dots & [K^{1n}] & \dots & [K^{1M}] \\ [K^{21}] & [K^{22}] & \dots & [K^{2n}] & \dots & [K^{2M}] \\ \vdots & \vdots & & \vdots & & \vdots \\ [K^{m1}] & [K^{m2}] & & [K^{mn}] & & [K^{mM}] \\ \vdots & \vdots & & \vdots & & \vdots \\ [K^{M1}] & [K^{M2}] & & [K^{Mn}] & & [K^{MM}] \end{bmatrix} \begin{Bmatrix} \{\delta^1\} \\ \{\delta^2\} \\ \vdots \\ \{\delta^n\} \\ \vdots \\ \{\delta^M\} \end{Bmatrix} = \begin{Bmatrix} \{F^1\} \\ \{F^2\} \\ \vdots \\ \{F^m\} \\ \vdots \\ \{F^M\} \end{Bmatrix}$$

or (5.10)

$$[K]\{\delta\} = \{F\}$$

Thus, if the harmonic overall stiffness matrices $\left[K^{mn}\right]$ and the harmonic overall force vectors $\left\{F^{m}\right\}$ m,n=1,2,....,M are assembled from the harmonic element stiffness matrices $\left[k^{mn}\right]_e$ and harmonic element force vectors $\left\{f^{m}\right\}_e$ according to the procedure given in the previous section, then the overall stiffness matrix $[K]$ and overall force vector $\{F\}$ can be formed as in equation (5.10).

5.2 General Form of the Harmonic Overall Stiffness Matrix.

The harmonic element stiffness matrix relates the harmonic nodal displacements to the harmonic nodal loads of a particular element. The harmonic overall stiffnes matrix has been shown to be an assemblage of the harmonic stiffness matrices of all the elements. It follows, therefore, that in the overall structure, when two nodes are not connected by a single element, then the locations, in the overall stiffness matrix, at the intersection of rows and columns that correspond to the degrees of freedom of these nodes, contain zero values.

In the semi-analytic approach used here, because of the nature of the division of the plate, any node will be connected by elements to two other nodes at most. In fig.(5.1), node 1, with degrees of freedom 1 and 2, is not directly connected to node 3, with degrees of freedom 5 and 6. Therefore, the locations, in the harmonic overall stiffness matrix, at the intersections of row 1 with columns 5 and 6, row 2 with columns 5 and 6, row 5 with columns 1 and 2 and row 6 with columns 1 and 2, all contain zero values. The same applies to the degrees of freedom of nodes 4, 5, etc..

Accordingly, the general form of the harmonic overall stiffness matrix will be as given in fig.(5.2).

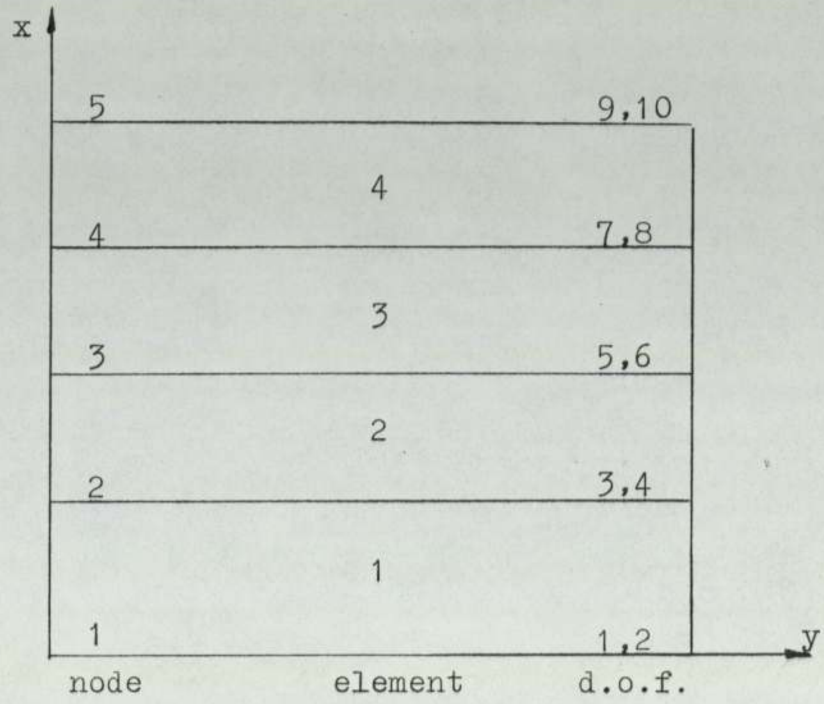

Fig.(5.1)

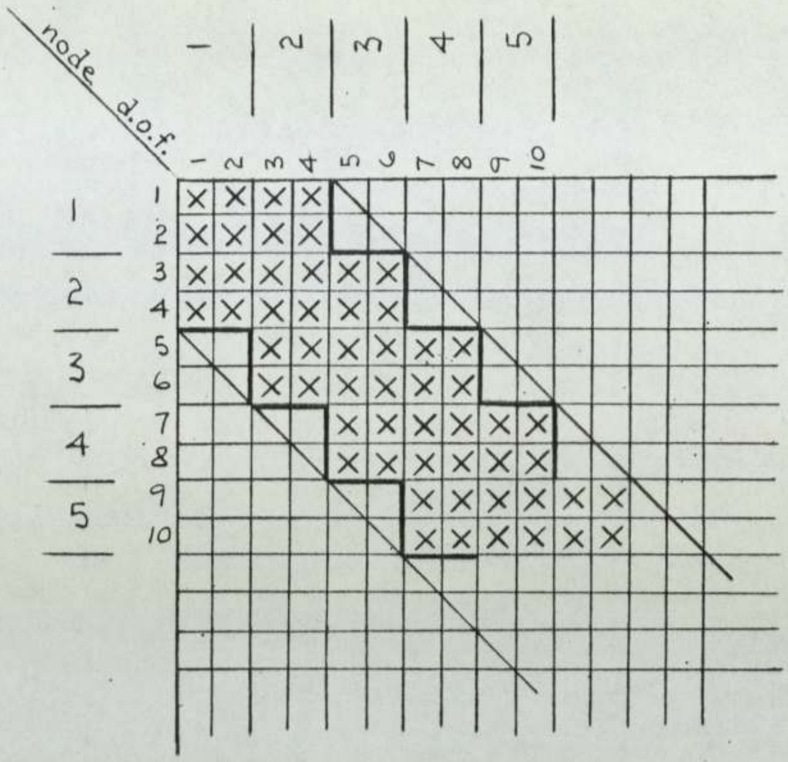

Fig.(5.2)

5.3 Grouping of the Harmonics.

Two major factors in any computer orientated numerical analysis are the computer storage requirement and the solution time. The nature of the overall stiffness matrix of a finite element method of analysis plays an important role in both factors. Generally the overall stiffness matrix is of a banded nature i.e. it contains zero elements at locations above and below a band centred about the leading diagonal. obviously, the smaller the bandwidth , the less computer storage is required and the faster is the solution. The bandwidth depends on the particular problem and the sequence in which the nodes are numbered.

In the semi-analytic approach to the plate bending problem the most favourable numbering sequence is the obvious one (fig.5.1) however, it will be seen that there is still room for improvement. The bandwidth in the overall stiffness matrix (equation 5.10) is large because the only zero elements in the matrix contributing towards the reduction of the bandwidth are those in the sub-matrices $[K^{1M}]$ and $[K^{M1}]$. This is illustrated by an example of a hypothetical problem with a total of three degrees of freedom and three harmonics, in which there is no connection between the first and the third degrees of freedom in the sense described in section (5.2). Fig.(5.3) shows the form of the overall stiffness matrix for this problem. There is a number of zeros in the harmonic matrices within the band, which has not been exploited for the reduction of the bandwidth.

The equilibrium equations of the problem can be rearranged such that all the zero elements of the sub-matrices $[K^{mn}]$ (m,n=1,2,3) are collected to the right, above the leading diagonal and to the left, below the leading diagonal, resulting in a reduced bandwidth. This is achieved by grouping together the harmonic nodal displacements of each node. Fig.(5.4) shows the rearranged equations with a more efficient form of the overall stiffness matrix.

In effect all that has been done here is that the equations and their various terms have been stated in a different order. For example, the second equation in the original set of equations stated:

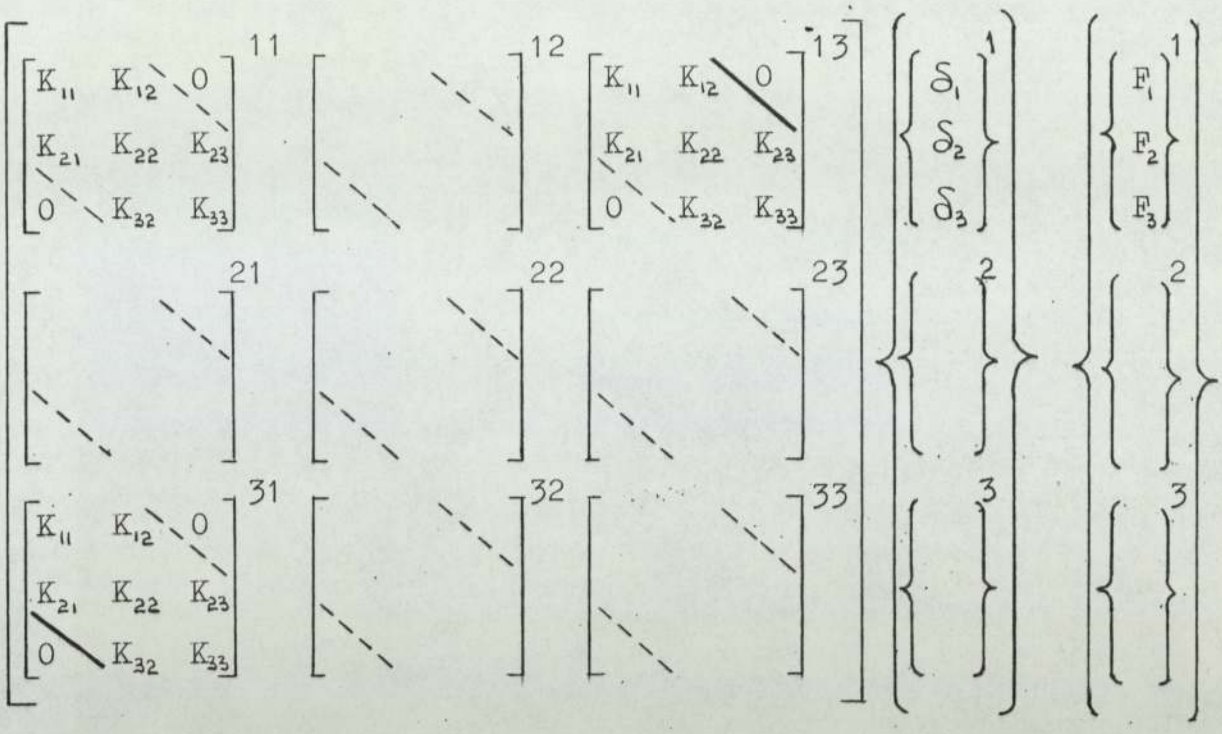

Fig.(5.3) Bandwidth of a 3 d.o.f., 3 harmonics problem.

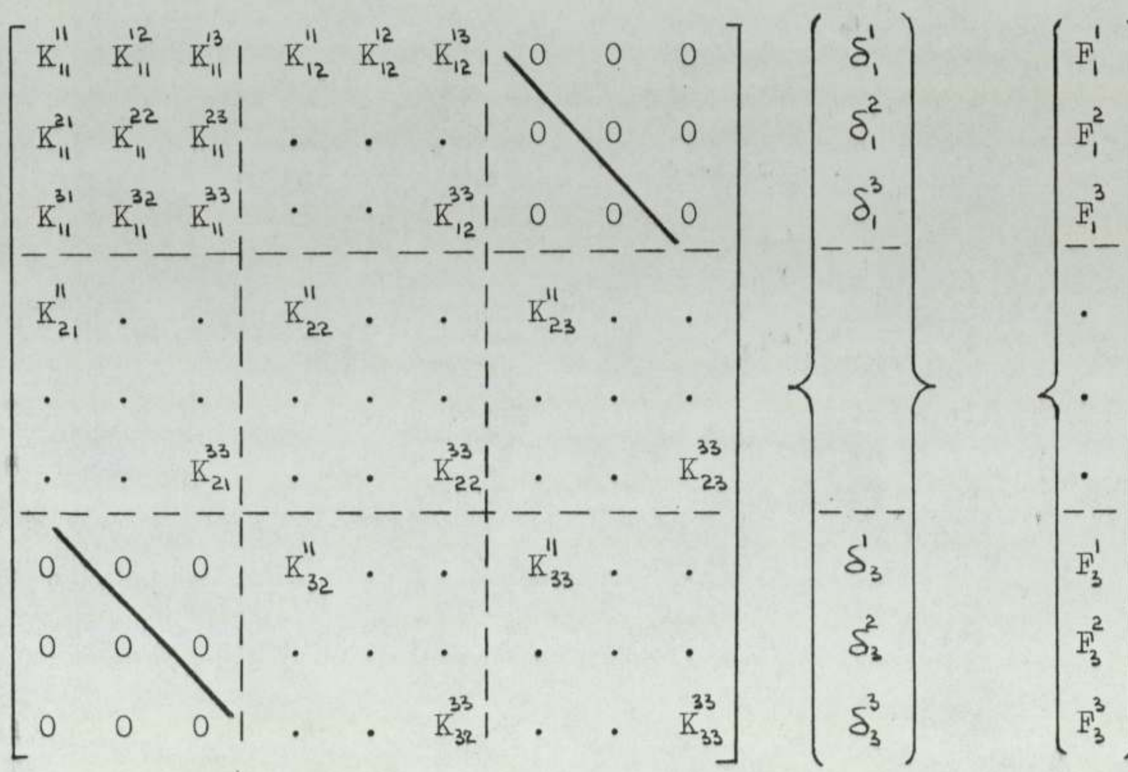

Fig.(5.4) Rearranged equations with the harmonics grouped together.

$$(K^{11}_{21}\,\delta^{1}_{1} + K^{11}_{22}\,\delta^{1}_{2} + K^{11}_{23}\,\delta^{1}_{3}\ ) + (K^{12}_{21}\,\delta^{2}_{1} + K^{12}_{22}\,\delta^{2}_{2} + K^{12}_{23}\,\delta^{2}_{3}\ )$$
$$+\ (K^{13}_{21}\,\delta^{3}_{1} + K^{13}_{22}\,\delta^{3}_{2} + K^{3}_{23}\,\delta^{3}_{3}\ ) = F^{1}_{2}$$

This equation is now the fourth equation in the rearranged set of equations which states:

$$K^{11}_{21}\delta^{1}_{1} + K^{12}_{21}\delta^{2}_{1} + K^{13}_{21}\delta^{3}_{1} + K^{11}_{22}\delta^{1}_{2} + K^{12}_{22}\delta^{2}_{2} + K^{13}_{22}\delta^{3}_{2}$$
$$+\ K^{11}_{23}\delta^{1}_{3} + K^{12}_{23}\delta^{2}_{3} + K^{13}_{23}\delta^{3}_{3} = F^{1}_{2}$$

which is identical to the original equation.

Symmetry of the overall stiffness matrix, which is important for the reduction of computer storage requirements and solution time, has been maintained.

Now, returning to the plate bending problem, the rearranged form of equations (5.10) then becomes:

$$\begin{bmatrix} [K^{rs}]_{11} & [K^{rs}]_{12} & \cdots & [K^{rs}]_{1j} & \cdots & [K^{rs}]_{1N} \\ [K^{rs}]_{21} & [K^{rs}]_{22} & \cdots & [K^{rs}]_{2j} & \cdots & [K^{rs}]_{2N} \\ \vdots & \vdots & & \vdots & & \vdots \\ [K^{rs}]_{i1} & [K^{rs}]_{i2} & \cdots & [K^{rs}]_{ij} & \cdots & [K^{rs}]_{iN} \\ \vdots & \vdots & & \vdots & & \vdots \\ [K^{rs}]_{N1} & [K^{rs}]_{N2} & \cdots & [K^{rs}]_{Nj} & \cdots & [K^{rs}]_{NN} \end{bmatrix} \begin{Bmatrix} \{\delta^{s}\}_{1} \\ \{\delta^{s}\}_{2} \\ \vdots \\ \{\delta^{s}\}_{j} \\ \vdots \\ \{\delta^{s}\}_{N} \end{Bmatrix} = \begin{Bmatrix} \{F^{r}\}_{1} \\ \{F^{r}\}_{2} \\ \vdots \\ \{F^{r}\}_{i} \\ \vdots \\ \{F^{r}\}_{N} \end{Bmatrix} \tag{5.11}$$

where

$$[K^{rs}]_{ij} = \begin{bmatrix} K^{11} & K^{12} \cdots & K^{1M} \\ K^{21} & K^{22} \cdots & K^{2M} \\ \vdots & \vdots & \vdots \\ K^{M1} & K^{M2} & K^{MM} \end{bmatrix}_{ij}$$

$$\{\delta^s\}_j = \left[\delta^1 \quad \delta^2 \quad \ldots . \quad \delta^M \right]_j^T$$

$$\{F^r\}_i = \left[F^1 \quad F^2 \quad \ldots . \quad F^M \right]_i^T$$

$$i, j = 1, 2, \ldots, N$$

N = total number of degrees of freedom.

M = number of harmonics.

5.4 Prescribed Displacements.

Before equations (5.11) can be solved, the prescribed displacements on the boundary edges parallel to the y-axis have to be incorporated into the equations.

In most cases the prescribed displacements are either zero deflection, as in the case of a simply supported edge, or zero deflection and zero rotation, as in the case of a clamped edge, or they may be non-existant , as in the case of a free edge. There is no reason, however, why problems with prescribed displacements other than zero should not be treated. It should be remembered, though , that the function which describes the non-zero displacement must satisfy the boundary conditions at the other two edges because these are built into the chosen eigenfunction.

The prescribed displacement has to be in a form suitable for insertion into the equations. This is achieved by harmonic analysis.

Let the prescribed displacement be $\delta^*(\xi)$, where $\xi = {}^y/_a$.

This displacement can be represented by a series of the same form as the assumed deflection function i.e.

$$\delta^*(\xi) = \sum_{m=1}^{\infty} \delta^{*m} \, Y_m(\xi) \tag{5.12}$$

where $Y_m(\zeta)$ is the beam eigenfunction of the particular problem and δ^{*m} is the harmonic prescribed displacement.

Multiplying both sides of equation (5.12) by $Y_n(\zeta)$ and integrating over the length of the edge gives:

$$\int_0^1 \delta^*(\zeta)\, Y_n(\zeta)\, d\zeta = \sum_{m=1}^{\infty} \delta^{*m} \int_0^1 Y_m(\zeta)\, Y_n(\zeta)\, d\zeta$$

Applying the orthogonality property of the beam eigenfunctions (appendix A2.2), the right-hand side is non-zero only when m=n. Therefore,

$$\delta^{*m} = \frac{\int_0^1 \delta^*(\zeta)\, Y_m(\zeta)\, d\zeta}{\int_0^1 Y_m^2(\zeta)\, d\zeta} \qquad (5.13)$$

$$m=1,2,\ldots,M$$

Thus, the harmonic prescribed displacement δ^{*m} can be evaluated for m=1,2,...,M.

In the cases where the prescribed displacement has a zero value, the harmonic prescribed displacement δ^{*m} is zero for all values of m (equation 5.13).

5.4.1 Statement of Prescribed Displacements

If the displacement is prescribed on the l^{th} degree of freedom, then

$$\{\delta^s\}_l = \{\delta^{*s}\} \qquad s=1,2,\ldots,M \qquad (5.14)$$

where $\{\delta^{*s}\}$ is obtained using equation (5.13).

Substitution of equations (5.14) into equations (5.11) yields:

$$\begin{bmatrix} [K^{rs}]_{11} & [K^{rs}]_{12} & \cdots & [K^{rs}]_{1l} & \cdots & [K^{rs}]_{1N} \\ [K^{rs}]_{21} & [K^{rs}]_{22} & \cdots & [K^{rs}]_{2l} & \cdots & [K^{rs}]_{2N} \\ \vdots & \vdots & & \vdots & & \vdots \\ [0^{rs}]_{l1} & [0^{rs}]_{l2} & \cdots & [I^{rs}]_{ll} & \cdots & [0^{rs}]_{lN} \\ \vdots & \vdots & & \vdots & & \vdots \\ [K^{rs}]_{N1} & [K^{rs}]_{N2} & \cdots & [K^{rs}]_{Nl} & \cdots & [K^{rs}]_{NN} \end{bmatrix} \begin{Bmatrix} \{\delta^s\}_1 \\ \{\delta^s\}_2 \\ \vdots \\ \{\delta^s\}_l \\ \vdots \\ \{\delta^s\}_N \end{Bmatrix} = \begin{Bmatrix} \{F^r\}_1 \\ \{F^r\}_2 \\ \vdots \\ \{\overset{*}{\delta}{}^s\}_l \\ \vdots \\ \{F^r\}_N \end{Bmatrix} \qquad (5.15)$$

where $[0^{rs}]$ and $[I^{rs}]$ are the null matrix and the identity matrix respectively, both of order M.

It is apparent from equations(5.15) that the symmetry of the overall stiffness matrix has been disturbed. To remedy this, each equation

$$[K^{rs}]_{i1} \ \{\delta^s\}_1 + [K^{rs}]_{i2} \ \{\delta^s\}_2 + \cdots + [K^{rs}]_{il} \ \{\delta^s\}_l + \cdots$$

$$+ [K^{rs}]_{iN} \ \{\delta^s\}_N = \{F^r\}_i \qquad i=1,2,\ldots,N \quad i \neq l$$

is considered in turn and the term $[K^{rs}]_{il} \ \{\delta^s\}_l$ is taken to the right hand side after substituting for $\{\delta^s\}_l$ from equation (5.14). Thus the i^{th} equation becomes:

$$[K^{rs}]_{i1} \ \{\delta^s\}_1 + [K^{rs}]_{i2} \ \{\delta^s\}_2 + \cdots + [0^{rs}]_{il} \ \{\delta^s\}_l + \cdots$$

$$+ [K^{rs}]_{iN} \ \{\delta^s\}_N = \{F^r\}_i - [K^{rs}]_{il} \ \{\overset{*}{\delta}{}^s\}$$

With this process carried out for all, but the lth , of the matrix equations in (5.15), these equations become:

$$\begin{bmatrix} [K^{rs}]_{11} & [K^{rs}]_{12} & \cdots & [0^{rs}]_{1l} & \cdots & [K^{rs}]_{1N} \\ [K^{rs}]_{21} & [K^{rs}]_{22} & \cdots & [0^{rs}]_{2l} & \cdots & [K^{rs}]_{2N} \\ \vdots & \vdots & & \vdots & & \vdots \\ [0^{rs}]_{l1} & [0^{rs}]_{l2} & \cdots & [I^{rs}]_{ll} & \cdots & [0^{rs}]_{lN} \\ \vdots & \vdots & & \vdots & & \vdots \\ [K^{rs}]_{N1} & [K^{rs}]_{N2} & & [0^{rs}]_{Nl} & & [K^{rs}]_{NN} \end{bmatrix} \begin{Bmatrix} \{\delta^s\}_1 \\ \{\delta^s\}_2 \\ \vdots \\ \{\delta^s\}_l \\ \vdots \\ \{\delta^s\}_N \end{Bmatrix}$$

$$= \begin{Bmatrix} \{F^r\}_1 - [K^{rs}]_{1l} \{\delta^{*s}\} \\ \{F^r\}_2 - [K^{rs}]_{2l} \{\delta^{*s}\} \\ \vdots \\ \{\delta^{*s}\} \\ \vdots \\ \{F^r\}_N - [K^{rs}]_{Nl} \{\delta^{*s}\} \end{Bmatrix} \qquad (5.16)$$

The symmetry of the overall stiffness matrix has, thus, been restored.

5.5 Solution of the Equations.

Having modified the equilibrium equations, to include the statement of prescribed displacements, they are ready for solution.

There are many methods for the solution of a large system of equations each of which may be more suitable for one system of equations than for another. One of the more efficient methods for the solution of equations whose coefficient matrix is symmetric and positive definite is the Cholesky Decomposition Method [37].

Fung [38] shows, on thermodynamics grounds, that the strain energy function of a solid body must be positive definite, i.e. it must be non-negative and it is zero only in the natural state. The positive definiteness of the strain energy implies certain relationships between the stiffness (or influence) coefficients. In the equation $U = \{\delta\}^T[K]\{\delta\}$, when $U > 0$ for $\delta_i \neq 0$ and $U=0$ for $\delta_i = 0$, then the sum of the coefficients K_{ii} and the determinant $|K_{ij}|$ are both positive.

Symmetry of the matrix $[K]$ is established on the basis of the reciprocal theorem [38].

Thus, the coefficient matrices arising from a displacement (or equilibrium) formulation to the finite element method are symmetric and positive definite. Consequently the Cholesky Decomposition Method for the solution of equations is applicable here.

The Cholesky Decomposition Method is based on the following theorem:

If $[K]$ is a symmetric positive definite matrix, then there exists a real non-singular lower triangular matrix

[L] such that

$$[L][L]^T = [K].$$

where

$$l_{ij} = 0 \quad \text{for } i < j$$

The elements of [L] are obtained thus: Modifying the usual rules of matrix multiplication to include the symmetric property of [K] and triangular property of [L], the following equations are obtained.

$$k_{ii} = \sum_{r=1}^{i} l_{ir}\, l_{ir} \qquad i=1,2,\ldots n \tag{5.17}$$

$$k_{ij} = \sum_{r=1}^{j} l_{ir}\, l_{jr} \qquad \begin{array}{l} i=2,3,\ldots n \\ j=1,2,\ldots i-1 \end{array} \tag{5.18}$$

where n is the order of the matrix [K].

Equation (5.17) may be re-written as:

$$k_{ii} = l_{ii}\, l_{ii} + \sum_{r=1}^{i-1} l_{ir}\, l_{ir} \qquad \text{from which:}$$

$$l_{ii} = (k_{ii} - \sum_{r=1}^{i-1} l_{ir}^2)^{\frac{1}{2}} \qquad i=2,3,\ldots n \tag{5.19}$$

when $i = 1$, $l_{11} = k_{11}$

Similarly from equation (5.18)

$$k_{ij} = l_{ij}\, l_{jj} + \sum_{r=1}^{j-1} l_{ir}\, l_{jr}$$

Therefore,

$$l_{ij} = (k_{ij} - \sum_{r=1}^{j-1} l_{ir}\, l_{jr}) \;/\; l_{jj} \qquad \begin{matrix} i=2,3,\ldots n \\ j=1,2,\ldots i-1 \\ i>j \end{matrix} \qquad (5.20)$$

Alternate evaluation of equations (5.19) and (5.20) gives all the elements of the matrix $[L]$. The solution of the equations $[K]\{\delta\} = \{F\}$, then, proceeds in the following steps:

$$[K]\{\delta\} = \{F\}$$

or

$$[L]\,[L]^T\{\delta\} = \{F\}$$

Letting $\{Y\} = [L]^T\{\delta\}$, the equation becomes:

$$[L]\{Y\} = \{F\}$$

Hence $\{Y\}$, hence $\{\delta\}$.

An element by element process is given by

$$\begin{aligned} y_i &= (b_i - \sum_{r=1}^{i-1} l_{ir}\, y_r) \;/ l_{ii} \\ \delta_i &= (y_i - \sum_{r=1}^{n} l_{ri}\, \delta_r) \;/ l_{ii} \end{aligned} \qquad i=1,2,\ldots n \qquad (5.21)$$

This method of solution is easily adapted to take advantage of the banded nature of the matrix $[K]$. In this case, the operations involved in arriving at equations (5.19), (5.20) and (5.21) are carried out with the convention that $k_{ij}=0$ for $|i-j|>(B-1)$ where B is the semi-bandwidth [39]. This, in fact, is the statement of a banded matrix.

5.6 Solution of the Problem.

The solution of the equations yields the harmonic nodal displacement parameters from which all the necessary information for the solution of the plate stressing problem can be obtained.

5.6.1 Deflections and Rotations.

The deflection and rotations anywhere on the plate may be evaluated by using equation (4.10) i.e.

$$w = \sum_{m=1}^{M} [N] \{\delta^m\}_e Y_m$$

$$\theta_x = -\frac{\partial w}{\partial x} = -\sum_{m=1}^{M} [N'] \{\delta^m\}_e Y_m \qquad (5.22)$$

$$\theta_y = \frac{\partial w}{\partial y} = \sum_{m=1}^{M} [N] \{\delta^m\}_e Y'_m$$

Generally, the deflection and the rotations are evaluated at a discrete number of points along each node in order to obtain an overall picture of the state of displacement of the plate. Thus, substituting the appropriate values of x and y into equations (5.22), the displacements on the nodes are given by:

$$w_k = \sum_{m=1}^{M} w_{km} Y_m (y=y_o)$$

$$(\theta_x)_k = \sum_{m=1}^{M} \theta_{km} Y_m (y=y_o) \qquad k=1,2,\ldots,nnode \qquad (5.23)$$

$$(\theta_y)_k = \sum_{m=1}^{M} w_{km} Y'_m (y=y_o)$$

where nnode is the total number of nodes.

Y_m and Y'_m are evaluated at the appropriate points, $y=y_o$, on the nodes.

5.6.2 Moments, Shearing Forces and Stresses.

The bending and twisting moments are evaluated from equations (4.11) and (4.15), i.e.

$$M = \begin{Bmatrix} M_x \\ M_y \\ M_{xy} \end{Bmatrix} = D[D^*] \sum_{m=1}^{M} \begin{bmatrix} -[N''] \; Y_m \\ -[N] \; Y''_m \\ -2[N'] \; Y'_m \end{bmatrix} \{\delta^m\}_e$$

The principal moments M_p which represent the maximum and minimum values of the bending moments, and the pertinent angle α at which they occur, and the maximum and minimum twisting moments M_{nt} [4] are given by:

$$(M_p)_{\substack{max \\ min}} = \frac{M_x + M_y}{2} \pm \frac{1}{2} \sqrt{(M_x - M_y)^2 + 4M_{xy}^2}$$

$$\tan 2\alpha = \frac{2M_{xy}}{M_x - M_y}$$

$$(M_{nt})_{\substack{max \\ min}} = \pm \frac{1}{2} \sqrt{(M_x - M_y)^2 + 4M_{xy}^2}$$

The shearing forces are obtained from equations (2.9)

i.e. $$\{Q\} = \begin{Bmatrix} Q_x \\ Q_y \end{Bmatrix} = -D \begin{Bmatrix} \left(\dfrac{\partial^3 w}{\partial x^3} + \dfrac{\partial^3 w}{\partial x \, \partial y^2}\right) \\ \left(\dfrac{\partial^3 w}{\partial y^3} + \dfrac{\partial^3 w}{\partial y \, \partial x^2}\right) \end{Bmatrix}$$

Substituting for w from equation (4.10) the shearing forces will be:

$$\begin{Bmatrix} Q_x \\ Q_y \end{Bmatrix} = -D \sum_{m=1}^{M} \begin{bmatrix} ([N'''] \, Y_m + [N'] \, Y''_m) \\ \\ ([N] \, Y'''_m + [N''] \, Y'_m) \end{bmatrix} \{\delta^m\}_e$$

The effective shearing forces are similarly evaluated from expressions (2.18) and (4.10).

$$\{V\} = \begin{Bmatrix} V_x \\ V_y \end{Bmatrix} = -D \sum_{m=1}^{M} \begin{bmatrix} ([N'''] \, Y_m + (2-\nu)[N'] \, Y''_m) \\ \\ ([N] \, Y'''_m + (2-\nu)[N''] \, Y'_m) \end{bmatrix} \{\delta^m\}_e$$

The stresses are evaluated using expressions (2.11). Thus,

$$\{\sigma\} = \begin{Bmatrix} \sigma_x \\ \sigma_y \\ \tau_{xy} \end{Bmatrix} = \frac{6}{h^2} \begin{Bmatrix} M_x \\ M_y \\ M_{xy} \end{Bmatrix}$$

Similarly, the principal stresses and maximum shearing stress are obtained.

The matrices $[N]$, $[N']$ and $[N'']$ in the expressions above are evaluated at the appropriate node, and the functions Y_m, Y'_m, Y''_m and Y'''_m are evaluated at the appropriate value of y.

CHAPTER 6

CHAPTER SIX.

DEVELOPMENT OF THE COMPUTER PROGRAM.

6.1 Introduction.

The process, for the analysis of plate bending problems, which was outlined in the previous chapters, has to be written in the form of a computer program.

To recapitulate, this process consisted of the following steps:

1. The plate is divided, in one direction, into a suitable number of strip elements and a suitable number of modes is decided upon.
2. Information regarding the dimensions, rigidity and applied load for each element is made available.
3. The stiffness matrix and load vector are evaluated for each element and for each mode.
4. The overall stiffness matrix and overall force vector are assembled.
5. The overall stiffness matrix and overall force vector are modified to include the statement of prescribed displacements.
6. The equations are solved yielding the harmonic nodal displacement parameters.
7. The deflection, rotations, moments, shear forces and stresses are calculated at a discrete number of points on the plate.

Whenever possible and, indeed, whenever it is more efficient, the systematic execution of these operations by the computer is carried out using self-contained program segments called "Procedures".

6.2 Division of the Plate into Strip Elements.

Once the oerientation of the plate is decided upon with respect to the direction in which the analytic function is applied, there will be only one way in which the plate may be divided into strip elements, and provided that the elements, local and global nodal lines and local and global degrees of freedom (d.o.f.) are always numbered in the same sequence, fig.(6.1), then many of the required variables may be obtained from other variables, thus, the input information, for which data preparation is required, is reduced.

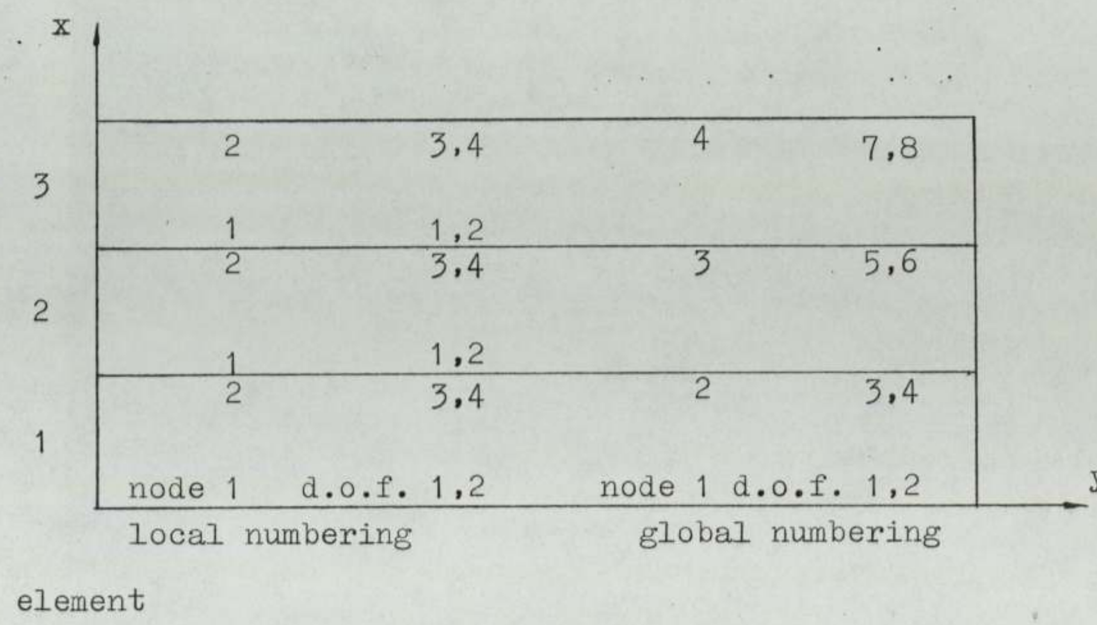

Fig.(6.1)

The relationship between the global node number and the element number will always be:

$$n_g = e + n_l - 1$$

where n_g is the global node number , e is the element number and n_l is the local node number =1,2.

The relationship between the element member and the global d.o.f. will be:

$$d_g = 2(e-1) + d_l$$

where d_g is the global d.o.f. and d_l is the local d.o.f.

$d_l = 1,2,3,4.$

The local d.o.f. 1,2,3,4 refer to the deflection and rotation parameters of the first node and deflection and rotation of the second node respectively.

6.3 Plate Flexural Rigidity and Applied Distributed Pressure.

In this section reference is made to the flexural rigidity only, but the procedure applies equally to a distributed pressure, if any is applied.

The flexural rigidity may be available in a form suitable for direct input into the computer as in the cases of uniform rigidity or variable rigidity approximated by step-wise uniformity. On the other hand, it may be available as a function of the co-ordinates x and y and the variation is such that it requires a better approximation than step-wise uniform. In this case, the flexural rigidity may be treated as step-wise linear (section 4.7.2). For this purpose, the strip element is assumed to be divided into a number of steps over each of which the rigidity is assumed to vary according to the equation

$$D_s = D_{1s}\,x + D_{2s}\,y + D_{3s} \tag{6.1}$$

where s is the step number.

In some cases the constants D_{1s}, D_{2s} and D_{3s} are readily available and may be read-in into the computer directly as in the case where the true variation of the rigidity is linear. In other cases, these constants may be evaluated from the actual values of the rigidity at the corners of each step. To this end, a procedure LSTSQR has been written. Referring to fig.(6.2), the input parameters to this procedure are:

1. The step number,
2. The element number,
3. Values of x and y at points 1,2,3 and 4
4. Values of D at the same points.

Fig.(6.2)

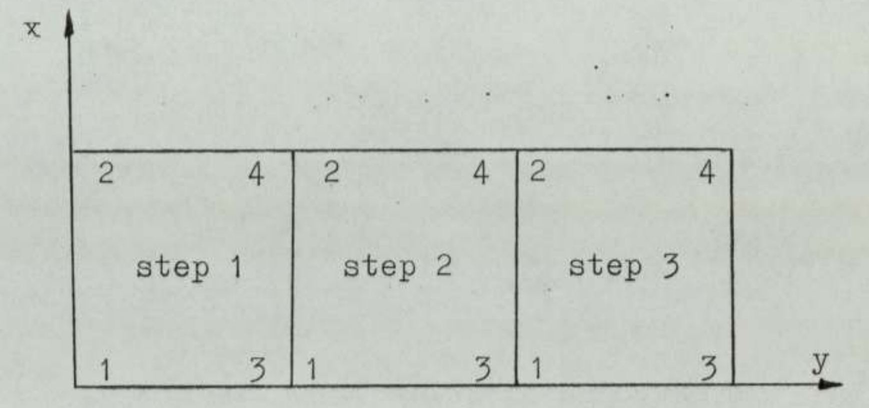

The first three quantities are obtained automatically from other input parameters. The values of D must be read in the following sequence: four values for the first step, $(D)_1$, $(D)_2$, $(D)_3$ and $(D)_4$ and two values for each subsequent step, $(D)_3$ and $(D)_4$. The values of $(D)_1$ and $(D)_2$ for step s(>1) are taken equal to $(D)_3$ and $(D)_4$, respectively, for step (s-1).

The procedure LSTSQR is based on the theory outlined in appendix (5). Its output are the coefficients of the linear equation (6.1).

The same procedure is used, when necessary, for variable applied distributed pressure, by changing the procedure's dummy variables to those relating to the load. This, however, is carried out automatically.

6.4 The Harmonic Element Stiffness Matrix and Harmonic Element Force Vector.

To obtain these quantities, equations (4.22) and (4.30) are used. In these equations, integrals of the analytic functions, integrals of products of these functions and integrals of various derivatives of these functions have to be evaluated.

In chapter seven, section (7.4), a discussion regarding the numerical instability of the higher modes of the analytic functions will be given and a modification of these functions will be suggested. It is the modified form of the analytic functions that the computer program processes.

A real procedure HARM has been written to give the roots, μ_r, of the characteristic equations for any specified eigenfunction for all desired modes (r=1,2,...,M). Specification of the function is carried out using a variable which denotes the boundary conditions of the function. Another variable is used to indicate cases of symmetry about y=a/2 in order to deal with odd modes only (section 4.3) and reduce computer storage requirement and analysis time.

The procedure IY evaluates the integral of the analytic functions, $\int Y_m \, dy$, for m=1,2,...,M and for the specified end limits. This procedure calls up two other procedures, IFI, which evaluates the integrals of the trigonometric and exponential functions that constitute the analytic function, and CI, which evaluates the coefficients of these functions for the specified boundary conditions.

The procedure IYY evaluates the integral of products of the analytic functions and their required derivatives $\int \Phi_r^{mn}$ dy equation (4.23) for m,n=1,2,...,M and for the specified end limits. This procedure also calls up two other procedures, IFIFI for integrating products of trigonometric and exponential functions, and CI as before.

The procedures IY and IYY also evaluate the integrals $\int y \, Y_m$ dy and $\int y \, \Phi_r^{mn}$ dy respectively. These integrals are necessary when the distributed pressure and flexural rigidity are assumed to be piece-wise linear.

6.5 The Variable Bandwidth, One-Dimensional Array Scheme for the Storage of the Stiffness Matrix.

The overall stiffness matrix K contains many zeros which would have to be stored if any of the mose widely used storage schemes was employed. A method, developed by Alan Jennings [40] in conjunction with an equation solving procedure, is the variable bandwidth, one-dimensional array scheme for symmetric matrices. This method reduces the storage requirement by storing the elements below the leading diagonal in sequence by rows with all the elements preceeding the first non-zero in each row omitted.

An address array is used to locate the position of the elements in the leading diagonal for each row.

In this way, a matrix K_{ij}, such as shown in Fig.(6.3) would be stored as the one-dimensional array K_l' .

$$\begin{bmatrix} 1.0 & 0.5 & 0 & 0 & 0 & 0 \\ 0.5 & 2.2 & 0.8 & 1.1 & 0 & 0 \\ 0 & 0.8 & 2.7 & 0 & 0 & 0.2 \\ 0 & 1.1 & 0 & 3.1 & 0.1 & 0 \\ 0 & 0 & 0 & 0.1 & 3.0 & 0 \\ 0 & 0 & 0.2 & 0 & 0 & 2.9 \end{bmatrix}$$

Fig.(6.3)

The one-dimensional array will be

l	1	2	3	4	5	6	7	8	9	10	11	12	13	14
K'_l	1.0	0.5	2.2	0.8	2.7	1.1	0	3.1	0.1	3.0	0.2	0	0	2.9

The address array A will be

r	1	2	3	4	5	6
A_r	1	3	5	8	10	14

The r^{th} integer of the address array, A_r , indicates that the leading diagonal element of the r^{th} row of matrix K_{ij} (i.e. K_{rr}) is the $(A_r)^{th}$ element of the array K'_l (i.e. K'_{A_l}).

A simple relationship for the correspondence of one element in the matrix to the same element in the array is

$$K(i,j) = K'(A_i - i + j).$$

This relationship applies only to the elements following the first non-zero element in each row of the lower triangle.

6.5.1 Algorithm for Forming the Address Array.

Since the division of the plate can only be carried out in a unique way from the point of view of arrangement of the strip elements, the overall stiffness matrix will always be of the same form. Fig.(6.4) shows this form, based on grouping the harmonics together (section 5.3).

Taking advantage of this fact a simplified algorithm for forming the address array can be written. The variables involved in the algorithm are:

NHARM	the number of modes (harmonics).
m	current mode number.
r	current row number in the overall stiffness matrix.
OVADD [r]	the address of the diagonal element of the $r^{th.}$ row in the overall stiffness matrix.
i	current node number.
TNNODE	total number of nodes.

Referring to fig.(6.4), the following relationships are obtained:

The number of rows for the first two nodes

$$= 2 \text{ (nodes) } \times 2 \text{ (d.o.f./node) } \times \text{NHARM}$$

$$= 4\text{NHARM}.$$

For these rows, the address is

$$\text{OVADD}[r] = \text{OVADD}[r-1] + r \qquad r=1,2,\ldots,4\text{NHARM};\ \text{OVADD}[0]=0.$$

For subsequent rows:

$$\left.\begin{array}{l} r = (i-1)\,2\text{NHARM} + m \\ \text{OVADD}[r] = \text{OVADD}[r-1] + 2\text{NHARM} + m \end{array}\right\} \begin{array}{l} i = 3,4,\ldots,\text{TNNODE} \\ m = 1,2,\ldots,2\text{NHARM} \end{array}$$

Based on the above relationships, the procedure ADDARRAY is written. The flow diagram for ADDARRAY is given in fig.(6.5).

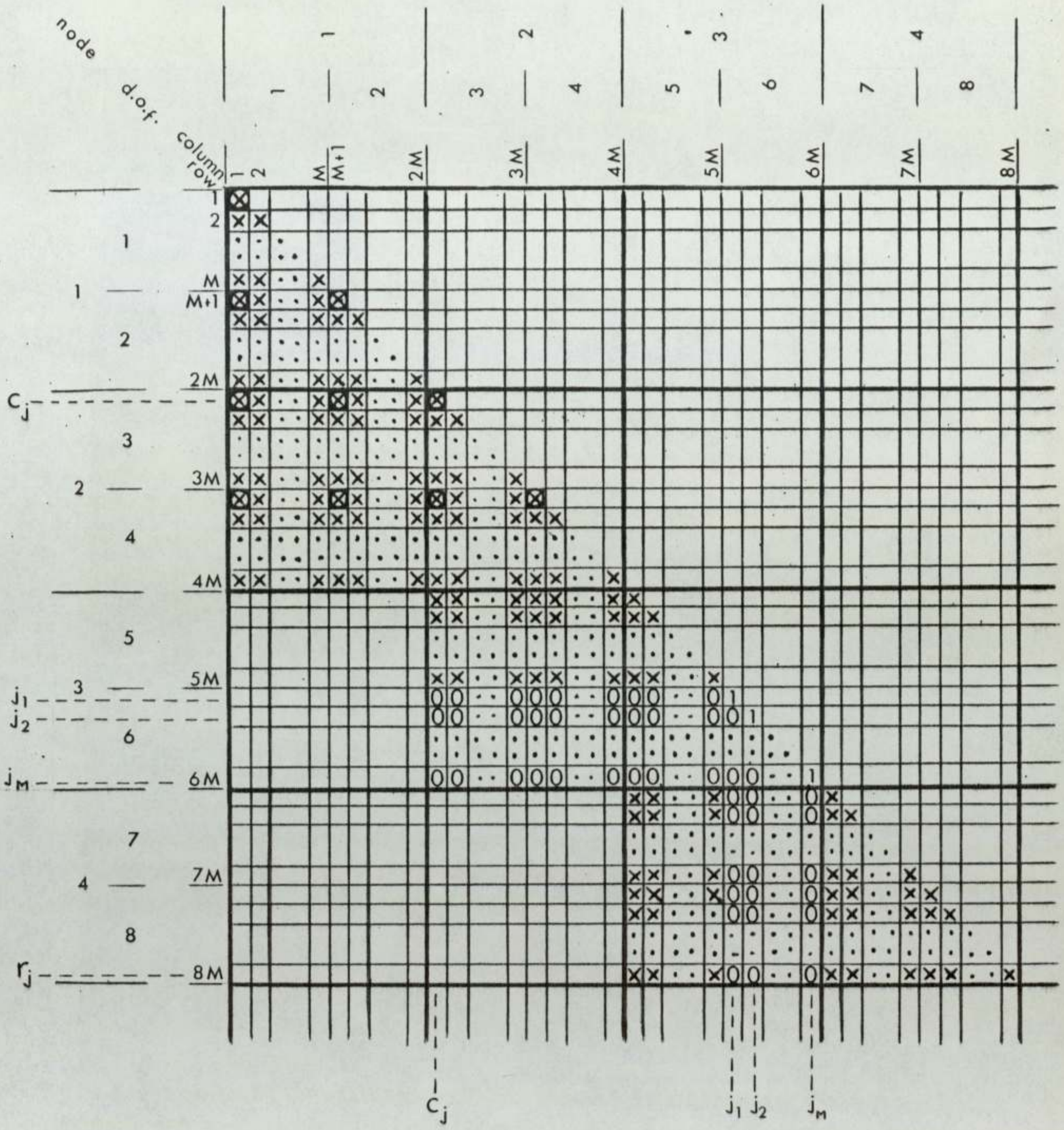

Fig.(6.4) Typical Overall Stiffness Matrix showing non-zero locations, x, and contribution of the first element for m=n=1, ⊗, and the modification necessary for statement of the prescribed displacement on an arbitrary degree of freedom 6.

Fig.(6.5). Flow diagram for the procedure ADDARRAY

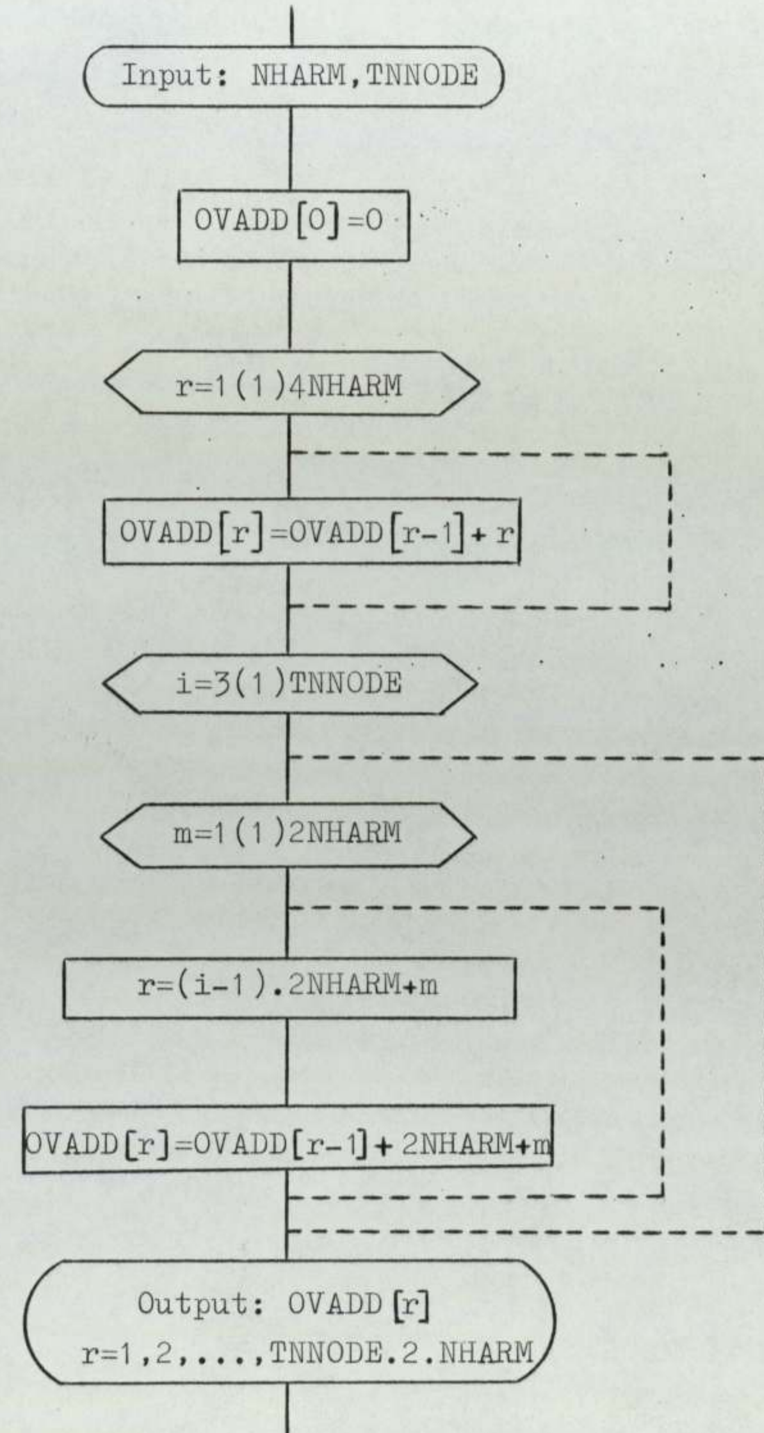

6.5.2 Algorithm for the Assembly of the Overall Stiffness Array and Overall Force Vector.

Following the process outlined in sections (5.1.2) and (5.3), a procedure ASSEMBLY has been written to form the overall stiffness matrix, as a variable bandwidth one dimensional array, and the overall force vector.

The variables involved in this algorithm, in addition to those previously used, are:

i,j	current row and column numbers in the overall stiffness matrix.
s,t	current row and column numbers in the harmonic element stiffness matrix.
k	element number.
ii,jj	global degrees of freedom.
HEK	harmonic element stiffness matrix.
HEF	harmonic element force vector.
l	location in the overall stiffness array corresponding to location ij in the overall stiffness matrix.
OVK	overall stiffness array.
OVF	overall force vector.

From previous considerations and with the aid of fig.(6.4), the following relationships are obtained:

$$ii = 2(k-1) + s \qquad s = 1,2,3,4$$

$$jj = 2(k-1) + t \qquad t = 1,2,3,4$$

$$i = \mathrm{NHARM}\,(ii-1) + n \qquad n = 1,2,\ldots,\mathrm{NHARM}$$

$$j = \mathrm{NHARM}\,(jj-1) + m \qquad m = 1,2,\ldots,\mathrm{NHARM}$$

$$l = \mathrm{OVADD}[i] - i + j$$

The overall stiffness array and overall force vector will then be given by:

OVK [l] = OVK [l] + HEK [s,t] and

OVF [i] = OVF [i] + HEF [s] .

Based on these relationships, the flow diagram for the procedure ASSEMBLY will be as given in fig.(6.6).

6.6 Algorithm for the Statement of the Prescribed Displacement.

A procedure GEOMBC has been developed to modify the overall stiffness array and the overall force vector to include the statement of prescribed displacements on the boundary edges normal to the x-axis. The procedure is based on the theory given in section (5.4.1).

Because it is extremely difficult to develop a general method to deal with any prescribed displacement function, the procedure, in its present form, had been written in such a way as to accept zero prescribed displacements and allow a simple modification, to be carried out by the user, in order to accomodate a specific prescribed displacement function. The positions on the procedure where a user must carry out these modifications are indicated on the flow diagram (fig.6.7). Variables not previously used are:

NPD	number of prescribed displacements.
p	current number of prescribed displacement.
PD[p]	value of prescribed displacement.
DF[p]	the degrees of freedom on which the displacements are prescribed.

j	row number of each harmonic corresponding to DF [p].
b	total number of rows above and below j.
c_j	column number of the first non-zero element of the j^{th} row = row number of the first non-zero element of the j^{th} column (by symmetry).
r_j	row number of the last non-zero element in the j^{th} column.
TOTDF	total number of degrees of freedom.
i,j	current location where modification to the overall stiffness array is taking place.

Once again referring to fig.(6.4), the following relationships may be obtained:

If DF [p] = 1 or 2 or (TOTDF-1) or TOTDF then

b = 4NHARM - 1 , otherwise b = 6NHARM - 1 .

$$j = (DF[p] - 1) \times NHARM + m \qquad m=1,2,\ldots,NHARM$$

$$c_j = j - (OVADD[j] - OVADD[j-1]) + 1$$

$$r_j = b + c_j$$

The flow diagram for the procedure GEOMBC is given in fig.(6.7).

Fig.(6.4) gives an example of the modification to the overall stiffness matrix and fig.(6.8) shows a modified force vector.

Fig.(6.6). Flow diagram for the procedure ASSEMBLY

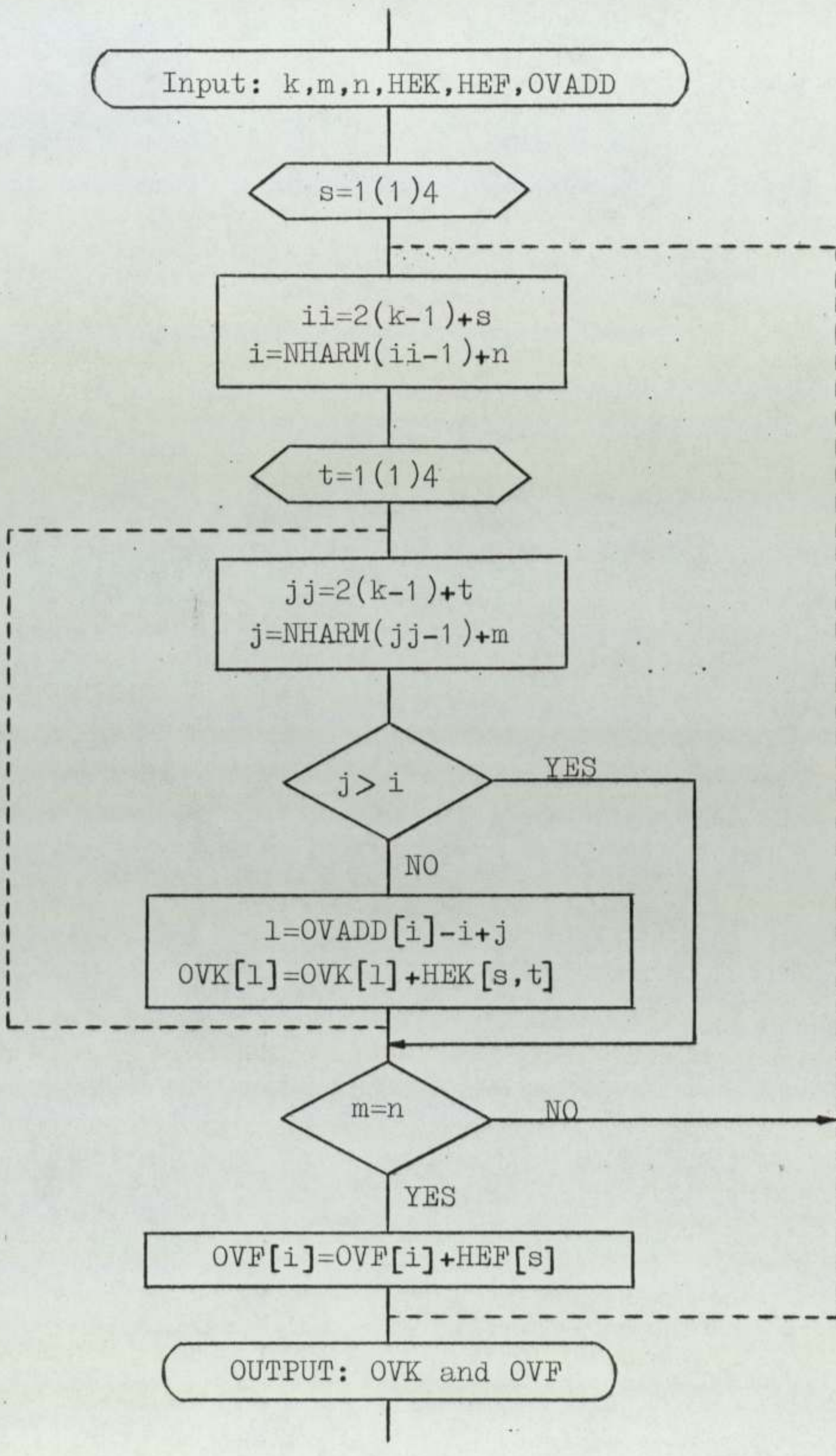

Fig.(6.7). Flow diagram for the procedure GEOMBC

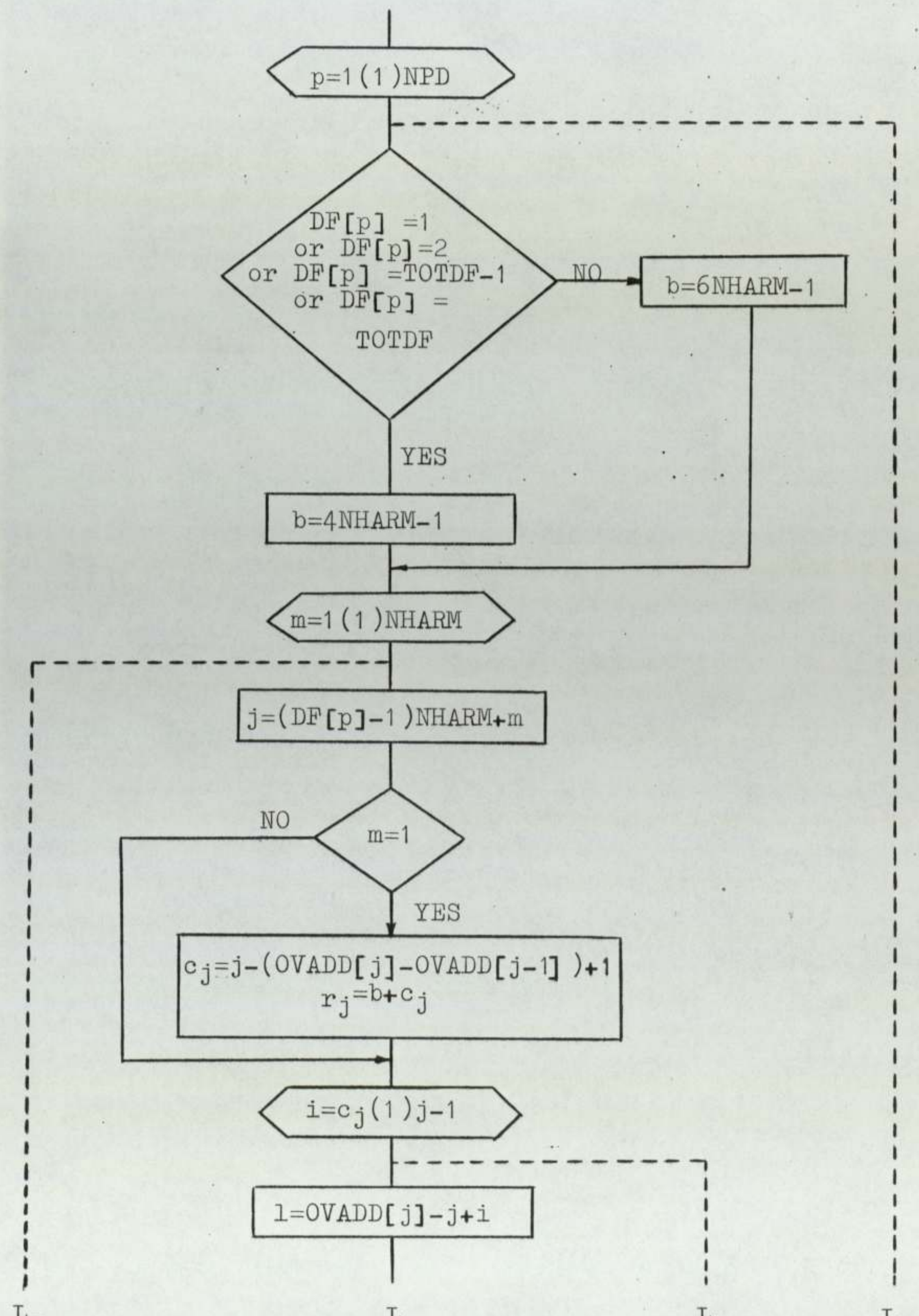

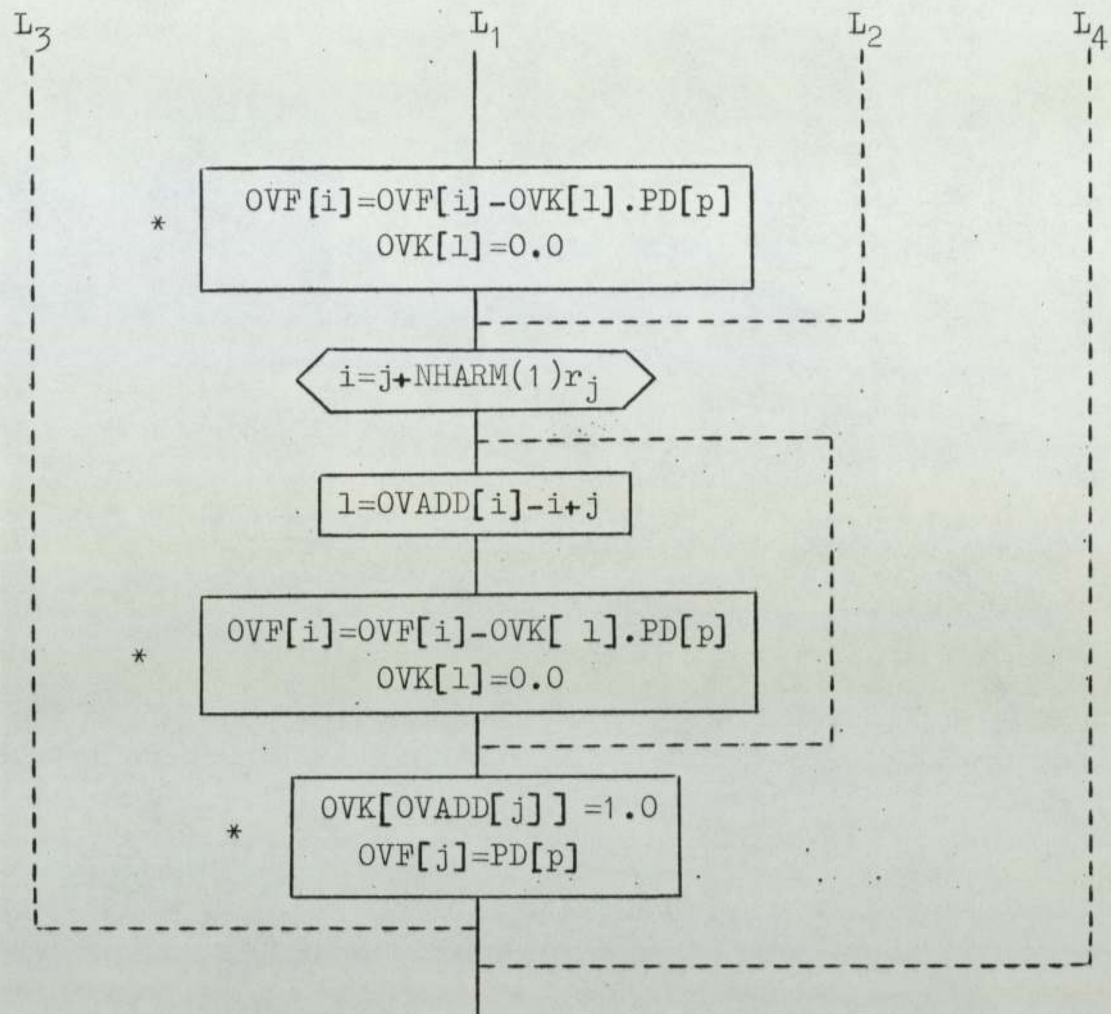

If the prescribed displacement is not zero,then a harmonic analysis of the function representing the prescribed displacement must be carried out as laid down in section (5.4). The resulting harmonic prescribed displacement must, then, replace PD[p] at the indicated positions (*).

Fig.(6.8) Typical Overall Force Vector modified to account for prescribed displacement on global d.o.f. 6 . The original forces are designated by x.

6.7 Solution of the Equations.

The algorithm used for this purpose is SYMVBSOL which was developed by Alan Jennings [41] for the solution of variable bandwidth positive definite equations. It is based on the Cholesky Factorization Method, a description of which was given in section (5.5).

The algorithm solves the system of equations [A] [X] = [B] where [A] is a symmetric positive definite matrix of order N stored in variable bandwidth one dimensinal form, and [B] is an N x R matrix of R right hand sides. The solution [X] overwrites [B].

The algorithm is a generalisation of the fixed bandwidth method developed by Martin and Wilkinson [39].

6.8 Solution of the Problem.

SYMVBSOL yields the harmonic nodal displacement parameters. From these, the deflection, rotation, moments, shear forces and stresses are obtained by using the expressions developed in section (5.6).

6.9 The Overall Picture.

A brief description of the computer program as a whole is given in the form of a flow diagram (fig.6.9). The procedures which may be called for some of the operations are indicated.

Additional variables are:

QTYPE	type of the applied distributed pressure. More detailed description of this variable is given in section (6.10).

Fig.(6.9). A general flow diagram for the complete program.

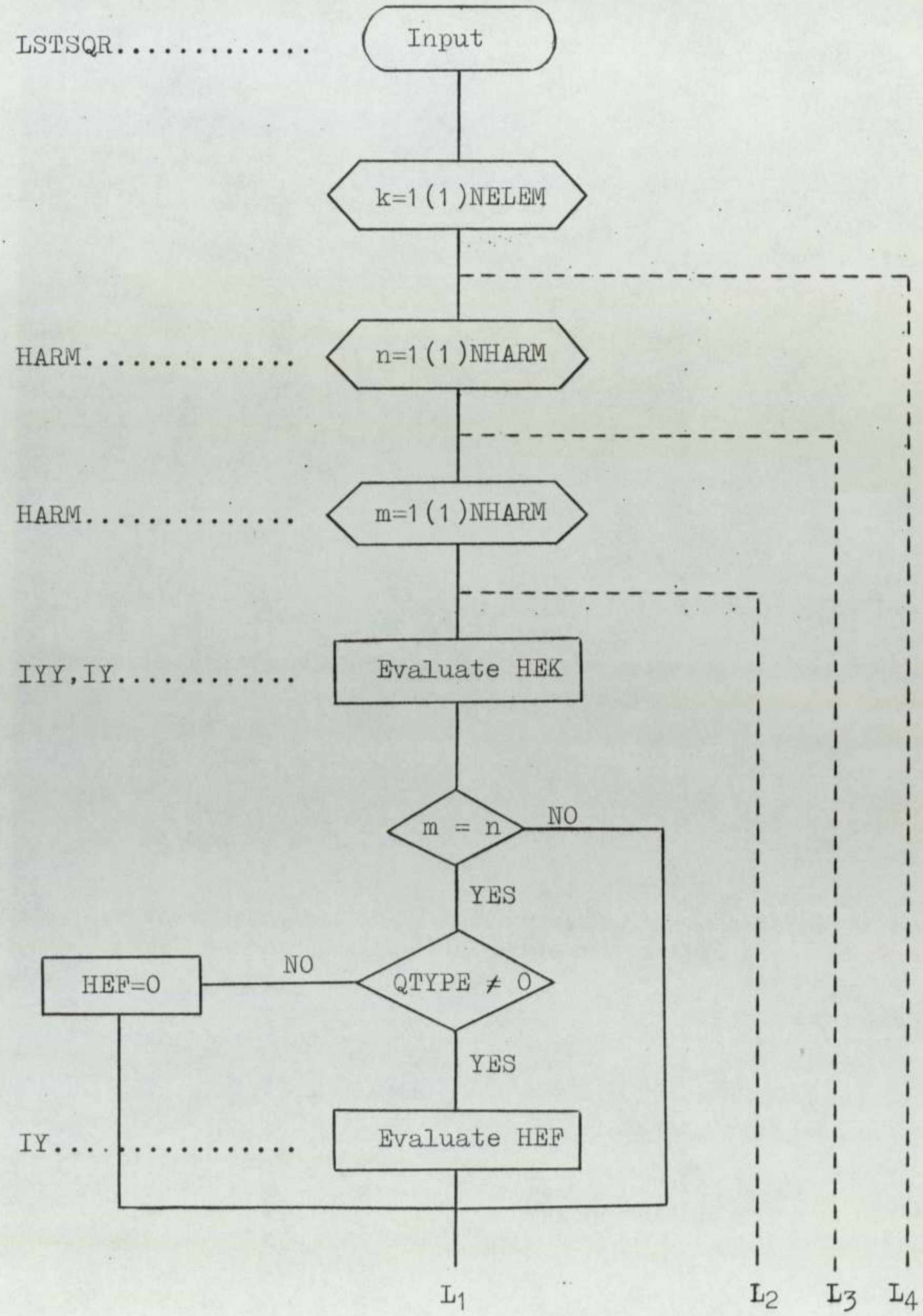

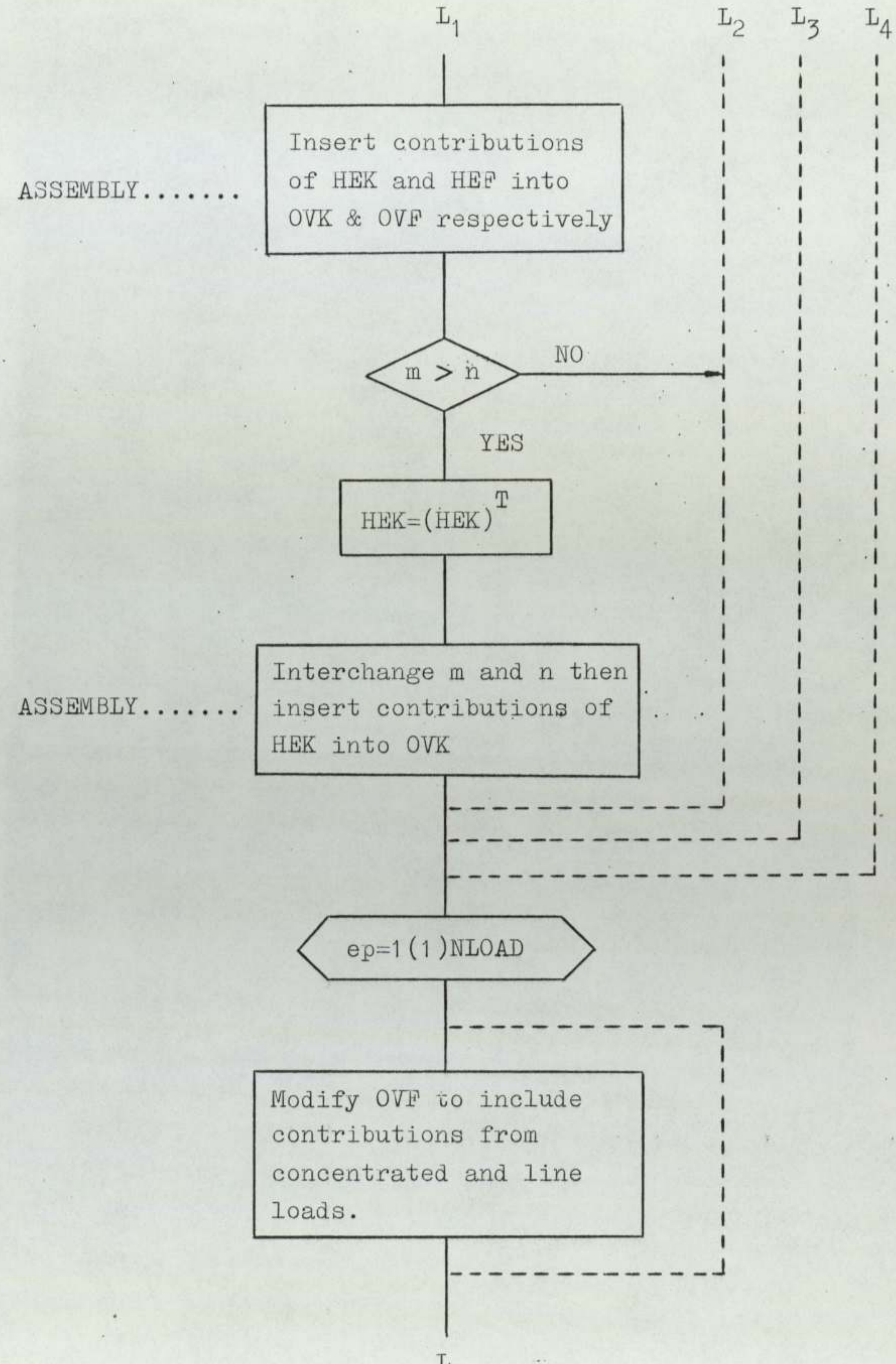
L1
L2
L3
L4
ASSEMBLY.......
Insert contributions of HEK and HEF into OVK & OVF respectively
m > n
NO
YES
HEK=(HEK)T
ASSEMBLY.......
Interchange m and n then insert contributions of HEK into OVK
ep=1(1)NLOAD
Modify OVF to include contributions from concentrated and line loads.
L5

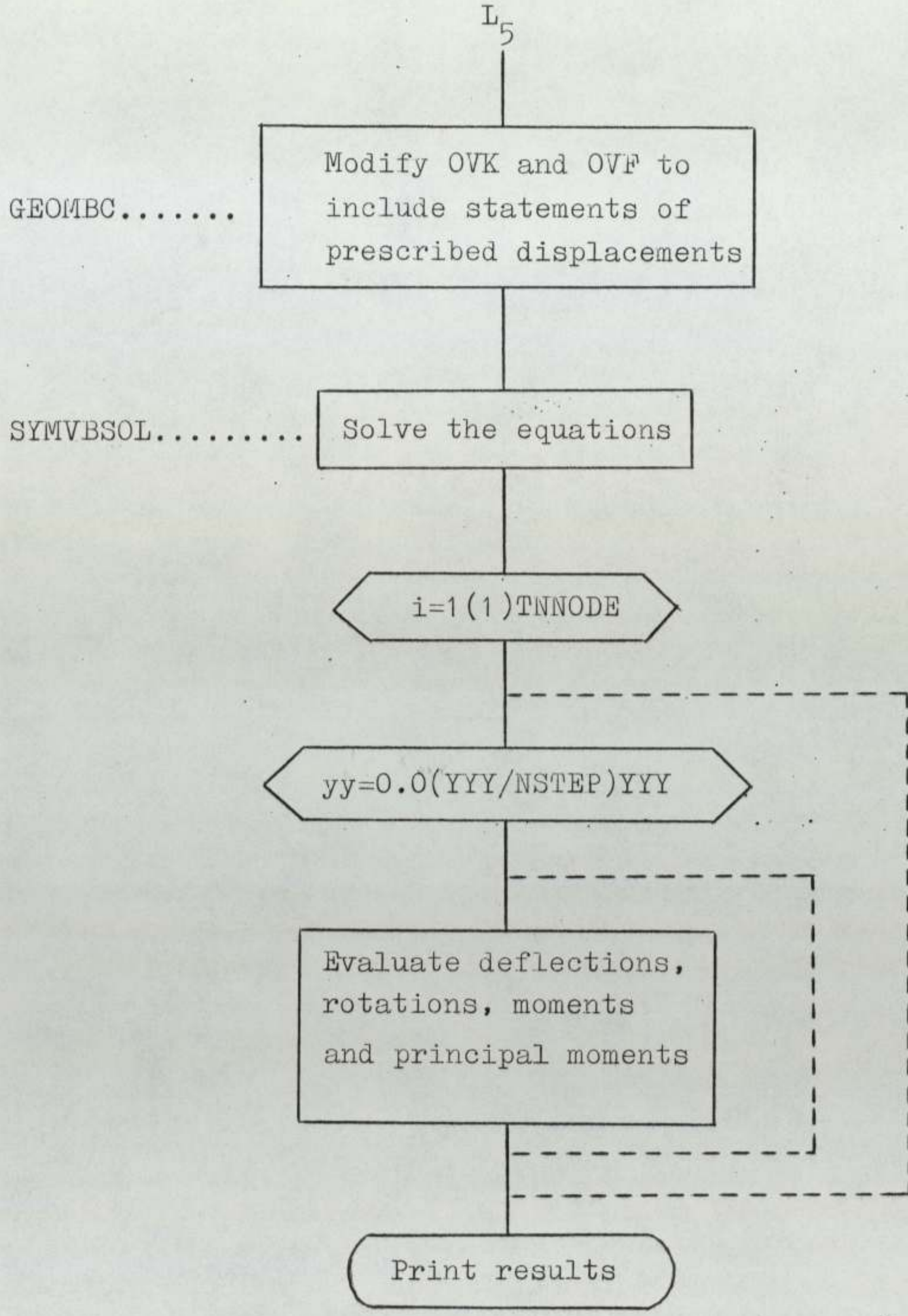
L5
Modify OVK and OVF to include statements of prescribed displacements
GEOMBC.......
SYMVBSOL.........
Solve the equations
i=1(1)TNNODE
yy=0.0(YYY/NSTEP)YYY
Evaluate deflections, rotations, moments and principal moments
Print results

NLOAD	number of concentrated and line loads acting simultaneously.
ep	current concentrated or line load.
yy	current value of y at which results are required.
YYY	final value of y at which results are required.
NSTEP	number of steps from y=0 to y=YYY at which results are required.

6.10 The Input Data

A listing of the required input data and the definition of the variables used for the input will now be given.

Statements will be made regarding the number of steps into which the elements are divided. Strictly speaking these are inaccurate. They refer to the number of steps into which the integrals in the analytic function are divided for the purpose of evaluation of the element stiffness matrix and element load vector. If the plate and the applied load are uniform for a particular element, then the number of steps for this element should be given as 1.

No reference is made to Young's Modulus, E, or plate thickness, h, because at the time of program development, results were checked against analytical results. The latter are usually quoted as a function of the flexural rigidity D. Therefore, it was felt that it would be more convenient to use D directly. It is, now, necessary to evaluate D manually if an analysis is required for a specific plate thickness. Alternatively, a simple modification to the program would be necessary to allow the use of E and h directly.

At the end of the section, a specific example will be given to act as a guide to data preparation should this guide be necessary.

The data must be given in the order in which they are listed below. In the case of some array variables, a loop is used together with a counter (i, ep or k). The loop is to ensure that the variables are read in the correct sequence. The counters should not be assigned any values. They are not variables.

In the listing below

I	refers to integer variable
R	refers to real variable
A	refers to real array
IA	refers to integer array

Variable	Type	Definition
NSETS	I	The number of sets of data to be analysed in one run.
BC	I	The boundary conditions of the analytic function. This variable should be assigned one of the following integers as appropriate: 1 for simply supported-simply supported. 2 for clamped-clamped. 3 for free-free. 4 for clamped-free. 5 for simply supported-clamped. 6 for simply supported-free .

Variable	Type	Definition
A	R	The length of the plate in the direction of the analytic function. In the case of a free edge function it is suggested that, in order to reduce the residual moment and shear force at the free edge, a rectangular extension of width 0.2A should be added to the whole length of the free edge. The rigidity of the extension should be assigned a zero value. In this case the value of A would be 1.2, for one free edge and 1.4 for two free edges, times the actual value of A. The variables DTYPE and QTYPE should then be assigned the appropriate integers for variable rigidity and load. The example at the end of the section will clarify this procedure.
NELEM	I	Number of strips.
NHARM	I	Number of harmonics.
YYY	R	The results are given for a number of points on each nodal line. These points start at y=0 and go up to y=<u>YYY</u> in <u>NSTEP</u> equal steps.
NSTEP	I	Defined above.

Variable	Type	Definition
NPD	I	The total number of prescribed displacements (on the edges not described by the analytic function). If there are no prescribed displacements (when both edges are free), then the integer 0 should be assigned to this variable.
MNS	I	Maximum number of steps into which any of the strips is divided. This integer is necessary for reserving the storage requirement of some of the arrays.
V	R	Poisson's Ratio.
SYMM	I	This variable should be assigned the values 1 if the problem is symmetric about y=A/2 0 otherwise.
QTYPE	I	The type of applied distributed load. One of the following values should be assigned to this variable. 0 when no distributed load is applied. 111 for uniformity throughout the whole plate. 11 for uniformity throughout each strip. 1 for uniformity throughout each step. 2 linear variation. Required coefficients of the linear equation $Q=Q_1x+Q_2y+Q_3$ are available. 3 linear variation. Coefficients of the linear equation are to be evaluated using the procedure LSTSQR.

Variable	Type	Definition
		Only one of the above integers should be read for the whole problem.
DTYPE	I	The type of plate rigidity. A convention identical to that for the applied distributed load is employed here (except, of course, for the integer 0 which does not apply here).
NLOAD	I	The total number of concentrated and line loads (forces and moments) acting simultaneously. If none, the integer 0 should be assigned.
i=1		
DF[i]	IA	The global degree of freedom on which the displacements are prescribed. The relationship between the global d.o.f. and the node number is d.o.f.=2 x node number - 1 for deflection =2 x node number for rotation. If the deflection is prescribed on nodal line 1 (simply supported edge) then DF[i]=1, and if the rotation is specified on nodal line 6 (line of symmetry) then DF[i]=12. If NPD had been read as 0 (free edges), no values should be assigned to DF[i] or PD[i].
i ⩽ NPD		
PD[i]	A	The value of the prescribed displacement.
i=i+1		

Variable	Type	Definition
		Only a 0.0 value may be dealt with. A simple modification to the program is necessary to deal with other types of prescribed displacements. This modification is indicated in section (6.6).

If NLOAD = 0 then the five sets of variables below are not assigned any values.

ep=1

Variable	Type	Definition
P[ep]	A	Value of the concentrated load or line load (per unit length).
PTYPE[ep]	IA	The type of the load above: 1 for line force 21 for line moment M_x 22 for line moment M_y 3 for concentrated force 41 for concentrated moment M_x 42 for concentrated moment M_y
NODENO [ep]	IA	The global number of the nodal line to which the load above is applied.
C[ep]	A	The value of y at which the load is applied in the case of concentrated loads or the lower limit of y for line loads.
DP[ep]	A	This variable is only assigned a value in the case of line loads. It refers to the upper limit of y.

ep=ep+1

ep $\leqslant$ NLOAD

Variable	Type	Definition
k=1		
BE[k]	A	The width of the strip.
NS[k]	IA	The number of steps for each strip.
EL[k,es]	A	The end limit of each step (i.e. the upper value of y). All the values (for es=1,2,...NS[k]) should be given for the current strip. These end limits are as shown below for the strip k.
k=k+1		

k ≤ NELEM

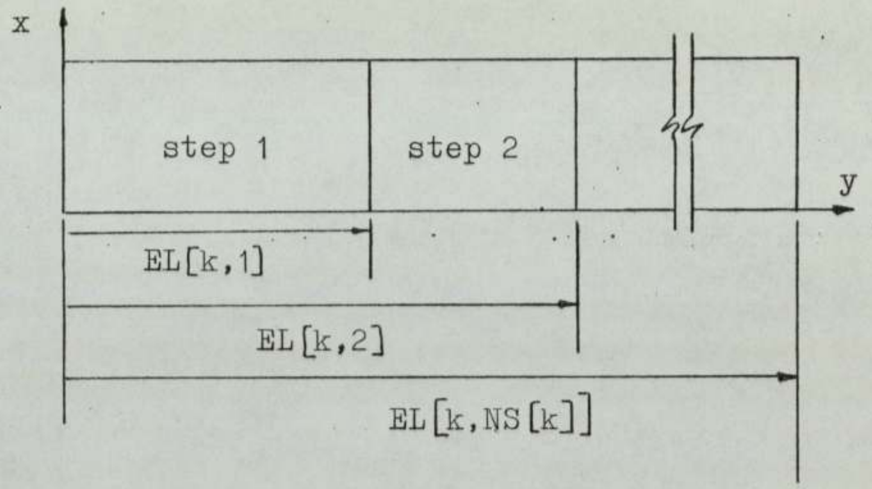

Q1 [k,es] Q2 [k,es] Q3 [k,es]	A	The applied distributed load. It is assumed to be of the form $Q=Q_1\ x + Q_2\ y + Q_3$. The values of Q1, Q2 and Q3 depend on QTYPE which has been assigned a value earlier. When QTYPE = 0 No values are assigned to Q1, Q2 or Q3. When QTYPE = 111 One value, Q3, has to be given here.

Variable	Type	Definition
		When QTYPE = 11 , NELEM values of Q3 have to be read in succession.
		When QTYPE = 1 , NS[1],NS[2],....., NS[NELEM] values of Q3 have to be read in succession.
		When QTYPE = 2 , NS[1],NS[2],....., NS[NELEM] values of Q1, Q2 and Q3 have to be read in succession. The values of Q1, Q2 and Q3 have to be read together for each step of each strip
		When QTYPE = 3 , values of Q1, Q2 and Q3 will be evaluated using LSTSQR. Values of Q should be read for each step of each strip according to the sequence below.

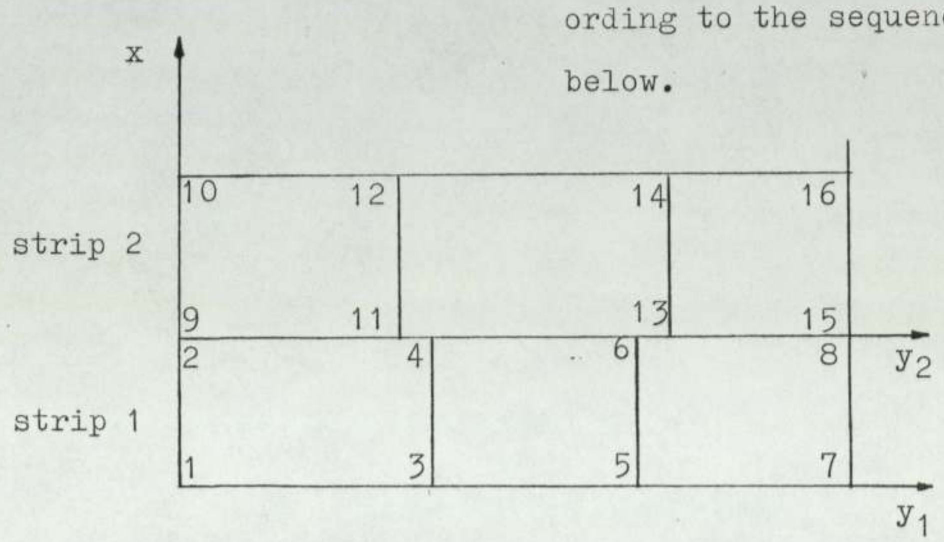

Variable	Type	Definition
D1[k,es] D2[k,es] D3[k,es]	A	The rigidity of the plate is assumed to be of the form $D=D_1\ x + D_2\ y + D_3$. The values of D1, D2 and D3 depend on DTYPE and the convention is identical to the one used for the applied pressure, except for 0 which does not apply here.

A listing of the complete program is given in Appendix (6).

6.10.1. A Sample of Input Data.

The Problem

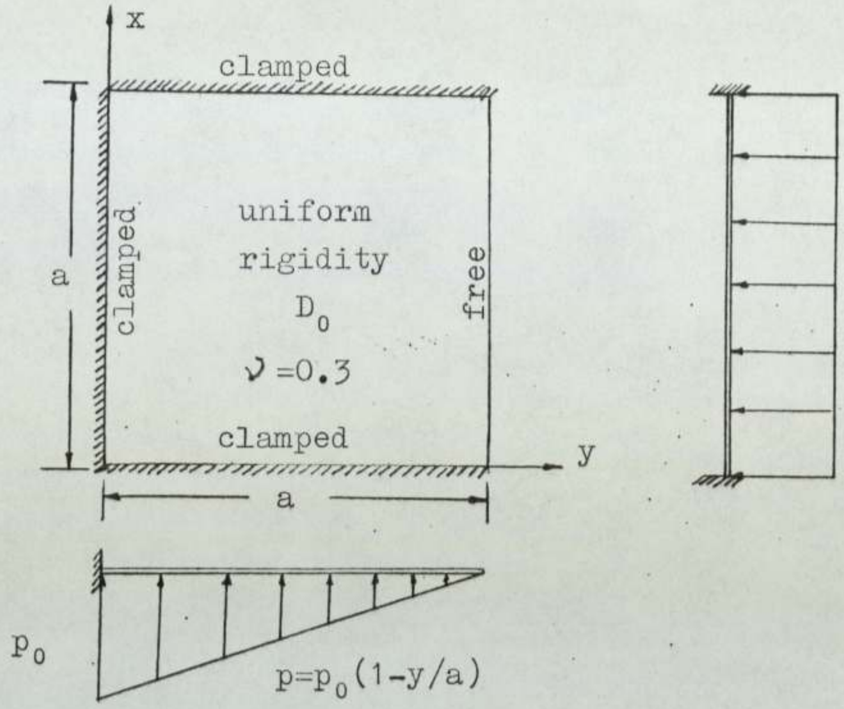

The Discretized Plate

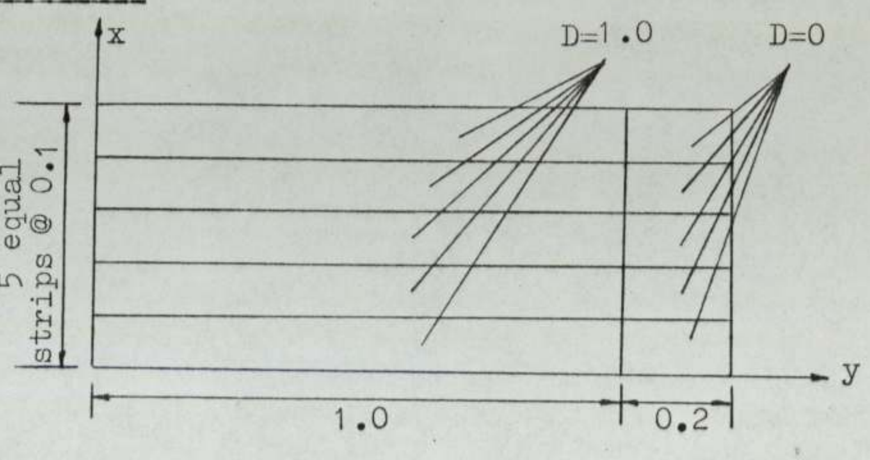

Replacing a, p_0 and D_0 by 1.0 implies that the results will be the factors α and β in the following:

$$\text{deflection} = \alpha p_0 \ a^4/D_0$$

$$\text{moment} = \beta \, p_0 \ a^2$$

Results are required at six equispaced points from the clamped edge to the free edge, on all nodal lines

Values of Q and D.

For each element

$$Q = \underline{0.0}\ x + \underline{(-1.0)}\ y + \underline{1.0} \quad \text{for the first step,}$$

and

$$Q = \underline{0.0}\ x + \underline{0.0}\ y + \underline{0.0} \quad \text{for the second step.}$$

Also for each element,

$$D = 1.0 \quad \text{for the first step,}$$

and

$$D = 0.0 \quad \text{for the second step.}$$

The Input Data

```
1
4  1.2  5  7  1.0  5  4  2  0.3  0  2  1  0
1  0.0  2  0.0  11  0.0  12  0.0
0.1  2  1.0  1.2    0.1  2  1.0  1.2    0.1  2  1.0  1.2
0.1  2  1.0  1.2    0.1  2  1.0  1.2
0.0  -1.0  1.0    0.0  0.0  0.0    0.0  -1.0  1.0
0.0  0.0  0.0    0.0  -1.0  1.0    0.0  0.0  0.0
0.0  -1.0  1.0    0.0  0.0  0.0    0.0  -1.0  1.0
0.0  0.0  0.0
1.0  0.0    1.0  0.0    1.0  0.0    1.0  0.0    1.0  0.0
```

CHAPTER 7

CHAPTER SEVEN.

ASSESSMENT OF ACCURACY.

7.1 Introduction.

It is practically impossible to assign an "accurate" figure to the relative error in the analysis of plates by the finite element method. This is because of the number of possible sources of error and their varying magnitude.

Inherent errors arise from inaccurate data. Material properties and applied loads are known to a limited degree of accuracy. Boundary conditions are only an idealization of the actual situations as is the geometry of the structure in many cases. These errors arise in the solution of most engineering problems, even in so-called exact solutions. Other sources of errors are due to assumptions made in the development of the theory, such as those made in developing the classical theory of plates (section 2.1.2).

In numerical methods of analysis other sources of error are introduced. In the finite element method, for example, the continuum is divided into a discrete number of elements. Increasing the number of elements improves the accuracy because it brings the discretized structure closer to the continuum, but on the other hand, it increases the number of equations to be solved, thus increasing truncation and round off errors which are inevitable in machine calculations. Numerical stability plays an important role in reducing the effects of truncation errors. This factor, or the lack of it, is a characteristic of the system of equations, which are dependant on the problem and the functions employed to approximate the solution of the problem.

Although the error cannot be quantified in absolute terms, it is possible to establish criteria upon which this error and its order of magnitude depends.

Understanding the sources of error and their order of magnitude builds confidence in the method of analysis.

In this chapter a study of the limitations of the classical theory of plates, the numerical stability and convergence of results will be carried out.

7.2 Limitations of the Classical Theory of Plates.

In chapter two the expressions for the stresses in a laterally loaded plate were derived after making certain assumptions, regarding the nature of the deformations, based on other assumptions about the deflection in relation to the thickness, and the thickness in relation to the in-plane dimensions. The conditions under which these assumptions can be considered as valid may be established by carrying out an order of magnitude analysis.

It was assumed that the normal stress σ_z and the shearing stresses τ_{xz} and τ_{yz} in the direction normal to the plane of the plate are negligible.

Dym and Shames [24] carried out an order of magnitude study on all stresses for comparison purposes. A portion of the plate, with an in-plane dimension of length L, was considered.

Consideration of the equilibrium of forces and moments on the portion gave the following order of magnitude equations:

$$O(\sigma_x) = O(\sigma_y) = O(\tau_{xy}) = O(pL^2/h^2)$$

$$O(\tau_{xz}) = O(\tau_{yz}) = O(pL/h) \qquad (7.1)$$

$$O(\sigma_z) = O(p)$$

where O is the order of magnitude, p is the applied pressure and h is the thickness of the plate.

From equations (7.1) it can be seen that the transverse shearing stresses τ_{xz} and τ_{yz} are smaller than the mid plane shearing stress τ_{xy} by a factor $O(L/h)$ and the transverse normal stress σ_z is smaller than the mid plane normal stresses σ_x and σ_y by a factor $O(L^2/h^2)$. Therefore, if $L/h > 10$ then the assumptions made regarding σ_z, τ_{xz} and τ_{yz} being negligible are valid to a reasonable degree of accuracy.

The expressions for the strains in the plate were derived on the basis that the middle surface is the neutral surface. This amounts to neglecting the stress and strain on this surface. Timoshenko [23] examines the implication of this assumption by considering the bending of a circular plate. A geometrical investigation of the deflected surface leads to an upper limit for the circumferential strain at the edge of the plate. Comparison of this strain with the maximum bending strain leads to the conclusion that the latter is about $\frac{3h}{2w}$ times the former, where h is the thickness of the plate and w is the maximum deflection. It follows, then, that the equations derived in section (2.1.3) on the assumption that the middle surface of the plate is its neutral surface, are acceptable if the deflection is small when compared to the thickness of the plate.

7.3 Numerical Instability - General Discussion.

In section (4.3) the question of numerical stability was briefly mentioned. This very important subject will be discussed further here.

Mikhlin [28] demonstrated how the choice of functions, in the Ritz procedure for the solution of variational problems, can drastically affect the numerical stability of the Ritz coefficients.

The problem Mikhlin used for his demonstration was that of the variational problem

$$F(u) = \int_0^1 (u'^2 - 2\,\frac{1}{1+x}\,u)\,dx \qquad u(0)=0,$$

The system of co-ordinate functions chosen to represent the solution was that of a polynomial, i.e.

$$u = \sum_{k=1}^{M} a_k\ \varphi_k \quad . \qquad \text{where} \quad \varphi_k = x^k$$

The normal Ritz method was followed to establish a set of linear equations with unknowns a_k (k=1,2...M), (analogous to displacements). The use of exact numbers in the coefficients of a_k (stiffnesses) and in the right-hand sides (forces) gave an exact solution for a_k which was then rounded to four decimal places. The solutions a_k for different values of M showed the dependence of a_k on M though these values tended to stabilize non-uniformly. More significant, is the fact that when the right hand sides were rounded to four decimal places before the equations were solved, the solutions a_k diverged as M was increased. So, theoretically, to improve the accuracy of the Ritz solution more terms have to be taken (i.e. M should be increased) and yet with an increase in M there was a sharp increase in the error.

The reason for this paradox lies in the nature of the system of equations. Two or more equations contain coefficients that are almost equivalent. This causes ill-conditioning of the system of equations and consequently any small error in the coefficients or in the right hand sides is magnified many times in the solution.

It is not easy to detect ill-conditioning. However, the stability of the solution vector for a different number of terms is a good indication.

It is more difficult to deal with ill-conditioning, once it is present and prevention in this case is far better than cure! Prevention is achieved by the right choice of co-ordinate functions. If a system of co-ordinate functions is chosen such that the solution vector is independent (or almost independent) of the number of terms taken, then the stability of the system of equations will be ensured. In terms of matrix notation, this implies that the off-diagonal terms in the coefficients matrix are zeros (or much smaller than the diagonal terms).

Orthogonal functions satisfy this requirement. These functions are defined by the identity

$$\int_0^1 \varphi_i(x) \cdot \varphi_j(x)\, dx = \delta_{ij} = \begin{cases} 0 & i \neq j \\ 1 & i = j \end{cases}$$

7.4 Numerical Instability of the Beam Eigenfunctions.

The use of orthogonal functions in a boundary value problem results in a numerically stable system of equations. However, before this stage is reached some integrals of the form $\int Y_m(\xi)\, Y_n(\xi)\, d\xi$ have to be evaluated for a number of values of m and n. It is at this stage that the beam functions for the clamped-clamped, free-free and clamped-free cases become troublesome. The trouble arises from the algebraic operations on the trigonometric functions whose values remain in the range ± 1.0, and the hyperbolic functions whose values increase rapidly as their arguments increase. This, coupled with the fact that the computer can work with only a limited number of significant figures, causes the beam eigenfunctions to become unstable at high modes.

To illustrate this problem, the clamped-clamped function,

$$Y_m = \sin m\xi - \text{sh}\, m\xi - \left(\frac{\sin m - \text{sh}\, m}{\cos m - \text{ch}\, m}\right)(\cos m\xi - \text{ch}\, m\xi),$$ will

be evaluated for the fourth mode, where m=14.137, for ξ=0.70736.

The function will be evaluated using a floating decimal point arithmetic in the way that a computer would carry out the operations. The computer will be assumed to be capable of storing real numbers to an accuracy of four significant figures. Thus,

$$Y_m = -5440 \times 10^{-4} - 1101 \times 10^1 - \left(\frac{1000 \times 10^{-3} - 6896 \times 10^2}{1669 \times 10^{-7} - 6896 \times 10^2}\right) \times (-8391 \times 10^{-4} - 1101 \times 10^1)$$

$$= -1101 \times 10^1 - \left(\frac{-6896 \times 10^2}{-6896 \times 10^2}\right) \times (-1101 \times 10^1)$$

$$= 0000 \times 10^1$$

Clearly, this value is inaccurate because Y_m should only be zero at ξ=0 and ξ=1.0.

If, on the other hand, the arithmetic operations were carried out in a different order, then a different value for Y_m would be obtained, viz.

$$Y_m = -5440 \times 10^{-4} + 1000 \times 10^{-3} \times 8391 \times 10^{-4} - 1101 \times 10^{1}$$
$$+ 1000 \times 10^{-3} \times 1101 \times 10^{1}$$

$$= 2951 \times 10^{-4} = 0.2951$$

Although this value is closer to the truth than the first one, there is still a little inaccuracy arising from the evaluation of the factor $\propto_m = \frac{\sin m - \text{sh } m}{\cos m - \text{ch } m}$, because the values of sin m and cos m are lost when compared with sh m and ch m. The inaccuracy is reduced by using the exponential form of the hyperbolic functions and rearranging the terms thus:

$$Y_m = \sin m\xi - \text{sh } m\xi - \propto_m(\cos m\xi - \text{ch } m\xi)$$

$$= \sin m\xi - \propto_m \cos m\xi - \tfrac{1}{2}\left[e^{m\xi}(1-\propto_m) - e^{-m\xi}(1+\propto_m)\right]$$

$$= \sin m\xi - \propto_m \cos m\xi - \tfrac{1}{2}\left[e^{m\xi}\left(\frac{\cos m - \sin m - e^{-m}}{\cos m - \text{ch } m}\right)\right.$$
$$\left. - e^{-m\xi}\left(\frac{\cos m + \sin m - e^{m}}{\cos m - \text{ch } m}\right)\right]$$

Evaluating the rearranged form of Y_m for the same values of m and ξ and working to four significant figures yields

$$Y_m = 2791 \times 10^{-4} = 0.2791$$

This value for Y_m is undoubtedly more accurate because the expression from which it was evaluated is of such a form that inherent error sources cause a much less serious round off error to take place, The higher degree of accuracy of the rearranged form of the beam eigenfunctions can be verified by evaluating the original expression to a larger number of significant figures. Working to nine figures, the original form of the eigenfunction gives:

$$Y_m = 279129201 \times 10^{-9}$$

$$= 0.2791$$

The numerical instability of the beam eigenfunction was demonstrated by evaluating the function with an accuracy of four significant figures. However, when the integral of the product of the various modes of the function are evaluated, this numerical instability takes place, even when the working accuracy is increased to twelve significant figures, at about the fourth mode. This is because the evaluation of the integral of the products of the function involves evaluation of trigonometric and hyperbolic functions with arguments composed of the sum of the two arguments involved in the original product.

Working with the rearranged form of the eigenfunction greatly reduces the round off errors and eliminates numerical instability allowing higher mode analysis provided that they are within the range of capability of the computer to handle real numbers.

7.5 Roots of the Characteristic Equation.

With emphasis on the effect of the number of significant figures on the stability of the beam functions, it becomes necessary that the roots of the characteristic equations are evaluated to a higher degree of accuracy than that given in table (4.1).

The I.C.L. 1905E computer used for processing of the program works with an accuracy of 11 significant figures. The roots of the characteristic equations should, therefore, be obtained to at least the same degree of accuracy.

For this purpose a computer program NEWTON was written on the basis of Newton's Iterative Method for the solution of equations [42] with the values in table (4.1) as initial guesses. A brief account of the method and a listing of the computer program are given in appendix (4) together with the first ten roots of each equation.

7.6 Numerical Stability and "Convergence" Tests.

That the finite element method produces converging results as the mesh is made finer has been discussed by many authors. Not so in the case of the semi-analytic method. Therefore, before the semi-analytic computer program can be used with confidence, it needs to be confirmed that numerical stability and convergence are assured. Also, the effects of load and rigidity variation on numerical stability and convergence have to be established.

For this purpose, a series of tests were carried out. The computer program was run to solve problems of plates having different boundary conditions, loading and rigidities.

In all cases, the number of strips into which the plate was divided and the boundary conditions on the edges parallel to the direction of the analytic functions, were kept the same throughout. Therefore, the subjects of examination in these tests were the beam eigenfunctions.

The behaviour of these functions was studied by examining the solution vectors (i.e. the nodal displacement parameters) for various values of M, the number of harmonics.

If in one approximation the analytic function is truncated to (M-1) harmonics and in a further approximation M harmonics are taken, then the optimum in numerical stability, in this context, occurs when the solutions $\delta^{m,M}$ $(m=1,2,\ldots M-1)$, where the superfix m,M signifies the m^{th} mode of a set of M harmonics, from the second approximation are identical to the solutions $\delta^{m,M-1}$ $(m=1,2,\ldots M-1)$, from the first approximation, i.e. when the solutions (i.e. the displacement parameters) are totally independent of the number of harmonics, M, (section 7.3). In the event when such independence is lacking, a measure of numerical stability is obtained by comparing the solutions $\delta^{m,M-1}$ with $\delta^{m,M}$ $(m=1,2,\ldots M-1)$. It is desirable that the relative difference between $\delta^{m,M-1}$ and $\delta^{m,M}$ should be small and decreasing, as M increases, until it vanishes (for a certain number of significant figures) when M exceeds a reasonably small value.

The term "rate of convergence" will be used throughout the discussions on these tests. It is intended to mean the rate at which the deflections and the bending moments approach a limiting value. Since no comparison with "exact" deflections and moments is made, the term "convergence" is, strictly speaking, inaccurate. In fact, it will be shown, in a later section, that convergence cannot be achieved through a unilateral increase in either the number of strips or the number of harmonics.

A measure of the "rate of convergence" is obtained by estimating the truncation error. To this end, the maximum deflection was evaluated for a number of large values of M (12, 13 and 14) to ensure that a stable limiting value for the deflection is obtained, which is then compared with the maximum deflection for a small value of M (say 3 to 7) and a relative error is obtained. This error will be called the truncation error, which, together with the truncation error for the bending moment M_y obtained on the same basis, serves as a comparative guide to the number of harmonics required for a satisfactory level of accuracy.

Whilst remembering that the truncation errors would be somewhat larger for the effective shear force, since this force is a function of the third derivatives of the deflection, these errors will not be discussed for the individual cases of boundary conditions because in the majority of plate problems the most important quantities are those pertaining to the bending moments.

7.6.1 Uniform Plates Under Uniform Pressure.

The first set of tests was on a square uniform plate under uniform pressure, with two opposite edges simply supported. The boundary conditions at the other two edges being described by the various analytic functions.

In all cases in this set of tests, only half the plate was considered by making use of symmetry about x=a/2. The appropriate boundary conditions at the line of symmetry being zero normal rotation. This half of the plate was divided into five equal strips which is equivalent, from the point of view of accuracy, to dividing the whole plate into ten strips. Symmetry of the problem about y=a/2 was also exploited, whenever possible, by considering odd modes only (section 4.3). The dimensions and other necessary information are given in fig.(7.1).

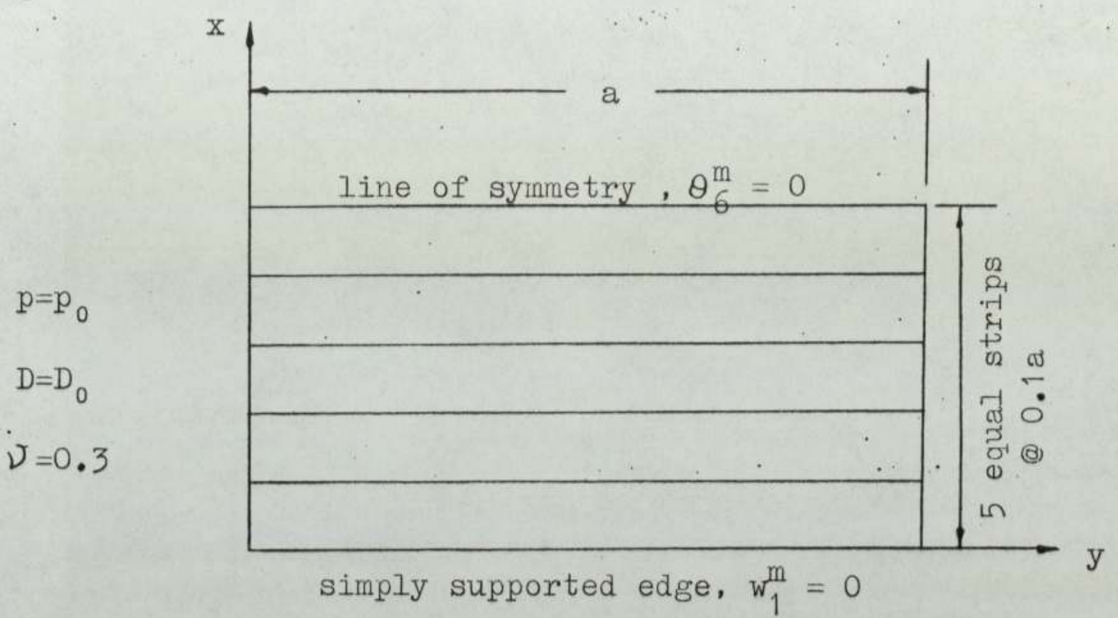

Fig.(7.1)

The results which are listed in the form of tables in appendix (7) give the values of the deflection parameters, $w_6^{m,M}$, on nodal line 6 for a number of values of M and for m=1,2,.....,M. The properties exhibited by these results are also exhibited, more or less, by the displacement parameters on other nodal lines. When this is not the case, the values of the displacement parameters will be given for the nodal lines which show a marked variation from $w_6^{m,M}$.

The results of the first test will now be discussed. No comparison with analytical or other solutions will be carried out at this stage.

(a) Simply Supported - Simply Supported Function.

The feature that the results of this case (table 7.1) highlights is the total independence of the solution vector (the displacement parameters w_6^m and not the deflection) from the value of M. This property was anticipated when the reasons for the uncoupling of the modes were discussed in section (4.7.2). The case of simply supported - simply supported edges is, therefore, the optimum in numerical stability.

Truncating the series for maximum deflection and maximum bending moment M_y, both at the centre of the plate in this case, to 3 harmonics results in truncation errors of about 0.025% and 0.65% respectively. These figures imply an excellent "rate of convergence" for both the deflection and the bending moment functions.

It should be considered, for the sake of comparison with other cases, that because of symmetry about y=a/2 in this case the computer program neglected the skew symmetric modes (even modes) of the function. Consequently, although the program dealt with three modes only, effectively the results are equivalent to those from a six mode analysis.

(b) Clamped - Clamped Function.

The results for this case are given in table (7.2). The dependence of the solutions on M is apparent but this dependence reduces rapidly and the solutions stabilize and become independent of M, for the given number of significant figures, for $M > 3$.

The truncation errors in the maximum deflection, at the centre of the plate, and the maximum bending moment, M_y at the middle of the clamped edge, for M=3 are about 0.5% and

3.3% respectively. This indicates that the series for the deflection converges very rapidly, whereas the bending moment series has a comparatively slow rate of convergence. However, taking one further harmonic in the series reduces the truncation error for the bending moment to about 1.9% which is quite acceptable.

Once again only symmetric modes are considered and the implication is as before.

(c) Simply Supported - Clamped Function.

Table (7.3) gives the results for this case. The solutions stabilize (in the sense described earlier) uniformly for all modes and become virtually independent of M for $M > 5$.

The "rates of convergence" of the series for the deflection and the maximum bending moment are less rapid than the previous cases. Truncation of these series to 3 harmonics results in truncation errors of about 0.3% for the deflection at $x=0.5a$, $y=0.4a$ and 8.5% for the maximum bending moments. Increasing the number of harmonics to seven reduces the truncation error in the maximum bending moment to 1.5%.

The problem in this case is not symmetric about $y=a/2$. Consequently, all the harmonics in the function had to be considered.

(d) Simply Supported - Free Function.

Numerical stability and "convergence" were examined for this case, first by solving the problem as in the previous cases, then the method suggested in section (4.6) was employed, whereby the free edge was simulated by replacing the original plate by one with an imaginary extension having zero flexural rigidity.

Table (7.4a) gives the results from the "standard" method. The dependence of the solution vector on M decreases slightly less rapidly than in the previous cases. Nevertheless, the tendency to stabilize is quite apparent in the solutions.

The "rate of convergence" for the bending moment M_y at the centre is very low. The truncation error, for M=7, in the central bending moment M_y is about 6% and that for the maximum deflection is about 1%.

The normal bending moment at the middle of the free edge, which should have a zero value, was in fact approaching a value comparable to that of the bending moment M_y at the centre. This residual bending moment is due to the fact that the beam eigenfunction for a free edge does not satisfy the natural boundary conditions of a plate exactly. This point was discussed in section (5.5).

Applying the method of simulated free edge, the results of which are shown in table (7.4b), the numerical stability is found to be of a similar character to that in the "standard" method. The truncation errors, however, are greatly reduced. Truncation of the series to 7 harmonics results in a truncation error of about 0.1% for the maximum deflection and 0.7% for the bending moment M_y at the centre of the plate. Significantly, the normal bending at the middle of the free edge is now less than $^1/6$th that for the centre of the plate. Moreover, this bending moment continues to approach zero.

Thus, by applying this method, the "rate of convergence" was substantially improved whilst the numerical stability of the solution was maintained.

(e) <u>Free - Free Function</u>

Having established (case d) that simulating the free edge condition, rather than applying the function directly, improves the "convergence" and maintains the numerical stability of the function, the method was applied to this case at both edges. The results are given in table (7.5).

The stability of the solution vector in this case is of a similar nature to case (d).

The "rate of convergence" is very good for the maximum deflection but relatively low for the bending moment M_y at the centre. Truncation of the series to 7 harmonics was necessary to obtain results with an acceptable truncation error, in which case the truncation error for the deflection is about 0.1% and for the moment M_y about 1.2%.

With M=7, the normal bending moment at the free edge is small when compared with the maximum bending moment (less than 1/10th) and continuing to approach zero.

(f) <u>Clamped - Free Function.</u>

Once again the free edge was simulated, as before. The solutions, which are given in table (7.6), show that numerical stability of the beam function for this case of boundary conditions, is about the same as in case (e).

The error in a seven mode truncation of the series for the maximum deflection, which occurs at the middle of the free edge, is about 0.1% and that for the maximum bending moment, which is the normal moment at the middle of the clamped edge, is about 2%.

"Convergence" of the normal bending moment at the middle of the free edge is good. Its value, for M=7, is less than

1/20th the value of the maximum bending moment.

7.6.2 Uniform Plates Under Varying Load.

In the previous section, numerical stability and "convergence" were studied for plate problems under uniform pressure which, mathematically, is the most ideal case to deal with and consequently it must be the case which would give the best results from the point of view of stability and "convergence". In this section the effect of variation, in the load, on numerical stability and "convergence" is studied. One case of boundary conditions is examined, that of a clamped-clamped plate under a central point load. Since the latter is the most severe type of load variation a liberal estimate of the effect of variation in load will be obtained by comparing results from this case with those from the clamped-clamped plate under uniform pressure. The clamped-clamped plate is taken, merely, as an example which is moderate in its behaviour in respect of numerical stability and "convergence".

The dimensions and divisions of the plate are as given in fig.(7.1). The uniform pressure is replaced by a concentrated force, P, applied to the middle of nodal line 6.

Table (7.7) gives the deflection parameters on nodal line 3 which is away from the point of application of the concentrated force. As can be seen from these results, the numerical stability and "convergence" rate are excellent. In fact, only three harmonics are required to keep truncation errors under 0.01% for the deflection at x=0.2a, y=0.5a, fig (7.1), and under 1.0% for the bending moment M_y at x=0.2a, y=0.0.

The deflection parameters on nodal line 6, where the concentrated force is applied, do not exhibit the same high level of numerical stability and "convergence" rate. Table (7.7b) shows that the solutions become uniformly stable for all modes for $M > 7$. Compared with the case of uniform pressure, the stabilization process in this case is inferior.

The rate of "convergence" is also lower than that for the case of uniform pressure. With three harmonics, the truncation error is about 1.4% for the maximum deflection and 7.5% for the maximum bending moment M_y compared with 0.05% and 3.3% respectively for the case of uniform pressure. The number of harmonics has to be increased to 9 in order to reduce these errors to 0.15% for the deflection and 2.8% for the bending moment. Thus, 9 terms are required to maintain a truncation error comparable to that produced by the uniform pressure case. It should be remembered, though, that the rate of "convergence" is very low at the nodal line on which the force is applied. Away from this line, the rate of "convergence" is very good.

Although the solution of the plate problem under a concentrated load does not involve an explicit representation of the load by a series, nevertheless, the harmonic deflection parameters are, in effect, the result of a harmonic forcing function. Therefore, the load is implicitly represented by a series of the same form as the deflection. The low rate of "convergence" near the point of application of the load is, thus, a demonstration of the relatively inferior quality of the series representation of a unit impulse function.

7.6.3 Varying Flexural Rigidity, Uniform Load.

When the plate rigidity varies with y, the computer program evaluates the integrals that appear in the element stiffness matrix, in a discrete number of steps. Within each step the rigidity is either constant or linearly varying (section 4.7.2). The consequence of the variation in the rigidity is that the orthogonality property of the beam eigenfunctions becomes inapplicable because the eigenfunctions are orthogonal with respect to a weighting function of unity. When the rigidity D is a function of the same independent variable as the eigenfunctions (i.e. y), it has to go under the integral sign. Thus, the weighting function is not unity. If the integral is evaluated in steps with a constant value for D over each step, then the interval of the integration is not correct for the orthogonality property to apply. Since the orthogonality property of the beam eigenfunctions is responsible for the stability of the solution, this stability and the "convergence" of the solutions will have to be examined for the cases when it is not possible to apply the orthogonality property.

The most severe case of rigidity variation is abrupt step variation in general and that which includes a zero or an infinite portion, (a hole or a rigid inclusion), in particular.

The problem examined here is that of a square plate of side length a, with a central square hole of side length 0.4a under uniform pressure p. Two opposite edges are simply supported and the other two clamped. The analytic function describes the latter conditions.

Once again, symmetry about two axes is exploited and only half the plate is considered. This half is divided into five equal strips as shown in fig.(7.2).

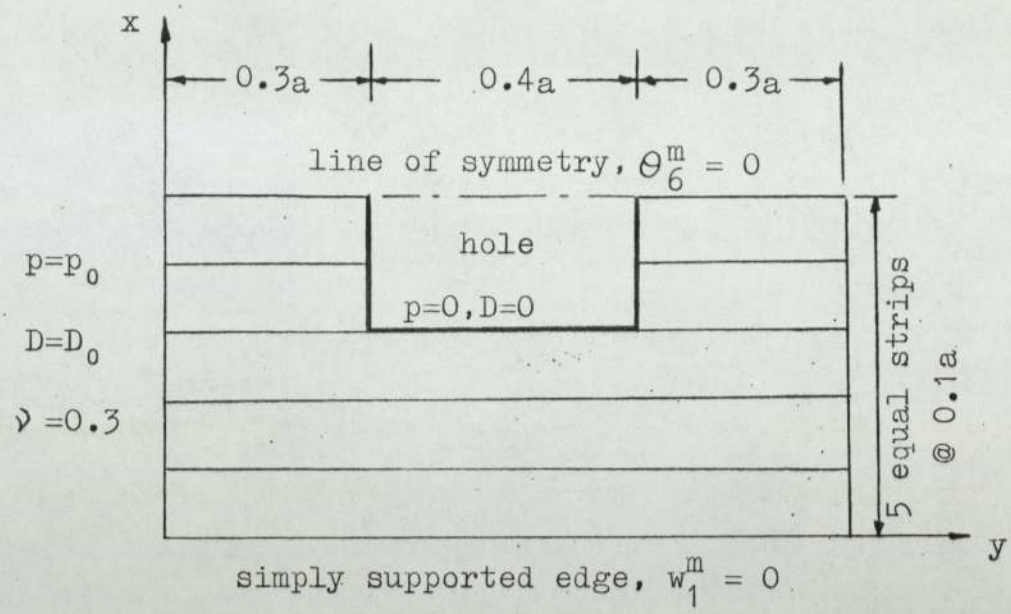

Fig.(7.2)

Table (7.8), appendix (7) gives the solution vector, for various values of M, for the deflection parameters at nodal line 6. The solutions are reasonably stable for small values of M, but as M increases the variations in the values of the harmonic displacement parameters become large. An interesting feature becomes apparent from evaluating the deflection and the bending moment at a number of points for various values of M. Although the deflection parameters vary appreciably for M=11,12, and 13, the deflection and the bending moment M_y, which are functions of these parameters, do not show the same amount of variation. In fact, they continue to "converge". The reason for this, apparently illogical, situation lies in the fact that the deflection curve on a section of the plate through the hole is not unique. The true deflection curve has an undefined portion at the hole. In attempting to describe this curve by a set of continuous functions the undefined portion may be assigned any arbitrary shape which smoothly joins the portions either side of the hole (fig.7.3). The function representing curve A will, then, differ from that which represents B or C. Therefore, the deflection parameters for these deflection curves will be different. This explanation is verified by evaluating the deflection at a point within the region of the hole. It will be found that the variation in the deflection for M=11,12 and 13 is substantial.

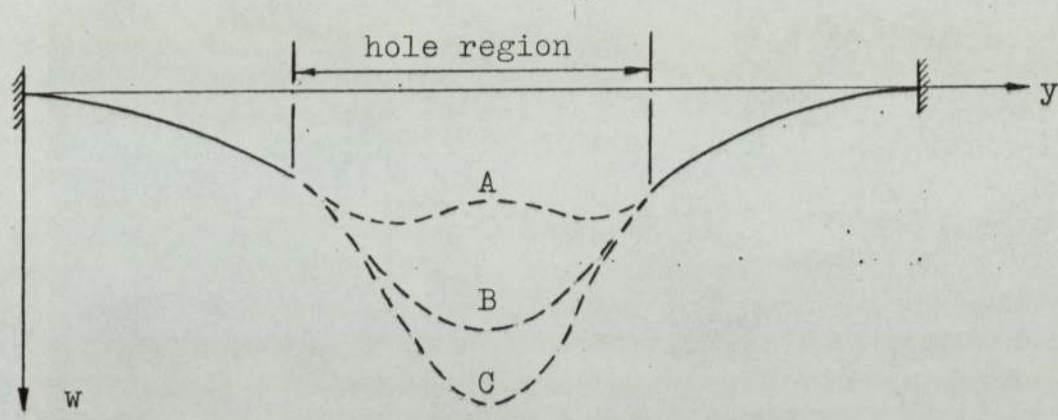

Fig.(7.3)

The arbitrary shape of the deflection curve in the region of the hole does not, in itself, affect the value of the potential energy of the system because of the zero value assigned to the flexural rigidity of that portion. However, it may cause the solution to become unstable. In this case the difficulty is overcome by assigning a very small value to the flexural rigidity of the hole region (say 10^{-6} times the rigidity elsewhere) thus making the deflection curve unique. It should be mentioned here that in the tests carried out for plates with holes, no numerical instability was encountered when the value zero was assigned to the hole region.

Six term truncation of the analytic function results in a truncation error of about 0.15% in the deflection at $x=0.5a$, $y=0.3a$ and 1.0% in the bending moement M_y at the middle of the clamped edge. Since the analytic functions are continuous and so are their second derivatives the bending moments normal to the edge of the hole cannot be expected to have a zero value as the case should be. However, a value which is amll when compared with the maximum bending moment within the plate should be acceptable. In this case the value of M_y at $x=0.5a$, $y=0.3a$ is about 1% of the value of M_y at the middle of the clamped edge.

It is anticipated that numerical stability and "convergence" would reduce with a redcution in the size of the hole relative to the overall dimensions of the plate. This is due, once again, to the representation of a discontinuous function by a set of continuous functions. This point is made clear by the two diagrams in figs.(7.4a) and (7.4b).

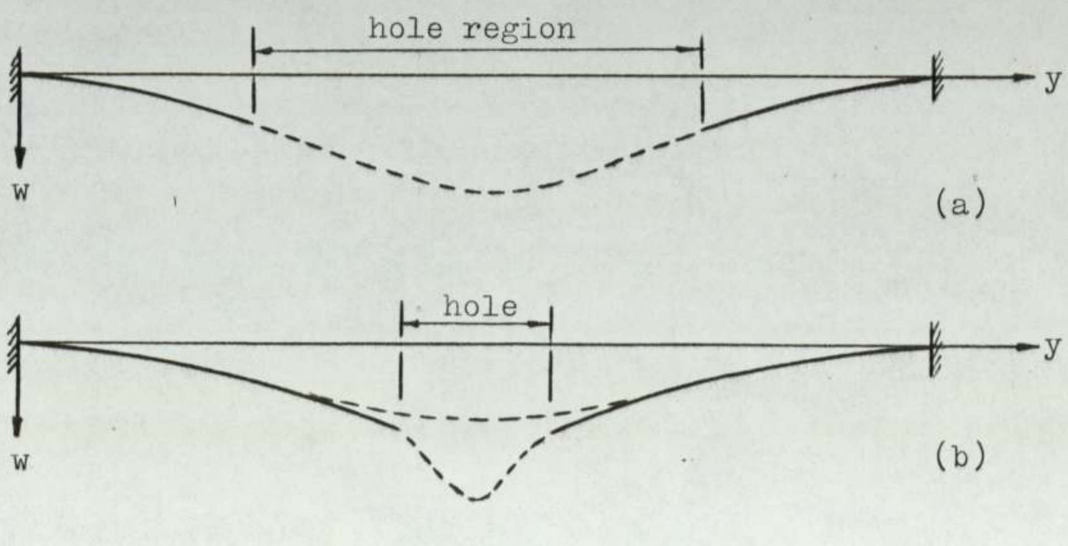

Fig.(7.4)

The number of harmonics required to represent, accurately, the curve in fig.(7.4b) is much greater than those necessary for the curve in fig.(7.4a), because of the rapid change in the slope of the former. Truncation to few terms would cause some error near the hole. This error may not be very large for the deflection but it would be magnified upon differentiation. The consequences on the values of the bending moments near the hole are then obvious.

The case of a plate with a rigid inclusion has been examined although no results are given here. It is not possible to assign an infinite value to the rigidity of the inclusion, but a large value (say 10^6 times the rigidity elsewhere) serves the purpose well. For a small rigid inclusion, the solution vector is stable and the "convergence" rate is similar to that for the plate with a hole. However, the effect of the size of the rigid portion on stability and "convergence" would be opposite to that for the plate with a hole, i.e. as the size of the rigid portion increases relative to the overall dimensions of the plate, stability, "convergence" and accuracy are reduced. The self-explanatory diagrams in figs. (7.5a) and (7.5b), and a similar argument to that for the plate with a hole, confirm this point.

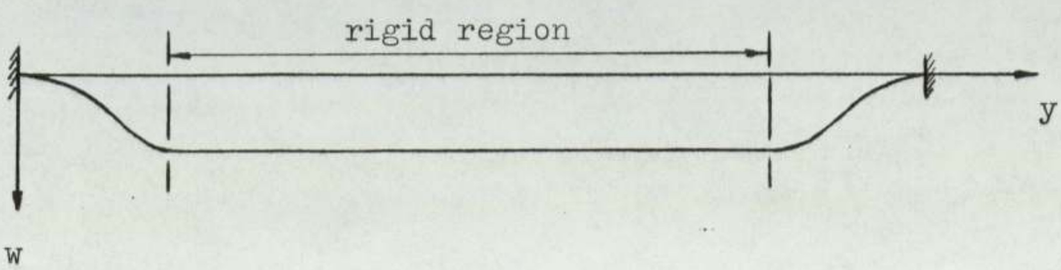

Fig.(7.5 a)

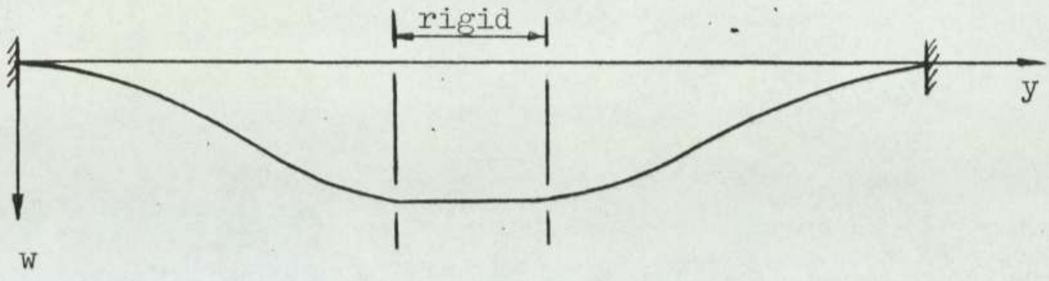

Fig.(7.5 b)

7.6.4 Concluding Remarks.

In the last three sub-sections the beam eigenfunctions were tested for numerical stability and "convergence" under the favourable conditions of uniformity of load and flexural rigidity and under the adverse conditions of load concentration and step variation of flexural rigidity. These functions proved to be quite stable and "convergent" to varying degrees, though "convergence" was not, yet, shown to be towards the correct solution. This will, in fact, be the subject of a later section in this chapter.

The results of the tests give a guide to the number of harmonics necessary to produce a certain degree of accuracy, assuming for the moment that results do converge towards the correct solution, when a particular function is used. They also give a guide to the choice of function in a problem where an alternative is available. For example, if the plate is simply supported-simply supported on two opposite edges and clamped-clamped on the other two edges then the plate should be divided into strips whose y axis is perpendicular to the simply supported edges so that the analytic function for the simply supported edges is employed, rather than the one for clamped edges because the former has proved to "converge" more rapidly than the latter.

The statements made in this chapter regarding "convergence" refer to the convergence of the analytic function when applied to the discretised plate rather than the continuum. Because the problem is formulated on the basis of minimum potential energy, which is a function of the bending and twisting moments, and they, in turn, are functions of the two variables (x,y), convergence to the "exact"solution can never be achieved by taking more and more harmonics whilst keeping down the number of strips and vice versa. This is closely analogous to the division of the continuum into finite elements in the standard finite element technique where the mesh has to be made finer in both directions for convergence to occur. The number of harmonics taken in a semi-analytic technique may be regarded as divisions in one of the two directions.

7.7 Discretization of the Plate.

In the finite element method, the rate of convergence can be seriously affected by the manner of division of the continuum into elements. For rectangular elements, it has been shown [10] that, if the displacements vary at about the same rate in each direction, then the error in the solution, for a fixed number of elements, is least when the ratio of the lengths of the elements, the aspect ratio, approaches 1.0. That is, when the rectangular elements are closest to squares. This statement assumes that the displacement function employed in the analysis possesses geometric isotropy, i.e. it must not have a preferential direction. For example, if a polynomial is employed, then any term in x (say x^2) must have a counterpart in y (y^2) and vice versa. Functions employed in a finite element formulation are usually geometrically isotropic.

In the semi-analytic method, the function which describes the variation of deflection in one direction is entirely different to the one describing the deflection variation in the other direction. Thus, the statements made regarding the aspect ratio and the geometric isotropy do not apply directly here.

The process of discretization in the semi-analytic method requires two decisions to be made. The first is with regard to the orientation of the plate with respect to the direction of the divisions. The second is with regard to the choice of the number of harmonics in conjunction with the number of strips and a certain degree of accuracy.

If a problem of a long plate is considered, one may be tempted to orientate the plate such that the analytic function describes the deflection variation in the long direction so that the division into strips may be carried out in the short direction "because fewer strips would be required in this direction than if the orientation was the other way round". It will be shown, here, that this is not necessarily the case. In plate bending problems, when the aspect ratio of the plate is large the variation of deflection and moments in the long direction, away from the edges at the extreme points of this direction, is very small, whilst that in the short direction is large. Timoshenko shows [23] that for a uniformly loaded simply supported rectangular plate, the variation is negligible if the aspect ratio of the plate exceeds 3. In these cases, the plate may be considered as an infinite strip without a serious loss in accuracy.

Consequently, when the semi-analytic method is used in the analysis, the cubic model which is used to describe the deflection variation across the "width" of the strip can give as good an accuracy when wide strips are used in the long direction as it would when narrow strips are used in the short direction. It follows, then, that divisions in the long direction of the plate need not imply a larger number of strips. To confirm this argument, the problem of a simply supported uniformly loaded rectangular plate with an aspect ratio of 4.0 is solved for the two orientations shown in figs.(7.6a) and (7.6b) and the deflections and bending moments across the centre-lines, figs.(7.7) and (7.8), are compared. In both cases the plate is divided into six strips and the series truncated to 3 harmonics. Symmetry about the centre lines was not exploited so as not to introduce factors outside those involved in the comparison.

The graphs of variation of deflection and bending moment across the centre lines of the plate, for the two orientations show that the results are very nearly the same. In fact, the maximum values of deflection and bending moment from the plate with the wide short strips (fig.7.6a) are slightly closer to the exact values than those from the plate with the narrow long strips. This confirms the statements made earlier.

The question of choice of number of harmonics in conjunction with the number of strips is difficult because of the number of factors that affect the rate at which the solution approaches a limiting value with an increase in the number of harmonics (section 7.6). Therefore, no general rule can be established which relates the number of harmonics to the number of strips for a given accuracy. However, two points must be emphasised. The first is that an increase in the number of harmonics has a more adverse effect on computer storage requirement and solution time than an increase in the number of strips because major parts of the total computer storage requirement and solution time are proportional to NB and NB^2 [39] respectively, where N is the final number of equations to be solved and B is the semi bandwidth.

$$N = (NELEM + 1) \times 2 \times NHARM \qquad \text{and}$$

$$B = 4\ NHARM \qquad \text{(fig. 6.4)}$$

Therefore,

$$NB = 8\ (NELEM + 1)\ NHARM^2 \qquad \text{and}$$

$$NB^2 = 32(NELEM + 1)\ NHARM^3.$$

The second point is that a unilateral increase in the number of harmonics or the number of strips does not produce convergence to the exact solution. To demonstrate this point, the problem of a square simply supported plate under a central concentrated load was solved for a combination of values of NELEM and NHARM. The central deflection was compared with that from a series solution [23] and the error in each case was evaluated.

Fig.(7.9) shows the lines of constant error for the various values of NELEM and NHARM. These lines confirm the statements made earlier that convergence to the exact solution can never be achieved by increasing the number of harmonics without increasing the number of strips and vice versa. The lines also show that, for the case considered, optimum convergence is obtained when the number of harmonics is equal to or one greater than the number of strips. It should be emphasised, however, that if this is to be taken as a guide to the discretization process it must be considered in conjunction with the findings of section (7.6) which indicated a substantial variation in the rate of convergence depending on boundary conditions, applied load and flexural rigidity.

Symmetry, or the lack of it, also plays a part in the discretization process. In the case considered, for example, half the plate and odd modes only were taken. For identical accuracy and the same number of harmonics the whole plate would have had to be divided into twice the number of strips. It follows, then, that for a plate in which one of the edges parallel to the y-axis is other than simply supported while the remaining conditions are the same as before, the optimum number of strips must be about twice the number of harmonics. Similar argument applies if symmetry about $y=a/2$ was disturbed by, say, shifting the point load slightly along the y-axis. In this case the optimum number of harmonics would be about twice the number of strips into which half the plate is divided.

As in any idealization or discretization process, local zones where the geometry, applied load or properties of the structure show a severe variation, the divisions near these zones should be made finer. Unfortunately, such local refinement is not possible in the y-direction because it would mean an increase in the number of harmonics for the strips near the peculiar zones and this would result in an excess in the number of d.o.f. of these strips. Consequently, incompatibility would arise at inter-element boundaries.

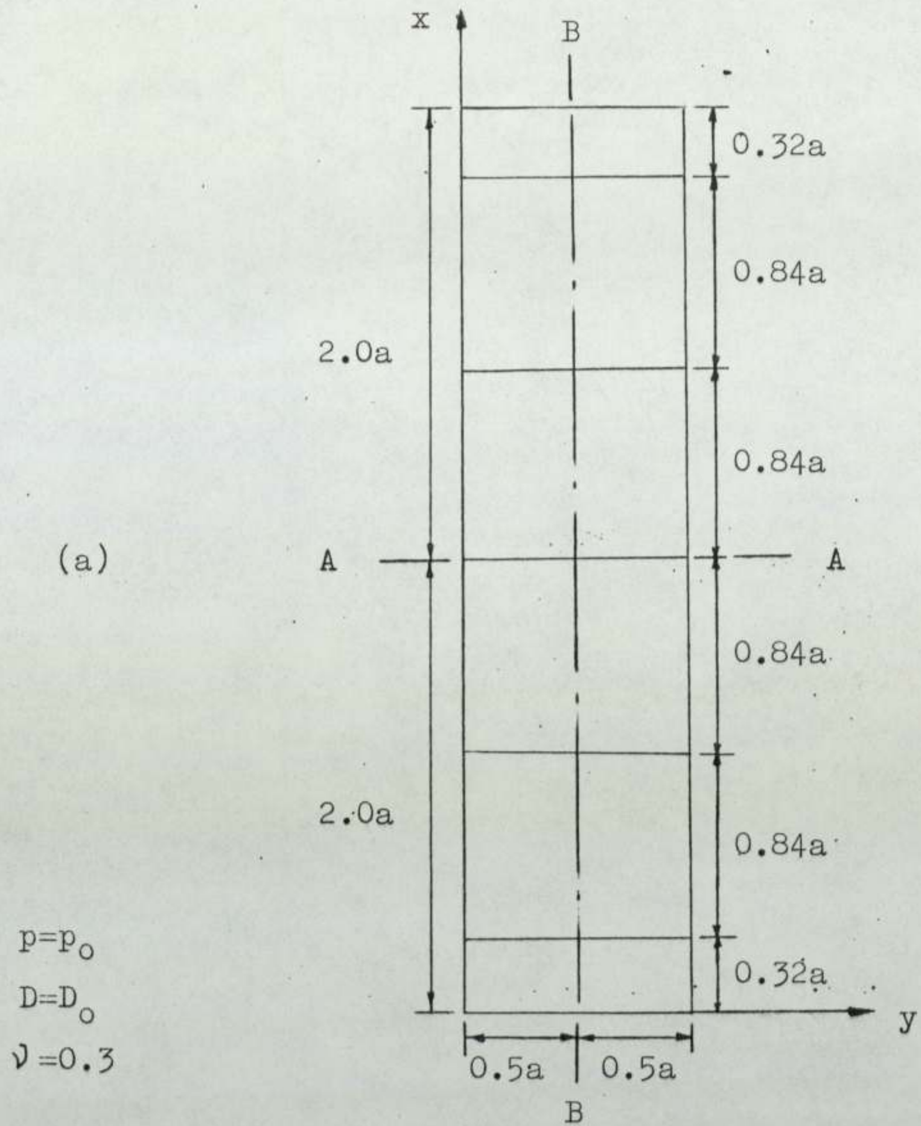

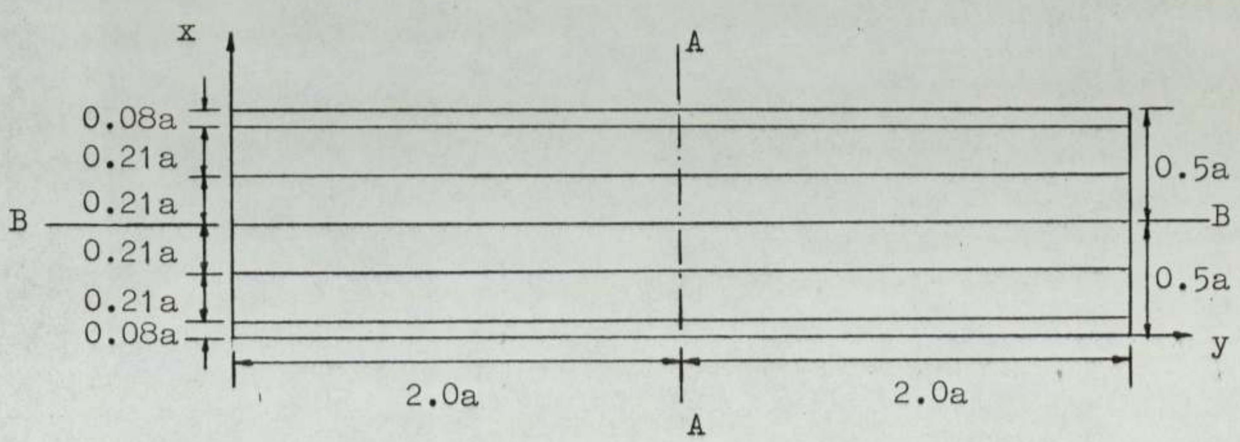

(b)

Figs.(7.6) Uniformly loaded simply supported rectangular plate in two orientations.

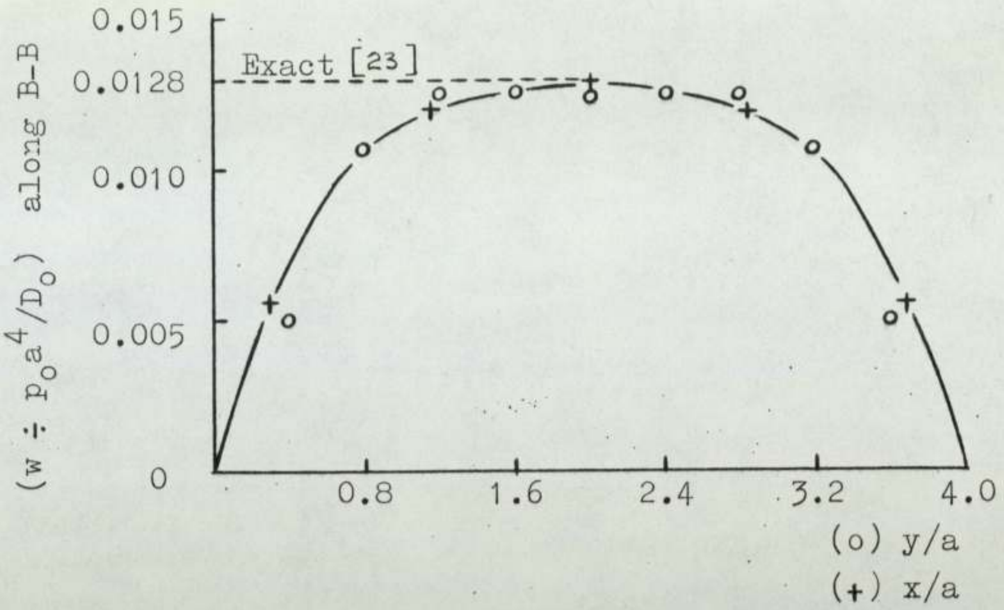

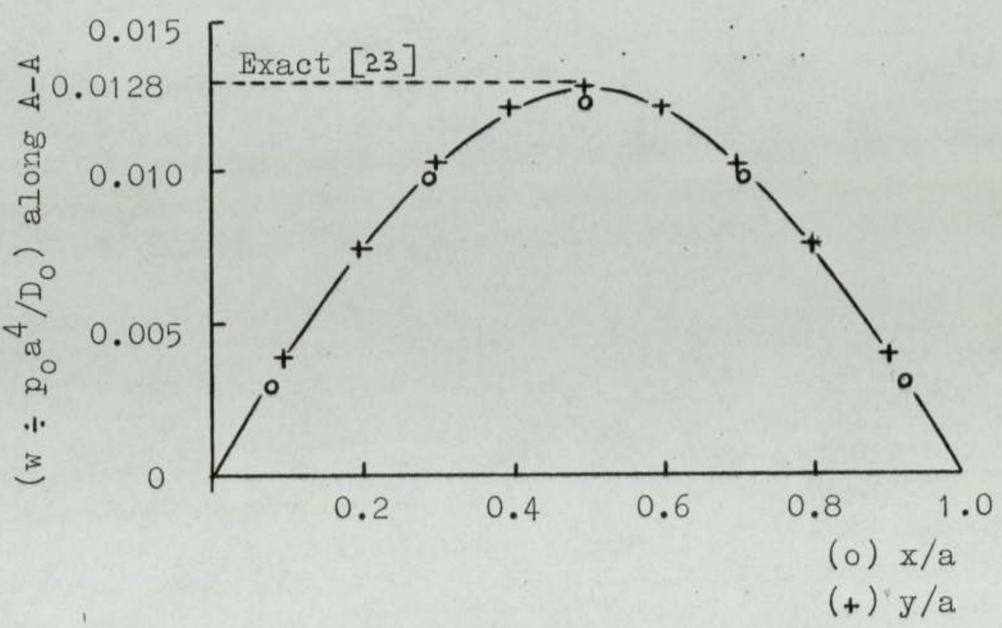

Figs.(7.7) Deflections along A-A and B-B

(+) results from orientation (a).

(o) results from orientation (b).

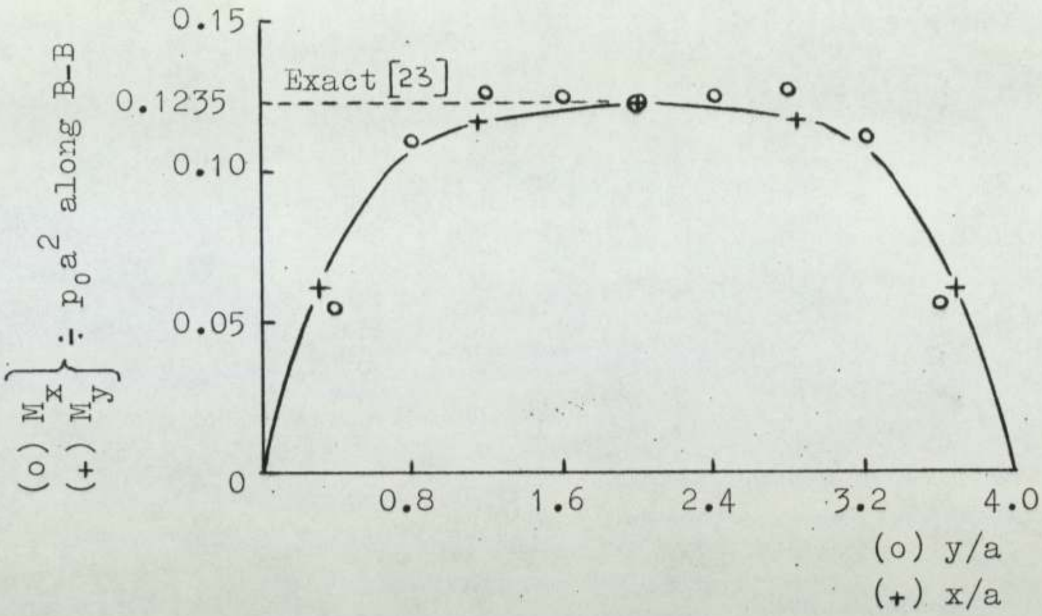

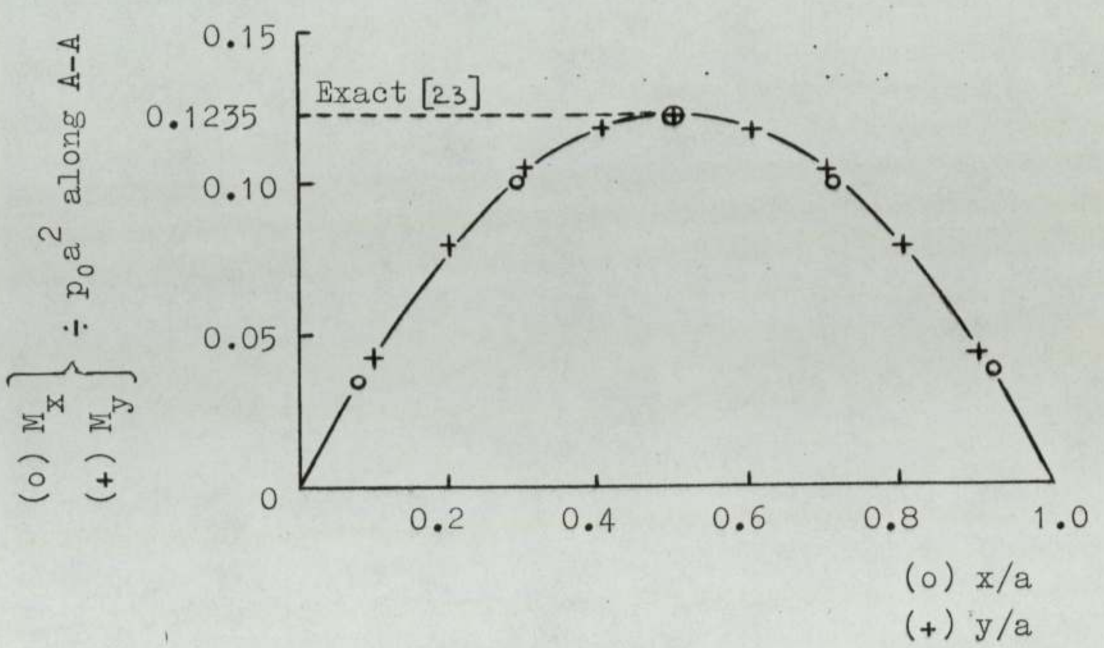

Figs.(7.8) Bending Moments along A-A and B-B

(+) results from orientation (a)
(o) results from orientation (b)

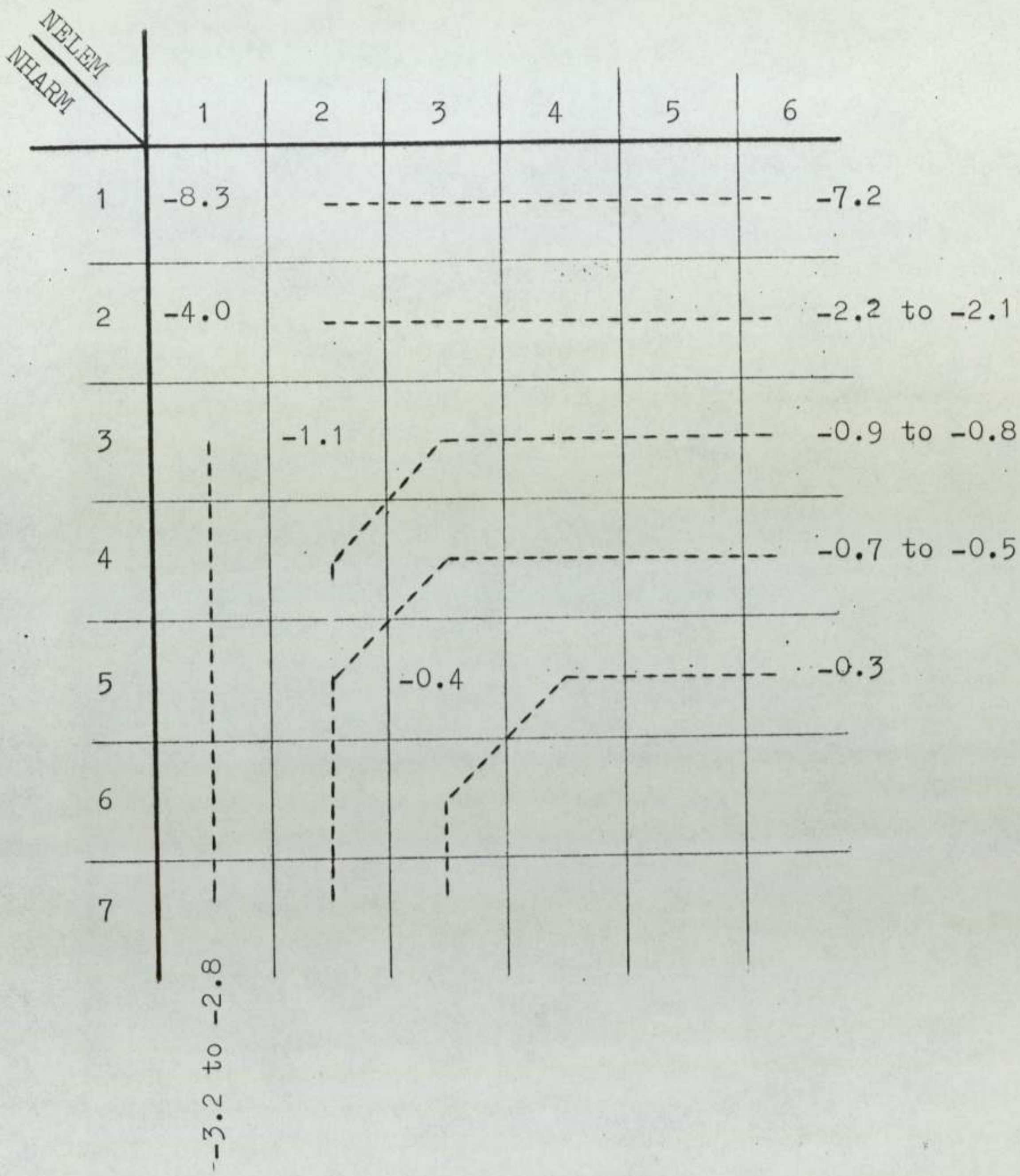

Fig.(7.9) Lines of constant % error in the central deflection for a combination of values of NELEM, the number of strips, and NHARM, the number of harmonics, for a simply supported square plate under a central concentrated force.

7.8 A Check on Accuracy.

In section (7.6), the analytic functions were tested for convergence for a number of cases of boundary and loading conditions and rigidity variation. Although it was established that these functions do converge, this convergence was not shown to be towards the correct solution. In this section, the results from the semi-analytic method, for a number of problems, are compared with results from other methods, some of which are analytical and others are numerical.

The test cases represent all the boundary conditions which are described by the analytical functions. The loading conditions include uniform pressure, linearly varying pressure and uniform line moment. The problem of a plate whose rigidity varies according to some known function and that of a plate with a hole were also solved.

The test cases and their solutions are given in figs. (7.10) through (7.24) and tables (7.9) and (7.10).

Whenever possible, symmetry of the plate about one or both centre lines was exploited by considering one half of the plate in the x-direction and odd modes only in the y-direction.

In the case of a free edge perpendicular to the y-direction the method suggested in section (4.6) was implemented, whereby the free edge was simulated by adding a zero flexural rigidity extension to the plate at the free edge in order to reduce the errors due to the residual normal bending moment at this edge. Where the free edge is perpendicular to the x-direction, the strip at the boundary was made narrower than the remaining strips aiming at the same goal as before.

Cases (i) and (ii) represent the same problem in a differing orientation. It is intended to demonstrate the effect of orientation, hence the analytic function used, on the accuracy of the results.

Whenever the solutions are available for a number of points on the plate, the comparisons are carried out graphically, otherwise maximum deflections and maximum bending moments are compared.

The series solutions for the problems in cases (i) and (ii) are from refs. [43], [44] and [45] and are based on the analytical methods discussed in section (2.3). For the remaining cases the references from which the solutions are obtained are given with the figures.

The letters designating the boundary conditions are self-explanatory. In each case the division of the plate and the necessary information regarding the applied load, the properties of the plate and the number of harmonics, M, are given with the relevant figure. In some of the figures, the identifier BM is used to mean either M_x or M_y as appropriate.

CASE (i) SS-SS-C-F

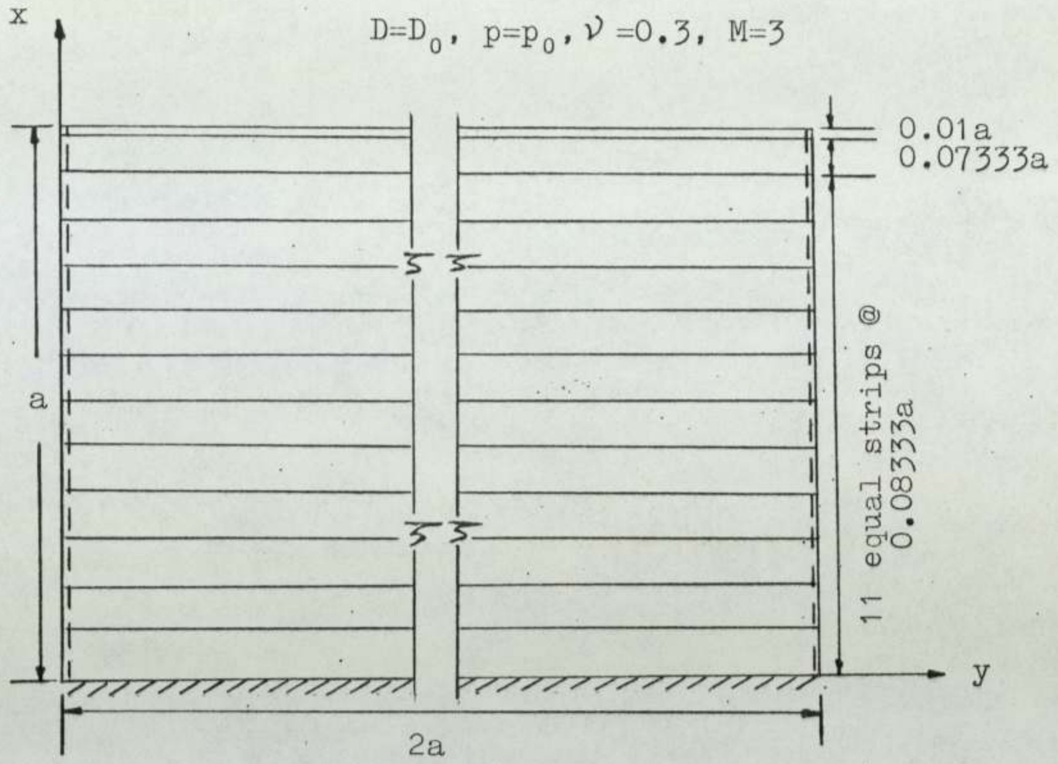

Fig.(7.10)

CASE (ii) C-F-SS-SS

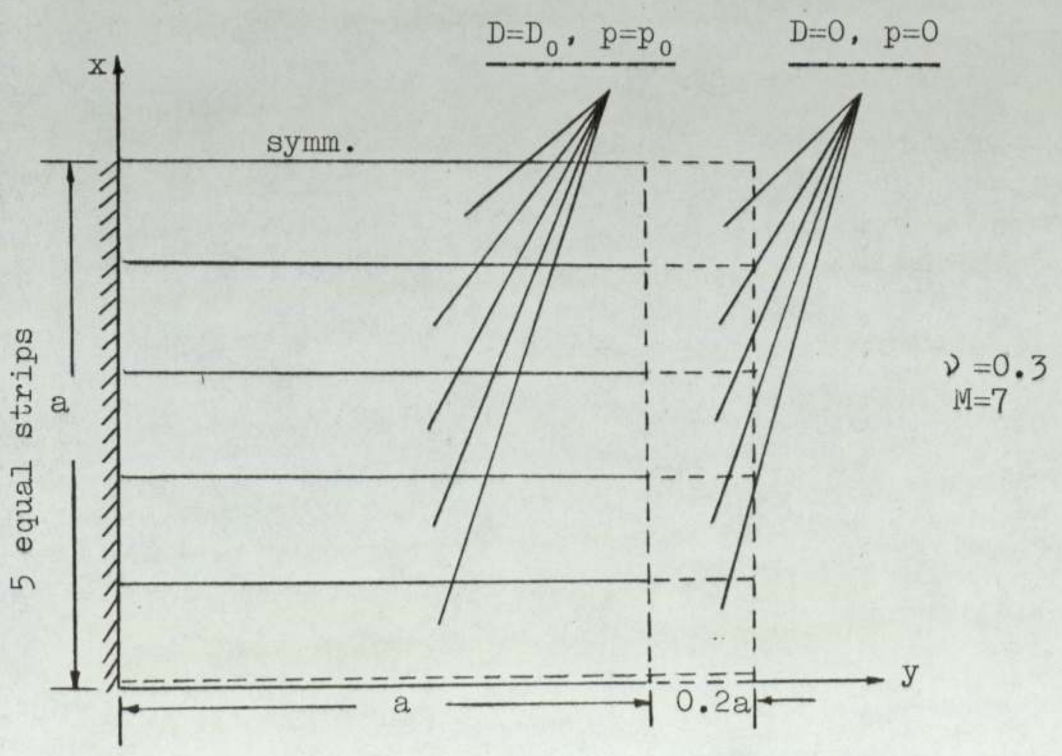

Fig.(7.11)

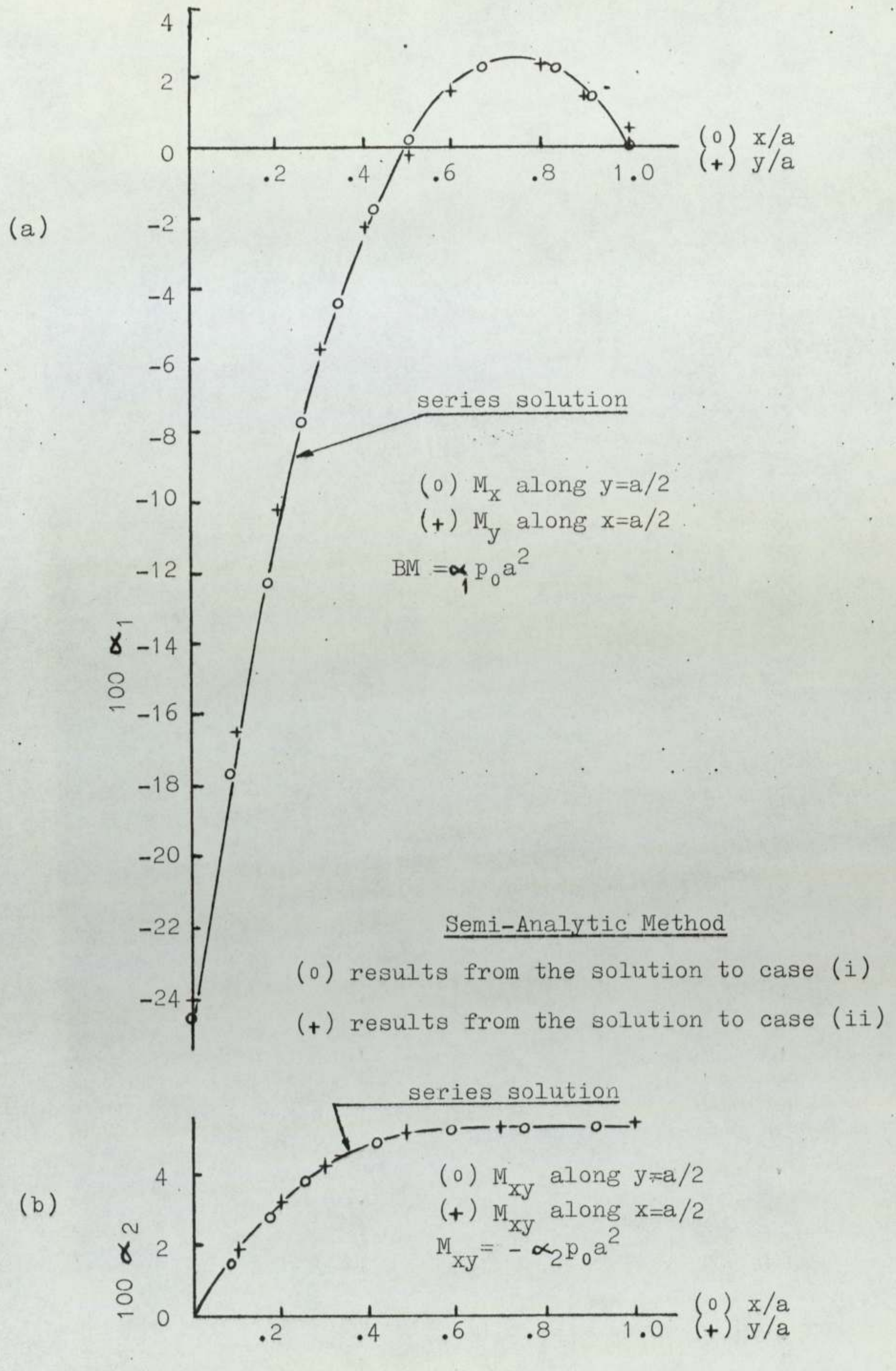

Figs.(7.12) Solutions to cases (i) and (ii)

(c)
(d)
(e)

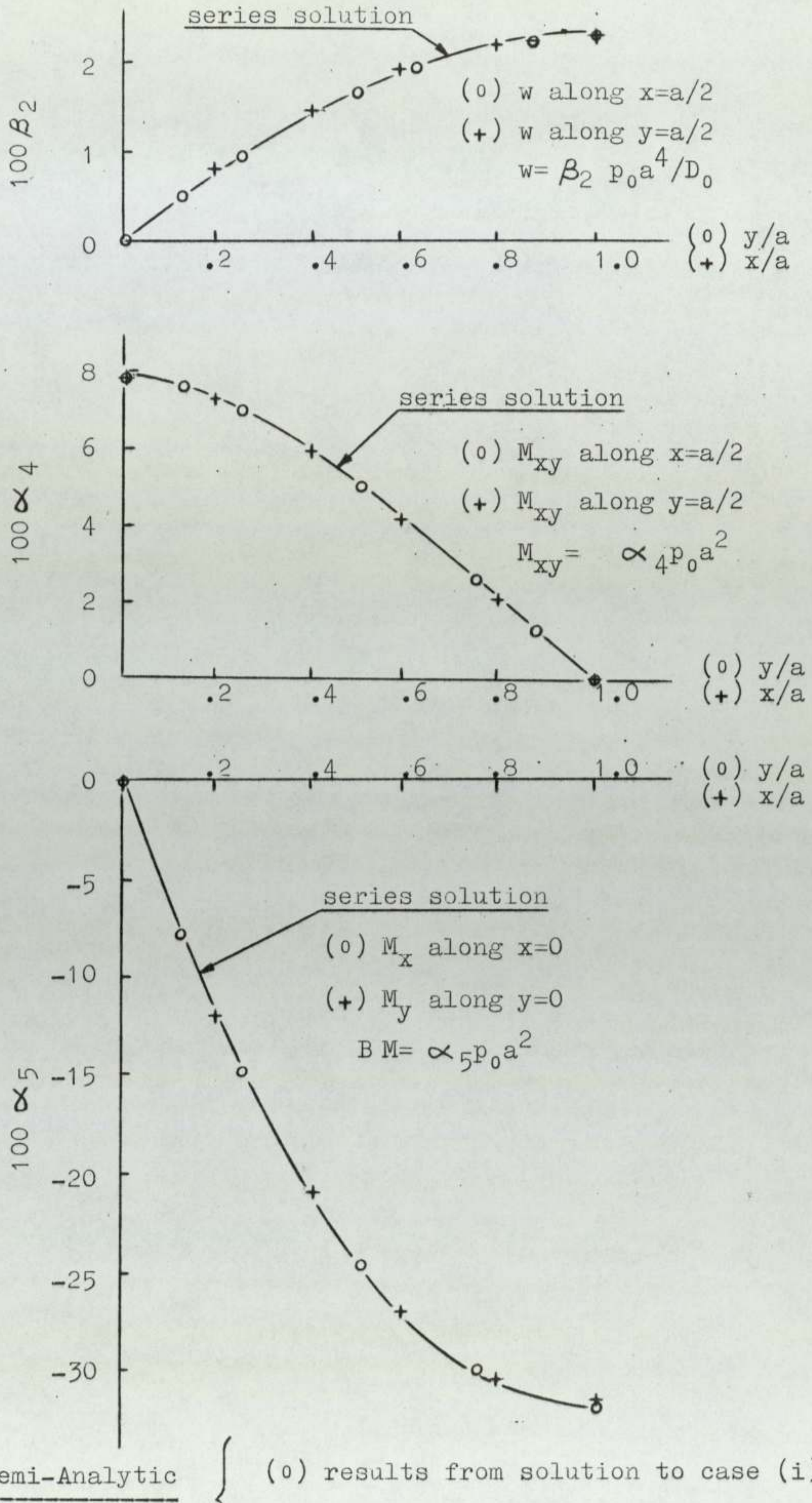

Semi-Analytic Method
(o) results from solution to case (i)
(+) results from solution to case (ii)

(f)

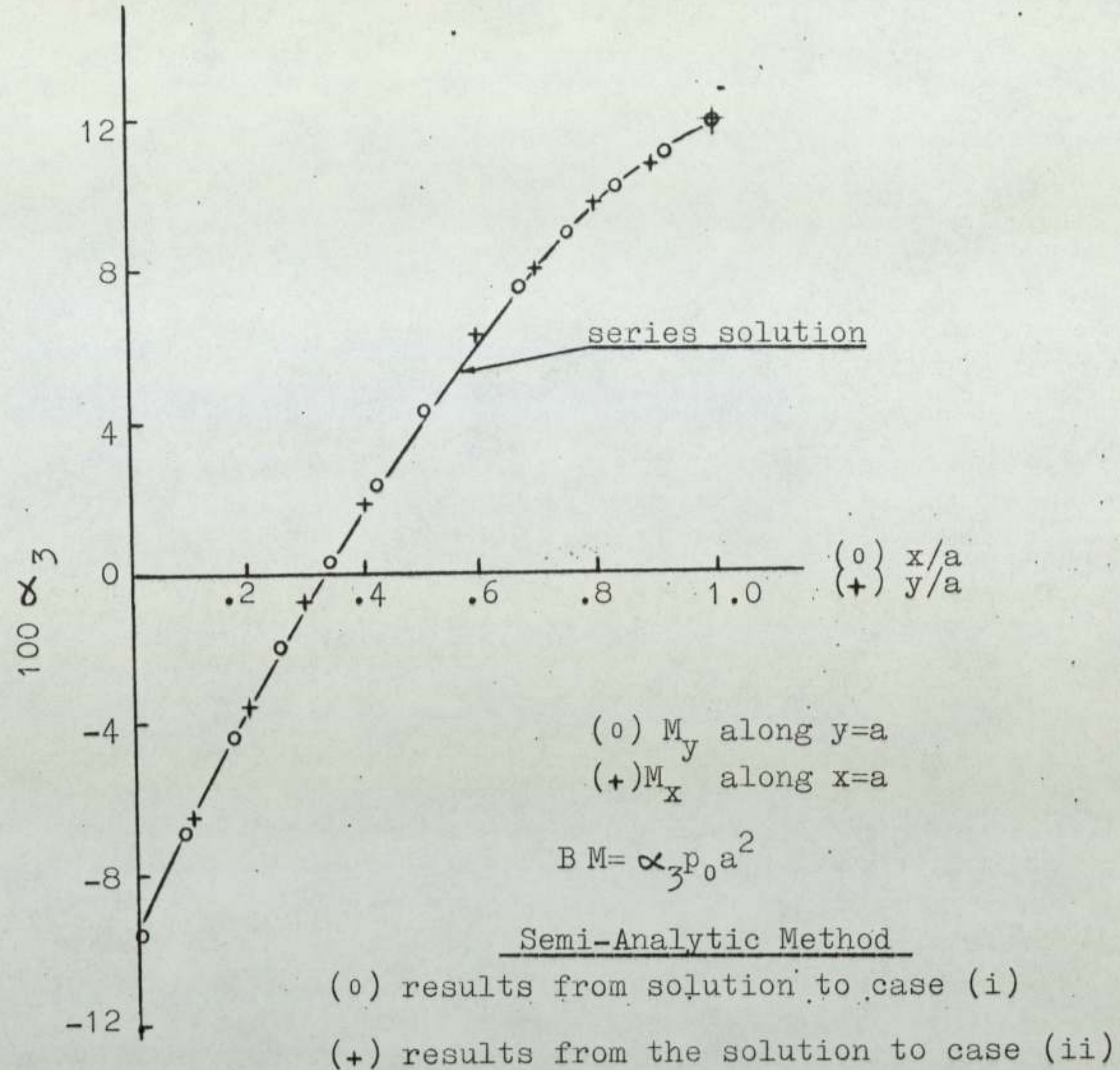

12
8
4
0
-4
-8
-12
$100\,\alpha_3$
.2
.4
.6
.8
1.0
(o) x/a
(+) y/a
series solution
(o) M_y along y=a
(+) M_x along x=a
B M= $\alpha_3 p_0 a^2$
Semi-Analytic Method
(o) results from solution to case (i)
(+) results from the solution to case (ii)

(g)

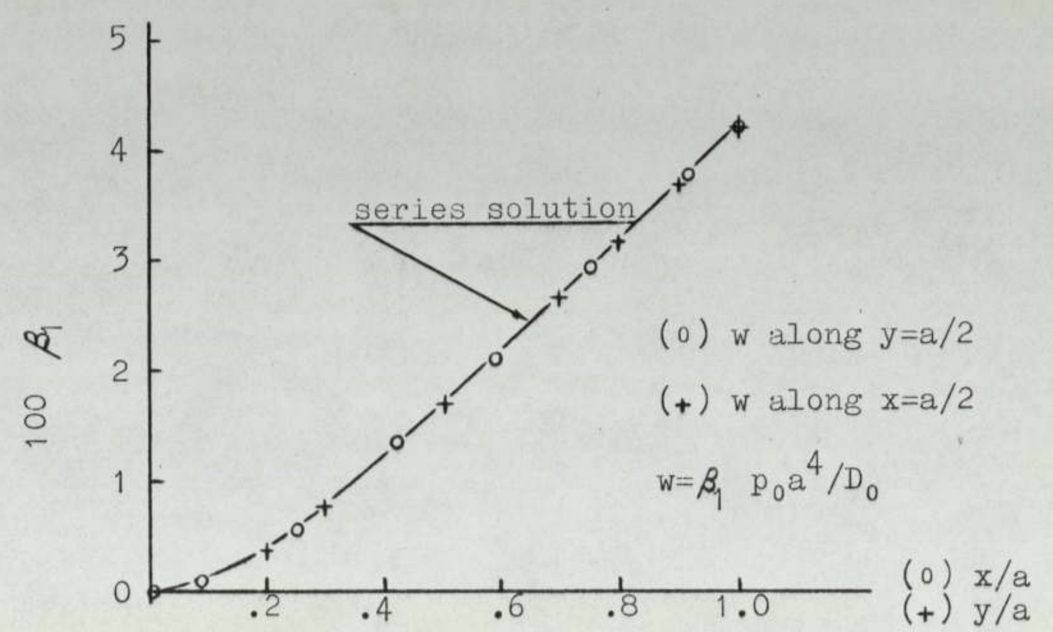

5
4
3
2
1
0
$100\,\beta_1$
.2
.4
.6
.8
1.0
(o) x/a
(+) y/a
series solution
(o) w along y=a/2
(+) w along x=a/2
$w=\beta_1\ p_0a^4/D_0$

CASE (iii) S-C-C-C

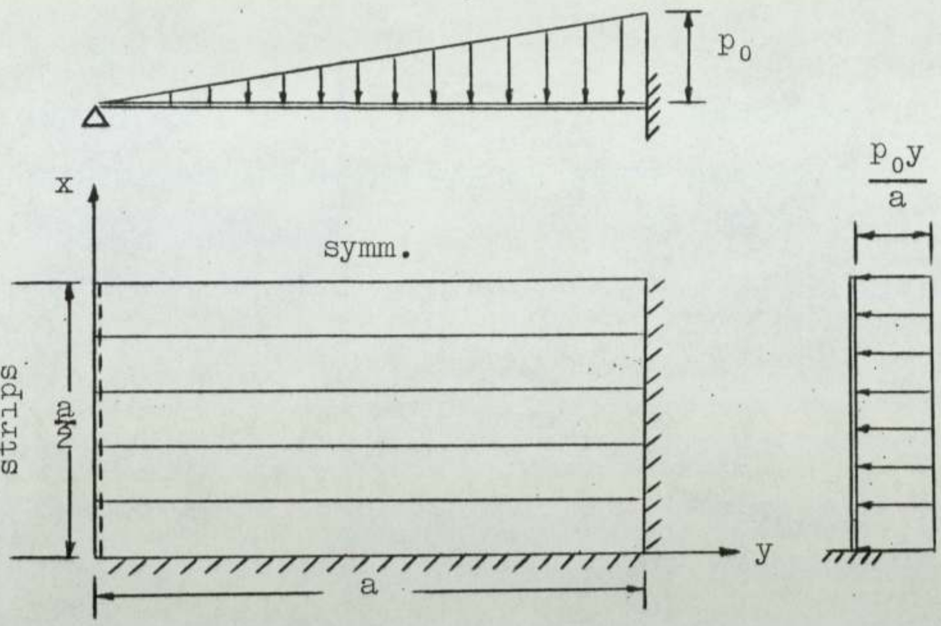

$D=D_0$, $\nu=0.2$, M=5

Fig.(7.13)

CASE (iv) C-C-C-F

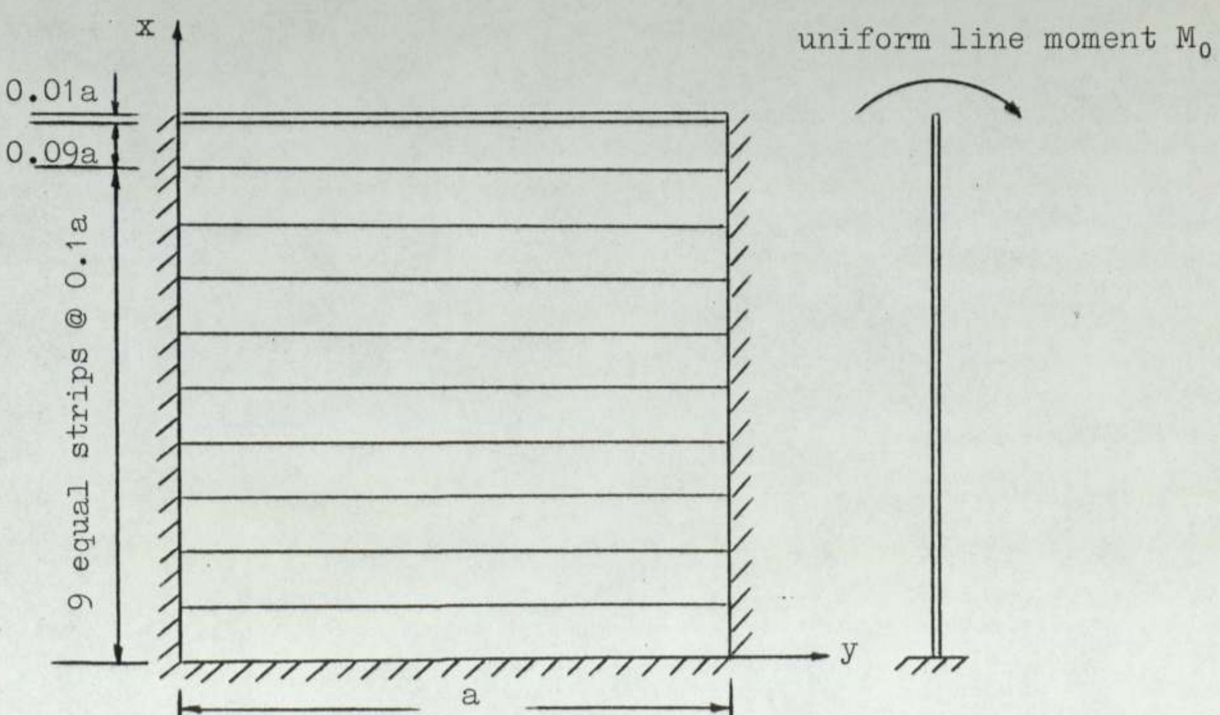

$D=D_0$, $\nu=0.2$, M=7

Fig.(7.14)

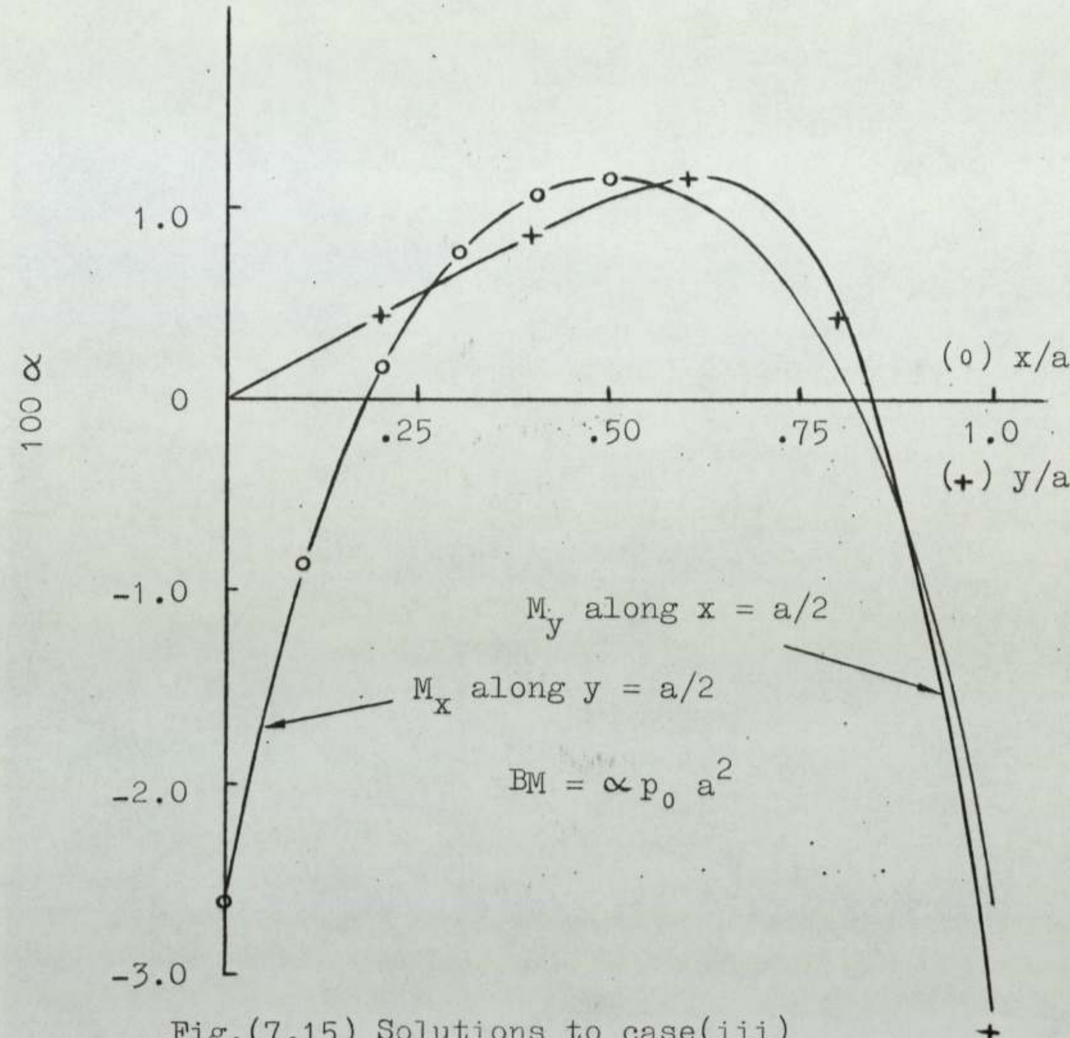

Fig.(7.15) Solutions to case(iii)

—— Finite Difference Method (ref.[46])

(+),(o) Semi-Analytic Method

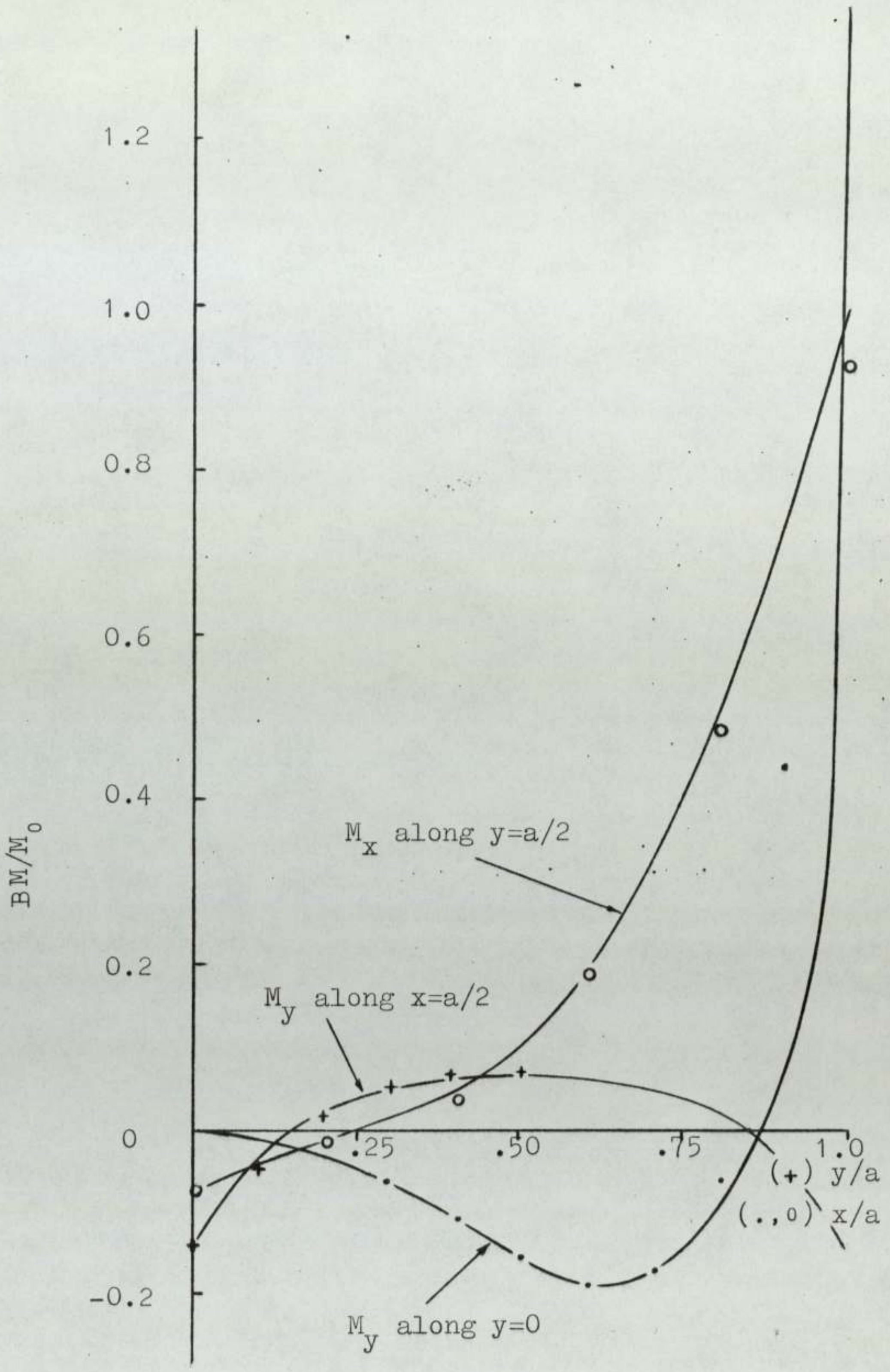

Fig.(7.16) Solutions to case (iv)

——— Finite Difference Method (ref.[46])

(+),(o),(.) Semi-Analytic Method

CASE (v) S-F-SS-SS

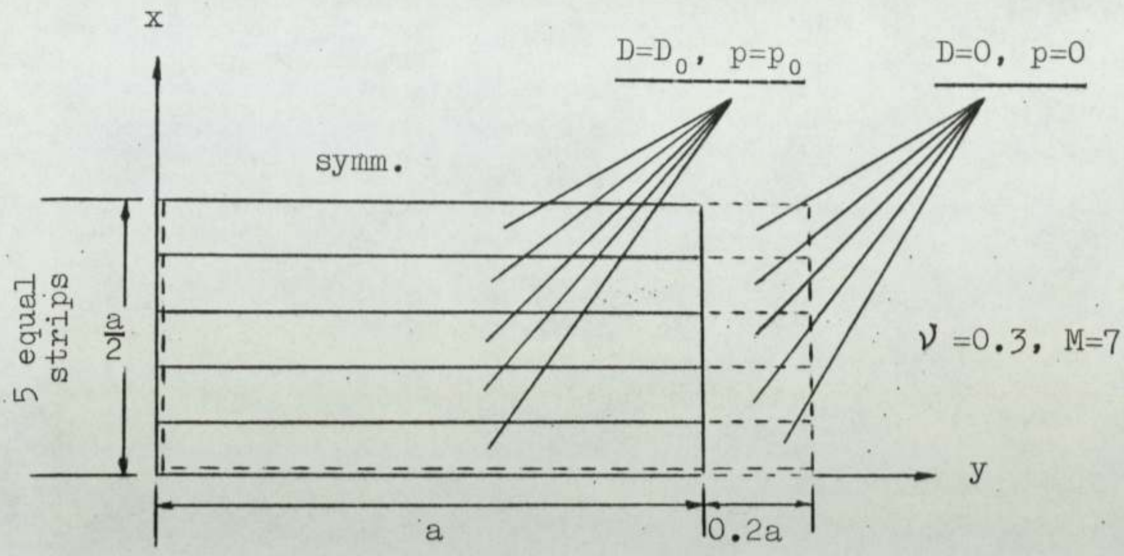

Fig.(7.17)

CASE (vi) F-F-SS-SS

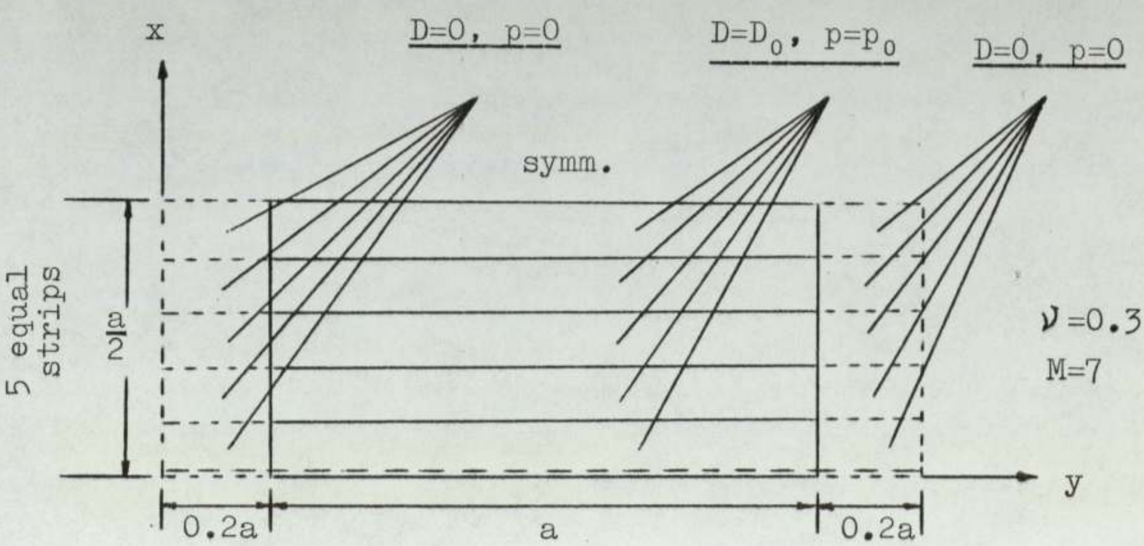

Fig.(7.18)

Table (7.9) Deflection and Bending Moments for case (v)

	x=a/2, y=a		x=a/2, y=a/2	
	$(w)_{max} \div \frac{p_0 a^4}{D_0}$	$(M_x)_{max} \div p_0 a^2$	$M_x \div p_0 a^2$	$M_y \div p_0 a^2$
Semi-Analytic	0.01285	0.114	0.080	0.039
Exact [23]	0.01286	0.112	0.080	0.039

Table (7.10) Deflections and Bending Moments for case (vi)

	x=a/2, y=a		x=a/2, y=0.7a		
	$(w)_{max} \div \frac{p_0 a^4}{D_0}$	$(M_x)_{max} \div p_0 a^2$	$w \div \frac{p_0 a^4}{D_0}$	$M_x \div p_0 a^2$	$M_y \div p_0 a^2$
Semi-Analytic	0.01501	0.1327	0.01309	0.1233	0.0270
Exact [23]	0.01509	0.1318	0.01309	0.1225	0.0271

CASE (vii) Variable Thickness

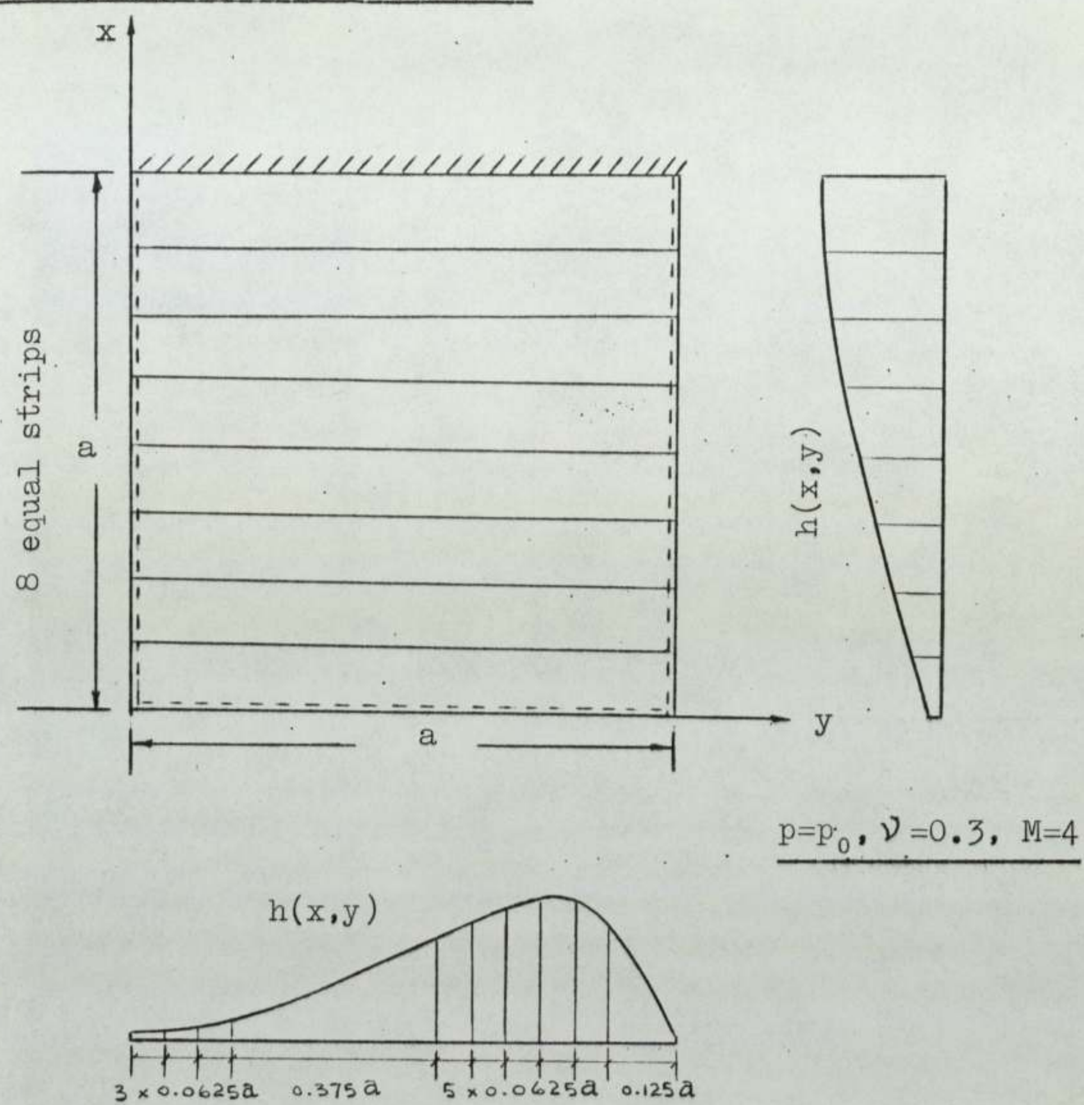

The thickness, h, is given by:

$$h=2\sin\left(\frac{\pi}{6}+\frac{\pi x}{3a}\right)\left[0.1674+2.175\left(1-\frac{y}{a}\right)^{\frac{1}{2}}\left(\frac{y}{a}\right)\right]$$

The rigidity, D(x,y) is expressed in terms of the rigidity, D_0, at x=0, y= $\frac{5a}{8}$ at which point h=1.

The integral in the y-direction is divided into 10 steps for each strip as shown.

Fig.(7.19)

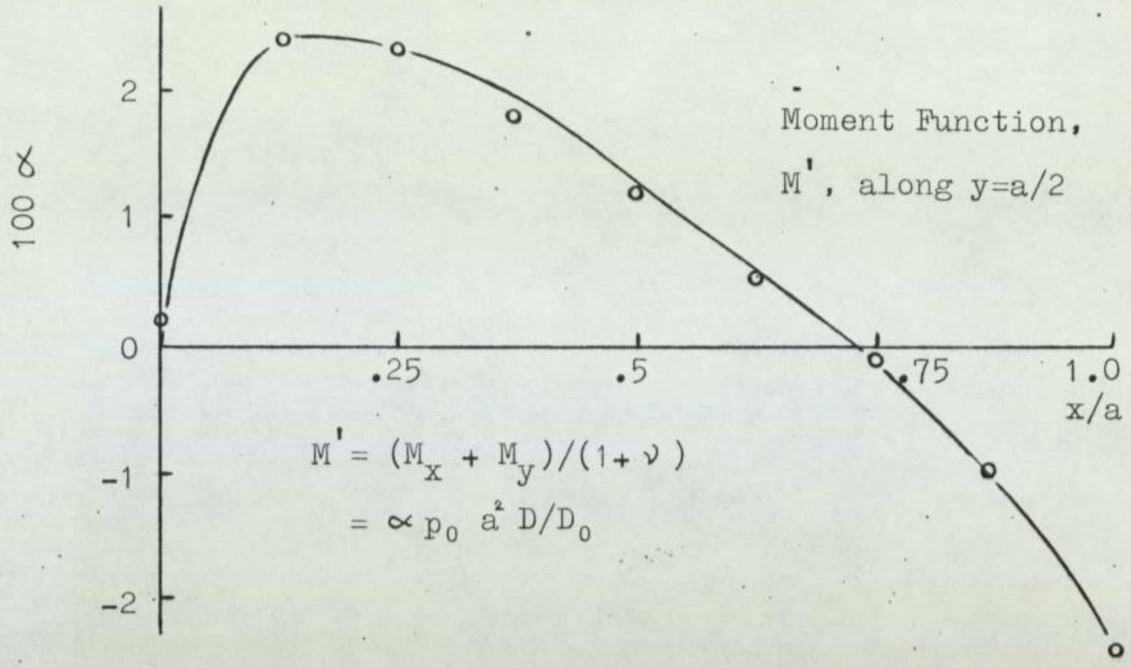

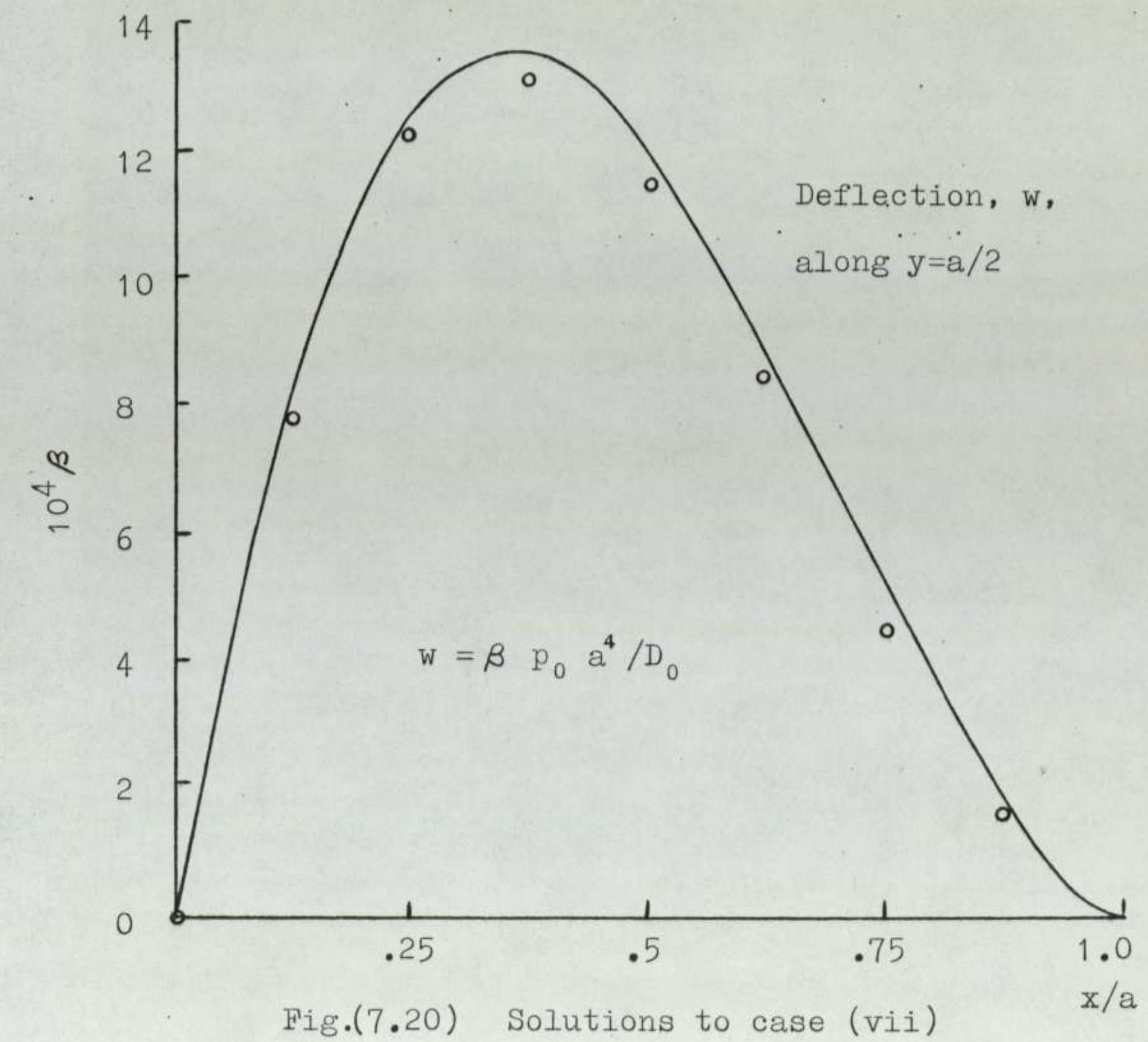

Fig.(7.20) Solutions to case (vii)

—— Finite Difference Method with pure-resistance electrical analogue computer (ref. [30])

(o) Semi-Analytic Method

CASE(viii) <u>Simply Supported Square Plate With a Square Central Hole</u>

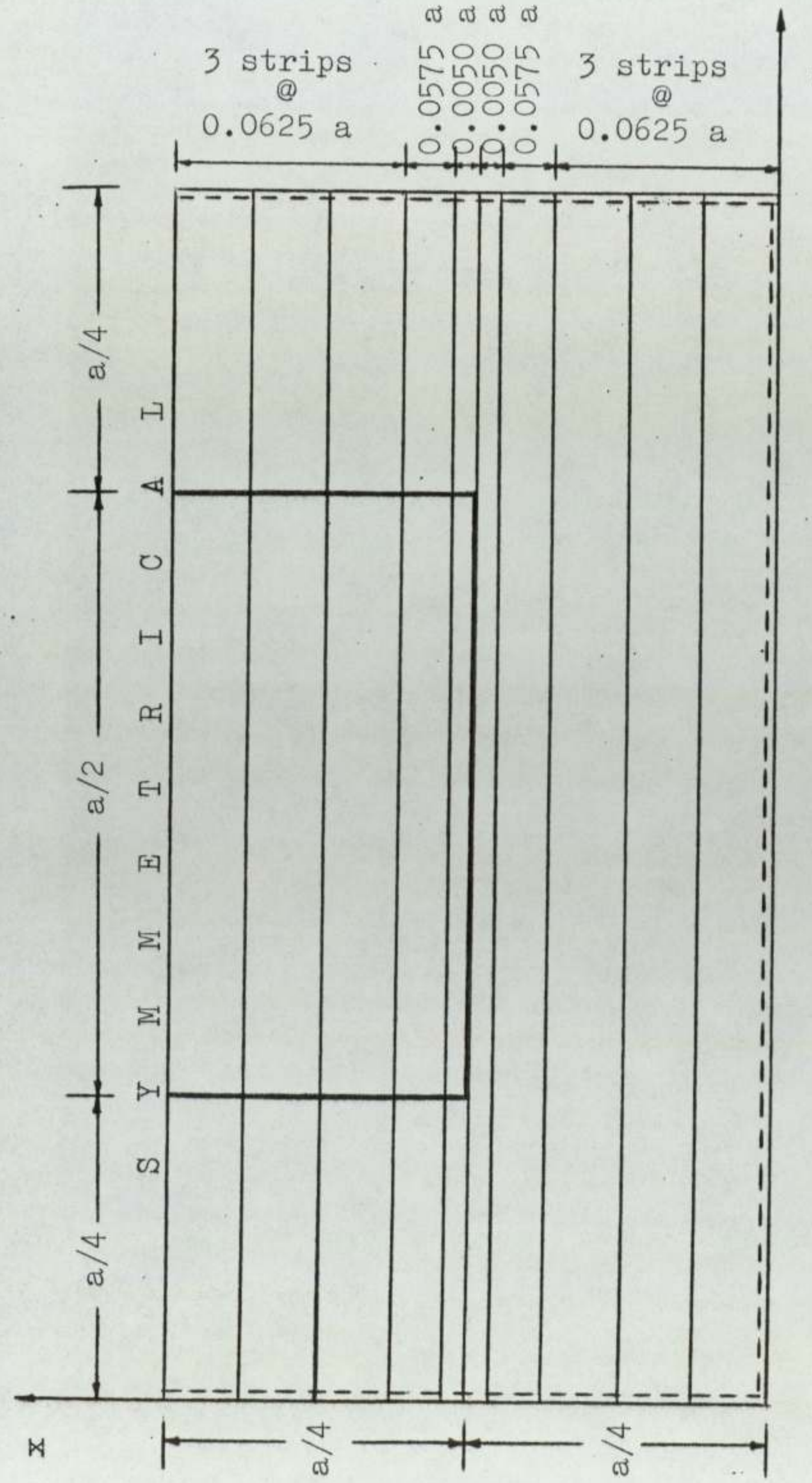

Fig.(7.21)

Over the hole region $D = 0$, $p = 0$

Elsewhere $D = D_0$, $p = p_0$ $\nu = 0.3$ $M = 7$

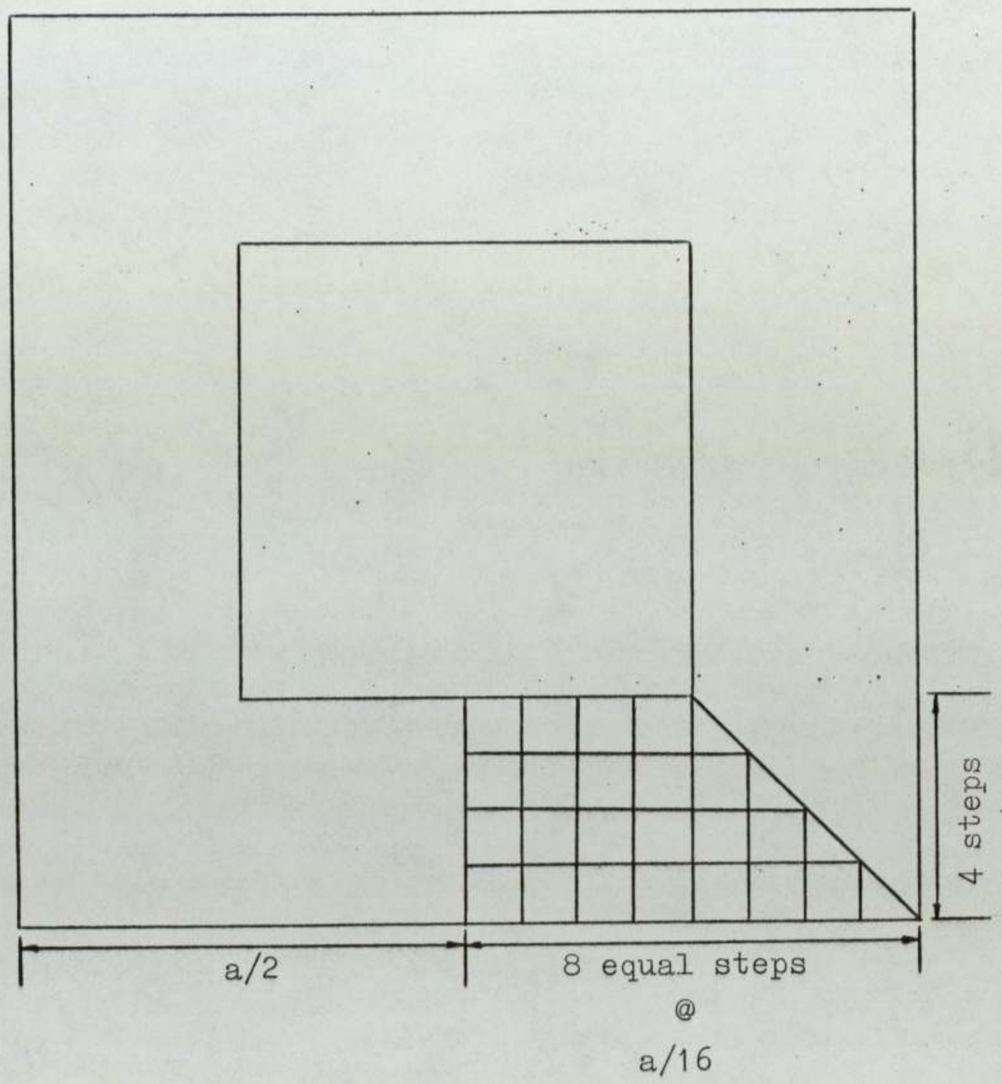

Fig.(7.22) Locations at which the bending and twisting moments in fig.(7.23) are given.

2.36	2.47	2.62	3.11				
0.01	0.00	0.00	0.00	singular			
0.00	0.49	0.98	1.63				
1.97	2.01	2.13	2.41	2.54	1.73		
0.70	0.72	0.79	0.97	1.39	1.72		
0.00	0.47	0.96	1.54	2.30	2.55		
1.43	1.46	1.55	1.66	1.66	1.37	0.98	
0.91	0.93	0.97	1.03	1.12	1.17	0.98	
0.00	0.46	0.94	1.46	2.03	2.46	2.68	
0.77	0.78	0.82	0.87	0.85	0.74	0.57	0.30
0.66	0.66	0.68	0.69	0.70	0.68	0.57	0.33
0.00	0.46	0.94	1.45	1.97	2.45	2.78	3.06

$\begin{Bmatrix} M_y \\ M_x \\ M_{xy} \end{Bmatrix}$

Simply Supported Edge

Fig.(7.23a) Values of M_y , M_x , M_{xy} from the modified Rayleigh-Ritz finite element solution (ref.[47]).

All values to be multiplied by $p_0 \, a^2/100$

Locations are shown in fig.(7.22).

2.39	2.44	2.59	2.89				
0.00	0.01	0.03	0.16	singular			
0.00	0.48	1.02	1.87				
1.99	2.03	2.17	2.62	2.60	1.69		
0.70	0.72	0.80	1.04	1.39	1.72		
0.00	0.47	0.97	1.53	2.34	2.52		
1.45	1.48	1.57	1.65	1.62	1.37	1.00	
0.92	0.93	0.98	1.06	1.20	1.18	1.00	
0.00	0.46	0.94	1.47	2.10	2.44	2.65	
0.79	0.80	0.84	0.90	0.89	0.76	0.59	0.38
0.67	0.68	0.69	0.70	0.70	0.70	0.60	0.37
0.00	0.46	0.93	1.44	1.96	2.43	2.77	3.00

$\begin{Bmatrix} M_y \\ M_x \\ M_{xy} \end{Bmatrix}$

Simply Supported Edge

Fig.(7.23b) Values of M_y , M_x , M_{xy} from the Semi-Analytic solution to case (viii).

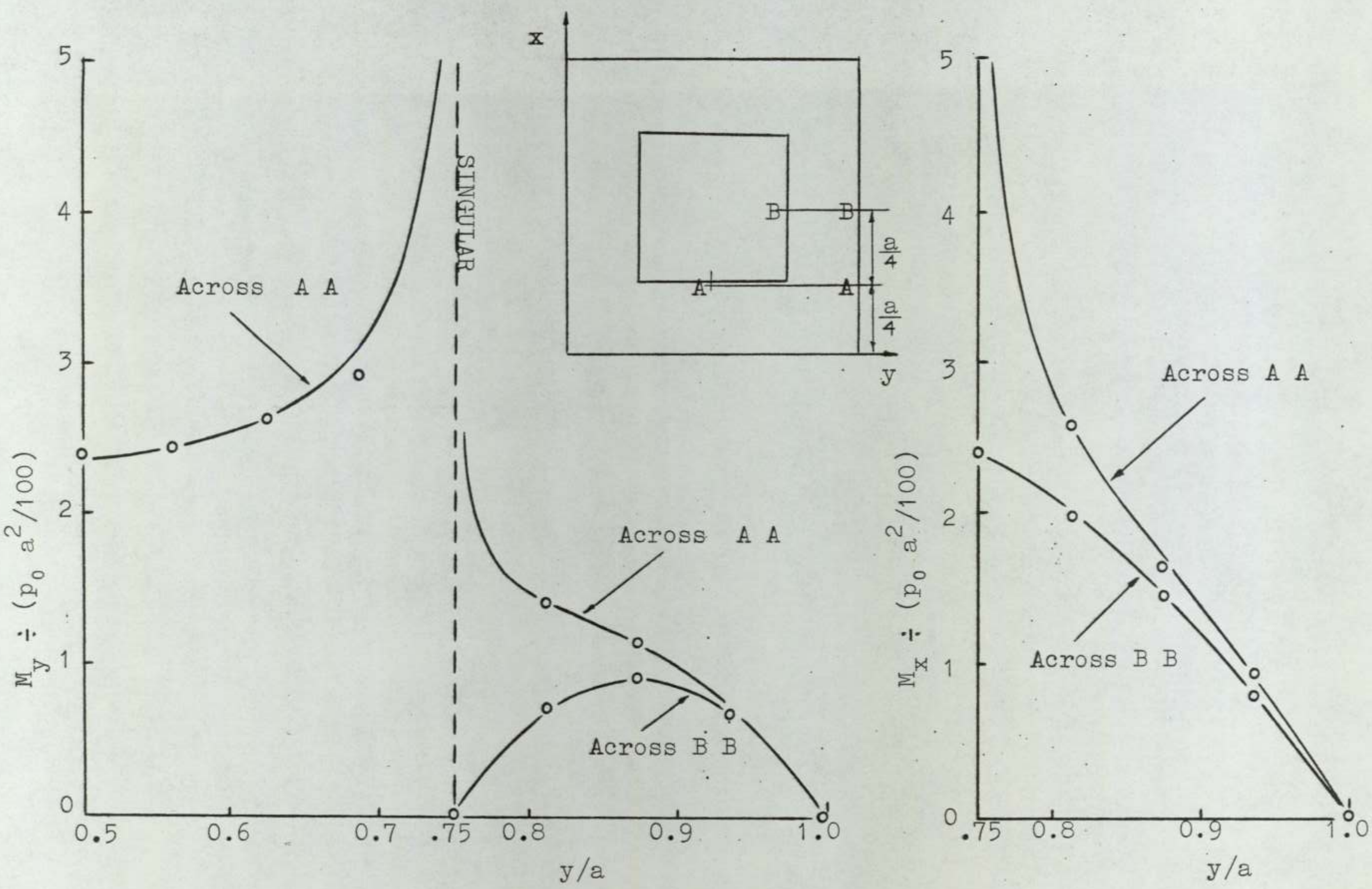

Fig.(7.24) Solutions to case (viii)

— From ref.[47]

o From Semi-Analytic Method

7.8.1 Discussion of Results.

In the preceeding section, a thorough check on the accuracy of the semi-analytic method was carried out for a number of problems.

It can be seen that the agreement of the solutions from the semi-analytic method with those from other methods, some of which are "exact", is excellent in all cases but one and for most points on the plate for which the solutions are available. The only exception is the bending moement M_y along y=0, (fig.7.16), in the solution to the problem of case (iv). The discrepency between the value of this moment as obtained from the finite difference method with that from the semi-analytic is comparatively large near the edge on which the uniform couple is applied. Elsewhere, however, the agreement between the solutions from the two methods is very good.

The accuracy of the results has proven to be, generally, extremely good. However, there are a few points which deserve particular attention.

In section (7.6) when the numerical stability and convergence of the various beam eigenfunctions were tested, it was discovered that these properties are superior in the case of simply supported-simply supported functions, to those in other functions. The problems in cases (i) and (ii) were intended to confirm this point. They represent the same problem in differing orientations. In the first case, the simply supported-simply supported function was used and in the second case, the clamped-free function was used. Results of comparable accuracy were obtained for both cases. However, the plate in the first case was divided into 13 strips and 3 harmonics, whereas in the second it was necessary to divide half the plate into 5 strips and 7 harmonics. Now, since the computer time required for the solution of the equations, which ususally constitutes a considerable proportion of the overall time required for the solution of the problem, is proportional to NB^2 (section 7.7), the values of this quantity for the two cases will be 12096 and 65856 respectively. Thus, to obtain similar accuracy from the two functions, the clamped-free problem requires considerably more computer time than does the simply supported-simply supported problem. This confirms the superiority of the behaviour of the simply supported function.

Exact solution for cases (v) and (vi) were only available for two points on the plate. Comparison with the solutions from the semi-analytic method (tables 7.9 and 7.10) shows that the error in the deflection is less than 0.6% and the error in the bending moments is less than 2%, for the given number of strips and harmonics. An increase in the number of strips and the number of harmonics would improve accuracy.

The problem of a plate with a hole (case viii) is of particular interest because of its frequent occurrence in civil engineering where it is necessary to provide a hole in a slab floor for lifts, say. The problem is important, in practice, because of the uncertainty about the effect of the singularity of the bending moments at the corners of the hole and the extent of propagation of any errors this singularity may cause.

Morley [47] developed a method of solution, for this type of problem, which employs triangular finite elements together with eigenfunctions that satisfy, exactly, the homogeneous differential equation of the plate and the boundary conditions along the inner edges. The principle of minimum complementary energy was used in the formulation (i.e. the force formulation). The values of bending and twisting moments for a simply supported square plate with a central square hole, under uniform pressure are given in fig.(7.23) in which (a) gives these values from the Morley solution and (b) gives the values from the semi-analytic method.

The agreement between the solutions is excellent on all but a few points near the corner. At these points the maximum error in the bending moments is 7.0%. Because the semi-analytic mathod uses a continuous function with continuous derivatives, the bending moments at the corners have a finite though large values. Acknowledging the singularity of the moments at the corners, these values are ignored.

Thus, the semi-analytic method gave very good results for the problem of a plate with a hole, with no special modification to the formulation. The strips nearest the edge of the hole were made narrower than the rest to reduce the effects of error propagation.

7.8.2 Comparison of the Rate of Convergence in the Semi-Analytic Approach and Other Formulations of the Finite Element Method.

In the finite element method, the problem may be formulated with the displacements, forces or both as unknown parameters. In these cases the formulations are called displacement, force or mixed respectively. With each formulation various types of elements and functions may be employed [10], [35]. These yield solutions of varying rates of convergence.

Desai and Abel [10] compared the rates of convergence of a number of types of elements employed in the analysis of a simply supported square plate under a central concentrated force. The basis for comparison was the percent error in the central deflection as a function of NB^2, where N is the number of equations arising from the analysis of the discretized structure and B is the semi bandwidth of the equations. NB^2 is a measure of computer time required for the solution of the equations [39].

Against some of the elements in Desai and Abel's example, the rate of convergence of the central deflection of the same problem, obtained by the semi-analytic method, is compared here.

A brief description of the elements, the formulation and comparison of their rates of convergence are given in fig.(7.25). This shows that the results from the semi-analytic approach converge much more rapidly than any of the other elements or formulations given. Conversely, for similar accuracies, the semi-analytic solution requires considerably less computer time .

Fig.(7.25) also shows that the semi-analytic solution represents a lower bound to the exact solution.

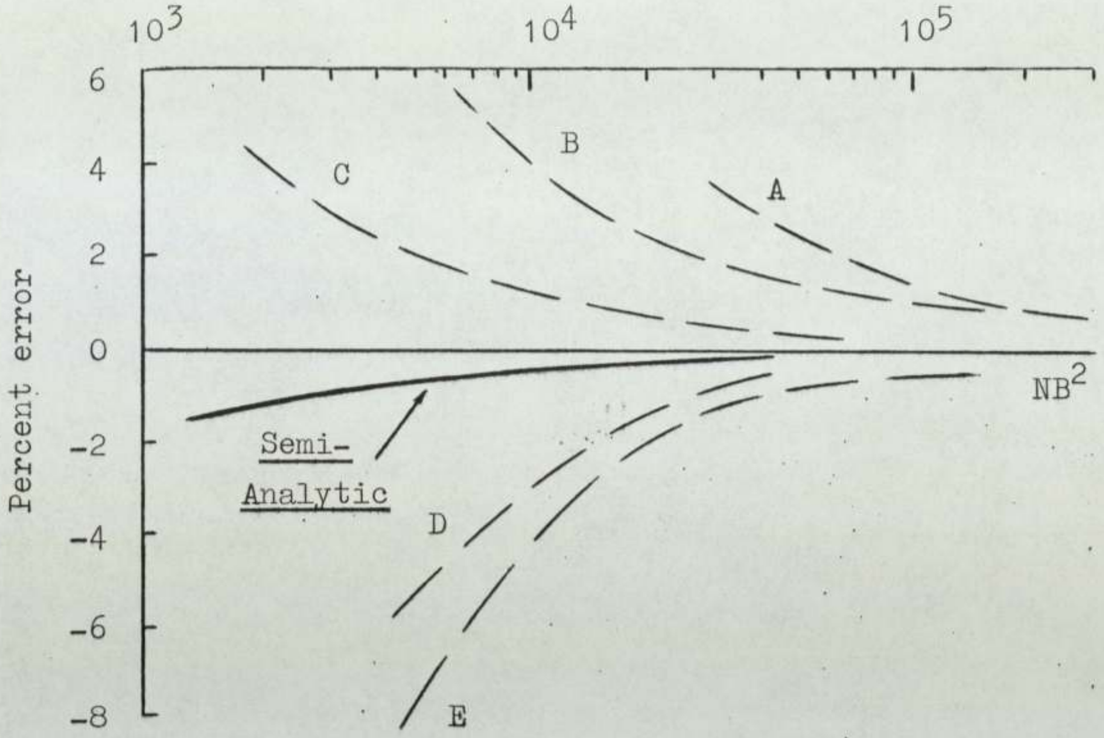

Symbol	Approach	Description of Element
A	Force	2 triangles; linear moments.
B	Displacement	rectangle; cubic model.
C	Displacement	rectangle; cubic beam function plus uniform twist.
D	Mixed	4 triangles; cubic displacements, quadratic stress parameters.
E	Displacement	rectangle; cubic Hermitian polynomial model.

Fig.(7.25) Comparison of the rate of convergence of the central deflection, for a simply supported square plate with a central point load, from the Semi-Analytic approach with other approaches to the Finite Element Method.

7.9 Experimental Tests.

In the previous section, results from the computer program, for various cases of loading and boundary conditions were compared with known published results in order to test the accuracy of the semi-analytic method. It was felt that experience in an experimental procedure for the analysis of plates would be desireable. At the same time a further check on the applicability of the semi-analytic method to plate bending problems with rigidity variation, may be obtained through the experimental procedure. For these purposes, the Moire Technique, which was developed by Ligtenberg [48], for the experimental analysis of laterally loaded plates was used.

7.9.1 The Moire Apparatus.

The Moire apparatus (fig.7.26) consists of a steel structure on which a curved screen is mounted. The surface of the screen, which is in the form of a circular cylinder segment, is covered with ruled paper. The lines being equispaced and parallel to the axis of the cylinder. The screen can be rotated so that the lines may be set to any desired angle from the vertical, and its position may be adjusted in three directions. A camera, which is mounted behind the screen, views, through a hole in the screen, a model of the plate which acts as a first surface mirror, in front of the screen. The model is fixed to the structure by means of G-clamped. Loading of the structure is achieved through levers attached to the structure behind the model. Illumination of the screen, which is necessary for the photography process, is achieved by means of photo-flood lamps positioned, on the structure, at such

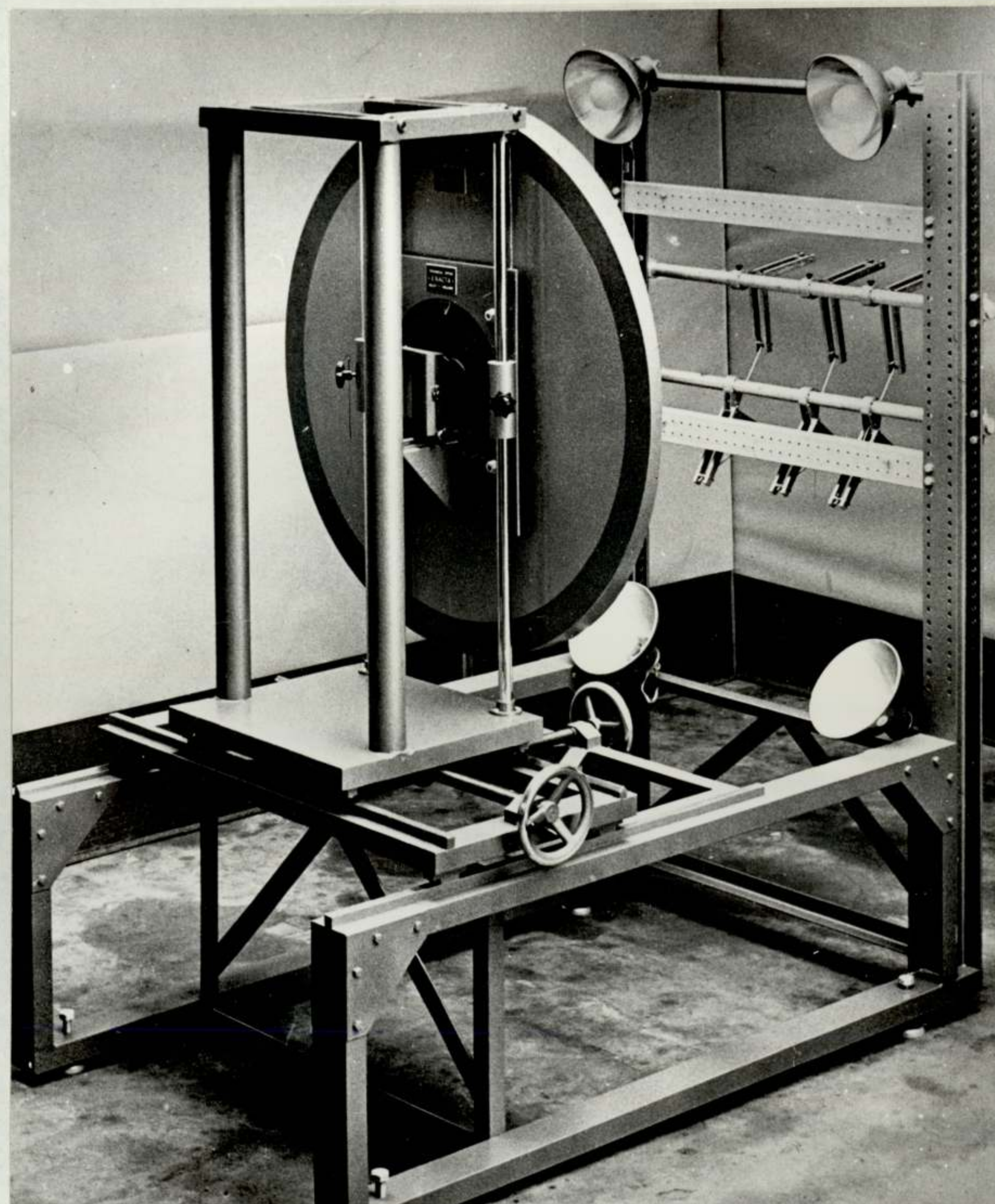

Fig. (7.26) The Moire Apparatus.

points as to ensure even distribution of light on the screen and avoid glare from reaching the camera lens.

7.9.2 Fundamentals of the Moire Method.

In this method the model of the slab, which is positioned in front of the illuminated, lined screen, acts as a first surface mirror reflecting the images of the lines on to the photographic plate (fig.7.27).

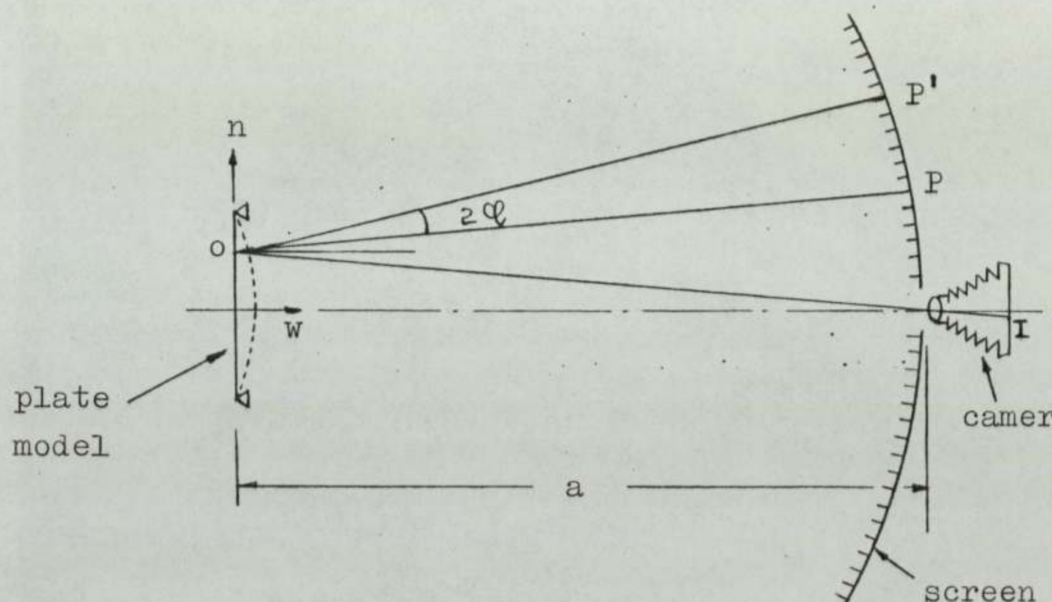

Fig.(7.27)

When a photograph is taken of the unloaded model, this photograph will record the undistorted image of the lines as reflected by the model. In particular a point P on the screen will appear as the image I on the Photographic plate. If, then, the model is deflected by the load, the image of a different point P' will coincide with I. Now, whenever such points as PP' are a certain constant distance apart, their images will coincide at such points on the photographic plate as I. These images will form a line called a "fringe".

On the basis of small deflections theory of plate flexure, the angle P'OP can be shown to be twice the angle of rotation φ in the direction normal to the lines of the screen. Thus, referring to fig.(7.28), the following relationships can be obtained:

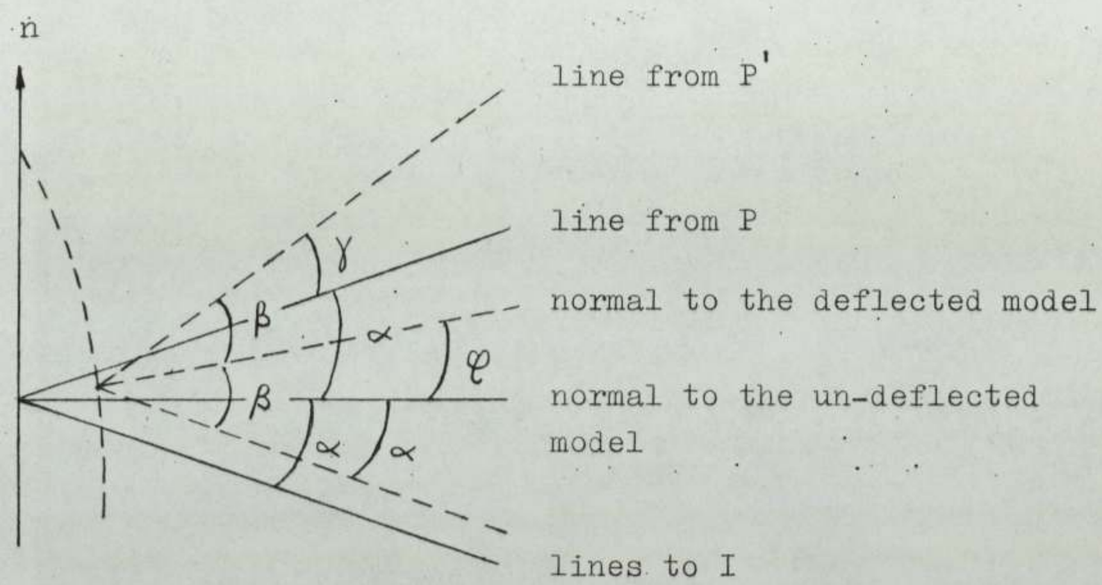

Fig.(7.28)

$$\gamma = \beta - (\alpha - \varphi).$$

$$\beta = \alpha + \varphi$$

$$= 2\varphi \qquad \text{where} \quad \varphi = \frac{\partial w}{\partial n}$$

Thus, the fringe is the line on which the slope, normal to the direction of the lines, has a specific constant value. The value of the slope pertinent to a particular fringe is established only if the slope is known along a certain line on the slab. This situation is often possible as in the case of zero slopes due to clamped edges or lines of symmetry.

Once the fringe pertinent to the zero slope is established, it is assigned the integer value 0 called the "fringe order". The order of the remaining fringes will, then, be obtained by assigning the integer values 1,2,3,... to neighbouring fringes on one side of the zero order fringe and -1,-2,-3,... to neighbouring fringes on the other side. The sign of the fringe order depends on the sign of the slope.

Between two consecutive fringes, the values of PP' will differ by an amount, d, equal to the distance between two lines on the screen, and for small deflections, the slopes, φ , will differ by an amount d/2a, where a is the distance from the model to the screen (fig.7.27).

Thus, a graph of the variation of the slope in any direction may be obtained from the photograph of the fringe patterns. This process will be shown for a specific case later. Fringe patterns obtained whilst the lines are in a direction normal to the x-axis of the plate model give the slope $\frac{\partial w}{\partial x}$ and those obtained whilst the lines are in a direction normal to the y-axis of the model give the slope $\frac{\partial w}{\partial y}$. Second derivatives, hence bending and twisting moments, are obtained by graphical differentiation and the deflection, w, is obtained by graphical integration.

The slope curve may be drawn without actually assigning a zero slope axis, and differentiation of the slope curve does not require that the line of zero slope be known although the correct signs must be established. The curvature curve may then be assigned a zero curvature axis to which other values of the curvature are related. It is unlikely that neither the slope nor the curvature is known at some point on the plate.

7.9.3 Technical Details.

Ligtenberg [48] showed that a radius of 3.5a for the circular cylinder, of which the screen is a segment, gives results with acceptable accuracy. The lines on the screen were found to give the clearest fringe patterns when the ruling was chosen as d/2 white and d/2 black where d is the distance between the centres of lines. Also, d should be chosen to be between 0.004a and 0.002a.

Almost any material which can be made reflective on one side may be used for the model. However, Perspex was found to be very satisfactory.

7.9.4 Experimental Details.

The experiences of other users of the Moire Apparatus, [49] and [50], were taken as a guide for the experimental work conducted here.

5 mm thick black perspex was used for the models of the plates which were to be analysed. Sufficient illumination of the screen was achieved by using four 500 watt. photo-flood lamps. A bellows-type camera with a 1:4.5/13.5 cm lens was used to take the photographs of the fringe patterns on a Kodalith Ortho (sheet) Film, Type 3. A diaphragm setting of f16 and exposure time of 45 seconds gave very good results. The relevant screen dimensions were a=86cm (based on R=3.5a) and d/2a = 0.00125.

7.9.5 Details of the Test Cases.

The Moire method was used to determine the slopes in three different plate problems, namely a square clamped plate with uniform rigidity under uniform pressure (fig.7.29a), a square clamped plate with a central portion whose thickness is twice that of the rest of the plate, also under uniform pressure (fig.729b), and a square clamped plate with a central square hole, under two concentrated loads (fig.7.29c).

To simulate the clamped edge condition the perspex plate was sandwiched between a pair of steel frames and the assembly was effectively made rigid at the boundary by a number of bolts (fig.7.30).

7.9.6 Experimental Procedure.

The procedure detailed here was carried out for each test case in turn.

The perspex plate was mounted, in its assembly, on the structure of the Moire Apparatus. The screen was adjusted to the required distance from the plate, and rotated so that the lines were parallel to the x-direction of the plate. The photoflood lamps were directed towards the screen so that the latter was evenly illuminated. The camera was, then, adjusted so that the image of the ruled lines, as reflected by the perspex plate onto the ground glass of the camera, was in focus. The sheet film was then placed in the camera, the diaphragm set to f16 and the film was exposed for 45 seconds. The load was then applied to the back of the plate and the same sheet film was exposed for the same length of time. The screen was then rotated through 90 degrees so that the lines were parallel

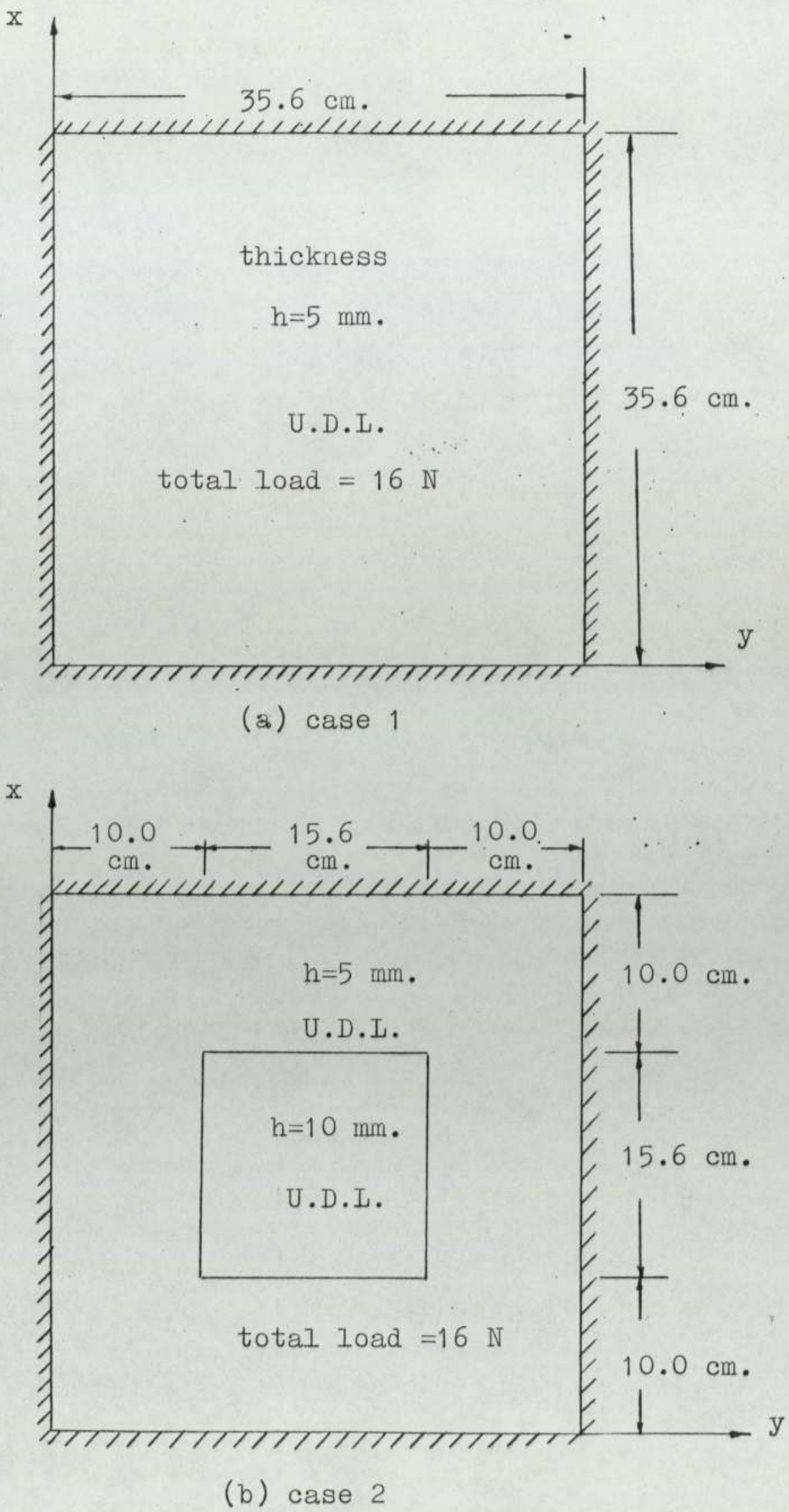

Fig.(7.29) Details of experimental test cases.

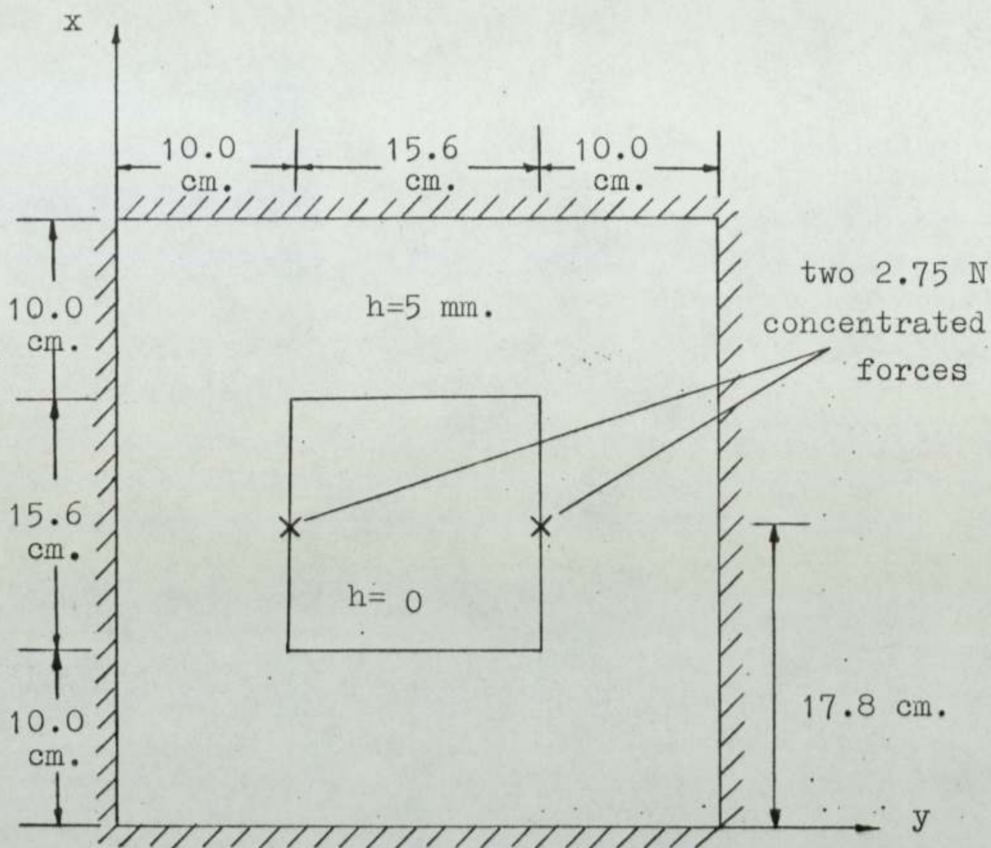

Fig.(7.29 c) case 3.

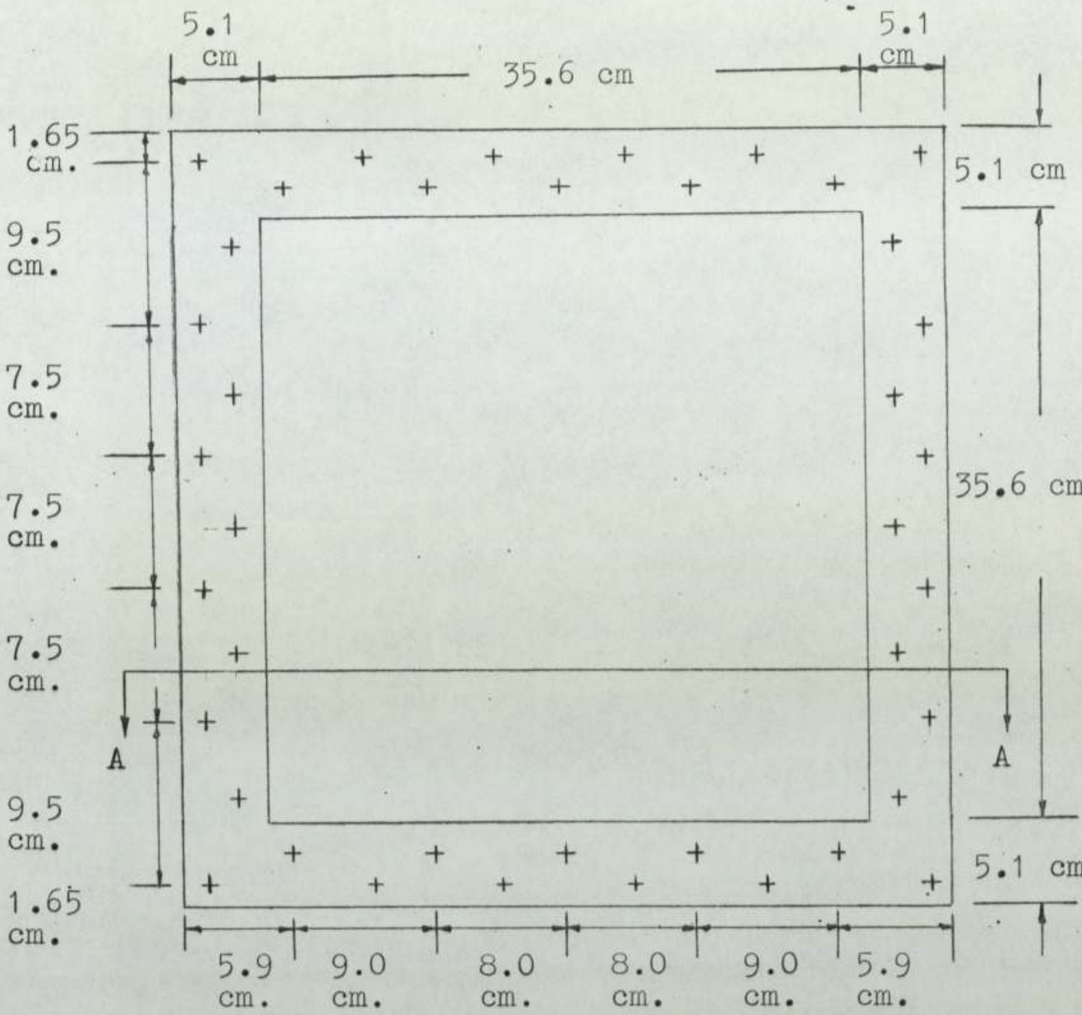

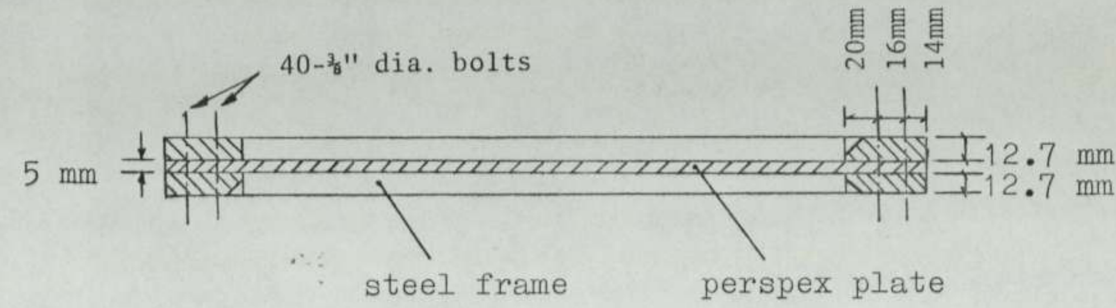

Section A-A

Fig.(7.30)

Details of clamping

to the y-direction and the process was repeated with a new film.

To save on loading and unloading time, the procedure for the second orientation of the screen was carried out by photographing the loaded plate first, then the load was removed and the new film was exposed for the zero-load state.

The exposed films were developed and printed giving contours of the slopes $\frac{\partial w}{\partial x}$ and $\frac{\partial w}{\partial y}$.

The application of concentrated forces was straight forward. That of the distributed loads, on the other hand, required the use of 3" thick foam rubber and a ½" thick plank of wood (fig.7.31).

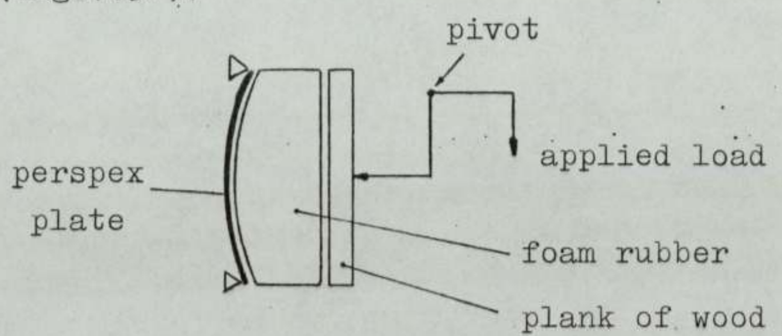

Fig.(7.31)

The load, when applied to the centre of the wooden plank, caused the foam rubber to compress appreciably in relation to the deflection of the perspex. Thus a state of uniformity in the applied load was achieved to a good degree of accuracy.

7.9.7 <u>Analysis of the Moire Fringes.</u>

The fringe photographs represent contours of slopes. The variation of the slope across a section of the plate may be obtained from the photographs thus:

A line XX (fig.7.32) is drawn on the photograph at the required section. This line will intersect with the fringe patterns at a number of points. Lines are drawn, on a graph paper, normal to XX at the points of intersection of XX with the fringes. The points necessary to draw the slope curve are obtained by fixing a point P on one of the normal lines and fixing other points on other normal lines in increments of d/2a (=0.00125 in this case) as in fig.(7.32). The direction of the increments relative to the first point is established on physical grounds. A zero slope axis ox is assigned if a point of zero slope is known. When a fringe crosses the line XX at more than one point, then the value of the slope at the normal lines emanating from these points should be the same (because the fringes represent lines of constant slope). The scale of photograph governs the scale on the axis ox. If the photograph is s times smaller than the model of the plate, then, the actual distance between the normal lines should be multiplied by s to give the distance on the model.

If the above procedure is carried out for two photographs of slopes in directions normal to one another, the bending and twisting moments may be obtained by appropriate graphical differentiation. The deflection is obtained by graphical integration of the slope curve.

Converting results from the model to those for the prototype, then, has to be carried out [48]. However, since in this case the experiment is aimed at comparing experimental results with those from the computer program, the slopes will represent sufficient and convenient quantities for comparison as they are obtained directly from both the experiment and the computer program. Further, the perspex plate will be assumed

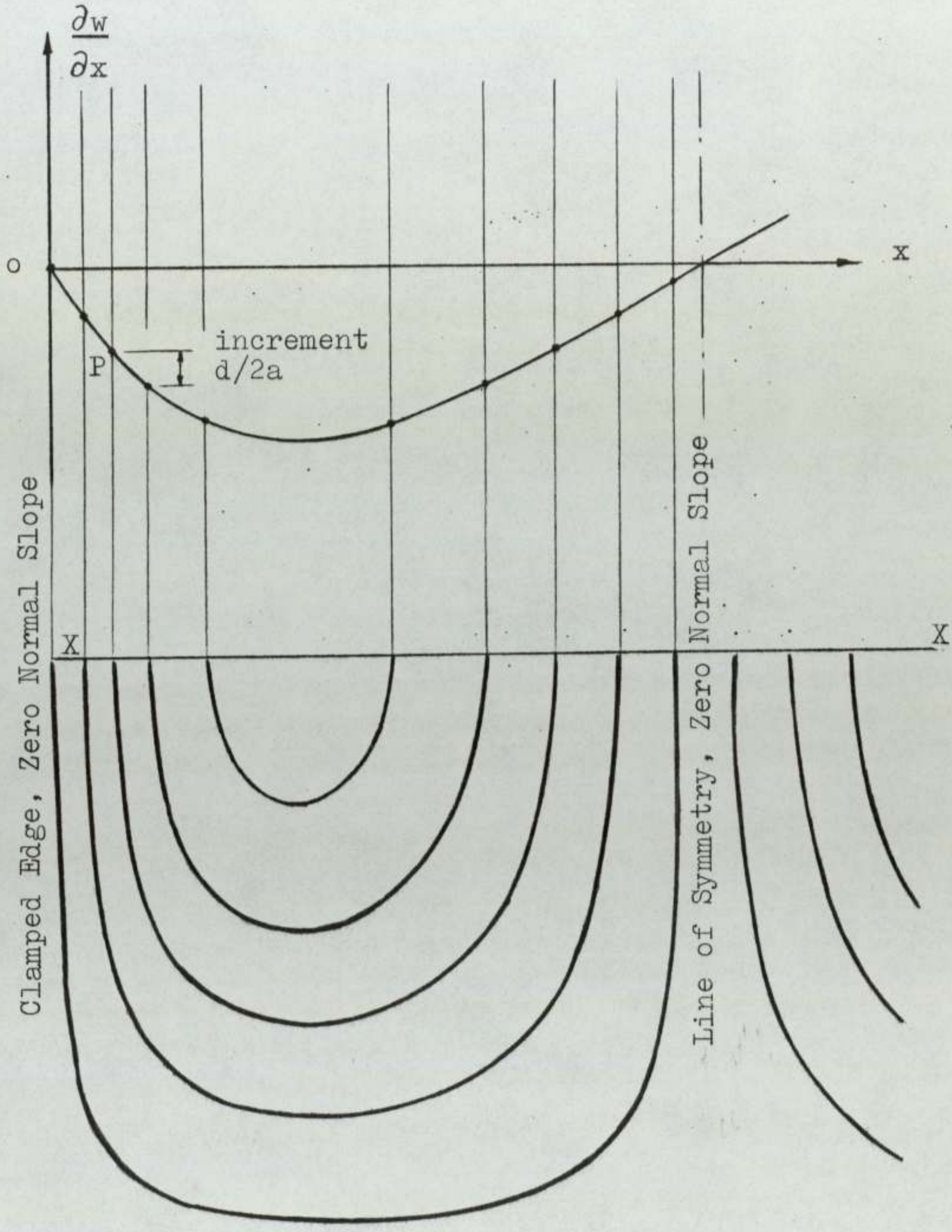

Fig.(7.32) Method of plotting the slope curve from the Moire' Fringes.

to be the prototype rather than a model. Therefore, no further work will be carried out on the experimental slope curves after they are plotted.

7.9.8 Comparison of Results from the Experiment with Tnose from the Computer Program.

The three cases shown in figs.(7.29a), (7.29b) and (7.29c) were analysed using the computer program. It was necessary to obtain the value of the flexural rigidity of the perspex. To this end, the experimental procedure suggested by Ligtenberg [48] was followed, using the specially designed rig. In this procedure a square piece of perspex was simply supported at three corners and loaded at the fourth by a concentrated force. If the x and y axes are taken along the diagonals, the bending and twisting moments will be constant everywhere: $M_x = - M_y = P/2$, $M_{xy} = 0$ where P is the applied point load [48]. The Moire technique will, consequently, yield parallel equi-spaced diagonal straight fringes from which the flexural rigidity of the perspex employed in the experiment can be found, viz.

$$D = \frac{P}{2} \cdot \frac{s}{(1-\nu)} \frac{2a}{d}$$

where s is the distance between the fringes.

Using this procedure and a given value of 0.335 for ν [48], the value of the flexural rigidity of the perspex used in the experiments was found to be 373 N.cm.

Figs.(7.33), (7.34) and (7.35a) show the photographs of fringe patterns for the slopes $\frac{\partial w}{\partial x}$ for the problems in test

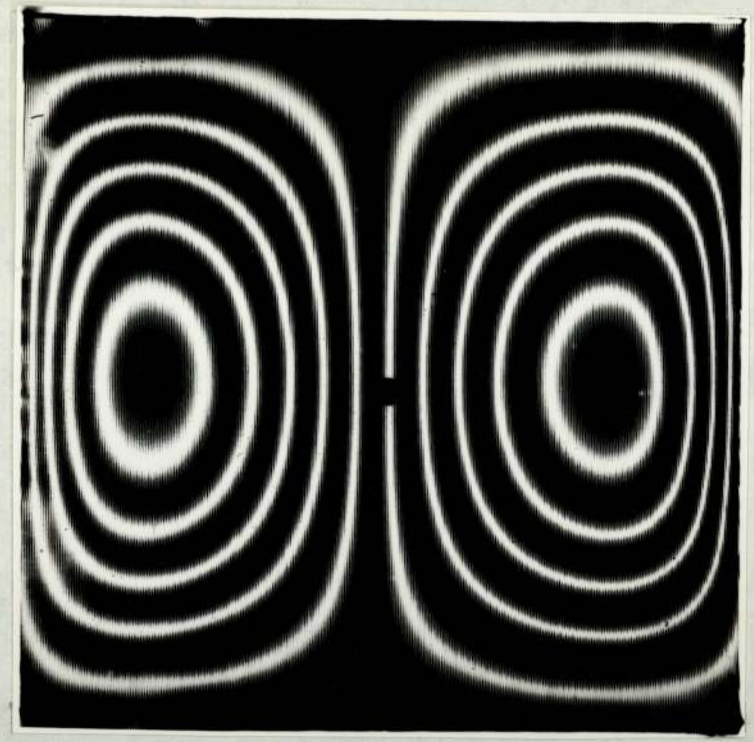

Fig. (7.33) Fringe photograph of the slope $\frac{\partial w}{\partial x}$ for the problem in test case (1).

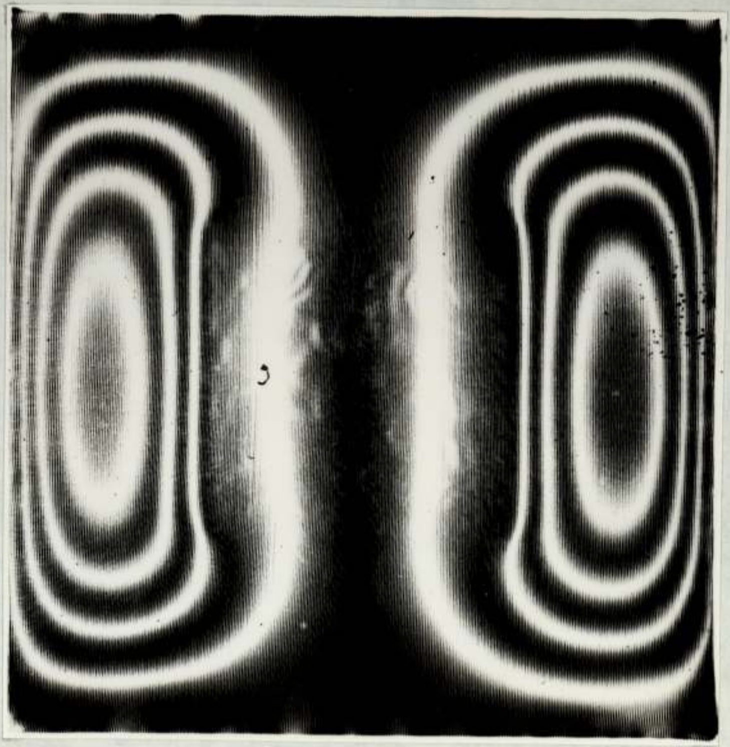

Fig. (7.34) Fringe photograph of the slope $\frac{\partial w}{\partial x}$ for the problem in test case (2).

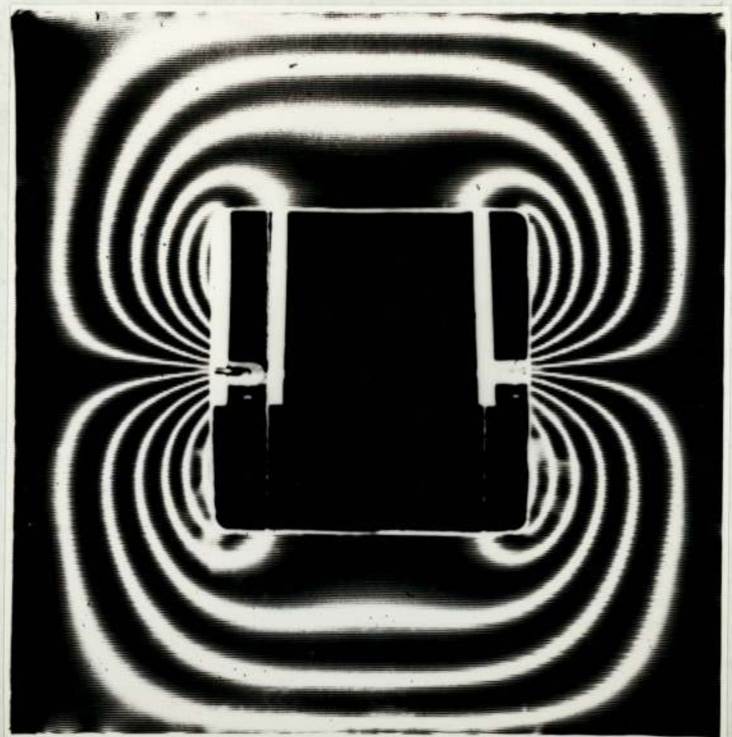

Fig. (7.35a) Fringe photograph of the slope $\frac{\partial w}{\partial x}$ for the problem in test case (3).

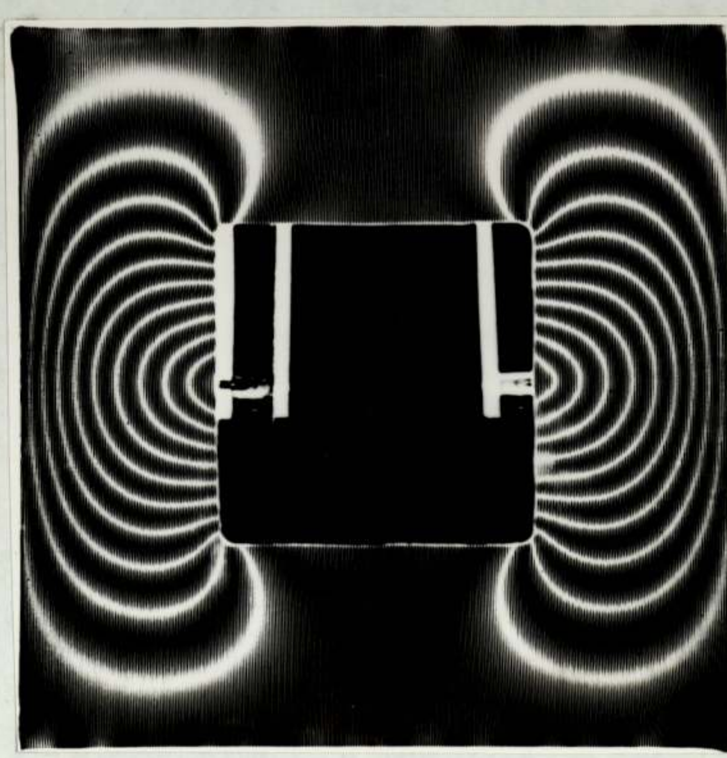

Fig. (7.35b) Fringe photograph of the slope $\frac{\partial w}{\partial y}$ for the problem in test case (3).

cases (1), (2) and (3) respectively. Fig.(7.35b) gives the fringe pattern for the slope $\frac{\partial w}{\partial y}$ for the problem in test case (3).

These fringe patterns were analysed as described in section (7.8.7) and the variations of the slopes across a section of the plate were plotted (figs.7.36, 7.37, 7.38a and 7.38b). Because of symmetry of the problems (skew-symmetry of slopes) the slopes are given for half the way across the plate. The corresponding slopes from the computer program were also indicated. It can be seen that in cases (1) and (2) the agreement between the experiments and the semi-analytic method on the values of the slope $\frac{\partial w}{\partial x}$ along y=17.8 cm, is very good. Similar agreement was obtained for the slope $\frac{\partial w}{\partial y}$ along y=6.0 cm for case (3). The slope $\frac{\partial w}{\partial x}$ along the same section of case (3), on the other hand, shows a relatively large difference in the values of the two methods. There is no apparent, analytical, reason for the error, particularly since the section for which the slope is plotted is some distance from the hole. Therefore, the discrepency can only be attributed to experimental errors. A possible source of error is the vulnerability of the perspex to the temperature and the humidity of the surroundings.

7.9.9 Concluding Remarks.

The experiment was conducted for two reasons. The first was to compare results from the computer program with those from a source other than an analytical or a numerical one. The second reason was to attain a first hand knowledge of the

Moire technique for the experimental analysis of plates. Both aims were achieved successfully.

It is felt that there are too many inherent sources of error and practical difficulties to allow the technique to be as simple to apply as it, otherwise, is. Considerable difficulty was encountered in ensuring that a uniform load is evenly distributed over the area of the plate. The levers used for the application of the load and their means of attachment to the structure of the apparatus were too bulky to allow the application of more than two, vertically separated levers. The method of applying the uniform load via a plank of wood and foam rubber is sound in theory, but in practice it was found that serious deviations from uniformity could arise if the lever load is not absolutely horizontal and centrally applied to the wooden plank. Checks had to be carried out to ensure that the foam rubber deflected identical amounts at all corners around the back of the plate.

Although a case of simply supported edges was not analysed it is anticipated that this would present considerable practical difficulties in ensuring that friction, between the edge of the model and the steel support, which have to maintain contact to prevent deflection, does not inhibit rotation.

The effects of temperature and humidity on the behaviour of the perspex model were reported by another user of the apparatus [50]. These were confirmed when, on a number of occasions, the experiment was repeated for the same problem, within a short space of time, and was found to give somewhat different results.

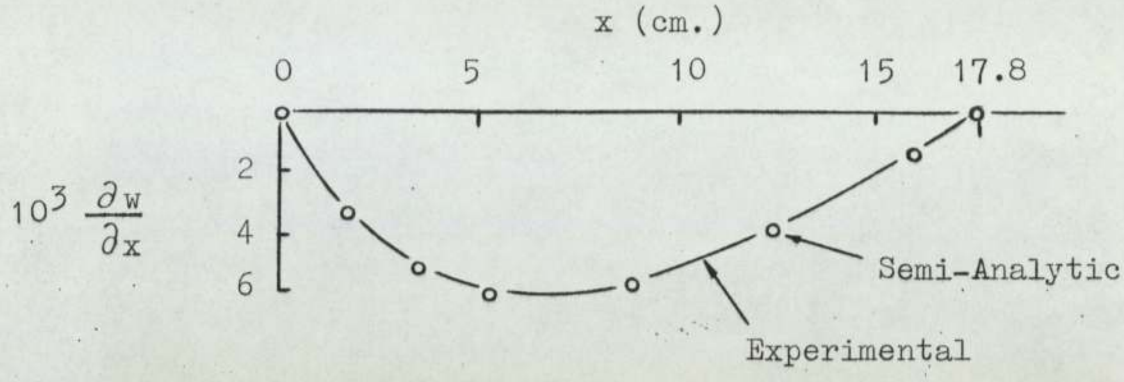

Fig.(7.36) Experimental and Semi-Analytic values of the slope $\frac{\partial w}{\partial x}$ along $y = 17.8$ cm., for case (1).

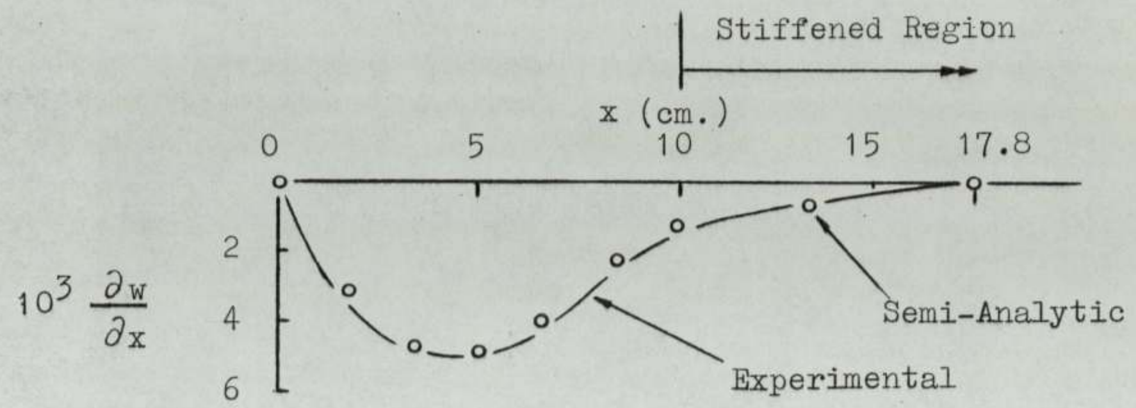

Fig.(7.37) Experimental and Semi-Analytic values of the slope $\frac{\partial w}{\partial x}$ along $y = 17.8$ cm., for case (2).

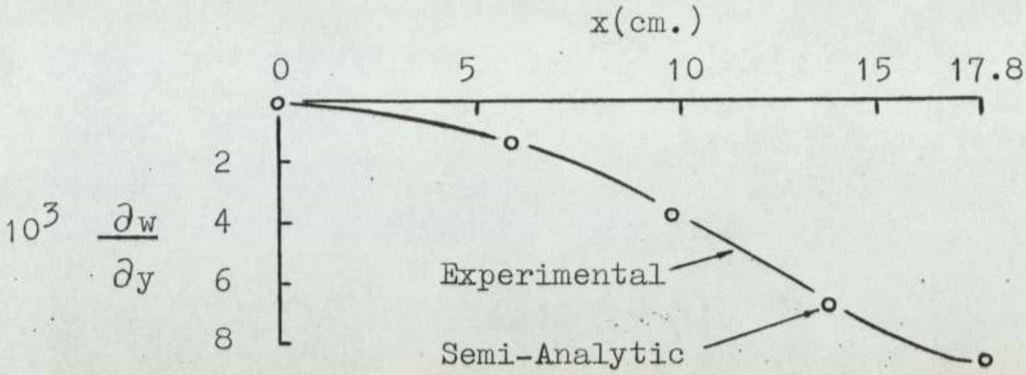

Fig.(7.38a) Experimental and Semi-Analytic values of the slope $\frac{\partial w}{\partial y}$ along y = 6.0 cm., for case (3).

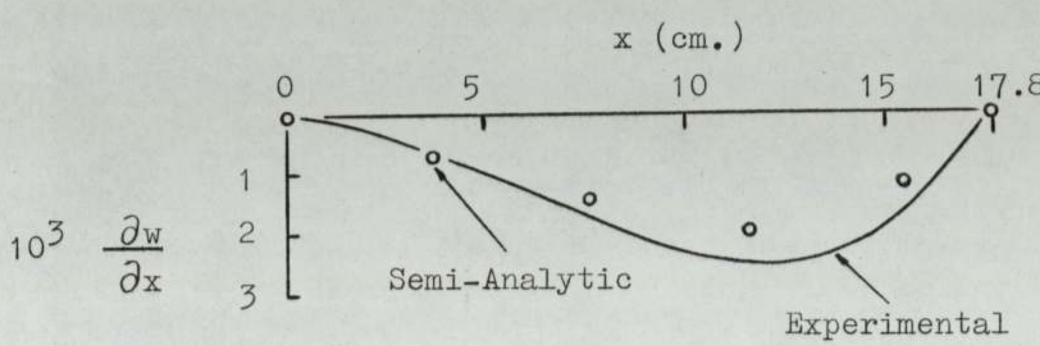

Fig.(7.38b) Experimental and Semi-Analytic values of the slope $\frac{\partial w}{\partial x}$ along y = 6.0 cm., for case (3).

CHAPTER 8

CHAPTER EIGHT

CONCLUSIONS

8.1 Preliminary Investigations.

The aim of the project was to develop a computer program, based on a semi-analytic finite element formulation, for the solution of rectangular plate problems with any combination of simply supported, clamped and free boundary conditions and with any variation in flexural rigidity and loading. The computer program was to be used to examine various aspects of the semi-analytic method and to explore its potential.

This method required that the deflection of the plate in one direction be described by a set of continuous functions which satisfies the boundary conditions at the extreme points in this direction. For these functions, the eigenfunctions of free vibration of a beam were used for their orthogonality property. This property reduces the amount of work necessary for the analysis and ensures numerical stability of the final set of simultaneous algebraic equations.

Preliminary investigations included a study of the applicability of the boundary conditions implied by the beam eigenfunctions to the edge of a rectangular plate (section 4.6). It was discovered that the free edge beam function does not, exactly, satisfy the boundary conditions of a free plate edge. There remained, in fact, a residual normal bending moment and a residual shearing force at the free edge of the plate. It has been shown in section (2.2) that for approximate solutions by the principle of minimum potential energy, it is only the geometric boundary conditions that must be satisfied exactly. However, the inadequate representation of the natural boundary conditions implies an inherently imperfect satisfaction of the equilibrium conditions. Exact satisfaction of the natural boundary conditions enhances the approximate solution and, thus, improves the rate of convergence of the method. A device to reduce the error in the approximate solution was developed on the basis of a proposed method of dealing with variable flexural rigidity. This device involved adding a rectangular extension to the plate at the free edge and assigning a zero value to the flexural rigidity of the extension thus simulating the free edge situation. The implementation of this idea, after the development of the computer program, proved very successful as shown by the results of sub-section (7.6.1d).

Another preliminary investigation indicated that the eigenfunctions for the cases of clamped-clamped, free-free and clamped-free edges are numerically unstable when the integrals of their products were evaluated at the fifth and higher modes with the 11 significant figure accuracy provided by the I.C.L.1905E computer employed for the analysis. This was a serious disadvantage for a method of analysis which could, otherwise, claim to require only a small computer for processing the program. A modification to the representation of these functions was envisaged whereby the hyperbolic functions which appear in the eigenfunctions were replaced by their exponential equivalent and the terms rearranged so that they are evaluated, by the computer, in a specific order. When this idea was implemented, the numerical instability was eliminated and it was possible to include any mode in the analysis provided that the numbers involved in this mode were within the capability of the computer to handle real numbers. The computer used in the analysis had a range of $\pm 5.6 \times 10^{76}$ allowing up to twenty-two modes to be included in the analysis.

8.2 The Semi-Analytic Finite Element Computer Program.

The computer program, which was developed on the basis of the semi-analytic method, utilized six sets of analytic functions, namely the simply supported-simply supported, clamped-clamped, free-free, clamped-free, simply supported-clamped and simply supported-free beam eigenfunctions. It was necessary to modify the representation of the second, third and fourth of these functions in order to eliminate an inherent numerical instability.

The analysis of problems of plates with variable flexural rigidity $D(x,y)$ requires the evaluation of integrals of products of the analytic functions and their derivatives, weighted by the variable quantity $D(x,y)$. To allow for any type of rigidity variation, as part of this investigation, these integrals are evaluated over a number of steps, which is specified by the user of the program, within each of which the rigidity is assumed to be either constant or linearly varying as desired. A variation in the applied pressure is similarly treated.

In developing the computer program, a maximum reduction in computer storage requirement and solution time was aimed at. For this purpose, the bandwidth of the overall stiffness matrix was minimized by grouping together all the harmonics of each element in corresponding locations in the harmonic overall stiffness matrix. The effectiveness of this scheme was demonstrated in section (5.3). A compact storage scheme was used in which the overall stiffness matrix is stored as a one-dimensional variable bandwidth array.

Efficiency of the program was improved, whenever possible, by using self-contained program segments called "Procedures".

8.3 Further Investigations.

Following the development of the computer program, a series of tests were carried out to investigate various aspects of the semi-analytic method.

The first of these tests was aimed at making a comparison between various cases of boundary and loading conditions and rigidity variation from the point of view of numerical stability of the solution vector and the rate at which the maximum deflection and maximum bending moment approach a limiting value (the term "rate of convergence" will be used here although the limiting value was not, at that stage, shown to be the correct one).

In this test, all the plates were divided into the same number of strips and the boundary conditions at the edges parallel to the direction in which the analytic functions applied were maintained throughout. Thus, the analytic functions were, in this test, the subject of scrutiny.

It was established from the results of this test that, for uniform plates under uniform pressure, the "rate of convergence" of the maximum deflection and maximum bending moment varied depending on the eigenfunction used. The simply supported-simply supported function gave the highest "rate of convergence". The clamped-clamped and simply supported -clamped functions were slightly inferior, followed by the free-free, simply supported-free and clamped-free functions in that order. In all these cases, the solution vectors were perfectly stable.

The effect of load variation on the "rate of convergence" was examined in the case of the clamped-clamped function. This function was chosen because of its previously established moderate behaviour in respect of stability and "convergence". The uniform pressure in the first case was replaced by a central point load and the results were compared. Comparison indicated that the effect of load concentration was, predictably, to reduce the "convergence rate" near the applied load whilst away from the point of application of the load a high "rate of convergence" was maintained. Numerical stability was, again, at no risk.

The effect of rigidity variation was examined next, through the severe case of a plate with a hole. The function for which the results were compared was, again, the clamped-clamped eigenfunction. The hole region was assigned a zero-value rigidity. The results showed that the effect of the hole on the "rate of convergence", for the case considered, was small. It was argued, however, that this could well deteriorate if the size of the hole was reduced in comparison with the overall dimensions. The solution vector, in this case, tended to be unstable at modes higher than the tenth. This was explained to be due to the fact that the actual deflection curve is discontinuous across the hole region and in attempting to describe this curve by a continuous function, the latter would give an arbitrary, non-unique shape at the hole region. This did not, however, affect the solution away from the hole. Although no problems were encountered from assigning a zero value to the rigidity of the hole region, it is feared that under further accumulative adverse conditions (size of hole, load concentration, boundary conditions), the numerical instability may cause a break-down in the solution. If this occurs, it is suggested that rigidity of the hole region be assigned a small non-zero value (say 10^{-6} times the rigidity elsewhere).

The results from these tests gave a guide to the most favourable orientation of the plate with respect to the direction of the analytic function. They also gave a comparative guide to the number of harmonics necessary for various cases of boundary and loading conditions and rigidity variation.

The effect of aspect ratio of the strip and the effect of a unilateral increase in the number of harmonics or the number of strips on the rate of convergence were examined next. If the direction along which the eigenfunctions are used specifies the "length" of the strip, while that along which the cubic model is used specifies the "width" of the strip, then, it was concluded, that a plate with a large aspect ratio does not necessarily require more strips if it were divided such that the width of the strips was in the long direction of the plate than if it were divided the other way round. It was argued that this is so because generally the variation of the deflection in the long direction of a long plate is less severe than in the short direction. Consequently, relatively wide strips, whose width is in the "long" direction of the plate, could give results as accurate as narrow strips whose width is in the short direction.

The problem of a simply supported square plate under a central concentrated force was solved for a combination of values of NELEM, the number of strips, and NHARM, the number of harmonics. Lines of constant % error in the central deflection were plotted. These demonstrated that for an optimum improvement in accuracy, the values of NELEM and NHARM must be increased at about the same rate. It was clear that an increase in one of these quantities beyond a certain value, whilst maintaining the value of the other, would not improve accuracy.

A thorough check on accuracy, i.e. convergence to the "true" answer, followed these tests. Eight ptoblems, for which solutions by other methods were available, were solved by the semi-analytic computer program. They included all the eigenfunctions, load variation and rigidity variation and the severe case of a plate with a hole. Agreement with other methods, some of which were "exact", was, generally, excellent. The results from the case of the plate with a hole were particularly interesting because of the singularity of the bending moments at the re-entrant corners of the hole. The semi-analytic method gave values for the bending and twisting moments, a short distance away from the hole, that are in close agreement with the results from a modified Rayleigh-Ritz finite element solution which takes account of the singularities. Thus, the extent of propagation of error due to the use of a continuous function to describe a singular one was very limited.

In the test cases considered throughout this project, a feature of the semi-analytic method was quite obvious. This is the remarkably low volume of data necessary for the analysis. In the majority of cases, no more than ten minutes of manual work was necessary to prepare the data. Another feature was the low cost (time) of processing the program. To give a figure for the time required to solve a particular problem could be misleading if it is not compared with solution time from other methods using the same computer. However, an idea can be obtained by comparing the rates of convergence of the semi-analytic method with other methods for the solution of the same problem. This was carried out.

The percentage error in the central deflection of a simply supported square plate under a central concentrated force was plotted against NB^2, where N is the number of equations arising from the analysis and B is the semi-bandwidth of the overall stiffness (influence) matrix. NB^2 is proportioned to the time required by any computer to solve the equations. Solution of the equations usually constitute a large part of the overall time required to process the program. The convergence curve from the semi-analytic method was compared with convergence curves from other formulations to the finite element method (section 7.8.2). For any given accuracy, the value of NB^2 from the semi-analytic method is many times less than that from any of the formulations considered.

Thus, the semi-analytic method has been shown to obtain a solution to simple and moderately complex rectangular plate problems with a low computer storage and time requirement and with very little effort in data preparation, in comparison with other finite element formulations for the same accuracy of solution.

It is appreciated that the term "simple and moderately complex problems" is imprecise. However, if the development of the computer program and the results of the tests are considered, a less broad statement may be made regarding computer time and data preparation effort. These quantities will increase when the plate problem requires the evaluation of the integral of the eigenfunctions at a large number of steps because of a continuous non-linear change in the rigidity throughout the plate, or when it is necessary to use a large number of harmonics. In these situations the advantages of the semi-analytic method will be reduced.

8.4 Experimental Tests.

The results obtained from the semi-analytic program and compared with other methods should have been enough to confirm the applicability of the semi-analytic method to various rectangular plate problems. The experimental tests, therefore, were carried out mainly to gain experience in an experimental technique which claims to be fast, simple and accurate, rather than to confirm the results obtained from the semi-analytic method. The main objective was achieved. However, it was felt that the results produced by the method were too sensitive to factors outside the control of the experimentor, such as temperature and humidity. Difficulty was also encountered in applying a uniform pressure.

8.5 Suggestions for Further Work.

Efficiency in the computer program and extensive exploration of the capability of the semi-analytic method were always aimed at in the given time for this project. However, there remains a number of ideas that may warrant attention if further improvement of the efficiency of the program and further tests on the capability of the method are sought. Some of these ideas will be given here.

The method of simulating a free edge in the cases when such an edge is described by the eigenfunctions had been successfully implemented. However, in the time given it was not possible to modify the computer program to simulate the free edge automatically. At present, therefore, if the free edge is to be simulated in the way described earlier, then this has to be carried out by treating the plate with zero rigidity extension as a new problem of a plate with step variation in its rigidity with what this implies in increase of data preparation. Therefore, it is worthwhile, if an improvement is sought, to modify the computer program to carry out the process automatically.

Another area of possible improvement in the computer program is the method of reading the types of distributed load and rigidity. At present only one type of each is allowed. Thus if on one element the variation in the applied load is linear, whilst on all other elements the distribution is uniform, then, the variation has to be assumed to be linear throughout and consequently zero coefficients of x and y have to be read for all elements whose load distribution is uniform.

It should be possible to modify the program to allow a different type of load and rigidity to be read for each element.

The program, in its present form, evaluates the integrals of the analytic functions and their derivatives for a number of steps between any limits specified by the user. This is carried out for each harmonic and for each strip. It is thought that it may be possible to evaluate, and store in a separate file, all the necessary integrals for all boundary conditions, for a pre-specified number of values of the dependent variable so that whenever the integrals are required between certain limits, the value can be obtained directly (from the file) by subtracting the value of the integral at the lower limit from that at the upper limit. Intermediate values may be obtained by interpolation. This process, if possible, would drastically reduce the time required by the computer to evaluate the integrals.

The method of solution, at present, is based on the assumption that the boundary conditions along each edge are homogeneous, so that in any one problem, only one set of eigenfunctions is used. It is possible, and not too difficult, to modify the program such that the choice of boundary conditions specified by the eigenfunctions are dependent on the element number, i.e. to allow mixed boundary conditions to be treated. The outcome of this is, however, not known at this stage, because the use of different eigenfunctions for two neighbouring elements will cause discontinuity of deflection as well as slope to occur across the element boundaries. Displacement functions with discontinuous slopes have been successfully used with convergent results, but no reports have been found regarding the use of functions with discontinuous deflections across plate element boundaries. A possible alternative method of treating mixed boundary conditions is available with the program as it stands. This method, however, applies only to a mixture of clamped and free boundary conditions along one or two opposite edges. The method involves using the clamped function throughout and adding a rectangular extension to the edge and assigning a large value to the rigidity of the extension where the edge should be clamped and a zero value where the edge should be free. This method has not been tested, but on the basis of experience with the computer program it is anticipated that simulation of the boundary conditions in this way would be successful.

Another possible area where tests would be useful is the application of the method to plates of the form shown in fig.(8.1). The boundary conditions on one or two opposite edges may, in these cases, be either clamped or free.

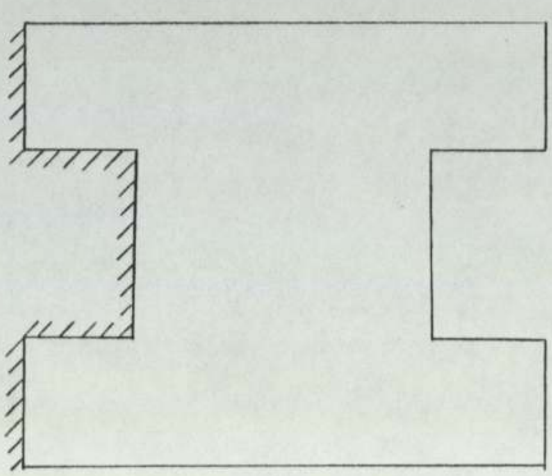

Fig.(8.1)

This type of problem would be solved by completing the large rectangle, using the clamped function throughout and assigning a very large value to the rigidity of the added portions (say 10^6 times that of the plate).

Thus, the semi-analytic method has been shown to be a powerful and, within the limitations of the geometry of the edges, a versatile method for the solution of plate bending problems.

ACKNOWLEDGEMENT

The author would like to thank:

His Supervisor, Mr. T. H. Richards, for his advice and encouragement given throughout the course of this project.

His wife who, somehow, managed to keep-house, go to work and type a very difficult manuscript.

Financial Support for a major part of the course of this investigation was provided by the Science Research Council and for a further part by the University of Aston in Birmingham. The author is grateful to both bodies.

APPENDICES Page

APPENDIX 1

Integration of Terms in the Potential Energy Expression (2.15)

$$\int \delta w_{xx}\, dx = \int \delta\left(\frac{\partial^2 w}{\partial x^2}\right) dx = \int \frac{\partial^2}{\partial x^2}(\delta w)\, dx$$

$$= \frac{\partial}{\partial x}(\delta w) = \delta\left(\frac{\partial w}{\partial x}\right) = \delta w_x .$$

$$\int_0^a \int_0^b w_{xx}\, \delta w_{xx}\, dxdy = \int_0^a \left[w_{xx}\, \delta w_x - \int w_{xxx}\, \delta w_x\, dx \right]_{x=0}^{x=b} dy$$

$$= \int_0^a \left[w_{xx}\, \delta w_x - w_{xxx}\, \delta w + \int w_{xxxx}\, \delta w_x \right]_{x=0}^{x=b} dy$$

$$= \int_0^a \int_0^b w_{xxxx}\, \delta w\, dxdy + \int_0^a \left[w_{xx}\, \delta w_x \right]_{x=0}^{x=b} dy$$

$$- \int_0^a \left[w_{xxx}\, \delta w \right]_{x=0}^{x=b} dy$$

$$\int_0^a \int_0^b w_{yy}\, \delta w_{yy}\, dxdy = \int_0^a \int_0^b w_{yyyy}\, \delta w\, dxdy + \int_0^b \left[w_{yy}\, \delta w_y \right]_{y=0}^{y=a} dx$$

$$- \int_0^b \left[w_{yyy}\, \delta w \right]_{y=0}^{y=a} dx$$

$$\int_0^a \int_0^b w_{xx}\, \delta w_{yy}\, dxdy = \int_0^b \left[w_{xx}\, \delta w_y - w_{xxy}\, \delta w_y\, dy \right]_{y=0}^{y=a} dx$$

$$= \int_0^b \left[w_{xx}\, \delta w_y - w_{xxy}\, \delta w + \int w_{xxyy}\, \delta w\, dy \right]_{y=0}^{y=a} dx$$

$$= \int_0^a \int_0^b w_{xxyy}\, \delta w\, dxdy + \int_0^b \left[w_{xx}\, \delta w_y \right]_{y=0}^{y=a} dx$$

$$- \int_0^b \left[w_{xxy}\, \delta w \right]_{y=0}^{y=a} dx$$

$$\int_0^a \int_0^b w_{yy}\, \delta w_{xx}\, dxdy$$

$$= \int_0^a \int_0^b w_{xxyy}\, \delta w\, dxdy + \int_0^a \Big[w_{yy}\, \delta w_x \Big]_{x=0}^{x=b} dy - \int_0^a \Big[w_{yyx}\, \delta w \Big]_{x=0}^{x=b} dy.$$

$$\int_0^a \int_0^b w_{xy}\, \delta w_{xy}\, dxdy = \int_0^b \Big[w_{xy}\, \delta w_x - w_{xyy}\, \delta w_x\, dy \Big]_{y=0}^{y=a} dx$$

$$= \int_0^b \Big[w_{xy}\, \delta w_x \Big]_{y=0}^{y=a} dx - \int_0^a \int_0^b w_{xyy}\, \delta w_x\, dxdy$$

$$= \Big\{ \Big[w_{xy}\, \delta w - \int w_{xxy}\, \delta w\, dx \Big]_{x=0}^{x=b} \Big\}_{y=0}^{y=a}$$

$$- \int_0^a \Big[w_{xyy}\, \delta w - \int w_{xxyy}\, \delta w\, dx \Big]_{x=0}^{x=b} dy$$

$$= \int_0^a \int_0^b w_{xxyy}\, \delta w\, dxdy - \int_0^b \Big[w_{xxy}\, \delta w \Big]_{y=0}^{y=a} dx$$

$$- \int_0^a \Big[w_{xyy}\, \delta w \Big]_{x=0}^{x=b} dy + \Big\{ \Big[w_{xy}\, \delta w \Big]_{x=0}^{x=b} \Big\}_{y=0}^{y=a}$$

APPENDIX 2

A2.1 Eigenfunctions of Free Vibration of Uniform Beams.

The eigenfunctions of the free vibration of a homogeneous beam are known [36] to satisfy the differential equations.

$$\frac{d^4Y}{dy^4} = \frac{\mu^4}{a^4} Y \tag{A2.1}$$

whose general solution is in the form

$$Y = A \sin \frac{\mu y}{a} + B \cos \frac{\mu y}{a} + C \text{ sh } \frac{\mu y}{a} + D \cosh \frac{\mu y}{a} \tag{A2.2}$$

where A, B, C and D are arbitrary constants dependent on the boundary conditions of the beam, μ is a parameter related to the natural frequencies, a is the length of the beam.

For the clamped-clamped beam, the boundary conditions are

$$Y = Y' = 0 \quad \text{at} \quad y = 0 \quad \text{and} \quad y = a$$

From these conditions, the four following equations are obtained:

$$\begin{aligned} &B + D = 0 \\ &A + C = 0 \\ &A \sin\mu + B \cos\mu + C \text{ sh}\mu + D \text{ ch}\mu = 0 \\ &A \cos\mu - B \sin\mu + C \text{ ch}\mu + D \text{ sh}\mu = 0 \end{aligned} \tag{A2.3}$$

Using the first two of equations (A2.3) to eliminate D and C from the third and fourth equations, the following relationships will be obtained.

$$\begin{aligned} &A (\sin\mu - \text{sh}\mu) + B(\cos\mu - \text{ch}\mu) = 0 \\ &A (\cos\mu - \text{ch}\mu) - B(\sin\mu + \text{sh}\mu) = 0 \end{aligned} \tag{A2.4}$$

For arbitrary values of A and B, the determinant of the coefficients in equations (A2.4) has to be zero:

$$\begin{vmatrix} (\sin\mu - \mathrm{sh}\mu) & (\cos\mu - \mathrm{ch}\mu) \\ (\cos\mu - \mathrm{ch}\mu) & (\sin\mu + \mathrm{sh}\mu) \end{vmatrix} = 0 \qquad \text{(A2.5)}$$

Equation (A2.5) yields the characteristic equation of the system, i.e.

$$\cos\mu \ \ \mathrm{ch}\mu = 1 \qquad \text{(A2.6)}$$

Equation (A2.6) is a transcendental equation whose roots may be obtained by one of a number of methods [5].

The first four roots of the equation are

$$\mu_1 = 4.73004 \ , \ \mu_2 = 7.85320 \ , \ \mu_3 = 10.9956 \ , \ \mu_4 = 14.1372$$

$$\text{for } r > 4 \qquad \mu_r \approx (2r+1)\,\pi/2.$$

From equation (A2.4)

$$B = - \frac{\sin\mu - \mathrm{sh}\mu}{\cos\mu - \mathrm{ch}\mu} A = \frac{\cos\mu - \mathrm{ch}\mu}{\sin\mu + \mathrm{sh}\mu} A$$

Since the constant A is arbitrary, the value 1.0 can be assigned to it. Equation (A2.2), after substituting for B, C and D in terms of A, then becomes:

$$Y_r = \left[\sin \frac{\mu_r y}{a} - \mathrm{sh}\,\frac{\mu_r y}{a} - \alpha_r(\cos \frac{\mu_r y}{a} - \mathrm{ch}\,\frac{\mu_r y}{a})\right]$$

where $\alpha_r = \dfrac{\sin \mu_r - \mathrm{sh}\, \mu_r}{\cos \mu_r - \mathrm{ch}\, \mu_r}$.

The eigenfunctions for beams with any other boundary conditions are similarly obtained.

A2.2 Orthogonality Property of the Beam Eigenfunctions.

Since the eigenfunctions satisfy the differential equation

$$Y^{IV} = \lambda^4 Y$$

where

$$Y^{IV} = \frac{d^4Y}{dy^4} \quad , \quad \lambda = \frac{\mu}{a} \quad ,$$

two modes r and s($r \neq s$) of the eigenfunction will satisfy the equations

$$Y_r^{IV} = \lambda_r^4 Y_r \quad , \quad Y_s^{IV} = \lambda_s^4 Y_s \qquad (A2.7)$$

Multiplying the first of equations (A2.7) by Y_s and the second by Y_r then subtracting, yields:

$$Y_r Y_s = \frac{1}{(\lambda_r^4 - \lambda_s^4)} \left[Y_s Y_r^{IV} - Y_r Y_s^{IV} \right] \qquad (A2.8)$$

Integrating both sides of equation (A2.8) over the length of the beam, the right hand side being integrated twice by parts, gives:

$$\int_0^a Y_r Y_s \, dy = \frac{1}{(\lambda_r^4 - \lambda_s^4)} \left[Y_s Y_r''' - Y_r Y_s''' - Y_s' Y_r'' + Y_r' Y_s'' \right]_0^a$$

(A2.9)

On substituting the end limits, each of the four products on the right hand side of equation (A2.8) reduces to zero. The first pair because, either the deflection is zero (simply supported or clamped) or the shear force is zero (free). The third and fourth terms vanish because either the slope or the moment is zero.

Therefore, for a uniform beam:

$$\int_0^a Y_r \, Y_s \, dy = 0 \quad (r \neq s) \qquad (A2.10)$$

It can be shown, similarly, that

$$\int_0^a Y_r'' \, Y_s'' \, dy = 0 \quad (r \neq s) \qquad (A2.11)$$

These properties are called the orthogonality properties of the beam eigenfunctions.

When r=s , let the integral be

$$I = \int_0^a Y_r \, Y_r \, dy \qquad (A2.12)$$

Substituting for Y_r from (A2.7), I becomes:

$$I = \frac{1}{\lambda_r^4} \int_0^a Y_r \, Y_r^{IV} \, dy \qquad (A2.13)$$

Integrating by parts and applying the preceeding argument regarding the end limits, the integral reduces to:

$$I = -\frac{1}{\lambda_r^4} \int_0^a Y_r' \, Y_r''' \, dy \qquad (A2.14)$$

and on repeating the process:

$$I = \frac{1}{\lambda_r^4} \int_0^a \left[Y_r'' \right]^2 \, dy \qquad (A2.15)$$

From equations (A2.12), (A2.14) and (A2.15) the following is obtained:

$$4I = \int_0^a \left\{ Y_r^2 + \frac{1}{\lambda_r^4} \left[Y_r''\right]^2 - \frac{2}{\lambda_r^4} Y_r' \, Y_r''' \right\} dy \qquad (A2.16)$$

Now, substituting the expression (A2.2), i.e.

$Y_r = A \sin \mu_r y + B \cos \mu_r y + C \operatorname{sh} \mu_r y + D \operatorname{ch} \mu_r y$, into equation (2.16) then integrating, gives for the integral:

$$I = (A^2 + B^2 + D^2 - C^2) \frac{a}{2} \qquad (A2.17)$$

The values of A, B, C and D for various boundary conditions are as given in table (4.1)

The integrals of products of derivatives of the eigenfunctions are similarly evaluated.

A2.3 Orthogonality of the Rigid Body Modes.

The rigid body displacement and rigid body rotation for the free-free beam were taken as 1 and $(\frac{1}{2} - \frac{y}{a})$ respectively. Now for the orthogonality property to be maintained, the following conditions have to be satisfied:

$$\int_0^a 1 . Y_r \, dy = \int_0^a (\tfrac{1}{2} - \tfrac{y}{a}) \, Y_r \, dy = \int_0^a 1 . (\tfrac{1}{2} - \tfrac{y}{a}) \, dy = 0$$

where Y_r is the eigenfunction for the free-free beam.

It is immediately apparent that the third condition is satisfied. For the first and second conditions, Y_r is replaced by $\frac{1}{\lambda_r^4} Y_r$ from equation (A2.7).

Thus:

$$\int_0^a 1 \,.\, Y_r \, dy = \frac{1}{\lambda_r^4} \int_0^a Y_r^{IV} \, dy$$

$$= \frac{1}{\lambda_r^4} \left[Y_r''' \right]_0^a = 0 \quad \text{since the shear force}$$

is zero at both ends.

$$\int_0^a \left(\tfrac{1}{2} - \tfrac{y}{a}\right) Y_r \, dy = \frac{1}{\lambda_r^4} \int_0^a \left(\tfrac{1}{2} - \tfrac{y}{a}\right) Y_r^{IV} \, dy.$$

Integrating the right hand side by parts gives:

$$\int_0^a \left(\tfrac{1}{2} - \tfrac{y}{a}\right) Y_r \, dy = \frac{1}{\lambda_r^4} \left[\left(\tfrac{1}{2} - \tfrac{y}{a}\right) Y_r''' + \tfrac{1}{a} \int Y_r''' \, dy \right]_0^a$$

$$= \frac{1}{\lambda_r^4} \left[\left(\tfrac{1}{2} - \tfrac{y}{a}\right) Y_r''' + \tfrac{1}{a} Y_r'' \right]_0^a$$

$= 0$ by applying the argument regarding the end conditions.

It can be shown similarly, that for the simply supported-free case:

$$\int_0^a \frac{y}{a} \,.\, Y_r \, dy = 0$$

APPENDIX 3

A3.1 The Constituent Matrices in the Harmonic Element Stiffness Matrix $\left[k^{jm}\right]_e$, Equation (4.27)

$$[J]_1 = \int_0^b B^T D^* B \, dx = \begin{bmatrix} \frac{12}{b^3} & & \text{symm.} & \\ \frac{6}{b^2} & \frac{4}{b} & & \\ \frac{-12}{b^3} & \frac{-6}{b^2} & \frac{12}{b^3} & \\ \frac{6}{b^2} & \frac{2}{b} & \frac{-6}{b^2} & \frac{4}{b} \end{bmatrix}$$

$$[J]_2 = \int_0^b \bar{\bar{B}}^T D^* B \, dx = -\nu \begin{bmatrix} \frac{6}{5b} & \frac{11}{10} & \frac{-6}{5b} & \frac{1}{10} \\ \frac{1}{10} & \frac{2b}{15} & \frac{-1}{10} & \frac{-b}{30} \\ \frac{-6}{5b} & \frac{-1}{10} & \frac{6}{5b} & \frac{-11}{10} \\ \frac{1}{10} & \frac{-b}{30} & \frac{-1}{10} & \frac{2b}{15} \end{bmatrix}$$

$$[J]_3 = [J]_2^T$$

$$[J]_4 = \int_0^b \bar{B}^T D^* \bar{B} \, dx = 2(1-\nu) \begin{bmatrix} \frac{6}{5b} & & \text{symm.} & \\ \frac{1}{10} & \frac{2b}{15} & & \\ \frac{-6}{5b} & \frac{-1}{10} & \frac{6}{5b} & \\ \frac{1}{10} & \frac{-b}{30} & \frac{-1}{10} & \frac{2b}{15} \end{bmatrix}$$

$$[J]_5 = \int_0^b \bar{\bar{B}}^T \, D^* \, \bar{\bar{B}} \, dx = \begin{bmatrix} \frac{13b}{35} & & & \text{symm.} \\ \frac{11b^2}{210} & \frac{b^3}{105} & & \\ \frac{9b}{70} & \frac{13b^2}{420} & \frac{13b}{35} & \\ \frac{-13b^2}{420} & \frac{-b^3}{140} & -\frac{11b^2}{210} & \frac{b^3}{105} \end{bmatrix}$$

$$[J]_{11} = \int_0^b x \, B^T \, D^* \, B \, dx = \begin{bmatrix} \frac{6}{b^2} & & & \text{symm.} \\ \frac{2}{b} & 1 & & \\ \frac{-6}{b^2} & \frac{-2}{b} & \frac{6}{b^2} & \\ \frac{4}{b} & 1 & \frac{-4}{b} & 3 \end{bmatrix}$$

$$[J]_{12} = \int_0^b x \, \bar{\bar{B}}^T \, D^* \, B \, dx = -\nu \begin{bmatrix} \frac{1}{10} & \frac{b}{5} & \frac{-1}{10} & \frac{-b}{10} \\ 0 & \frac{b^2}{30} & 0 & \frac{-b^2}{30} \\ \frac{-11}{10} & \frac{-b}{5} & \frac{11}{10} & \frac{-9b}{10} \\ \frac{b}{10} & 0 & \frac{-b}{10} & \frac{b^2}{10} \end{bmatrix}$$

$$[J]_{13} = [J]_2^T$$

$$[J]_{14} = \int_0^b x \, \bar{B}^T \, D^* \, \bar{B} \, dx = 2(1-\nu) \begin{bmatrix} \frac{3}{5} & & & \text{symm.} \\ \frac{b}{10} & \frac{b^2}{30} & & \\ \frac{-3}{5} & \frac{-b}{10} & \frac{3}{5} & \\ 0 & \frac{-b^2}{60} & 0 & \frac{b^2}{10} \end{bmatrix}$$

$$[J]_{15} = \int_0^b x \;\bar{\bar{B}}^T \; D^* \; \bar{\bar{B}} \; dx = \begin{bmatrix} \frac{3b^2}{35} & & & \text{symm.} \\ \frac{b^3}{60} & \frac{b^4}{280} & & \\ \frac{9b^2}{140} & \frac{b^3}{60} & \frac{2b^2}{7} & \\ \frac{-b^3}{70} & \frac{-b^4}{280} & \frac{-b^3}{28} & \frac{b^4}{168} \end{bmatrix}$$

A3.2 The Integrals $\int \Phi_r^{mn} \, dy$ and $\int y \; \Phi_r^{mn} \, dy$ in the Harmonic Element Stiffness Matrix (Equation 4.27) Between Arbitrary Limits.

These integrals involve products of the functions $\sin m\xi$ $\cos m\xi$, $e^{m\xi}$, and $e^{-m\xi}$ and $\sin n\xi$, $\cos n\xi$, $e^{n\xi}$ and $e^{-n\xi}$, where $\xi = y/a$. A total of 16 integrals need to be evaluated.

The integration of these functions is carried out either by parts or by using well-known relationships between products of the functions and functions of the sum or the difference of their arguments. The results are:

For $m \neq n$

$$\int e^{n\xi} \sin m\xi \;\; d\xi \;=\; \frac{e^{n\xi}}{m^2 + n^2} \, (-m \cos m\xi \; + n \sin m\xi \,)$$

$$\int e^{n\xi} \cos m\xi \;\; d\xi \;=\; \frac{e^{n\xi}}{m^2 + n^2} \, (m \sin m\xi \; + n \cos m\xi \,)$$

Six more integrals are obtained from the two above simply by replacing n by -n and by interchanging m and n.

$$\int e^{n\xi} \, e^{m\xi} \;\; d\xi = \frac{1}{m + n} \, (\, e^{n\xi} \;\; e^{m\xi} \,).$$

Three more integrals are obtained from the one above as described before.

$$\int \sin n\zeta \quad \cos m\zeta \quad d\zeta \ = \frac{1}{m^2 - n^2}\,(m \sin m\zeta \quad \sin n\zeta + n \cos m\zeta \quad \cos n\zeta\ )$$

One more integral is obtained from he one above by interchanging m and n.

$$\int \sin n\zeta \quad \sin m\zeta \quad d\zeta \ = \frac{1}{m^2 - n^2}\,(-m \cos m\zeta \quad \sin n\zeta + n \sin m\zeta \quad \cos n\zeta\ )$$

$$\int \cos n\zeta \quad \cos m\zeta \quad d\zeta \ = \frac{1}{m^2 - n^2}\,(m \sin m\zeta \quad \cos n\zeta - n \cos m\zeta \ \sin n\zeta\ )$$

For m=n

$$\int \sin^2 m\zeta \quad d\zeta \ = \frac{1}{2}\,(- \frac{1}{2m} \sin 2m\zeta \ + \zeta\ )$$

$$\int \cos^2 m\zeta \quad d\zeta \ = \frac{1}{2}\,(\frac{1}{2m} \sin 2m\zeta \ + \zeta\ )$$

$$\int \sin m\zeta \quad \cos m\zeta \quad d\zeta \ = - \frac{1}{4m} \cos 2m\zeta \ .$$

Integrals of the form $\int y\, \Phi_r^{mn}\, dy$ are obtained by integrating by parts using the relationships already established.

A3.3 The Vectors Involved in the Harmonic Element Force Vector (Equation 4.35).

$$\int_0^b [N]^T \, dx = \left[\frac{b}{2} \quad \frac{b^2}{12} \quad \frac{b}{2} \quad -\frac{b^2}{12}\right]^T$$

$$\int_0^b x\, [N]^T \, dx = \left[\frac{3b^2}{20} \quad \frac{b^3}{30} \quad \frac{7b^2}{20} \quad -\frac{b^3}{20}\right]^T$$

APPENDIX 4

A4.1 Newton's Iterative Method.

Newton's Method involves making a guess x_{n-1} at the solution of the equation $f(x)=0$ then using the tangent to the function at x_{n-1} to obtain the next approximation and so on as shown by fig.(A4.1).

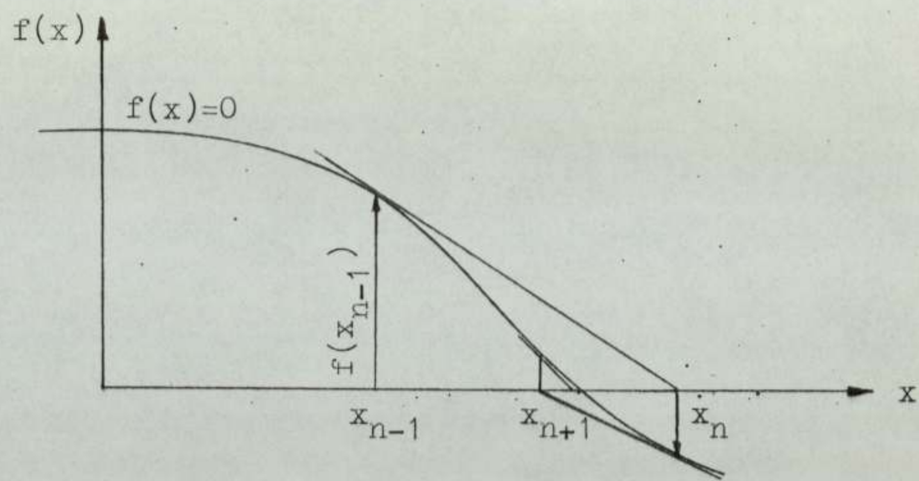

Fig.(A4.1)

The recurrence formula will be given by:

$$f'(x_{n-1}) = \frac{f(x_{n-1})}{x_{n-1} - x_n}$$

i.e. $$x_n = x_{n-1} - \frac{f(x_{n-1})}{f'(x_{n-1})}$$

The convergence can be shown to be approximately quadratic, i.e. the number of significant figures almost doubles with each iteration [42].

A4.2 Listing of the Computer Program NEWTON

```
'BEGIN'
'REAL' E,C,S,CH,SH,Y,PI,T,TH; 'INTEGER' I;  'ARRAY' A[1:10];
  PI:=4.0*ARCTAN(1,0);
  A[1]:=1.87510;  A[2]:=4.69409;  A[3]:=7.85476;  A[4]:=10.9955;
  A[5]:=14.1372;  'FOR' I:=6,7,8,9,10 'DO' A[I]:=(I-0.5)*PI;
  WRITETEXT('('''('4C 17S')'ROOTS%OF%CHARACTERISTIC%EQN%%COS(M)*COSH
(M)+1=0'('1C 17S')'---------------------------------------------------
  '('3C 17S')'MODE%NO.'('6S')'ROOT'('1C 17S')'--------%%%%%----
  '('2C 17S')'')');
  'FOR' I:=1 'STEP' 1 'UNTIL' 10 'DO'
'BEGIN'
NEWTON1:
  E:=EXP(A[I]);  C:=COS(A[I]);  S:=SIN(A[I]);  CH:=(E+1/E)/2;
  SH:=(E-1/E)/2;  Y:=A[I]-(C*CH+1)/(C*SH-S*CH);
  'IF' ABS(Y-A[I]) > 1.0 & -9  'THEN'
'BEGIN'
  A[I]:=Y;  'GOTO' NEWTON1;
'END';
  PRINT(I,2,0);  SPACE(4);  PRINT(Y,2,10);  NEWLINE(2); SPACE(17);
'END';
  NEWLINE(2);
  A[1]:=4.73004;  A[2]:=7.85320;  A[3]:=10.9956;  A[4]:=14.1372;
  A[5]:=17.2788;  'FOR' I:=6,7,8,9,10 'DO' A[I]:=(I+0.5)*PI;
  WRITETEXT('('''('1C 17S')'ROOTS%OF%CHARACTERISTIC%EQN%%COS(M)*COSH
(M)-1=0'('1C 17S')'---------------------------------------------------
  '('3C 17S')'MODE%NO.'('6S')'ROOT'('1C 17S')'--------%%%%%----
  '('2C 17S')'')');
  'FOR' I:=1 'STEP' 1 'UNTIL' 10 'DO'
'BEGIN'
NEWTON2:
  E:=EXP(A[I]);  C:=COS(A[I]);  S:=SIN(A[I]);  CH:=(E+1/E)/2;
  SH:=(E-1/E)/2;  Y:=A[I]-(C*CH-1)/(C*SH-S*CH);
  'IF' ABS(Y-A[I]) > 1.0 & -9  'THEN'
'BEGIN'
  A[I]:=Y;  'GOTO' NEWTON2;
'END';
  PRINT(I,2,0);  SPACE(4);  PRINT(Y,2,10);  NEWLINE(2); SPACE(17);
'END';
  NEWLINE(2);
  A[1]:=3.92660;  A[2]:=7.06858;  A[3]:=10.2102;  A[4]:=13.3518;
  A[5]:=16.4934;  'FOR' I:=6,7,8,9,10 'DO' A[I]:=(I+0.25)*PI;
  WRITETEXT('('''('4C 17S')'ROOTS%OF%CHARAC%EQN%%TAN(M)=THAN(M)
  '('1C 17S')'-----------------------------------'('4C 17S')'MODE%
NO'('6S')'ROOT'('1C 17S')'--------%%%%%----'('2C 17S')'')');
  'FOR' I:=1 'STEP' 1 'UNTIL' 10 'DO'
'BEGIN'
NEWTON3:
  E:=EXP(A[I]);  T:=SIN(A[I])/COS(A[I]);  S:=1/COS(A[I]);
  TH:=(E-1/E)/(E+1/E);  SH:=2/(E+1/E);
  Y:=A[I]-(T-TH)/(S*S-SH*SH);
  'IF' ABS(Y-A[I]) > 1.0 & -9  'THEN'
'BEGIN'
  A[I]:=Y;  'GOTO' NEWTON3;
'END';
  PRINT(I,2,0);  SPACE(4);  PRINT(Y,2,10);  NEWLINE(2); SPACE(17);
'END';
'END';
```

A4.3 Roots of the Characteristic Equations for the Various Boundary Conditions.

(a) Roots of the Equation SIN $\mu_r = 0$

Simply Supported-Simply Supported

The roots of this equation are readily obtained by inspection.

$$\mu_r = r\pi \qquad r=1,2,\ldots,\infty$$

$$= 3.1415\ 9265\ 359$$

(b) Roots of the Equation COS μ_r * COSH $\mu_r - 1 = 0$

Clamped-Clamped and Free-Free.

Mode No. (r)	Root (μ_r)
1	4.7300 4074 48
2	7.8532 0462 42
3	10.9956 0783 81
4	14.1371 6549 14
5	17.2787 5965 77
6	20.4203 5224 58
7	23.5619 4490 27
8	26.7035 3755 56
9	29.8451 3021 00
10	32.9867 2286 29

For r >10, $\mu_r = \frac{2r+1}{2}\pi$

(c) Roots of the Equation COS μ_r * COSH μ_r + 1 = 0

Clamped-Free

Mode No. (r)	Root (μ_r)
1	1.8751 0406 88
2	4.6940 9113 30
3	7.8547 5743 86
4	10.9955 4073 50
5	14.1371 6839 14
6	17.2787 5953 27
7	20.4203 5225 14
8	23.5619 4490 27
9	26.7035 3755 56
10	29.8451 3021 00

For r > 10,

$$\mu_r = \frac{2r - 1}{2}\pi$$

(d) Roots of the Equation TAN μ_r = TANH μ_r

Simply Supported-Clamped and Simply Supported-Free

Mode No. (r)	Root (μ_r)
1	3.9266 0231 22
2	7.0685 8274 57
3	10.2101 7612 30
4	13.3517 6877 78
5	16.4933 6143 20
6	19.6349 5408 52
7	22.7765 4673 88
8	25.9181 3939 25
9	29.0597 3204 61
10	32.2013 2470 01

For r > 10,

$$\mu_r = \frac{4r + 1}{4}\pi$$

APPENDIX 5

The Least Square Method.

This method is a general one [42] for obtaining the coefficients of a specified-order polynomial from a discrete number of points, when this number is larger than necessary to make the polynomial unique. The notion will become apparent from the application of the method to the problem at hand, i.e. that of obtaining a linear function of two independent variables from four points.

The required linear function is given by:

$$D = D_1 x + D_2 y + D_3 \tag{A5.1}$$

Let the four sets of values of D, x and y be given by D_i, x_i and y_i (i=1,2,3,4). Then the error at each of the four points arising from using equation (A5.1) will be:

$$(D_i - D_1 x_i - D_2 y_i - D_3) \quad i=1,2,3,4.$$

and the sum of the square of the errors will be:

$$S = \sum_{i=1}^{4} (D_i - D_1 x_i - D_2 y_i - D_3)^2$$

Minimizing S implies:

$$\frac{\partial S}{\partial D_1} = -2 \sum x_i(D_i - D_1 x_i - D_2 y_i - D_3) = 0$$

$$\frac{\partial S}{\partial D_2} = -2 \sum y_i(D_i - D_1 x_i - D_2 y_i - D_3) = 0$$

$$\frac{\partial S}{\partial D_3} = -2 \sum (D_i - D_1 x_i - D_2 y_i - D_3) = 0$$

Or

$$\sum x_i D_i = D_1 \sum x_i^2 - D_2 \sum x_i y_i - D_3 \sum x_i \qquad (A5.2)$$

$$\sum y_i D_i = D_1 \sum x_i y_i - D_2 \sum y_i^2 - D_3 \sum y_i \qquad (A5.3)$$

$$\sum D_i = D_1 \sum x_i - D_2 \sum y_i - 4 D_3 \qquad (A5.4)$$

Let $\sum x_i D_i = L$, $\sum x_i^2 = M$, $\sum x_i y_i = N$, $\sum x_i = P$

$\sum y_i D_i = Q$, $\sum y_i^2 = R$, $\sum y_i = S$, $\sum D_i = T$.

The summation everywhere is for i=1,2,3,4.

Equations (A5.2), (A5.3) and (A5.4) become:

$$L = M D_1 + N D_2 + P D_3$$

$$Q = N D_1 + R D_2 + S D_3$$

$$T = P D_1 + S D_2 + 4 D_3 .$$

These equations can be solved to give:

$$D_3 = \frac{1}{F_1^2/F_2 - (P^2/M - 4)} \left\{ T - \frac{PL}{M} + \frac{F_1}{F_2} \left(\frac{NL}{M} - Q\right) \right\}$$

$$D_2 = \frac{1}{F_2} \left[\frac{NL}{M} - Q - F_1 D_3 \right]$$

$$D_1 = (L - ND_2 - PD_3) / M.$$

where

$$F_1 = \frac{PN}{M} - S$$

$$F_2 = \frac{N^2}{M} - R$$

APPENDIX 6

Listing of the Complete Computer Program

```
'BEGIN'
'PROCEDURE'  LSTSQR(ES,K,Q1,Q2,Q3,X,Y,Q);
  'INTEGER'  ES,K;
  'ARRAY' Q1,Q2,Q3,X,Y,Q;
'BEGIN'
  'INTEGER'  I;
  'REAL' SXSQ,SXY,SX,SYSQ,SY,FACT1,FACT2,SXQ,SYQ,SQ;
  'IF' ES=1 ' THEN'
'BEGIN'
  'FOR' I:=1 'STEP' 1 'UNTIL' 4 'DO'
  Q[I]:=READ;
'END' 'ELSE'
  'FOR' I:=1,2 'DO'
'BEGIN'
  Q[I]:=Q[I+2];  Q[I+2]:=READ;
'END';
  SXSQ:=SXY:=SX:=SYSQ:=SY:=SXQ:=SYQ:=SQ:=0.0;
  'FOR' I:=1 'STEP' 1 'UNTIL' 4 'DO'
'BEGIN'
  SXSQ:=SXSQ+X[I]*X[I];   SXY:=SXY+X[I]*Y[I];   SX:=SX+X[I];
  SY:=SY+Y[I];    SQ:=SQ+Q[I];   SYSQ:=SYSQ+Y[I]*Y[I];
  SXQ:=SXQ+X[I]*Q[I];   SYQ:=SYQ+Y[I]*Q[I];
'END';
  FACT1:=SX*SXY/SXSQ-SY;  FACT2:=SXY*SXY/SXSQ-SYSQ;
  Q3[K,ES]:=(SQ-SX*SXQ/SXSQ+FACT1/FACT2*(SXY*SXQ/SXSQ-SYQ))/
            (FACT1*FACT1/FACT2-(SX*SX/SXSQ-4));
  Q2[K,ES]:=(SXY*SXQ/SXSQ-SYQ-FACT1*Q3[K,ES])/FACT2;
  Q1[K,ES]:=(SXQ-SXY*Q2[K,ES]-SX*Q3[K,ES])/SXSQ;
'END' OF PRO CEDURE LSTSQR ;
'PROCEDURE' GEOMBC (NHARM,TOTDF,NPD,DF,OVADD,OVF,OVK,PD);
  'INTEGER' NHARM,TOTDF,NPD;
  'ARRAY' OVF,OVK,PD;
  'INTEGER' 'ARRAY' DF,OVADD;
'BEGIN'
  'REAL' PI;
  'INTEGER'M,N,I,II,J,P,S,T;
  PI:=4.0*ARCTAN(1.0);
  'FOR'  P:=1 'STEP' 1 'UNTIL' NPD   'DO'
'BEGIN'
  'FOR'  M:=1 'STEP' 1 'UNTIL' NHARM 'DO'
'BEGIN'
  'FOR' II:=1 'STEP' 1 'UNTIL' TOTDF 'DO'
'BEGIN'
  'FOR'  N:=1 'STEP' 1 'UNTIL' NHARM 'DO'
'BEGIN'
  I:=(II-1)*NHARM+N;
  J:=(DF[P]-1)*NHARM+M;
  'IF' J<(I-(OVADD[I]-OVADD[I-1])+1)
  'OR' I<(J-(OVADD[J]-OVADD[J-1])+1) 'THEN' 'GOTO' MISS1;
  S:= 'IF' I>J 'THEN' I 'ELSE' J ;
  T:= 'IF' I>J 'THEN' J 'ELSE' I ;
  OVF[I,1]:=OVF[I,1]-OVK[OVADD[S]-S+T]*2*(1-(-1)↑M)*PD[P]/
  (PI*M);  'END';
MISS1:
'END';
  OVF[J,1]:=2*(1-(-1)↑M)*PD[P]/(PI*M);
  II:=(DF[P]-1)*NHARM+M;
```

```
  'FOR' I:=II+1 'STEP' 1 'UNTIL' NHARM*TOTDF 'DO'
'BEGIN'
  'IF' II<(I-(OVADD[I]-OVADD[I-1])+1) 'THEN' 'GOTO' MISS2;
  OVK[OVADD[I]-I+II]:=0.0;
MISS2:
'END';
  'FOR' J:=II-(OVADD[II]-OVADD[II-1])+1 'STEP' 1 'UNTIL' II-1
  'DO' OVK [OVADD [II] -II-J]:=0.0;
  OVK[OVADD[II]]:=1.0;
'END';
'END';
'END' OF PRO CEDURE GEOMBC ;
'PROCEDURE'  SYMVBSOL(A,L,S,B,N,R,FAIL);
  'VALUE' N,R;
  'ARRAY' A,L,B;
  'INTEGER''ARRAY' S;
  'INTEGER'  N,R;
  'LABEL' FAIL;
  'COMMENT' SOLVES AX=B, WHERE A IS A SYMMETRIC POSITIVE DEF -
       INITE MATRIX OF ORDER N STORED IN VARIABLE BAND FORM AND
       B IS AN N*R MATRIX OF R RIGHTHAND SIDES.THE SOLUTION X
            OVERWRITES B.
  REF. A. JENNINGS, THE COMPUTER JOURNAL ,1971, PAGE 446.;
'BEGIN'
  'INTEGER'  G,H,I,J,K,M,P,Q,T,U,V;
  'REAL' Y;
  H:=0;
  'FOR' I:=1 'STEP' 1 'UNTIL' N 'DO'
'BEGIN'
  T:=I+H-S[I]+1;
  G:=H+1;
  P:=S[T]-1;
  'FOR' J:=T 'STEP' 1 'UNTIL' I-1 'DO'
'BEGIN'
  Q:=P+1;  H:=H+1;
  P:=S[J];  K:=J+Q-P;
  V:=H-P;  U:=G;
  Y:=A[H];
  'IF' K>T 'THEN' U:=U+K-T;
  'FOR' U:=U 'STEP' 1 'UNTIL' H-1 'DO'
  Y:=Y-L[U]*L[U-V];
  Y:=Y/L[H-V];  L[H]:=Y;
  'FOR' M:=1 'STEP' 1 'UNTIL' R 'DO'
  B[I,M]:=B[I,M]-B[J,M]*Y;
'END' J ;
  Y:=A[H+1];
  'FOR' U:=G 'STEP' 1 'UNTIL' H 'DO'
  Y:=Y-L[U]↑2;
  'IF' Y 'LE' 0 'THEN'
'BEGIN'
  WRITETEXT('('[M]%IS%NOT%POSITIVE%DEFINITE')');
  'GOTO' FAIL;
'END';
  H:=H+1;  Y:=SQRT(Y);
  L[H]:=Y;
  'FOR' M:=1 'STEP' 1 'UNTIL' R 'DO'
  B[I,M]:=B[I,M]/Y;
```

```
'END' I ;
  'COMMENT' REDUCTION COMPLETE;
  'FOR' I:=N 'STEP' -1 'UNTIL' 1 'DO'
'BEGIN'
  Y:=L[H];
  'FOR' M:=1 'STEP' 1 'UNTIL' R 'DO'
  B[I,M]:=B[I,M]/Y;
  'IF' I=1 'THEN' 'GOTO' COMPLETE;
  J:=I; P:=S[I-1];
  'FOR' H:=H-1 'STEP' -1 'UNTIL' P+1 'DO'
'BEGIN'
  J:=J-1; Y:=L[H];
  'FOR' M:=1 'STEP' 1 'UNTIL' R 'DO'
B[J,M]:=B[J,M]-B[I,M]*Y;
'END' H ;
  H:=P;
COMPLETE:
'END' I ;
'END' OF PRO CEDURE SYMVBSOL ;

'REAL''PROCEDURE' HARM(N,BC,SYMM);
'INTEGER' BC,N,SYMM;
  'IF' BC=1 'THEN' HARM:=('IF' SYMM=1 'THEN' 2*N-1'ELSE' N)*3.1415926536
  'ELSE' ' IF' BC=2 'OR' BC=3 'THEN'
'BEGIN'
  'IF' SYMM=1 'THEN' HARM:=('IF' N=1 'THEN' 4.7300407448'ELSE' 'IF' N=2
  'THEN' 10.995607838'ELSE' 'IF' N=3 'THEN' 17.278759658'ELSE' 'IF' N=4
  'THEN' 23.561944903 'ELSE' (2*N-0.5)*3.1415926536)'ELSE'HARM:=('IF'N=1
  'THEN' 4.7 300407448'ELSE' 'IF' N=2
  'THEN'7.8532046242 'ELSE' 'IF' N=3 'THEN'10.995607838 'ELSE' 'IF' N=4
  'THEN'14.137165491 'ELSE' 'IF' N=5 'THEN'17.2787596577'ELSE'
  (N+0.5)*3.1415926536);
'END' 'ELSE'
  'IF' BC=4 'THEN' HARM:=('IF' N=1 'THEN' 1.8751040688'ELSE' 'IF' N=2
  'THEN' 4.6940911331'ELSE' 'IF' N=3 'THEN' 7.8547574385'ELSE' 'IF' N=4
  'THEN'10.995540735 'ELSE' 'IF' N=5 'THEN'14.137168391 'ELSE' 'IF' N=6
  'THEN'17 .278759533 'ELSE' 'IF' N=7 'THEN'20.420352251 'ELSE' 'IF' N=8
  'THEN' 23.561944903 'ELSE' (N-0.5)*3.1415926536) 'ELSE'
  'IF' BC=5 'OR' BC=6 'THEN' HARM:=('IF' N=1 'THEN' 3.9266023122'ELSE'
  'IF' N=2 'THEN' 7.0685827457 'ELSE' 'IF' N=3 'THEN' 10.210176123
  'ELSE' 'IF' N=4 'THEN' 13.3517687778 'ELSE' (N+0.25)*3.1415926536);
'PROCEDURE' MODIFIFI(M,N,Y,T,IFF);
'VALUE' M,N; 'REAL' M,N,Y; 'INTEGER' T; 'ARRAY' IFF;
'BEGIN'
  'INTEGER' I,J; 'REAL' S,D,SM,SN,DM,DN,A,B,XA,XB;
  'ARRAY' FM,FN[1:4],FF,IFFD[1:4,1:4];
  A:=M*Y; B:=N*Y; XA:=EXP(A); XB:=EXP(B);
  FM[1]:=COS(A); FM[2]:=SIN(A); FM[3]:=XA; FM[4]:=1/XA;
  FN[1]:=COS(B); FN[2]:=SIN(B); FN[3]:=XB; FN[4]:=1/XB;
  'FOR' I:=1,2,3,4 'DO' 'FOR' J:=1,2,3,4 'DO' FF[I,J]:=FM[I]*FN[J];
  S:=1/(M*M+N*N); SM:=S*M; SN:=S*N;
  IFF[1,3]:=SM*FF[2,3]+SN*FF[1,3]; IFF[3,1]:=SM*FF[3,1]+SN*FF[3,2];
  IFF[2,3]:=-SM*FF[1,3]+SN*FF[2,3]; IFF[3,2]:=SM*FF[3,2]-SN*FF[3,1];
  IFF[1,4]:= SM*FF[2,4]-SN*FF[1,4]; IFF[4,1]:=-SM*FF[4,1]+SN*FF[4,2];
  IFF[2,4]:=-SM*FF[1,4]-SN*FF[2,4]; IFF[4,2]:=-SM*FF[4,2]-SN*FF[4,1];
  IFF[3,3]:=FF[3,3]/(M+N); IFF[4,4]:=-FF[4,4]/(M+N);
```

```
  'IF' ABS(M-N)>0.1 'THEN'
'BEGIN'
  D:=1/(M*M-N*N); DM:=D*M; DN:=D*N;
  IFF[3,4]:=FF[3,4]/(M-N); IFF[4,3]:=-FF[4,3]/(M-N);
  IFF[1,1]:=DM*FF[2,1]-DN*FF[1,2]; IFF[2,2]:=-DM*FF[1,2]+DN*FF[2,1
];IFF[1,2]:=DM*FF[2,2]+DN*FF[1,1]; IFF[2,1]:=-DM*FF[1,1]-DN*FF[2,2
  ; 'END''ELSE'
'BEGIN'
  IFF[3,4]:=IFF[4,3]:=Y; IFF[1,1]:=SIN(2*A)/(4*M)+Y/2;
  IFF[2,2]:=-SIN(2*A)/(4*M)+Y/2; IFF[1,2]:=IFF[2,1]:=-COS(2*A)/
  (4*M); 'END';
  'IF' T=1 ' THEN'
'BEGIN'
  'FOR' I:=1,2,3,4 'DO' 'FOR' J:=1,2,3,4 'DO' IFFD[I,J]:=IFF[I,J];
  IFF[1,3]:=Y*IFF[1,3]-SM*IFFD[2,3]-SN*IFFD[1,3];
  IFF[3,1]:=Y*IFF[3,1]-SM*IFFD[3,1]-SN*IFFD[3,2];
  IFF[2,3]:=Y*IFF[2,3]+SM*IFFD[1,3]-SN*IFFD[2,3];
  IFF[3,2]:=Y*IFF[3,2]-SM*IFFD[3,2]+SN*IFFD[3,1];
  IFF[1,4]:=Y*IFF[1,4]-SM*IFFD[2,4]+SN*IFFD[1,4];
  IFF[4,1]:=Y*IFF[4,1]+SM*IFFD[4,1]-SN*IFFD[4,2];
  IFF[2,4]:=Y*IFF[2,4]+SM*IFFD[1,4]+SN*IFFD[2,4];
  IFF[4,2]:=Y*IFF[4,2]+SM*IFFD[4,2]+SN*IFFD[4,1];
  IFF[3,3]:=Y*IFF[3,3]-IFFD[3,3]/(M+N);
  IFF[4,4]:=Y*IFF[4,4]+IFFD[4,4]/(M+N);
  'IF' ABS(M-N)>0.1 'THEN'
'BEGIN'
  IFF[3,4]:=Y*IFF[3,4]-IFFD[3,4]/(M-N);
  IFF[4,3]:=Y*IFF[4,3]+IFFD[4,3]/(M-N);
  IFF[1,1]:=Y*IFF[1,1]-DM*IFFD[2,1]+DN*IFFD[1,2];
  IFF[2,2]:=Y*IFF[2,2]+DM*IFFD[1,2]-DN*IFFD[2,1];
  IFF[1,2]:=Y*IFF[1,2]-DM*IFFD[2,2]-DN*IFFD[1,1];
  IFF[2,1]:=Y*IFF[2,1]+DM*IFFD[1,1]+DN*IFFD[2,2];
'END''ELSE'
'BEGIN'
  IFF[3,4]:=IFF[4,3]:=Y*Y/2; IFF[1,1]:=Y*IFFD[1,1]-2/(4*M)*IFFD[2,
1]-Y*Y/4; IFF[2,2]:=Y*IFF[2,2]+2/(4*M)*IFFD[2,1]-Y*Y/4;
  IFF[1,2]:=IFF[2,1]:=Y*IFF[2,1]+SIN(2*A)/(8*M*M);
'END';
'END';
'END' OF PRO CEDURE MODIFIFI;
'PROCEDURE' MODCI(N,BC,C);
'VALUE' N; ' REAL' N; 'INTEGER' BC; 'ARRAY' C;
'BEGIN'
  'REAL' X,B,D,S,R;
  X:=EXP(N); B:=EVEN((BC+2)'/'2); D:=EVEN(BC);
  C[2,0]:=1.0;
  'IF' BC=1 'THEN' C[1,0]:=C[3,0]:=C[4,0]:=0.0 'ELSE'
  'IF' BC=2 'OR' BC=3 'OR' BC=4 'THEN'
'BEGIN'
  S:=(SIN(N)-B*(X-1/X)/2)/(COS(N)-B*(X+1/X)/2);
  R:=((COS(N)-SIN(N))-B/X)/(2*(COS(N)-B*(X+1/X)/2));
  C[1,0]:=-S; C[3,0]:=-D*R; C[4,0]:=D*(1+S)/2;
'END''ELSE'
'BEGIN'
  C[1,0]:=0.0; C[3,0]:=D*SIN(N)/(X-1/X); C[4,0]:=-C[3,0];
'END';
  C[1,1]:=N*C[2,0]; C[2,1]:=-N*C[1,0]; C[3,1]:=N*C[3,0];
```

```
  C[4,1]:=-N*C[4,0]; C[1,2]:=N*C[2,1]; C[2,2]:=-N*C[1,1];
  C[3,2]:=N*C[3,1]; C[4,2]:=-N*C[4,1];
'END' OF PROCEDURE MODCI;
'PROCEDURE' IYY(M,N,EL0,EL1,BC,I1);
'REAL' M,N,EL0,EL1;  'INTEGER' BC; 'ARRAY' I1;
'BEGIN'
  'INTEGER' I,J,T,T1;  'ARRAY' IFF,SIFF1[1:4,1:4],C,SCN,SCM[1:4,0:
  2]; MODCI(N,BC,C);
  'FOR' I:=1,2,3,4 'DO' 'FOR' J:=0,1,2 'DO' SCN[I,J]:=C[I,J];
MODCI(M,BC,C);
  'FOR' T:=0,1 'DO'
'BEGIN'
  MODIFIFI(M,N,EL1,T,IFF);
  'FOR' I:=1,2,3,4 'DO' 'FOR' J:=1,2,3,4 'DO' SIFF1[I,J]:=IFF[I,J
];MODIFIFI(M,N,EL0,T,IFF);
  'FOR' I:=1,2,3,4 'DO' 'FOR' J:=1,2,3,4 'DO'
  IFF[I,J]:=SIFF1[I,J]-IFF[I,J];
  T1:=T*10; 'FOR' I:=1,2,3,4,5 'DO' I1[T1+I]:=0.0;
  'FOR' I:=1,2,3,4 'DO' 'FOR' J:=1,2,3,4 'DO'
'BEGIN'
  I1[T1+1]:=I1[T1+1]+IFF[I,J]*C[I,0]*SCN[J,0];
  I1[T1+2]:=I1[T1+2]+IFF[I,J]*C[I,2]*SCN[J,0];
  I1[T1+3]:=I1[T1+3]+IFF[I,J]*C[I,0]*SCN[J,2];
  I1[T1+4]:=I1[T1+4]+IFF[I,J]*C[I,1]*SCN[J,1];
  I1[T1+5]:=I1[T1+5]+IFF[I,J]*C[I,2]*SCN[J,2];
'END';
'END';
'END' OF PROCEDURE  IYY;
'PROCEDURE'  MODIFI(M,Y,T,IF);
'VALUE' M; ' REAL' M,Y; 'INTEGER' T; 'ARRAY' IF;
'BEGIN'
'REAL' A,X1,X2,X3,X4,M2;
  A:=M*Y; X1:=COS(A); X2:=SIN(A);  X3:=EXP(A);  X4:=1/X3;
  IF[1]:=X2/M;  IF[2]:=-X1/M;  IF[3]:=X3/M;  IF[4]:=-X4/M;
'IF' T=1 'THEN'
'BEGIN'
  M2:=M*M;
  IF[1]:=Y*IF[1]+X1/M2; IF[2]:=Y*IF[2]+X2/M2;
  IF[3]:=Y*IF[3]-X3/M2; IF[4]:=Y*IF[4]-X4/M2;
'END';
'END' OFPROCEDURE MODIFI;
'PROCEDURE' IY(N,EL0,EL1,BC,I2,I12);
'REAL' N,EL0,EL1,I2,I12;  'INTEGER' BC;
'BEGIN'
  'INTEGER'  I,T; 'ARRAY' C[1:4,0:2],SIF,IF[1:4],II[0:1];
MODCI(N,BC,C);
  'FOR' T:=0,1 'DO'
'BEGIN'
   MODIFI(N,EL1,T,IF); 'FOR' I:=1,2,3,4 'DO' SIF[I]:=IF[I];
   MODIFI(N,EL0,T,IF); 'FOR' I:=1,2,3,4 'DO' IF[I]:=SIF[I]-IF[I];
   II[T]:=0.0;  'FOR' I:=1,2,3,4 'DO' II[T]:=II[T]+IF[I]*C[I,0];
'END';
  I2:=II[0];  I12:=II[1];
'END'OF PROCEDURE IY;
'PROCEDURE'  FI(N,Y,BC,FI0,FI1,FI2);
'REAL' N,Y,FI0,FI1,FI2;  'INTEGER' BC;
'BEGIN'
```

```
  'REAL'  A;  'INTEGER' I;  'ARRAY' C[1:4,0:2],F[1:4];
  A:=N*Y;
  F[1]:=COS(A);  F[2]:=SIN(A);  F[3]:=EXP(A);  F[4]:=1/F[3];
  MODCI(N,BC,C);  FI0:=FI1:=FI2:=0.0;
  'FOR' I:=1,2,3,4 'DO'
'BEGIN'
  FI0:=FI0+F[I]*C[I,0];
  FI1:=FI1+F[I]*C[I,1];
  FI2:=FI2+F[I]*C[I,2];
'END';
'END' OF PRO FI ;
'REAL' PI,A,B,E,G,H,YY,V,DD,F1,FF1,FF5,BA1,BA2,M,N,CM,CN,CM1,CN1,CM2,
  CN2,ALFM,ALFN,EX0,EX1,EX10,EX11,EX20,EX21,EX30,EX31,EX40,EX41,SH10,
  MPN,MMN,M2,SD1I1,SD1I2,SD1I3,SD1I4,SD1I5,SD2I11,SD2I12,SD2I13,SD2I1
  SD2I15,SD3I1,SD3I2,SD3I3,SD3I4,SD3I5,SQ1I2,SQ2I12,SQ3I2,I2,I12,PDA,
  FY,X0,X1,X2,X3,X4,X5,EL0,EL1,T1,T2,ALFMN,DEF,ROTX,ROTY,MX,MY,MXY,
  BA3,FI0,FI1,FI2,EL11,EL12,EL13,EL14,YYY,VX,VY,FFF1,SBK,XSX,
  FPM,PM1,PM2;
'INTEGER'K,NNN,MMM,I,J,NELEM,NHARM,MHARM,NN,NA,NB,IN,ID,IT,L,NSETS,
         TOTDF,S,T,  NDOF,NPD,NNODE,TNNODE,NS,ES,MNS,MSQ,NSQ,
         QTYPE,DTYPE,EP,NLOAD,BC,HDF,SYMM,NSTEP;
  NSETS:=READ;
'FOR'L:=1'STEP'1'UNTIL'NSETS'DO'
'BEGIN'
  PI:=4.0*ARCTAN(1.0);
  BC:=READ;  A:=READ;                 NELEM:=READ;  NHARM:=READ;  YYY:=REA
  NSTEP:=READ;
  NPD:=READ;  MNS:=READ;  V:=READ;  SYMM:=READ;  QTYPE:=READ;
  DTYPE:=READ;  NLOAD:=READ;
  NNODE:=NDOF:=2;  TNNODE:=NELEM+1;  TOTDF:=2*TNNODE;
'COMMENT' BC=1 REFERS TO SIMPLY SUPPORTED/SIMPLY SUPPORTED
             2 CLAMPED / CLAMPED,    3 FREE/FREE
             4 CLAMPED/FREE,  5 SIMPLY SUPPORTED/CLAMPED
             6 SIMPLY SUPPORTED/FREE ;
'BEGIN'
'INTEGER''ARRAY' OVADD[0:NHARM*TOTDF],NODE[1:NELEM,1:NNODE];
'PROCEDURE' ADDARRAY;
'BEGIN'
  'INTEGER' NHARM2,M,I,J;
  OVADD[0]:=0;  NHARM2:=2*NHARM;
  'FOR' M:=1 'STEP' 1 'UNTIL' NHARM2 'DO'  OVADD[M]:=OVADD[M-1]+M;
  'FOR' I:=2 'STEP' 1 'UNTIL' TNNODE 'DO'
  'FOR' M:=1 'STEP' 1 'UNTIL' NHARM2 'DO'
'BEGIN'
  J:=(I-1)*NHARM2+M;
  OVADD[J]:=OV ADD[J-1]+J-(I-2)*NHARM2;
'END';
'END' OF PROCEDURE ADDARRAY ;
  'FOR' K:=1 'STEP' 1 'UNTIL' NELEM 'DO'
  'FOR' S:=1 'STEP' 1 'UNTIL' NNODE 'DO'
  NODE[K,S]:=K+S-1;
ADDARRAY;


'BEGIN'
```

```
'PROCEDURE' ASSMBLY(K,N,M);
'INTEGER' K,N,M;
'COMMENT' THIS PROCEDURE CARRIES OUT THE ASSEMBLY OF THE OVERALL
          STIFFNESS MATRIX IN ONE DIMENSIONAL FORM AND THE ASSEMBLY
          OF THE FORCE VECTOR ;
'BEGIN'
  'INTEGER' S,I,II,T,J,JJ;
  'FOR' S:=1,2,3,4 'DO'
'BEGIN'
  II:=2*(K-1)+S;  I:=NHARM*(II-1)+N;
  'FOR' T:=1,2,3,4 'DO'
'BEGIN'
  JJ:=2*(K-1)+T;  J:=NHARM*(JJ-1)+M;
  'IF' J>I 'THEN' 'GOTO' KAM;
  OVK[OVADD[I]-I+J]:=OVK[OVADD[I]-I+J]+HEK[S,T];
'END';
KAM:
  'IF' M=N ' THEN'
  OVF[I,1]:=OVF[I,1]+HEF[S];
'COMMENT' THE HARMONIC FORCE VECTOR VARIES WITH N ONLY ;
'END';
'END' OF PROCEDURE ASSMBLY ;
'ARRAY' EL[1:NELEM,0:MNS],D1,D2,D3,Q1,Q2,Q3[1:NELEM,1:MNS],
  THEK,HEK[1:4,1:4],HEF[1:4],OVF[1:TOTDF*NHARM,1:1],
          OVK[1:OVADD[NHARM*TOTDF]],W[1:TOTDF*NHARM],
          HW[1:NHARM,1:TOTDF], X,Y,D,Q[1:4], PD[1:NPD+1],
              J1,J2,J3,J4,J5,J11,J12,J13,J14,J15[1:4,1:4],J6,J16[1:4],
 P,C,DP[1:NLOAD+1],II,IID,I1[1:20],FF2,FF3,FF4,FF6[1:NHARM],
  CI[1:4,0:2],BE[1:NELEM];
'INTEGER'' ARRAY' DF[1:NPD+1],NS[1:NELEM],PTYPE,NODENO[1:NLOAD+1];
  'FOR' I:=1 'STEP' 1 'UNTIL' NPD 'DO'
'BEGIN'
  DF[I]:=READ;   PD[I]:=READ;
'END';
  'FOR' EP:=1 'STEP' 1 'UNTIL' NLOAD 'DO'
'BEGIN'
  P[EP]:=READ;  PTYPE[EP]:=READ;  NODENO[EP]:=READ;  C[EP]:=READ;
  'IF' PTYPE[EP]=1 'OR' PTYPE[EP]=21 'OR' PTYPE[EP]=22 'THEN'
  DP[EP]:=READ;
'END';
'COMMENT' PTYPE INTEGERS REFER TO THE FOLLOWING:
  1     LINE FORCE
  21    LINE MOMENT M(X)
  22    LINE MOMENT M(Y)
  3     CONCENTRATED FORCE
  41    CONCENTRATED MOMENT M(X)
  42    CONCENTRATED MOMENT M(Y)  ;
  'FOR' I:=1 'STEP' 1 'UNTIL' OVADD[NHARM*TOTDF] 'DO'
  OVK[I]:=0.0;
  'FOR' I:=1 'STEP' 1 'UNTIL' TOTDF*NHARM 'DO'
  OVF[I,1]:=0.0;
  'FOR' K:=1 'STEP' 1 'UNTIL' NELEM 'DO'
'BEGIN'
BE[K]:=READ;  NS[K]:=READ;  EL[K,0]:=0.0;
  'FOR' ES:=1 'STEP' 1 'UNTIL' NS[K] 'DO'
  EL[K,ES]:=READ;
'END';
```

```
'COMMENT'  QTYPE AND DTYPE INTEGERS REFER TO THE FOLLOWING
  111  UNIFO RMITY THROUGHOUT THE WHOLE PLATE .ONE VALUE TO BE READ.
  11   UNIFORMITY THROUGHOUT EACH ELEM. A VALUE FOR EACH ELEM .
  1    UNIFORMITY THROUGHOUT EACH STEP.
  2    NON-UNIFORMITY . VALUES FOR Q1,Q2,Q3 AND / OR D1,D2, AND D3
       TO BE READ
  3    NON -UNIFORMITY . ABOVE VALUES TO BE EVALUATED FROM LSTSQR .
       VALUES OF Q AND / OR D TO BE READ FOR EACH STEP IN SUCH A
       SEQUENCE AS TO MAKE Q[3] AND Q[4] OF EACH STEP THE SAME AS
       Q[1] AND Q[2] OF THE NEXT STEP RESPECTIVELY . THUS FOR EACH
       ELEM 4 VALUES SHOULD BE READ FOR THE FIRST STEP AND TWO FOR
       SUBSEQUENT STEPS.
  0    NO DISTRIBUTED LOAD ;
  'IF' QTYPE=111 'THEN'
'BEGIN'
  Q3[1,1]:=READ;
  'FOR' K:=1 'STEP' 1 'UNTIL' NELEM 'DO'
  'FOR' ES:=1 'STEP' 1 'UNTIL' NS[K] 'DO'
'BEGIN'
  Q1[K,ES]:=Q2[K,ES]:=0.0;  Q3[K,ES]:=Q3[1,1];
'END';
'END' 'ELSE'
  'IF' QTYPE=11  'THEN'
'BEGIN'
  'FOR' K:=1 'STEP' 1 'UNTIL' NELEM 'DO'
'BEGIN'
  Q3[K,1]:=READ;
  'FOR' ES:=1 'STEP' 1 'UNTIL' NS[K] 'DO'
'BEGIN'
  Q1[K,ES]:=Q2[K,ES]:=0.0;  Q3[K,ES]:=Q3[K,1];
'END';
'END';
'END' 'ELSE'
  'IF' QTYPE=1   'THEN'
'BEGIN'
  'FOR' K:=1 'STEP' 1 'UNTIL' NELEM 'DO'
  'FOR' ES:=1 'STEP' 1 'UNTIL' NS[K] 'DO'
'BEGIN'
  Q3[K,ES]:=READ;  Q1[K,ES]:=Q2[K,ES]:=0.0;
'END';
'END' 'ELSE'
  'IF' QTYPE=2   'THEN'
'BEGIN'
  'FOR' K:=1 'STEP' 1 'UNTIL' NELEM 'DO'
  'FOR' ES:=1 'STEP' 1 'UNTIL' NS[K] 'DO'
'BEGIN'
  Q1[K,ES]:=READ; Q2[K,ES]:=READ; Q3[K,ES]:=READ;
'END';
'END' 'ELSE'
  'IF' QTYPE=3   'THEN'
'BEGIN'
  X[1]:=X[3]:=0.0;
  'FOR' K:=1 'STEP' 1 'UNTIL' NELEM 'DO'
'BEGIN'
  X[2]:=X[4]:=BE[K];
  'FOR' ES:=1 'STEP' 1 'UNTIL' NS[K] 'DO'
'BEGIN'
```

```
 Y[1]:=Y[2]:=EL[K,ES-1];  Y[3]:=Y[4]:=EL[K,ES];
 LSTSQR(ES,K,Q1,Q2,Q3,X,Y,Q);
'END';
'END';
'END';
 'IF' DTYPE=111 'THEN'
'BEGIN'
 D3[1,1]:=READ;
  'FOR' K:=1 'STEP' 1 'UNTIL' NELEM 'DO'
  'FOR' ES:=1 'STEP' 1 'UNTIL' NS[K] 'DO'
'BEGIN'
 D1[K,ES]:=D2[K,ES]:=0.0;  D3[K,ES]:=D3[1,1];
'END';
'END' 'ELSE'
  'IF' DTYPE=11 'THEN'
'BEGIN'
  'FOR' K:=1 'STEP' 1 'UNTIL' NELEM 'DO'
'BEGIN'
D3[K,1]:=READ;
  'FOR' ES:=1 'STEP' 1 'UNTIL' NS[K] 'DO'
'BEGIN'
 D1[K,ES]:=D2[K,ES]:=0.0;
 D3[K,ES]:=D3[K,1];
'END';
'END';
'END' 'ELSE'
  'IF' DTYPE=1 'THEN'
'BEGIN'
  'FOR' K:=1 'STEP' 1 'UNTIL' NELEM 'DO'
  'FOR' ES:=1 'STEP' 1 'UNTIL' NS[K] 'DO'
'BEGIN'
  D3[K,ES]:=READ;  D1[K,ES]:=D2[K,ES]:=0.0;
'END';
'END' 'ELSE'
  'IF' DTYPE=2 'THEN'
'BEGIN'
  'FOR' K:=1 'STEP' 1 'UNTIL' NELEM 'DO'
  'FOR' ES:=1 'STEP' 1 'UNTIL' NS[K] 'DO'
'BEGIN'
  D1[K,ES]:=READ;  D2[K,ES]:=READ;  D3[K,ES]:=READ;
'END';
'END' 'ELSE'
  'IF' DTYPE=3   'THEN'
'BEGIN'
  X[1]:=X[3]:=0.0;
  'FOR' K:=1 'STEP' 1 'UNTIL' NELEM 'DO'
'BEGIN'
  X[2]:=X[4]:=BE[K];
  'FOR' ES:=1 'STEP' 1 'UNTIL' NS[K] 'DO'
'BEGIN'
  Y[1]:=Y[2]:=EL[K,ES-1];  Y[3]:=Y[4]:=EL[K,ES];
  LSTSQR(ES,K,D1,D2,D3,X,Y,D);
'END';
'END';
'END';
  PDA:=PI/A;
```

```
WRITETEXT('('I%N%P%U%T%%%D%A%T%A%'('C')'==========
==========('2C')'DATA%SET%NO.')');  PRINT(L,2,0);
NEWLINE(2);
WRITETEXT('('DATA%OF%PLATE'('C')'--------------('2C')'
OVERALL%DIMENSIONS%ARE%%%A%=%')');  PRINT(A,0,4);
WRITETEXT('('%%%%B%=%')');
SBK:=0.0;  'FOR' K:=1 'STEP' 1 'UNTIL' NELEM 'DO'
SBK:=SBK+BE[K];  PRINT(SBK,0,4);  NEWLINE(2);
WRITETEXT('('NUMBER%OF%STRIPS%=')');  PRINT(NELEM,2,0);
WRITETEXT('('%%%%%NUMBER%OF%HARMONICS%=')');
PRINT(NHARM,2,0);  NEWLINE(2);
WRITETEXT('('THE%EDGES%Y=0%%AND%%Y=A%%ARE%%%')');
'IF' BC=1 'THEN' WRITETEXT('('SIMPLY%SUPPORTED-
SIMPLY %SUPPORTED')') 'ELSE'
'IF' BC=2 'THEN' WRITETEXT('('CLAMPED-CLAMPED')') 'ELSE'
'IF 'BC=3 'THEN' WRITETEXT('('FREE-FREE')') 'ELSE'
'IF' BC=4 'THEN' WRITETEXT('('CLAMPED-FREE')') 'ELSE'
'IF' BC=5 'THEN' WRITETEXT('('SIMPLY%SUPPORTED-CLAMPED')')
'ELSE' 'IF' BC=6 'THEN' WRITETEXT('('SIMPLY%SUPPORTED-
FREE')');
NEWLINE(2);
'IF' NPD=0 'THEN' WRITETEXT('('NO%DISPLACEMENTS%ARE%
PRESCRIBED%ON%THE%OTHER%EDGES.')') 'ELSE'
'BEGIN'
 WRITETEXT('('DISPLACEMENTS%PRESCRIBED%ON%THE%OTHER%EDGES%
 ARE%%%')' ); NEWLINE(2);  SPACE(15);
 'FOR' I:=1 'STEP' 1 'UNTIL' NPD 'DO'
'BEGIN'
 'IF' DF[I]'/'2=(DF[I]-1)'/'2 'THEN'
'BEGIN'
 WRITETEXT('('ZERO%DEFLECTION%PRESCRIBED%ON%NODAL%LINE%%')');
 PRINT((DF[I]+1)'/'2,3,0);  NEWLINE(2);  SPACE(15);
'END' 'ELSE'
'BEGIN'
 WRITETEXT('('ZERO%ROTATION%PRESCRIBED%ON%NODAL%
 LINE%%')');  PRINT((DF[I]+1)'/'2,3,0); NEWLINE(2);
 SPACE(15);
'END';
'END';
'END';
 NEWLINE(2);
 WRITETEXT('('STRIP%NO.%%STRIP%WIDTH%%NUMBER%OF%STEPS'('C')'
 ========%%==========%%==============('2C')'')');
 'FOR' K:=1 'STEP' 1 'UNTIL' NELEM 'DO'
'BEGIN'
 SPACE(3); PRINT(K,2,0); SPACE(5); PRINT(BE[K],0,4);
 SPACE(7); PRINT(NS[K],2,0);  NEWLINE(2);
'END';
 WRITETEXT('(''('C')'R%E%S%U%L%T%S'('C')'===========('2C')'
 %%Y/A%%%%%%X/B%%%%DEFLECTION%%%ROTATION%%%%%ROTATION%%%%%
 BENDING%MT.%%BENDING%MT.%%TWISTING%MT.%%PRINCIPAL%MOMENTS
 '('C 27S')'THETA%X%%%%%%THETA%Y'('11S')'MX'('11S')'MY'('13S')'
 MXY'('13S')'M1'('9S')'M2'('C')'%======%%======%%==========%%
 %========%%%%===========%%===========%%============%%
 ===============('2C')'')');
 'FOR' K:=1 'STEP' 1 'UNTIL' NELEM 'DO'
'BEGIN'
```

```
  B:=BE[K];
  'FOR' NNN:=1 'STEP' 1 'UNTIL' NHARM 'DO'
'BEGIN'
  'FOR' MMM:=NNN 'STEP' 1 'UNTIL' NHARM 'DO'
'BEGIN'
  'IF'BC=1'AND'(DTYPE=111'OR'DTYPE=11)'THEN'
'BEGIN'
  'IF' MMM 'NE' NNN 'THEN'
'BEGIN'
  'FOR' I:=1,2,3,4 'DO' 'FOR' J:=1,2,3,4 'DO'
  HEK[I,J]:=0.0;   'GOTO' ORTHO;
'END';
'END';
  N:=HARM(NNN,BC,SYMM);  M:=HARM(MMM,BC,SYMM);
  SD1I1:=SD1I2:=SD1I3:=SD1I4:=SD1I5:=SD2I11:=SD2I12:=SD2I13:=SD2I14:=
  SD2I15:=SD3I1:=SD3I2:=SD3I3:=SD3I4:=SD3I5:=0.0;
  'FOR' ES:=1 'STEP' 1 'UNTIL' NS[K] 'DO'
'BEGIN'
EL0:=EL[K,ES-1]/A;  EL1:=EL[K,ES]/A;
  'IF' BC=3 'OR' BC=6 'THEN'
'BEGIN'
  EL11:=EL1-EL0;  EL12:=EL1*EL1-EL0*EL0;  EL13:=EL1*EL1*EL1-EL0*EL0*EL0
; EL14:=EL1↑4-EL0↑4;
'END';
  'IF' BC=3 'THEN'
'BEGIN'
  'IF' MMM=NHARM-1 'AND' NNN=NHARM-1 'THEN'
'BEGIN'
  I1[1]:=EL11;  I1[11]:=EL12/2;
  I1[2]:=I1[12]:=I1[3]:=I1[13]:=I1[4]:=I1[14]:=I1[5]:=I1[15]:=0.0;
'GOTO' GLEN;
'END' 'ELSE' 'IF' (MMM=NHARM-1 'AND' NNN=NHARM) 'OR' (MMM=NHARM 'AND'
  NNN=NHARM-1) 'THEN'
'BEGIN'
  I1[1]:=EL12/2;  I1[11]:=EL13/3;
  I1[2]:=I1[12]:=I1[3]:=I1[13]:=I1[4]:=I1[14]:=I1[5]:=I1[15]:=0.0;
'GOTO' GLEN;
'END' 'ELSE'  'IF' MMM=NHARM-1 'THEN'
'BEGIN'
  IY(N,EL0,EL1,3,I2,I12);  I1[1]:=I2;  I1[11]:=I12;
  IY(N,EL0,EL1,2,I2,I12); I1[3]:=-N*N*I2;  I1[13]:=-N*N*I12;
  I1[2]:=I1[12]:=I1[4]:=I1[14]:=I1[5]:=I1[15]:=0.0;
'GOTO' GLEN;
'END' 'ELSE'  'IF' NNN=NHARM-1 'THEN'
'BEGIN'
  IY(M,EL0,EL1,3,I2,I12);  I1[1]:=I2;  I1[11]:=I12;
  IY(M,EL0,EL1,2,I2,I12);  I1[2]:=-M*M*I2;  I1[12]:=-M*M*I12;
  I1[3]:=I1[13]:=I1[4]:=I1[14]:=I1[5]:=I1[15]:=0.0;
'GOTO' GLEN;
'END';
'END';
  'IF' BC=3 'OR' BC=6 'THEN'
'BEGIN'
  'IF' MMM=NHARM 'AND' NNN=NHARM 'THEN'
'BEGIN'
  I1[1]:=EL13/3;  I1[11]:=EL14/4;  I1[4]:=EL11;  I1[14]:=EL12/2;
  I1[2]:=I1[12]:=I1[3]:=I1[13]:=I1[5]:=I1[15]:=0.0;
```

```
'GOTO' GLEN;
'END' 'ELSE' 'IF' MMM=NHARM 'THEN'
'BEGIN'
  IY(N,EL0,EL1,BC,I2,I12);  FI(N,EL1,BC,FI0,FI1,FI2);  I1[1]:=I12;
  I1[4]:=FI0;  I1[14]:=EL1*FI0-I2;  I1[13]:=EL1*EL1*FI1-2*EL1*FI0+2*I2;
  FI(N,EL0,BC,FI0,FI1,FI2);  I1[13]:=I1[13]-EL0*EL0*FI1+2*EL0*FI0;
  I1[4]:=I1[4]-FI0;  I1[14]:=I1[14]-EL0*FI0;
  IY(N,EL0,EL1,BC-1,I2,I12);  FI(N,EL1,BC-1,FI0,FI1,FI2);
  I1[11]:=EL1*EL1*FI1-2*EL1*FI0+2*I2;  I1[3]:=-N*N*I12;
  FI(N,EL0,BC-1,FI0,FI1,FI2);  I1[11]:=-(I1[11]-EL0*EL0*FI1+2*EL0*FI0)/
  (N*N);
  I1[2]:=I1[12]:=I1[5]:=I1[15]:=0.0;
'GOTO' GLEN;
'END' 'ELSE' 'IF' NNN=NHARM 'THEN'
'BEGIN'
  IY(M,EL0,EL1,BC,I2,I12);  FI(M,EL1,BC,FI0,FI1,FI2);  I1[1]:=I12;
  I1[4]:=FI0;  I1[14]:=EL1*FI0-I2;  I1[12]:=EL1*EL1*FI1-2*EL1*FI0+2*I2;
  FI(M,EL0,BC,FI0,FI1,FI2);  I1[12]:=I1[12]-EL0*EL0*FI1+2*EL0*FI0;
  I1[4]:=I1[4]-FI0;  I1[14]:=I1[14]-EL0*FI0;
  IY(M,EL0,EL1,BC-1,I2,I12);  FI(M,EL1,BC-1,FI0,FI1,FI2);
  I1[11]:=EL1*EL1*FI1-2*EL1*FI0+2*I2;  I1[2]:=-M*M*I12;
  FI(M,EL0,BC-1,FI0,FI1,FI2);  I1[11]:=-(I1[11]-EL0*EL0*FI1+2*EL0*FI0)/
  (M*M);
  I1[3]:=I1[13]:=I1[5]:=I1[15]:=0.0;
'GOTO' GLEN;
'END';
'END';
  IYY(M,N,EL0,EL1,BC,I1);
GLEN:
  I1[1]:=I1[1]*A; I1[2]:=I1[2]/A; I1[3]:=I1[3]/A;
I1[4]:=I1[4]/A; I1[5]:=I1[5]/A'3; I1[11]:=I1[11]*A*A;
I1[15]:=I1[15]/(A*A);
  SD1I1:=SD1I1+D1[K,ES]*I1[1];   SD2I11:=SD2I11+D2[K,ES]*I1[11];
  SD1I2:=SD1I2+D1[K,ES]*I1[2];   SD2I12:=SD2I12+D2[K,ES]*I1[12];
  SD1I3:=SD1I3+D1[K,ES]*I1[3];   SD2I13:=SD2I13+D2[K,ES]*I1[13];
  SD1I4:=SD1I4+D1[K,ES]*I1[4];   SD2I14:=SD2I14+D2[K,ES]*I1[14];
  SD1I5:=SD1I5+D1[K,ES]*I1[5];   SD2I15:=SD2I15+D2[K,ES]*I1[15];
  SD3I1:=SD3I1+D3[K,ES]*I1[1];
  SD3I2:=SD3I2+D3[K,ES]*I1[2];
  SD3I3:=SD3I3+D3[K,ES]*I1[3];
  SD3I4:=SD3I4+D3[K,ES]*I1[4];
  SD3I5:=SD3I5+D3[K,ES]*I1[5];
'END';
  'IF' NNN=1 'AND' MMM=1 'THEN'
'BEGIN'
  J1[1,1]:=J1[3,3]:=12/B'3; J1[2,1]:=J1[4,1]:=J11[1,1]:=J11[3,3]:=6/B'2;
  J1[2,2]:=J1[4,4]:=J11[4,1]:=4/B;  J1[3,1]:=-J1[1,1];  J1[3,2]:=J1[4,3]
  :=J11[3,1]:=-J1[2,1];  J1[4,2]:=J11[2,1]:=2/B;  J11[2,2]:=J11[4,2]:=1;
  J11[3,2]:=-J11[2,1];  J11[4,3]:=-J11[4,1];  J11[4,4]:=3;
  J2[1,1]:=J2[3,3]:=1.2/B;  J2[2,1]:=J2[4,1]:=J12[1,1]:=0.1;  J2[2,2]:=
  J2[4,4]:=2*B/15;  J2[3,1]:=-J2[1,1];  J2[3,2]:=J2[4,3]:=J12[1,3]:=-0.1
  ;  J2[4,2]:=-B/30;  J12[1,2]:=B/5;  J12[1,4]:=J12[4,3]:=-0.1*B;
  J12[2,1]:=J12[2,3]:=J12[4,2]:=J14[4,1]:=J14[4,3]:=0.0;  J12[2,2]:=
  J14[2,2]:=B*B/30;  J12[2,4]:=-J12[2,2];  J12[3,1]:=-1.1;J12[3,3]:=1.1;
  J12[3,2]:=-B/5;  J12[3,4]:=-0.9*B;  J12[4,1]:=J14[2,1]:=B/10;
  J12[4,4]:=J14[4,4]:=B*B/10;  J14[1,1]:=J14[3,3]:=0.6;  J14[3,1]:=-0.6;
```

```
  J14[3,2]:=-0.1*B;   J14[4,2]:=-B*B/60;
  J5[1,1]:=J5[3,3]:=13*B/35;  J5[2,1]:=11*B*B/210;  J5[2,2]:=J5[4,4]:=
  B↑3/105;  J5[3,1]:=9*B/70;  J5[3,2]:=13*B*B/420;  J5[4,1]:=-J5[3,2];
  J5[4,2]:=-B↑3/140;  J5[4,3]:=-11*B*B/210;
  J15[1,1]:=3*B*B/35;  J15[2,1]:=J15[3,2]:=B↑3/60;  J15[2,2]:=B↑4/280;
  J15[3,1]:=9*B*B/140;  J15[3,3]:=2*B*B/7;  J15[4,1]:=-B↑3/70;
  J15[4,2]:=-J15[2,2];  J15[4,3]:=-B↑3/28;  J15[4,4]:=B↑4/168;
  'FOR' I:=1 'STEP' 1 'UNTIL' 4 'DO'
  'FOR' J:=I 'STEP' 1 'UNTIL' 4 'DO'
'BEGIN'
  J4[I,J]:=J4[J,I]:=2*(1-V)*J2[J,I];  J14[I,J]:=J14[J,I]:=2*(1-V)*J14
  [J,I];  J5[I,J]:=J5[J,I];  J15[I,J]:=J15[J,I];
  J1[I,J]:=J1[J,I];  J11[I,J]:=J11[J,I];  J2[I,J]:=J2[J,I]:=-V*J2[J,I];
'END';
  J2[1,2]:=-1.1*V;  J2[3,4]:=1.1*V;
  'FOR' I:=1 'STEP' 1 'UNTIL' 4 'DO'
  'FOR' J:=1 'STEP' 1 'UNTIL' 4 'DO'
'BEGIN'
  J3[I,J]:=J2[J,I];  J12[I,J]:=-V*J12[I,J];  J13[J,I]:=J12[I,J];
'END';
'END';
  'FOR' I:=1 'STEP' 1 'UNTIL' 4 'DO'
  'FOR' J:=1 'STEP' 1 'UNTIL' 4 'DO'
  HEK[I,J]:=(SD1I1*J11[I,J]+(SD2I11+SD3I1)*J1[I,J]+
             SD1I2*J12[I,J]+(SD2I12+SD3I2)*J2[I,J]+
             SD1I3*J13[I,J]+(SD2I13+SD3I3)*J3[I,J]+
             SD1I4*J14[I,J]+(SD2I14+SD3I4)*J4[I,J]+
             SD1I5*J15[I,J]+(SD2I15+SD3I5)*J5[I,J]);
  'IF' MMM=NNN 'THEN'
'BEGIN'
  'IF' QTYPE 'NE' 0 'THEN'
'BEGIN'
  SQ1I2:=SQ2I12:=SQ3I2:=0.0;
  'FOR' ES:=1 'STEP' 1 'UNTIL' NS[K] 'DO'
'BEGIN'
EL0:=EL[K,ES-1]/A;  EL1:=EL[K,ES]/A;
  'IF' BC=3 'AND' NNN=NHARM-1 'THEN'
'BEGIN'
  I2:=EL1-EL0;  I12:=(EL1*EL1-EL0*EL0)/2;
'END' 'ELSE' 'IF' (BC=3 'OR' BC=6) 'AND' NNN=NHARM 'THEN'
'BEGIN'
  I2:=(EL1*EL1-EL0*EL0)/2;  I12:=(EL1↑3-EL0↑3)/3;
'END' 'ELSE'
  IY(N,EL0,EL1,BC,I2,I12);
  I2:=I2*A;  I12:=I12*A*A;
  SQ1I2:=SQ1I2+Q1[K,ES]*I2;  SQ2I12:=SQ2I12+Q2[K,ES]*I12;
  SQ3I2:=SQ3I2+Q3[K,ES]*I2;
'END';
  J6[1]:=J6[3]:=B/2;  J6[2]:=B*B/12;  J6[4]:=-J6[2];
  J16[1]:=3*B*B/20;  J16[2]:=B↑3/30;  J16[3]:=7*B*B/20;  J16[4]:=-B↑3/20;
  'FOR' I:=1 'STEP' 1 'UNTIL' 4 'DO'
  HEF[I]:=SQ1I2*J16[I]+(SQ2I12+SQ3I2)*J6[I];
'END' 'ELSE' 'FOR' I:=1,2,3,4 'DO' HEF[I]:=0.0;
'END';
ORTHO:
ASSMBLY(K,MMM,NNN);
  'IF' MMM>NNN 'THEN'
```

```
'BEGIN'
  'FOR' I:=1,2,3,4 'DO'  'FOR' J:=1,2,3,4 'DO' THEK[I,J]:= HEK[I,J];
  'FOR' I:=1,2,3,4 'DO'  'FOR' J:=1,2,3,4 'DO'  HEK[I,J]:=THEK[J,I];
ASSMBLY(K,NNN,MMM);
'END';
'END';
'END';
'END';
  'FOR' EP:=1 'STEP' 1 'UNTIL' NLOAD 'DO'
'BEGIN'
  HDF:=(NODENO[EP]*2-('IF' PTYPE[EP]=21 'OR' PTYPE[EP]=41 'THEN' 0
       'ELSE' 1 ))*NHARM-NHARM;
  'FOR' M:= 1 'STEP' 1 'UNTIL' NHARM 'DO'
'BEGIN'
  'IF' BC=3 'AND' M=NHARM-1 'THEN'
'BEGIN'
  'IF' PTYPE[EP]=1 'OR' PTYPE[EP]=21 'THEN'I2:=(DP[EP]-C[EP])/A 'ELSE'
  'IF'PTYPE[EP]=22 'OR' PTYPE[EP]=42 'THEN' I2:=0.0 'ELSE' I2:=1.0;
'END' 'ELSE' 'IF' (BC=3 'OR' BC=6) 'AND' M=NHARM 'THEN'
'BEGIN'
  'IF'PTYPE[EP]=1'OR'PTYPE[EP]=21'THEN'I2:=(DP[EP]*DP[EP]-C[EP]*C[EP])
  /(2*A*A)'ELSE' 'IF' PTYPE[EP]=22 'THEN' I2:=(DP[EP]-C[EP])/A
  'ELSE' 'IF' PTYPE[EP]=42 'THEN' I2:=1.0 'ELSE' I2:=C[EP]/A;
'END' 'ELSE'
'BEGIN'
  CM:=HARM(M,BC,SYMM);  CM1:=C[EP]/A;
  'IF' PTYPE[EP]=1 'OR' PTYPE[EP]=21 'OR' PTYPE[EP]=22 'THEN'
'BEGIN'
  CM2:=DP[EP]/A;  IY(CM,CM1,CM2,BC,I2,I12);
  'IF' PTYPE[EP]=22 'THEN' I2:=I12;
'END' 'ELSE'
'BEGIN'
  FI(CM,CM1,BC,FI0,FI1,FI2);
  'IF' PTYPE[EP]=42 'THEN' I2:=FI1 'ELSE' I2:=FI0;
'END';
'END';
  OVF[HDF+M,1]:=OVF[HDF+M,1]+I2*P[EP];
'END';
'END';
  'IF' NPD 'NE' 0 'THEN'
GEOMBC(NHARM,TOTDF,NPD,DF,OVADD,OVF,OVK,PD);
SYMVBSOL(OVK,OVK,OVADD,OVF,TOTDF*NHARM,1,FAIL);
  'FOR' I:=1 'STEP' 1 'UNTIL' TOTDF 'DO'
'BEGIN'
  'FOR' T:=1 'STEP' 1 'UNTIL' NHARM 'DO'
'BEGIN'
  HW[T,I]:=OVF[(I-1)*NHARM+T,1];

'END';
  NEWLINE(2);
'END';
  'FOR' YY:=0.0'STEP' YYY/NSTEP'UNTIL'YYY/0.999999'DO'
'BEGIN'
  'FOR' T:=1 'STEP' 1 'UNTIL' NHARM 'DO'
'BEGIN'
  'IF'(BC=3 'AND' T=NHARM-1) 'OR' (BC=3 'AND' T=NHARM) 'OR'
  (BC=6 'AND' T=NHARM ) 'THEN'
```

```
'BEGIN'
 'IF' (BC=3 'OR' BC=6) 'AND' T=NHARM 'THEN'
'BEGIN'
 FF3[T]:=YY/A;  FF2[T]:=FF6[T]:=0.0;  FF4[T]:=1.0;
'END' 'ELSE'
'BEGIN'
 FF3[T]:=1.0;  FF2[T]:=FF4[T]:=FF6[T]:=0.0;
'END';
'END' 'ELSE'
'BEGIN'
 F1:=HARM(T,BC,SYMM);  FY:=F1*YY/A;  X1:=EXP(FY);
MODCI(F1,BC,CI);
 FF3[T]:=COS(FY)*CI[1,0]+SIN(FY)*CI[2,0]+X1*CI[3,0]+CI[4,0]/X1;
 FF4[T]:=COS(FY)*CI[1,1]+SIN(FY)*CI[2,1]+X1*CI[3,1]+CI[4,1]/X1;
 FF2[T]:=COS(FY)*CI[1,2]+SIN(FY)*CI[2,2]+X1*CI[3,2]+CI[4,2]/X1;
 FF6[T]:=F1*(COS(FY)*CI[2,2]-SIN(FY)*CI[1,2]
 +X1*CI[3,2]-CI[4,2]/X1)/(A*A*A);
 FF4[T]:=FF4[T]/A;  FF2[T]:=FF2[T]/(A*A);
'END';
'END';
 XSX:=0.0;
 'FOR' I:=1 'STEP' 1 'UNTIL' TNNODE 'DO'
'BEGIN'
 DEF:=ROTX:=ROTY:=MX:=MY:=MXY:=VX:=VY:=0.0;
 'FOR' T:=1 'STEP' 1 'UNTIL' NHARM 'DO'
'BEGIN'
 DEF:=DEF+HW[T,2*I-1]*FF3[T];  ROTX:=ROTX+HW[T,2*I]*FF3[T];
 ROTY:=ROTY+HW[T,2*I-1]*FF4[T];
'END';
 PRINT(YY/A,1,3);  PRINT(XSX,1,3);
 XSX:=XSX+BE[I]/SBK;
 PRINT(DEF,0,4);  PRINT(ROTX,0,4);  PRINT(ROTY,0,4);
 'IF' I=1 'THEN'
'BEGIN'
 K:=1;  B:=BE[K];  BA1:=6/B'2;  BA2:=2/B;  BA3:=1;
'END' 'ELSE'
'BEGIN'
 K:=I-1;  B:=BE[K];  BA1:=-6/B'2;  BA2:=-1/B;  BA3:=4;
'END';
 'FOR' ES:=1 'STEP' 1 'UNTIL' NS[K] 'DO'
'BEGIN'
 'IF' EL[K,ES] 'GE' YY 'THEN'
'BEGIN'
 DD:=( 'IF' I 'NE' 1 'THEN' B*D1[K,ES] 'ELSE' 0 )+D2[K,ES]*YY+
 D3[K,E5]; 'GOTO' SAM1;
'END';
'END';
SAM1:
 'FOR' T:=1 'STEP' 1 'UNTIL' NHARM 'DO'
'BEGIN'
 FFF1:=(BA1*(HW[T,2*K-1]-HW[T,2*K+1])+BA2*(2*HW[T,2*K]+BA3*HW
 [T,2*K+2]));
 FF1:=FFF1*FF3[T];
 FF5:=-FF2[T]*HW[T,2*I-1];
 MX:=MX+DD*(FF1+V*FF5);
 MY:=MY+DD*(V*FF1+FF5);
```

```
  MXY:=MXY+(1-V)/2*DD*2*FF4[T]*HW[T,2*I];
'END';
  PRINT(MX,0,4);  PRINT(MY,0,4);  PRINT(MXY,0,4);
  FPM:=SQRT((MX-MY)↑2+4*MXY*MXY);
  PM1:=(MX+MY+FPM)/2;  PM2:=(MX+MY-FPM)/2;
  PRINT(PM1,0,4);  PRINT(PM2,0,4);
  NEWLINE(2);
'END';
  NEWLINE(3);
'END';
  WRITETEXT('('FOR%STRESSES%THE%RELEVANT%MOMENT%IS%
  MULTIPLIED%BY%%6/(H*H) '('C')'WHERE%H%IS%THE%THICKNESS%
  OF%THE%PLATE%AT%THE%POINT%UNDER%CONSIDERATION.')');
'END';
'END';
FAIL:
  NEWLINE(5);
'END';
'END';
```

APPENDIX 7

Tables of Harmonic Deflection Parameters From the Tests Described in Section (7.6).

M	$w_6^{1,M}$	$w_6^{2,M}$	$w_6^{3,M}$	$w_6^{4,M}$	$w_6^{5,M}$	$w_6^{6,M}$	$w_6^{7,M}$
1	4.1094						
2	4.1094	0.0505					
3	4.1094	0.0505	0.0042				
4	4.1094	0.0505	0.0042	0.0008			
5	4.1094	0.0505	0.0042	0.0008	0.0002		
6	4.1094	0.0505	0.0042	0.0008	0.0002	0.0001	
7	4.1094	0.0505	0.0042	0.0008	0.0002	0.0001	0.0000

All figures are to be multiplied by 10^{-3}

M	$w_{max.}$ $\div p_0 a^4/D_0$	$(M_y)_{max.}$ $\div p_0 \; a^2$
3	0.004063	0.048186
large	0.004062	0.047986

Table (7.1)

Simply Supported-Simply Supported

Uniform Pressure.

M	$w_6^{1,M}$	$w_6^{2,M}$	$w_6^{3,M}$	$w_6^{4,M}$	$w_6^{5,M}$	$w_6^{6,M}$	$w_6^{7,M}$	$w_6^{8,M}$
1	1.2060							
2	1.2147	0.0378						
3	1.2156	0.0378	0.0044					
4	1.2157	0.0378	0.0044	0.0010				
5	1.2157	0.0378	0.0044	0.0010	0.0003			
6	1.2157	0.0378	0.0044	0.0010	0.0003	0.0001		
7	1.2157	0.0378	0.0044	0.0010	0.0003	0.0001	0.0001	
8	1.2157	0.0378	0.0044	0.0010	0.0003	0.0001	0.0001	0.0000

All figures to be multiplied by 10^{-3}

M	$w_{max.}$ $\div p_0 a^4/D_0$	$(M_y)_{max.}$ $\div p_0 a^2$
3	0.0019179	-0.067144
4	0.0019170	-0.068289
large	0.0019169	-0.069670

Table (7.2)

Clamped - Clamped

Uniform Pressure

M	$w_6^{1,M}$	$w_6^{2,M}$	$w_6^{3,M}$	$w_6^{4,M}$	$w_6^{5,M}$	$w_6^{6,M}$	$w_6^{7,M}$	$w_6^{8,M}$
1	2.7078							
2	2.7242	-0.1068						
3	2.7328	-0.1094	0.0586					
4	2.7338	-0.1097	0.0587	-0.0073				
5	2.7345	-0.1099	0.0588	-0.0073	0.0060			
6	2.7346	-0.1100	0.0588	-0.0073	0.0060	-0.0012		
7	2.7347	-0.1100	0.0588	-0.0073	0.0060	-0.0012	0.0012	
8	2.7348	-0.1100	0.0588	-0.0073	0.0060	-0.0012	0.0012	-0.0002

All figures to be multiplied by 10^{-3}

M	$w \div p_o a^4/D_o$	$M_y \div p_o\ a^2$
	$x=0.5a, y=0.4a$	$x=0.5a, y=a$
3	0.0028281	-0.075941
7	0.0028367	-0.081767
large	0.0028363	-0.083

Table(7.3)

Simply supported-Clamped

Uniform Pressure

M	$w_6^{M,M}$	$w_6^{1,M}$	$w_6^{2,M}$	$w_6^{3,M}$	$w_6^{4,M}$	$w_6^{5,M}$	$w_6^{6,M}$	$w_6^{7,M}$
1								
2	1.3857	0.1098			All figures are to be multiplied by 10^{-2}			
3	1.3886	0.1134	0.0176					
4	1.3898	0.1139	0.0174	-0.0030				
5	1.3920	0.1143	0.0173	-0.0029	0.0031			
6	1.3934	0.1144	0.0172	-0.0029	0.0031	-0.0014		
7	1.3947	0.1144	0.0171	-0.0029	0.0030	-0.0014	0.0011	
8	1.3957	0.1144	0.0171	-0.0028	0.0030	-0.0014	0.0011	-0.0006

$w_6^{M,M}$ is the harmonic deflection parameter associated with the rigid body deflection mode.

M	$w_{max.} \div p_0 \ a^4/D_0$	$M_y \div p_0 \ a^2$ $x=0.5a, y=0.5a$	$M_y \div p_0 \cdot a^2$ $x=0.5a, y=a$
7	0.012689	0.03677	0.036616
large	0.012765	0.039	0.0368

Table (7.4a)

Simply Supported - Free.

Uniform Pressure.

M	$w_6^{M,M}$	$w_6^{1,M}$	$w_6^{2,M}$	$w_6^{3,M}$	$w_6^{4,M}$	$w_6^{5,M}$	$w_6^{6,M}$	$w_6^{7,M}$
1								
2	1.5564	0.1293						
3	1.6065	0.1161	0.0439					
4	1.6179	0.1121	0.0457	-0.0076				
5	1.6279	0.1079	0.0480	-0.0090	0.0057			
6	1.6312	0.1062	0.0491	-0.0098	0.0063	-0.0017		
7	1.6337	0.1046	0.0502	-0.0107	0.0070	-0.0022	0.0011	
8	1,6348	0.1038	0.0509	-0.0112	0.0074	-0.0025	0.0013	-0.0004

All figures are to be multiplied by 10^{-2}

$w_6^{M,M}$ is the harmonic deflection parameter associated with the rigid body rotation mode.

M	$w_{max.} \div p_0 a^4/D_0$	$M_y \div p_0 a^2$ x=0.5a,y=0.5a	$M_y \div p_0 a^2$ x=0.5a,y=a
7	0.012851	0.039486	0.00698
large	0.012840	0.03920	0.00000

Table (7.4b)

Simply Supported - Free.

Uniform Pressure.

M	$w_6^{M-1,M}$	$w_6^{M,M}$	$w_6^{1,M}$	$w_6^{2,M}$	$w_6^{3,M}$	$w_6^{4,M}$	$w_6^{5,M}$	$w_6^{6,M}$
1								
2					All figures are to be multiplied by 10^{-2}			
3	1.3993	0.0000	-0.1035					
4	1.4295	0.0000	-0.1190	-0.0198				
5	1.4368	0.0000	-0.1248	-0.0224	-0.0043			
6	1.4389	0.0000	-0.1274	-0.0241	-0.0054	-0.0011		
7	1.4400	0.0000	-0.1290	-0.0252	-0.0062	-0.0016	-0.0003	
8	1.4406	0.0000	-0.1300	-0.0260	-0.0067	-0.0019	-0.0001	

$w_6^{M-1,M}$ is the harmonic deflection parameter associated with the rigid body deflection mode.

$w_6^{M,M}$ is the harmonic deflection parameter associated with the rigid body rotation mode.

M	$w_{max.} \div p_0 a^4/D_0$	$M_y \div p_0 a^2$ $x=0.5a, y=0.5a$	$M_y \div p_0 a^2$ $x=0.5a, y=0.0$
7	0.015011	0.026963	0.00253
large	0.015011	0.0273	0.0000

Table (7.5)

Free - Free.

Uniform Pressure.

M	$w_6^{1,M}$	$w_6^{2,M}$	$w_6^{3,M}$	$w_6^{4,M}$	$w_6^{5,M}$	$w_6^{6,M}$	$w_6^{7,M}$	$w_6^{8,M}$	$w_6^{9,M}$	$w_6^{10,M}$
1	5.5743									
2	5.3202	1.1944								
3	5.6264	1.1518	0.3418							
4	5.6301	1.1487	0.3433	-0.0041						
5	5.6824	1.1257	0.3619	-0.0150	0.0421					
6	5.6870	1.1215	0.3646	-0.0171	0.0435	-0.0038				
7	5.7015	1.1095	0.3744	-0.0245	0.0494	-0.0080	0.0085			
8	5.7029	1.1080	0.3756	-0.0255	0.0501	-0.0086	0.0089	-0.0006		
9	5.7106	1.0997	0.3825	-0.0311	0.0546	-0.0120	0.0114	-0.0024	0.0022	
10	5.7104	1.0999	0.3823	-0.0309	0.0544	-0.0119	0.0113	-0.0023	0.0022	0.0000

All figures are to be multiplied by 10^{-3}

M	$w_{max.} \div p_0 \ a^4/D_0$	$M_y \div p_0 \ a^2$ x=0.5a,y=0.0	$M_y \div p_0 \ a^2$ x=0.5a,y=0.0
7	0.011235	-0.11455	0.005188
large	0.011245	-0.11700	0.000000

Table (7.6)

Clamped - Free.

Uniform Pressure.

M	$w_3^{1,M}$	$w_3^{2,M}$	$w_3^{3,M}$	$w_3^{4,M}$	$w_3^{5,M}$	$w_3^{6,M}$
1	1.9096					
2	1.9017	-0.0241				
3	1.9027	-0.0255	0.0039			
4	1.9028	-0.0251	0.0041	0.0001		
5	1.9028	-0.0253	0.0040	0.0001	0.0001	
6	1.9028	-0.0252	0.0040	0.0001	0.0001	0.0000

All figures are to be multiplied by 10^{-3}

M	$w \div P\ a^2/D_0$	$M_y \div P$
	$x=0.2a, y=0.5a$	$x=0.2a, y=0.0$
3	0.0031170	-0.082831
large	0.0031168	-0.083530

Table (7.7a)

Clamped - Clamped.

Point Load.

M	$w_6^{1,M}$	$w_6^{2,M}$	$w_6^{3,M}$	$w_6^{4,M}$	$w_6^{5,M}$	$w_6^{6,M}$	$w_6^{7,M}$	$w_6^{8,M}$	$w_6^{9,M}$	$w_6^{10,M}$
1	4.0751									
2	4.0357	-0.2186								
3	4.0460	-0.2136	0.0757							
4	4.0437	-0.2154	0.0747	-0.0246						
5	4.0447	-0.2145	0.0753	-0.0242	0.0132					
6	4.0444	-0.2149	0.0749	-0.0244	0.0131	-0.0066				
7	4.0446	-0.2147	0.0751	-0.0243	0.0132	-0.0065	0.0042			
8	4.0445	-0.2148	0.0750	-0.0244	0.0131	-0.0066	0.0041	-0.0025		
9	4.0445	-0.2148	0.0751	-0.0243	0.0131	-0.0065	0.0042	-0.0025	0.0017	

All figures are to be multiplied by 10^{-3}

M	$w_{max.} \div P\, a^2/D_0$ $x=0.5a, y=0.5a$	$(M_y)_{max.} \div P$ $x=0.5a, y=0.0$
3	0.0069476	-0.17782
9	0.0070200	-0.17015
Large	0.007030	-0.1655

Table (7.7b)

Clamped - Clamped.

Point Load.

M	$w_6^{1,M}$	$w_6^{2,M}$	$w_6^{3,M}$	$w_6^{4,M}$	$w_6^{5,M}$	$w_6^{6,M}$	. .	$w_6^{11,M}$	$w_6^{12,M}$	$w_6^{13,M}$
1	1.0648									
2	1.0766	-0.0106								
3	1.1214	-0.0302	0.0189							
4	1.1408	-0.0392	0.0238	-0.0027						
5	1.1581	-0.0513	0.0322	-0.0071	0.0018					
6	1.1633	-0.0554	0.0350	-0.0088	0.0025	-0.0002				
:	:	:	:	:	:	:				
11	1.4022	-0.2427	0.1852	-0.1159	0.0705	-0.0382	. .	0.0001		
12	0.9744	0.1007	-0.0990	0.0967	-0.0737	0.0497	. .	-0.0006	0.0001	
13	2.0276	-0.7504	0.6141	-0.4470	0.3052	-0.1899	. .	0.0028	-0.0006	0.0001

All figures are to be multiplied by 10^{-3}

M	w (x=0.5,y=0.3)	M_y (x=0.5,y=0.0)	M_y (x=0.5,y=0.3)
6	0.0012062	-0.054745	-0.00041389
11	0.0012074	-0.055141	-0.0010703
12	0.0012077	-0.055224	-0.0010659
13	0.0012078	-0.055147	-0.0009700

Table (7.8)

Clamped - Clamped.

Plate with a Hole.

REFERENCES.

1. Cheung Y.K., "The Finite Strip Method in the Analysis of Elastic Plates with Two Opposite Simply Supported Ends", Proc.Inst.Civ.Eng.,40,pp.1-7,1968.

2. Timoshenko S.P., History of Strength of Materials, McGraw-Hill, London,1953.

3. Love A.E.H., A Treatise on the Mathematical Theory of Elasticity, Dover Publication, New York,1944.

4. Szilard. R., Theory and Analysis of Plates-Classical and Numerical Methods, Prentice-Hall,Inc., New Jersey, 1974.

5. Salvadori M.G. and Baron M.L., Numerical Methods in Engineering, Prentice-Hall,Inc., New Jersey,1961.

6. Redshaw S.C., "A Three Dimensional Electrical Potential Analyser" British J. of Applied Physics, V.s, 1951, pp.291-295.

7. Hrenikoff A., "Solution of Problems of Elasticity by the Framework Method"., Trans.ASME,J.App.Mech.,8,Dec.1941, pp.A-169-A-175.

8. Turner M.J., Clough R.W., Martin G.C. and Topp L.J., "Stiffness and Deflection Analysis of Complex Structures". J.Aeron.Sci.,23,Sept.1956,pp.805-823.

9. Ghali A. and Neville A.M., Structural Analysis, Intext Educational Publishers,1972.

10. Desai C.S. and Abel J.F., Introduction to the Finite Element Method, Van Nostrand Reinhold Co.,1972.

11. Forray M.J., Variational Calculus in Science and Engineering, McGraw-Hill,1968.

12. Pin Tong and Pian T.H.H., "The Convergence of the Finite Element Method in Solving Linear Elastic Problems"., Int.J.Solids Structures,3,1967,pp.865-879.

13. Gould P.L., Szabo B.A., Brombolich L.J. and Tsai C., "High-Precision Plate and Shell Finite Elements". Developments in Mechanics,vol.6,Proc.12th Midwestern Mechanics Conference,Aug.1971.

14. Chakrabarti S., "Trigonometric Function Representation for Rectangular Plate Bending Elements", Int.J.Numerical Methods in Eng.,3,1971,pp.261-273.

15. Ergatoudis I., Irons B.M. and Zienkiewicz, "Curved, Isoparametric, 'Quadrilateral' Elements for Finite Element Analysis", Int.J.Solids Structures,4,1968,pp.31-42.

16. Irons B.M., "Engineering Applications of Numerical Integration in Stiffness Methods", AIAA J.,v.4,No.11, Nov.1966,pp.2035-2037.

17. Argyris J.H., "Matrix Analysis of Three Dimensional Media - Small and Large Displacements", AIAA J.,3,No.1, 1965,pp.45-51.

18. Strain M.N., Mathematical Methods for Technologists, The English Universities Press,1961.

19. Buell W.R. and Bush B.A., "Mesh Generation - A Survey", ASME Paper No.72-WA/DE-2.

20. Wilson E.L., "Structural Analysis of Axisymmetric Solids", AIAA J.,3,No.12,Dec.1965,pp.2269-2274.

21. Crose J.G., "Stress Analysis of Axisymmetric Solids with Asymmetric Properties", AIAA J.,10,No.7,July 1972, pp.866-871.

22. Cheung Y.K., "Finite Strip Method Analysis of Elastic Slabs", Proc.ASCE,94,EM6,(Dec.1968),pp.1365-1378.

23. Timoshenko S.P. and Woinowsky-Krieger S., Theory of Plates and Shells, McGraw-Hill Kogakusha,2nd.ed.,1959.

24. Dym C.L. and Shames I.H., Solid Mechanics-A Variational Approach, McGraw-Hill,1974.

25. Hussain K.M., Bending of Circular Plates, M.Sc. Thesis, Dept.Mech.Eng.,Univ. of Aston in Birmingham,1972.

26. Ayres F.Jr., Theory and Problems of Differential Equations,Schaum's Outline Series, McGraw-Hill,1952.

27. Mansfield E.H., The Bending and Stretching of Plates, Pergamon Press,Oxford,England,1964.

28. Mikhlin S.G., The Numerical Performance of Variational Methods, Wolers-Noordhoff,1971.

29. Palmer P.J. and Redshaw S.C., "Experiments with an Electrical Analogue for the Extension and Flexure of Flat Plates", Aeronaut.Quart.,6,1955,pp.13-30.

30. Harnden C.T. and Rushton K.R., "Numerical Analysis of Variable Thickness Plates", J. Strain Analysis,1,No.3, 1966,pp.231-238.

31. Richards T.H., "Thermal Stresses in a Thick-Walled Tube: An Experimental Study by Electrical Analogy", Int.J.Mech. Sci.Pergamon Press,7,1965,pp.103-113.

32. Yettram A.L. and Husain H.M., "Grid Framework Method for Plates in Flexure", J.Eng.Mech.Div.,Proc.ASCE,EM3, June 65,pp.53-64.

33. Woo C.W., Application of the Finite Element Method to the Design of Disc Type Wheels, Ph.D. Thesis,Dept. of Mech.Eng., Univ. of Aston in Birmingham,1971.

34. Cheung Y.K., "Folded Plate Structures by the Finite Strip Method", Proc.ASCE,95 ST,1969,pp.2963-79.

35. Zienkiewicz O.C., The Finite Element Method in Engineering Science, McGraw-Hill,London,1971.

36. Bishop R.E.D. and Johnson D.C., The Mechanics of Vibration, C.U.P.,1960.

37. Goult R.J., Hoskins R.F., Milner J.A. and Pratt M.J., Computational Methods in Linear Algebra, Stanley Thornes (Publishers),1974.

38. Fung Y.C., Foundations of Solid Mechanics, Prentice-Hall, Inc.,New Jersey,1965.

39. Martin R.S. and Wilkinson J.H., "Symmetric Decomposition of Positive Definite Band Matrices", Numerische Mathematik 7,1965,pp.355-361.

40. Jennings A., "A Computer Storage Scheme for the Solution of Symmetric Linear Simultaneous Equations", The Computer Journal,9,1966,pp.281-285.

41. Jennings A., "Solutions of Variable Bandwidth Positive Definite Simultaneous Equations", The Computer Journal, 1971,p446.

42. Scheid F., Numerical Analysis, Schaum's Outline Series, McGraw-Hill,1968.

43. Herrmann L.R., "A Bending Analysis for Plates", Proc. Conf.Matrix Methods in Structural Mechanics, Wright-Patterson Air Force Base, Ohio,1965.pp.577 - 602.

44. Herrmann L.R., "Finite Element Bending Analysis for Plates", J.Eng.Mech.Div.,Proc.ASCE,Oct.1967,pp.13-26.

45. Chatterjee A. and Setlur A.V., "A Mixed Finite Element Formulation for Plate Problems", Int.J.for Numerical Methods in Eng.,4,1972,pp.67-84.

46. Moody W.T., "Moments and Reactions for Rectangular Plates", Eng.Monograph No.27,U.S.Dept. of the Interior, Bureau of Reclamation,Denver,1963.

47. Morley L.S.D., "Bending of a Square Plate with Central Square Hole", Royal Aircraft Establishment,Technical Report 69031,Feb.1969.

48. Ligtenberg F.K., "The Moire Method-A New Experimental Method for the Determination of Moments in Small Slab Models", Proc.Soc.Expt.Stress Analysis,12,2,1955, pp.83-98.

49. Richards T.H., "Analogy Between the Slow Motion of a Viscous Fluid and the Extension and Flexure of Plates: A Geometric Demonstration by Means of Moire Fringes", British J. of App. Physics,2,June 1960,pp.244-254.

50. Elson M.G.J., Use of the Slab-Slice Analogy for the Study of Thermal Stress Problems, M.Sc. Thesis, Dept. of Mech.Eng.,College of Advanced Technology,Birmingham, 1965.